

Universität
Rostock



Traditio et Innovatio

**Bioenergetics, immunity and cellular and molecular
stress responses to ZnO nanoparticles are modulated
by environmental temperature and salinity in the blue
mussels *Mytilus edulis***

Cumulative Dissertation

For

Obtaining the academic degree

Doctor rerum naturalium (Dr. rer. Nat)

Department of Marine Biology

Institute of Bioscience

Faculty of Mathematics and Natural Sciences

University of Rostock

Submitted by

Fangli Wu

Born on 20.01.1993 in P. R. China

Rostock, 15.06.2022

Reviewer #1: Prof. Dr. Inna Sokolova

University of Rostock

Albert-Einstein-Str. 3

18059 Rostock, Germany

Reviewer #2: Dr. Till Luckenbach

Helmholtz-Zentrum für Umweltforschung UFZ

Permoserstr. 15, Raum: 229

04318 Leipzig, Germany

Jahr der Einreichung: 2022

Jahr der Verteidigung: 2023

Supervisor:

Prof. Dr. Inna Sokolova

Chair of Department of Marine Biology

Faculty of Mathematics and Natural Sciences

University of Rostock

Rostock, Germany

Erklärung

Hiermit versichere ich an Eides statt, dass ich die vorliegende Arbeit selbständig angefertigt und ohne fremde Hilfe verfasst habe. Dazu habe ich keine außer den von mir angegebenen Hilfsmitteln und Quellen verwendet. Die aus den benutzten Werken inhaltlich und wörtlich entnommenen Stellen sind als solche kenntlich gemacht.

Fangli Wu

Rostock, den 15.06.2022

Acknowledgement

First of all, I would like to express my deepest appreciation to my supervisor Prof. Dr. Inna Sokolova, who offered the excellent opportunity for my PhD studies in marine biology. I am very grateful for her constant guidance, great patience and nonstop encouragement, as well as for her tremendous support in my work and life. I have benefited immensely from her unique commitment to scientific research as well as from her example on getting along with people and dealing with matters. All these are inspiring me to be a responsible and knowledgeable researcher, which will benefit me forever.

This work was in part supported by the Research Training Group 'Baltic TRANSCOAST' funded by the DFG (Deutsche Forschungsgemeinschaft) under grant number GRK 2000 and the China Scholarship Council (CSC). I warmly thank the Baltic Transcoast group and greatly appreciate the DFG and the CSC for their financial support for my work.

My sincere thanks go to all my dear working group partners: Dr. Eugene Sokolov, PD. Dr. Stefan Forster, Holger Pielenz, Elke Meier, Andrea Mellin, Halina Falfushynska, Mirza Nusrat Noor, Andrei Khomich, Natascha Ouillon, Jennifer Steffen, Dr. Fouzia Haider, Hui Kong, Duy Nghia Pham, Torben Bruhns, Linda Adzigbli, Werna and Friederike Säring. Especially, I would like to thank Dr. Eugene Sokolov for his guidance on experimental operation and procedures, for his excellent cooperation and many discussions on experimental techniques.

I also sincerely thank my collaborators: Dr. Olaf Dellwig (Leibniz Institute for Baltic Sea Research Warnemünde, Rostock, Germany), Georg Schnell (Faculty of Mechanical Engineering and Marine Technology, University of Rostock, Germany), Christian Fettkenhauer (Anton Paar Germany GmbH, Ostfildern, Germany), Prof. Dr. Hermann Seitz (Faculty of Mechanical Engineering and Marine Technology, University of Rostock, Germany), Dr. Fei Ye and Dr Joydeep Dutta (KTH Royal Institute of Technology, Sweden) for their help with the metal determinations and the characterization of nanoparticles.

I greatly appreciate and wish to thank my parents and my brothers for their love. I also thank all friends in Germany: Dr. Yuya Hu, Dr. Shanshan Song, Dr. Rui Sang, Dr. Wei Zhou, Dan Wang, Xin Wang, Dr. Zhihong Wei, Kaicheng Zhang and Jiyun Zhang.

Finally yet importantly, I would like to thank my husband Wei Meng for his ardent love, great support and constant encouragements, which are essential for me.

Abstract

Shallow coastal habitats are commonly exposed to multiple stressors including pollution from point and non-point sources, fluctuations in temperature and salinity that can interactively affect the performance and health of keystone marine organisms including benthic ecosystem engineers such as the mussels. Engineered nanoparticles (nZnO) from multiple sources are contaminants of emerging concern (CECs) in coastal habitats especially in the closed inland basins such as the Baltic Sea. Toxicity of nanoparticles have raised concerns about their potential effects on coastal ecosystems, yet the mechanisms of the nanoparticle toxicity and their interactions with common abiotic stressors such as temperature and salinity are not well understood. The blue mussels of the genus *Mytilus* play important ecological and economical roles in temperate to subarctic coastal ecosystems and are biological indicator species for ecosystem health. Mussels can accumulate nanomaterials and are sensitive to their toxicity due to their filter-feeding habit. The aim of our present study was to investigate the combined effects of seasonal warming, acclimation at elevated temperatures and salinity stress on bioenergetics, immune and general cellular stress responses to nZnO nanoparticles pollution in the blue mussels *M. edulis*. To achieve this aim, we determined the combined effects of seasonality (winter and summer), warming (+5 °C above the season-specific ambient temperature), different salinity regimes (normal salinity 15, low salinity 5 and fluctuating salinity 5-15) as well as exposure to the environmentally relevant concentrations of nZnO (10 and 100 µg l⁻¹) for 21 days on key fitness-related traits including bioenergetics, innate immunity, and cellular stress response in the *M. edulis* from the Baltic Sea. Exposure to dissolved Zn (as ZnSO₄) was used to test whether the toxic effects of nZnO might be due to the potential release of Zn²⁺. Our study shows that nZnO exposures regulate the expression of immune-related genes and the immune-related functions in hemocytes, negatively affect the bioenergetics and cellular energy allocation in the whole soft tissue, and induce oxidative stress and apoptosis in gill and digestive gland in the mussels *M. edulis*, and that the immunomodulatory effects, bioenergetics responses and cellular stress responses of nZnO are strongly regulated by the elevated temperatures and the season as well as the environmental salinity regimes. Furthermore, the multi-biomarker analysis shows that the toxic effect of nZnO has different mechanisms and might be stronger than the effect of the equivalent concentrations of dissolved Zn in the mussels. Our study provided new insights into the bioenergetics, immunomodulation and cellular stress mechanisms underlying the combined effects of temperature and salinity variations with nZnO toxicity in the mussels and their implications for the survival and performance of the mussels' populations in polluted coastal areas.

Kurzfassung

Flache Küstenlebensräume sind häufig mehreren Stressoren ausgesetzt, darunter Verschmutzung sowie Temperatur- und Salzgehaltsschwankungen, die die Leistung und Gesundheit wichtiger Meeresorganismen, einschließlich benthischer Ökosystemingenieure wie Muscheln, interaktiv beeinflussen können. Technisch hergestellte Nanopartikel (nZnO) sind neu auftretende besorgniserregende Schadstoffe (Contaminants of Emerging Concern, CECs), insbesondere in geschlossenen Binnenbecken wie der Ostsee. Die Toxizität von Nanopartikeln hat Bedenken hinsichtlich ihrer potenziellen Auswirkungen auf Küstenökosysteme geweckt, doch die Mechanismen der Nanopartikeltoxizität und ihre Wechselwirkungen mit häufigen abiotischen Stressoren wie Temperatur und Salzgehalt sind nicht gut bekannt. Die Miesmuscheln der Gattung *Mytilus* sind ökologisch und ökonomisch wichtige Organismen in gemäßigten bis subarktischen Küstenökosystemen sowie Bioindikatorarten für die Ökosystemgesundheit. Muscheln können Nanomaterialien anreichern und sind aufgrund ihrer Filter-Fressgewohnheiten empfindlich gegenüber ihrer Toxizität. Das Ziel dieser Studie war es, die kombinierten Auswirkungen von Temperatur- und Salzstress auf die Bioenergetik, das Immunsystem und allgemeine zelluläre Stressreaktionen auf die nZnO-Nanopartikel bei der Miesmuschel *M. edulis* zu untersuchen. Dafür wurden die Muscheln der kombinierten Auswirkungen von Saisonalität (Winter und Sommer), Erwärmung (+5 °C über der jahreszeitspezifischen Umgebungstemperatur), verschiedenen Salzgehaltsregimen (normaler Salzgehalt 15, niedriger Salzgehalt 5 und schwankender Salzgehalt 5-15) sowie der umweltrelevanten Konzentrationen von nZnO (10 und 100 µg l⁻¹) für 21 Tage ausgesetzt, und die wichtige fitnessbezogene Merkmale, einschließlich Bioenergetik, angeborene Immunität und zelluläre Stressreaktion wurden gemessen. Die Exposition gegenüber gelöstem Zn (als ZnSO₄) wurde verwendet, um zu testen, ob die toxischen Wirkungen von nZnO auf die mögliche Freisetzung von Zn²⁺ zurückzuführen sein könnten. Unsere Studie zeigt, dass nZnO-Expositionen die Expression von immunbezogenen Genen und immunbezogenen Funktionen in Hämozyten ändern, die Bioenergetik und zelluläre Energieallokation im Körper negativ beeinflussen und oxidativen Stress und Apoptose in Kiemen und Verdauungsdrüsen von den Muscheln auslösen. Die immunmodulatorischen und bioenergetische Stresswirkungen von nZnO sind stark durch die erhöhten Temperaturen, Salinität und Saisonalität modifiziert. Darüber hinaus zeigt die Multi-Biomarker-Analyse, dass die toxische Wirkung von nZnO anders und teilweise stärker als die Wirkung auf die äquivalenten Konzentrationen von gelöstem Zn ist. Diese Arbeit liefert neue Erkenntnisse über die Bioenergetik, die Immunmodulation und die zellulären Stressmechanismen, die den kombinierten Auswirkungen erhöhter Temperatur- und Salzgehaltsschwankungen mit nZnO-Toxizität in den Muscheln zugrunde liegen, und deren Bedeutungen für die Lebensfähigkeit der Muschelpopulationen in verschmutzten Küstengebieten.

List of abbreviations

Ea	Total energy reserve
CEA	Cellular energy allocation
MTs	Metallothionein levels
ETS	Electron transport system
THC	Total hemocytes count
HM	Hemocytes mortality
AD	Adhesion capacity
Pha	Phagocytosis
NRU	Neutral red uptake
TLRb	Toll-like receptor b
TLRc	Toll-like receptor c
TNF	Tumor necrosis factor
TGF- β	Transforming growth factor-beta
C1	C1 complement domain-containing protein
C3q	Complement component C3-like protein
MyD88a	Myeloid differentiation primary response gene 88 a
MyD88a	Myeloid differentiation primary response gene 88 c
LPO	Lipid peroxidation
PC	Protein carbonyls
p53	Tumor protein p53
p38	p38 mitogen-activated protein kinases
JNK	C-Jun N-terminal kinase
COX	Cyclooxygenase
Bcl-2	B-cell lymphoma2
NF- κ B	Nuclear factor κ B (p100/p105)
PCA	Principal component analysis
DA	Discriminant analysis
NPs	Nanoparticles
nZnO	ZnO nanoparticles
C	Control (no Zn addition)
10 NP	10 μ g l ⁻¹ nZnO
100 NP	100 μ g l ⁻¹ nZnO
10 Zn	10 μ g l ⁻¹ dissolved Zn
100 Zn	100 μ g l ⁻¹ dissolved Zn
NS	Normal salinity 15
LS	Low salinity 5
FS	Fluctuating salinity between 15 and 5

Contents

1. General Introduction	1
1.1. Introduction.....	1
1.1.1. Coastal ecosystems under multiple stresses	1
1.1.2. nZnO as emerging contaminants in the coastal marine environments.....	2
1.1.3. The blue mussels <i>Mytilus edulis</i> as model organism in ecotoxicology	6
1.1.4. The interactive effects of nZnO and temperature on marine organisms.....	7
1.1.5. The interactive effects of nZnO and salinity on marine organisms.....	9
1.2. Objectives and experimental design of the present study.....	11
2. Immune responses of <i>M. edulis</i> to combined nZnO, temperature and salinity stress ...	15
2.1. Innate immune defense system of the bivalves.....	15
2.2. Bivalves immunity as a target for environmental nanoparticles.....	18
2.3. Hypotheses and approach to the study of nZnO immunotoxicity	20
3. Combined effects of nZnO, temperature and salinity on bioenergetics of the blue mussel <i>M. edulis</i>	22
3.1. Bioenergetics of the bivalves.....	22
3.2. Effect of nanoparticles on bioenergetics of the bivalves	25
3.3. Hypotheses and approaches to study the combined effects of nanopollutants and abiotic stressors on bioenergetics.....	26
4. Interactive effects of nZnO and temperature on cellular stress responses of the mussels <i>M. edulis</i>	28
4.1. Molecular and cellular stress responses of the bivalves.....	28
4.2. The oxidative stress response	29
4.3. Apoptosis regulation.....	29
4.4. Inflammatory responses.....	31
4.5. Hypotheses and approaches to study the cellular stress response	31
5. Summary and discussion.....	33
5.1. Immunotoxic mechanisms of nZnO in the context of environmental variability ...	34
5.2. Metabolic disturbance as a mechanism of nZnO toxicity in different environmental contexts	35
5.3. Cellular stress response in temperature-dependent nZnO toxicity mechanisms ..	37
6. References	39
7. Appendix.....	51
My contributions to the publications included in this thesis.....	51
7.1. Immune responses to ZnO nanoparticles are modulated by season and environmental temperature in the blue mussels <i>Mytilus edulis</i>	52
7.2. Interactive effects of salinity variation and exposure to ZnO nanoparticles on the innate immune system of a sentinel marine bivalve, <i>Mytilus edulis</i>	85
7.3. Season-dependent effects of ZnO nanoparticles and elevated temperature on bioenergetics of the blue mussel <i>Mytilus edulis</i>	102

7.4. Salinity-dependent effects of ZnO nanoparticles on bioenergetics and intermediate metabolite homeostasis in a euryhaline marine bivalve, <i>Mytilus edulis</i> ...	116
7.5. Interactive effects of ZnO nanoparticles and temperature on molecular and cellular stress responses of the blue mussel <i>Mytilus edulis</i>	135
Curriculum Vitae	169

1. General Introduction

1.1. Introduction

1.1.1. Coastal ecosystems under multiple stresses

Coastal ecosystems are among the most threatened in the world owing to habitat degradation, global climate change, urbanization and pollution [1, 2]. A recent comprehensive risk analysis of human activities listed chemical pollution as the highest risk faced by the coastal waters and biota [2]. With the widespread commercial and industrial application of manufactured nanoparticles, nanomaterials became important emerging pollutants that accumulate in the coastal environment posing a potential threat to coastal marine ecosystems, associated biota and human health [3, 4]. Coastal ecosystems are particularly vulnerable to emerging pollutants including nanomaterials, because they serve as the sinks of pollutants from land and river sources [4, 5]. However, the toxic mechanisms and effects of nanopollutants on marine organisms and ecosystems are not yet fully understood, especially in the context of natural changes of other abiotic stressors common in the coastal marine environments. Considering the impacts of global climate change and increasing human pressure on coastal ecosystems, it is essential to understand the physiological mechanisms that allow marine coastal organisms to survive and adapt to increasing pressure from multiple stressors and that set limits to their tolerance to combined stressors. This knowledge is essential for understanding the impacts of climate change and human activities on coastal biodiversity and ecosystem health and for developing policies to mitigate such impacts.

The Baltic Sea is a good model system representative of shallow coastal ecosystems under combined pressure of natural and abiotic stressors [6]. The Baltic Sea ecosystem is a hot spot for coastal ecotoxicology research serving as a model to gain valuable information about environmental risks from pollutant

toxicity [7]. The Baltic seawater has a long residence time (up to 25-40 years) and a slow exchange rate, resulting in the persistence of toxic substances in the Baltic environment [8]. This is a semi-enclosed shallow sea with an average depth of 53 m (86% of the Baltic Sea is shallower than 200 m and 20% of the Baltic Sea is shallower than 15 m). The Baltic Sea is connected to the Atlantic Ocean through the narrow and shallow waterway, resulting in limited water exchange with the North Sea [9]. The Baltic Sea is a non-tidal region, and its horizontal water flow is mainly due to wind and transverse density gradient caused by temperature and salinity gradient [10]. The Baltic Sea is greatly influenced by fresh water influx from land catchments, so that rainfall and river runoff account for one fortieth of the Baltic Sea water [8, 11]. This is one of the main reasons why the salinity of the Baltic Sea is lower than that of the open seas. The salinity of the Baltic Sea varies greatly in space, ranging from a minimum salinity of 1-2 (practical salinity units) in the north and east Baltic Sea to the maximum salinity of 20 in Kattegat. Salinity in the Baltic Sea fluctuates over time due to the changes of the saltwater influx, precipitation and evaporation [12]. Because of its shallow depth and locked inland position, the Baltic Sea is vulnerable to the ongoing climate change. By the end of this century, the summer average temperature of seawater in the Baltic Sea are predicted to rise by 2-4 °C, and the precipitation in the Baltic Sea will increase by 30% lead to the freshening of the surface Baltic seawater [13]. In addition, while many industrial legacy contaminants (such as trace metals and persistent organic pollutants) are now tightly controlled, the densely populated Baltic Sea coasts are increasingly exposed to emerging pollutants including engineered nanoparticles [14-16]. Hence, in the present study, the Baltic Sea was selected as an example of coastal ecosystem under multiple stresses and the Baltic populations of the mussels *Mytilus* was selected as our experimental species.

1.1.2. nZnO as emerging contaminants in the coastal marine environments

Manufactured nanomaterials (i.e. materials containing particles with one or

more dimensions < 100 nm) are increasingly used in industrial applications and consumer products, such as energy production, medicine and personal care products due to their stability and novel properties compared to those of bulk material [4]. A key feature of engineered nanomaterials, which renders them useful for many applications, is the improved reactivity due to the high surface to volume ratio; however, this characteristic (the small size of nanoparticles) also raises concerns about the environmental and human health hazard of nanomaterials during their production, use or release into the environment [4].

ZnO has been placed as a priority pollutant by the US EPA (US Environmental Protection Agency) [31] and as ecotoxic agent by the EU hazard classification [32] based on the toxic effects of dissolved Zn and bulk ZnO on organisms. The toxicity evaluation of nZnO is based on the hypothesis that its toxicity is mainly caused by ions released by ZnO nanoparticles [32]. Therefore, nZnO is classified as an ecotoxic substance in freshwater and marine environment by inference from Zn²⁺ toxicity [33]. Due to the rising concerns about the wide dispersive use of nZnO and insufficient information on its toxicity, nZnO has been placed as a priority pollutant urgently requiring investigation by ECHA (European Chemicals Agency, <https://echa.europa.eu>).

ZnO nanoparticles (nZnO) is a common type of metal-containing nanomaterials used in various products and applications [4, 17-19]. ZnO nanoparticles hold the third highest place (after SiO₂ and TiO₂) in terms of the global production volume with the annual production ranging from 550 to 10,000 tons based on different estimates [17, 20, 21]. ZnO nanoparticles are widely used in medicine, cosmetics, industry, agriculture, textiles and packaging as antibacterial agents, ultraviolet shielding agents, anti-corrosive agents, catalysts, antifouling agents and drug delivery systems [17, 18, 22-24]. This leads to the massive release on nZnO into the environment from the point- and non-point sources and raises concerns about the potential impact of the highly reactive nZnO on marine organisms, human health and the environment [4, 17, 18]. It is estimated that about 10% of

all produced nZnO is released into the environment, and more than 95% of them enter the aquatic environments from wastewater treatment plants, antifouling paints and personal care products accumulating in sediments and water including coastal areas [25, 26].

Due to the lack of the analytical methods to determine nZnO in complicated natural matrices (such as sediment or seawater), the quantitative evaluation of nZnO exposures in marine environment is facing challenges; however, the available probabilistic modeling-based estimates predict that environmental concentrations of nZnO reach hundreds ng l⁻¹ in the European surface waters [27-30] and up to 100 µg kg⁻¹ in the sediment [26, 29]. These environmentally relevant concentrations of nZnO raise concerns about the potential toxic effects of nZnO on marine organisms and the environment [4, 17].

It's worth noting that recent studies in freshwater mussels and amphibians show that nanoparticles including nZnO may show different toxic mechanisms from that of dissolved metals including ionic Zn²⁺ [34-38]. These findings challenge the assumption of the release of Zn²⁺ as the main toxic mechanism of ZnO nanoparticles that underlies current ecotoxicological risk assessments of nZnO [32]. There is increasing evidence that nZnO can exert toxicity not only by the release of zinc ions, but also by production of reactive oxygen species (ROS) and direct particle interaction causing physical damage through internalization [39, 40]. Furthermore, studies in mammals and marine mussels have found that the toxicity of nanoparticles depended on the size and shape of the nanostructures [41, 42], further lending support to the notion that nanoparticles' toxicity cannot be fully ascribed to the toxicity of the metal they contain. The mechanisms and impacts of nZnO toxicity therefore require further investigation, particularly in marine organisms that are potentially exposed to high nanoparticle load [43-48].

ZnO nanoparticles present a toxicity risk to a broad range of aquatic organisms including microorganisms, algae, invertebrates and vertebrates [47, 49]. Most

ecotoxicological studies of ZnO nanoparticles have been conducted on freshwater organisms using relatively high, not environmentally relevant concentrations of nZnO [34, 35, 37, 38, 40, 47, 49-52]. Similarly, most studies on the ecotoxicity of ZnO nanomaterials in marine organisms focused on the effects of high concentrations of these contaminants. Thus, recent studies in marine organisms including mussels, clams, oysters and amphipods have found that exposure to high concentrations (0.1-4 mg l⁻¹) of nZnO can affect the immune response [45, 48, 53, 54], impair feeding, growth and metabolism [55, 56], change cellular respiration and energy budgets [57], cause oxidative stress [58, 59] and negatively affect reproduction [55]. Interestingly, the effect of nZnO on these organisms is not simply dose-dependent. In addition, the potential ecotoxicological effects of the environmentally relevant concentrations of nanoparticles including nZnO in marine organisms have not been extensively studied [17, 26, 42].

The biological effects of nanoparticles including nZnO could be influenced by other environmental factors such as temperature, pH, salinity, or presence of other pollutants [48, 54, 60-62]. These interactions might be due to the direct impact of abiotic environment on the physicochemical properties of nanoparticles (such as the surface change and aggregation behavior) that influence the bioavailability and reactivity of nanoparticles [44, 63, 64], or indirect physiological effects of nanoparticles and other stressors on the organisms' metabolic machinery and cellular protective mechanisms [35, 50, 54, 64-67]. In polluted environments, the cumulative effects of stressors that act on the same pathways or molecular targets can complicate the interpretation and assessment of responses to nanoparticles. At present, only a handful of studies have investigated the interactive effects of nanopollutants and other abiotic stressors (such as temperature, salinity, or pH) on the physiological responses and fitness-related traits (including metabolism, immunity, cellular stress response, development, growth or reproduction) of marine organisms [35, 44,

50, 54, 64, 66, 67]. This limits our ability to understand the potential toxic effects of metal-containing nanopollutants such as nZnO in the naturally variable coastal environments and increases the uncertainty of environmental risk assessment of nanoparticles [68].

1.1.3. The blue mussels *Mytilus edulis* as model organism in ecotoxicology

The blue mussels (*Mytilus* spp.) play important ecological and economical roles in temperate to subarctic coastal ecosystems around the world [69, 70] and are common biological indicator species for assessment of the ecosystem health and environmental pollution monitoring [71, 72]. Mussels are common fouling organisms that form dense sediments (called mussel beds) on natural and artificial hard substrates in subtidal and intertidal zones of temperate to subarctic coastal ecosystems around the world [69, 70]. Fouling organisms are animal or plant species that exist in water and adhere to natural and artificial hard substrates immersed in water. When attached to the hull and water works, these organisms accumulate and grow, forming layers of sedimentary material harmful to the hull and the works. The production of marine mussels for human consumption (>15 million tons with a total value of over 20 billion US\$ per year) accounts for about 14% of the world's seafood production [73]. Most (89%) of the mussels' production comes from aquaculture, and only 11% comes from wild fisheries [73]. Notably, the seed resources for aquaculture production are mainly collected from natural populations [73]. Mussels serve as important ecosystem engineers in marine benthic habitats because they form mussel beds, providing refuge and food for many small organisms by increasing habitat complexity and contributing to the benthic-pelagic coupling and top-down control of the water quality. Owing to the ecological and economic importance of the mussels, their biology, ecology and physiology (including molecular and physiological stress mechanisms) are well understood [71, 74-78]. The knowledge of fundamental stress physiology of the mussels provides a solid foundation for biomarkers-based assessment of their health condition.

The blue mussels are filter-feeders that efficiently filter out and ingest particles of 4-35 μm size, and partially retain larger (35-100 μm) and smaller (<4 μm) particles [79, 80]. Thus, mussels can potentially accumulate nanoparticles and their aggregates [81] and are sensitive to their toxicity [35, 37, 42, 50, 82]. The Baltic blue mussel populations of the genus *Mytilus* represents natural hybrids of two closely related ecotypes *M. edulis* and *M. trossulus* [83], and the *Mytilus* population at our chosen study site (54°10'49.602"N, 12°05'21.991"E) has about 100% (mitochondrial) and 70% (nuclear) genetic background of *M. edulis* [83]. Thus, the present experimental mussels were designated as *M. edulis* due to the predominance of *M. edulis* genes in the studied natural hybrids [74, 83]. The mussels *M. edulis* are ecologically dominant and economically significant species in the Baltic Sea [84, 85] and are commonly exposed to emerging pollutants including engineered nanoparticles as well as to temperature and salinity variations in their habitats [48, 81]. Available studies showed that nZnO particles and their aggregates can be retained and ingested through the gills and the digestive tract, transported to internal organs including the digestive gland and internalized by endocytosis in mussels [60, 86, 87]. The gills (as a key place of nanomaterials uptake) and the digestive gland (as the main organ for nanomaterials accumulation) are considered sensitive tissues for nanoparticle toxicity in bivalves [87, 88], and were therefore used as target tissues in our present study. Furthermore, immune cells (hemocytes) of bivalves are among the earliest responders to abiotic stressors including metal-containing pollutants, salinity variations and temperature stress [89-92]. This makes the circulating hemocytes important stress-sensing tissues as well as a transport mechanism and target tissue for metal-containing nanoparticles warranting their consideration in the present analysis.

1.1.4. The interactive effects of nZnO and temperature on marine organisms

Temperature is an important environmental factor that affects all aspects of

ectotherms' performance, because it directly affects the rate of physiological and biochemical reactions, fluidity of biological membranes and structural stability of macromolecules such as DNA and proteins [93]. In temperate coasts, marine organisms are commonly affected by the elevated temperature due to seasonal warming and the global climate change [94]. Due to the climate change related to massive emissions of CO₂ in the atmosphere, the average surface seawater temperature is increasing at a rate of about 0.11-0.13 °C per decade [95] with even faster warming in semi-closed basins such as the Baltic Sea [96]. The recent global climate change consensus models predict that the global average air temperature will rise by 3-6 °C by the end of 21st century depending on to CO₂ emission scenario [94]. Northern and Central Europe are warming faster than the global average, and the average air temperature here is expected to rise by 5-8 °C by the end of 21st century [94]. In marine bivalves, elevated temperature can affect growth and reproduction [97], modulate the immune response [54, 98] and physiological energetics [99-102], and cause cellular damage due to elevated oxidative stress [101, 103-106]. This provides a physiological basis for potential interactive effects of nZnO toxicity and seawater warming on the physiological responses and fitness-related traits of marine bivalves in the context of the environmentally relevant thermal variability. Furthermore, the surface seawater temperature varies greatly in seasonal cycles and diurnal basis in the shallow coastal areas of the Baltic Sea, combined with the long-term warming trend due to the climate change [95, 107]. Thus, evaluation of the temperature-dependent biological responses to nanoparticles requires consideration of seasonality, which is an important factor affecting all aspects of temperate bivalve physiology including reproduction, immunity and stress responses to pollutants [77, 78, 108-112].

Studies have shown that temperature may regulate the responses to toxicants in aquatic organisms including marine bivalves [113]. Elevated temperatures due to the climate change and/or seasonal warming can strongly increase the toxicity of

metals such as Cd, Cu, and Pb in freshwater and marine organisms [106, 108, 113-115]. However, only a few studies have been done so far on the temperature-dependent biological responses to nanoparticles in freshwater and marine species [44, 50, 116]. Thus, toxic effects of nZnO increased in warming-exposed marine copepods *Tigriopus japonicus* (15→35°C) [116] and diatoms *Thalassiosira pseudonana* (10→30 °C) [44]. However, the effects of nZnO decreased during milder warming in marine diatoms *T. pseudonana* (10→25 °C) [44] and in freshwater mussels *Unio tumidus* (18→25 °C) [50]. Therefore, for evaluating the ecotoxicological effect of nanomaterials in organisms, it is of great importance to assess the potential impact of warming on the toxicity of nanoparticles in the context of the environmentally relevant thermal variability [62]. This is particularly important because both the organism's physiology and the physio-chemical properties of nanoparticles can be influenced by temperature [26, 44, 47, 93]. To close this important gap in our knowledge, we investigated the potential interactive effects of experimental temperature rise and seasonal warming and nZnO on key physiological responses of the blue mussels *Mytilus edulis* including immunity, bioenergetics and molecular and cellular stress response. The mussels were acclimated to different concentrations of nZnO under four temperature scenarios (see Chapter 1.2 for details of experimental design) that reflect the seasonal temperature change (10 °C in winter and 15 °C in summer) or mimic warming (+5 °C) such as occurs during heat waves and is similar to the warming predicted by the pessimistic end-of-century scenarios for the Baltic Sea (+5-8 °C) [13, 94]. To the best of our knowledge, this is the first study to investigate season- and warming-dependent effects on the key putative mechanisms of nZnO toxicity that play a central role in adverse health outcomes of nanoparticle exposures in the sentinel marine organisms, the blue mussel *M. edulis*.

1.1.5. The interactive effects of nZnO and salinity on marine organisms

Ambient salinity is a key environmental factor in shallow coastal areas, semi-

enclosed and closed basins and estuaries where salinity fluctuates due to evaporation, freshwater runoff, saltwater influx and precipitation [117, 118]. The seawater salinity in Baltic Sea varies spatially from 1 to 20 (practical salinity units) from southwest to northeast and fluctuates over time. The normal seawater salinity was 12-15 from the habitat salinity of the studied population *M. edulis*. Thus, the osmotic stress was low salinity 5 and fluctuating salinity 5-15 in the present study. Salinity variation is an important environmental stressors for coastal and marine organisms [7] and can strongly affect metabolism, biosynthetic activity, and osmoregulation of marine organisms including bivalves [119-122]. Furthermore, osmotic stress can modulate the immune functions, oxidative stress response, apoptosis and host-pathogen interactions of marine bivalves [121, 123-126]. This provides a physiological basis for potential interactive effects of nZnO toxicity and salinity on the bioenergetics, cellular stress response and immunity of marine bivalves in the coastal environments with variable salinity.

Earlier studies reported the interactions of salinity on the toxicity and bioavailability of nanoparticles in aquatic organisms including fish *Oryzias melastigma* and *Fundulus heteroclitus* [66, 127] , diatom *Thalassiosira pseudonana* [64] and copepod *Tigriopus japonicas* [128]. Furthermore, ambient salinity can directly affect nanoparticles' physicochemical properties (such as stability, aggregation, sedimentation and solubility) [44, 128] and thus potentially modulate the toxic effect of nZnO on organisms. However, potential mechanisms and interactive effects of salinity and nanopollutants on the health and performance of marine organisms including the mussels are not yet well understood and require further investigation. Therefore, in the second experimental series, we focused on the potential interactive effects of salinity stress and nZnO toxicity on marine mussels. We exposed the mussels to environmentally relevant nZnO during long-term acclimation to different salinity regimes (normal salinity 15, low salinity 5, or fluctuating salinity with the daily

change between salinity 15 and 5) (see Chapter 1.2 for details of the experimental design), and investigated the impact of these combined stressors on immunity and bioenergetics of the mussels.

1.2. Objectives and experimental design of the present study

The overarching objective of the present study was to improve our understanding of the combined effects of nZnO pollution and common abiotic stressors including elevated temperature (such as expected during seasonal warming or caused by climate change) and salinity variations on performance and health of keystone marine bivalves, the blue mussel *M. edulis* from the Baltic Sea. To achieve this objective, we focused on key fitness-related traits including cellular stress responses, bioenergetics and immune defense in the following specific aims:

- To investigate the potential temperature- and salinity-dependent immunotoxicity of nZnO for the immune cells (hemocytes) of the blue mussel *M. edulis* ([Publications 1 and 2](#)).
- To determine the interactive effects of nZnO, temperature and salinity variation on metabolism and energy homeostasis of the blue mussel *M. edulis* ([Publications 3 and 4](#)).
- To assess the combined effects of nZnO and elevated temperatures on the cellular stress responses related to the oxidative stress, apoptosis and inflammation pathways of the blue mussel *M. edulis* ([Publication 5](#)).

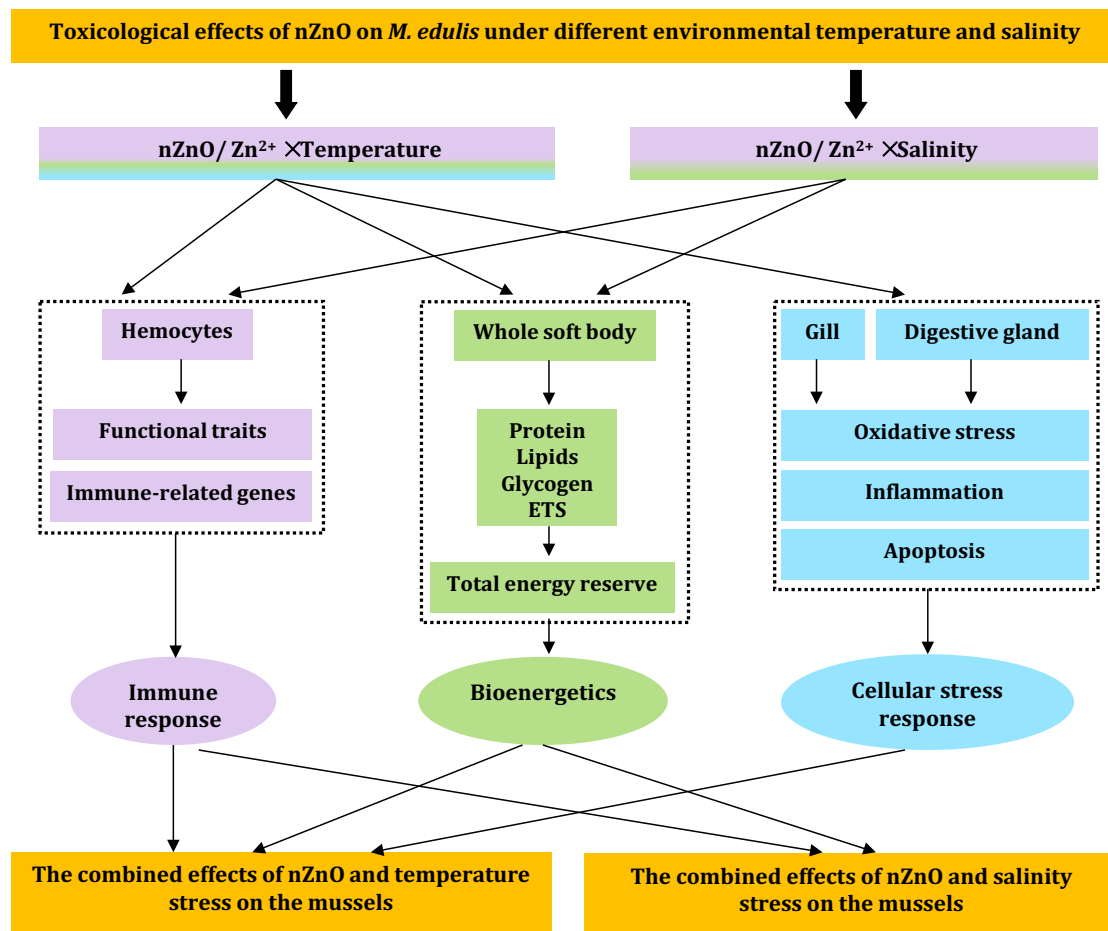


Figure 1. Concept of the experimental design for testing the toxicological effects of nZnO on *M. edulis* under different temperature and salinity regimes. ETS – mitochondrial electron transport system. The levels of the studied factors (temperature, salinity and Zn concentrations) are given in Figs. 2 and 3.

To address these research aims, two experimental series were carried out (Figure 1). In the first experimental series, we determined the combined effects of warming (+5 °C above the season-specific ambient temperature), seasonality (winter and summer) and exposure to different concentrations of nZnO or dissolved Zn on the immune response, bioenergetics and cellular stress response of *M. edulis*. A fully crossed experimental design was implemented using two seasons (winter and summer), two temperatures (ambient and elevated) and five Zn treatments: no Zn addition as a control, nZnO or Zn²⁺ at 10 µg l⁻¹ Zn and 100 µg l⁻¹ Zn (the low and high Zn levels, respectively) (Figure 2). Exposure to Zn²⁺

(added as ZnSO₄) was used to test whether the toxicity of nZnO can be attributed to the potential release of Zn²⁺ from nZnO (Figure 2). In winter, 10°C (ambient) and 15 °C (elevated) exposure temperature were used. In summer, the exposure temperatures were 15°C (ambient) and 20°C (elevated). All exposures were carried out for 21 days to allow acclimation and achieve a new physiological steady-state after an environmental shift in marine mussels [129, 130].

Experiment 1. The mussels under multi-stressors (nZnO/ Zn²⁺ × Temperature)

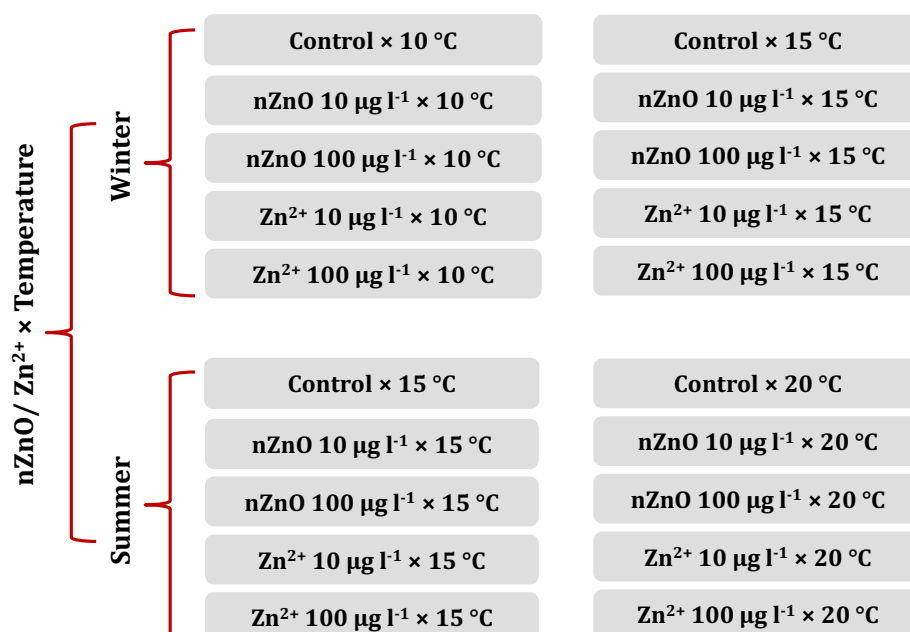


Figure 2. Levels of experimental factors used in the experimental design to test the combined effects of nZnO and temperature on the mussels. The mussels were exposed to two temperatures levels (10 and 15 °C as normal temperature for winter and summer, respectively; and 15 and 20 °C as elevated temperature for winter and summer, respectively) and five Zn treatments: no Zn addition as a control, nZnO or dissolved Zn at 10 µg l⁻¹ Zn and 100 µg l⁻¹ Zn (the low and high Zn levels, respectively).

In the second experimental series we focused on the combined effects of nZnO and salinity variations on immunity and bioenergetics. The mussels *M. edulis* were exposed for 21 days to nine treatments in a fully crossed experimental

design using three salinity regimes (normal salinity 15, fluctuating salinity 5-15, or low salinity 5) and three Zn treatments (no Zn addition as a control, nZnO or Zn^{2+} at $100 \mu\text{g l}^{-1}$ Zn) (Figure 3).

Experiment 2. The mussels under multi-stressors (nZnO/ Zn^{2+} × Salinity)

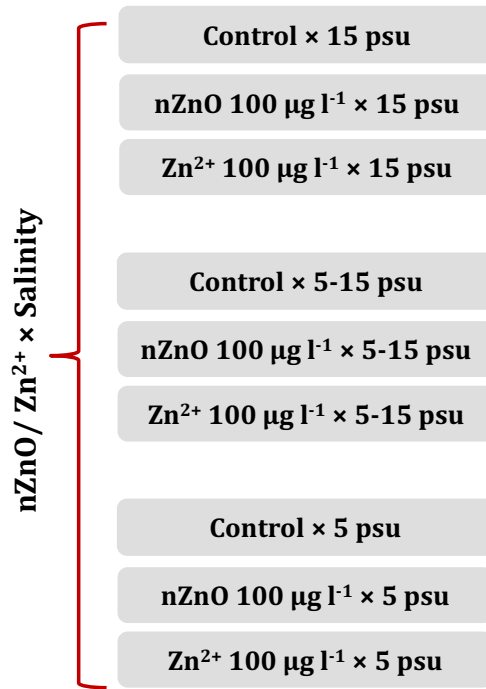


Figure 3. Levels of experimental factors used in the experimental design to test the combined effects of nZnO and salinity on the mussels. The mussels were acclimated to three salinity regimes (normal salinity 15, fluctuating salinity 5-15, or low salinity 5) and three levels of Zn exposure (no Zn addition as a control, nZnO or Zn^{2+} at the nominal concentrations of $100 \mu\text{g l}^{-1}$ Zn).

2. Immune responses of *M. edulis* to combined nZnO, temperature and salinity stress

2.1. Innate immune defense system of the bivalves

Marine bivalves including mussels are routinely exposed to high levels of viruses, bacteria and protozoans in their environments [131]. Lacking an adaptive immunity, the marine mussels rely on the efficiency of the innate immune system to defend against parasites, fungal, viral pathogens and tissue injury [132]. The innate immune defense of bivalves is mediated by coordinated action of cellular (hemocyte-mediated) defenses and humoral immunity involved in immune recognition, signal transduction, and expression of immune effectors [133, 134]. The cellular immune defense mainly includes phagocytosis or encapsulation, with subsequent elimination of the potential invasion target via enzymatic activity such as proteolysis in lysosomes and/or the release of cytotoxic metabolites such as ROS [133, 134]. The humoral immune response involves a series of molecular-mediated responses such as opsoninisation of the pathogen surface that promotes phagocytosis, cytokine production, classical complement activation, neutralization of pathogen-produced toxins and pathogen elimination [133, 134].

In bivalves, the innate immune defense system depends on hemocytes (the circulating cells in the hemolymph) for immune surveillance. Hemocytes are primarily responsible for the shell repair, tissue healing as well as the destruction of the pathogens and foreign bodies through oxidative burst, phagocytosis, and apoptosis and through production of the antimicrobial peptides and opsonizing molecules [135-138]. The common immune defense mechanisms in bivalves include production of oxygen and nitrogen radicals (ROS and NO), synthesis of cytokine-like proteins (e.g. TGF- β) and antimicrobial effectors (e.g. lectins and antimicrobial peptides including myticin, mytilin and defensin), activation of enzymatic cascades (e.g. lysosomal enzymatic reaction), encapsulation as well as

phagocytosis [133, 134]. Phagocytosis is a process of hemocytes to engulf cell debris and various non-self-particles (e.g. bacteria, zymosan, algae, and nanoparticles) to eliminate the potentially dangerous foreign materials and prevent their interactions with other tissues [139, 140]. Phagocytosis includes the adhesion of phagocytes to target particles, modification of the cytoskeleton, internalization, and destruction of the target particles within phagosomes by lysosomes [139, 141], oxidative burst releasing free radicals to kill the pathogen [141, 142] and production of antimicrobial factors [139, 143]. Encapsulation is a cellular immune response to non-self particles that are too big to be phagocytosed (e.g. multicellular parasites) [133, 134]. Encapsulation includes enclosing of the target particles by hemocytes, followed by the release of free radicals and other cytotoxic products by hemocytes for the elimination of the target [133, 144]. The cellular and humoral immune responses are generally carried out and coordinated by hemocytes that serve as a hub of innate immune response of bivalves.

2.1.1. Molecular mechanisms of immune recognition and signaling

Immune recognition is the initial step of the cellular immune response that involves recognizing non-self substances and altered-self particles such as injured host cells, and then initiating and activating the hemocytes-mediated immune response [133, 134]. Immune recognition is the process by which Pattern Recognition Receptors (PRRs), the molecules existing in hemolymph and hemocytes membranes, recognize and bind to pathogen-associated molecular patterns (PAMPs) [133, 134, 145, 146]. In bivalves, seven groups of the PRRs have been identified, including Toll-like receptors (TLRs), Gram-negative binding proteins (GNBPs), thioester-containing proteins (TEPs), scavenger receptors (SRs), C-type lectins, galectins family and peptidoglycan recognition proteins (PGRPs) [133].

Among PRRs, the TLRs that detect the PAMPs and then initiate immune response

play an important role in immune recognition of invertebrates including bivalves [147, 148]. This response was also found to be involved in the recognition of metal-containing nanoparticles in organisms including marine bivalves [149-151]. In addition, complement components including C3q proteins, which belongs to TEPs protein family, were also found to be involved in the regulate the immune recognition cascade to sense and opsonize nonself particles and injured host cells in invertebrates including bivalves [152-155]. Studies in marine bivalves have shown that the complement components including C1 and C3q are upregulated by toxic factors such as nanoparticles or by bacterial pathogens [156-160].

In bivalves, the innate immune system is highly regulated by different signaling pathways activated by PRRs in response to pathogen invasions, injury or environmental stress [133, 161]. Several conserved signaling pathways controlled by PPRs such as TLRs [162] or the complement system [133], have been identified in bivalves including MAPK pathway [163], JAK-STAT pathway [164], and the NF- κ B signaling pathways [165]. These pathways regulate production of various immune effectors that act as main executors for elimination of damaged host cells, pathogens and parasites. These pathways are also sensitive to the environmental stimuli such as salinity variations [166-168], temperature stress [169, 170], metal-containing nanoparticles [42, 151, 171-173] and dissolved metal stress [42, 156, 174]. Several groups of immune effectors has been identified and underlined in bivalves' immune response, including antimicrobial peptides (AMPs) such as myticin, mytilin and defensin, cytokines (e.g. TNF and TGF- β), complement components (e.g. C1 and C3q), lysozymes, lectins, free radicals (e.g. ROS and NO), antioxidant enzymes (e.g. catalase and superoxide dismutase), and acute phase protective proteins (e.g. metallothioneins (MTs) and heat shock proteins (HSPs)). The coordinated up- and downregulation of these factors plays a key role in fine-tuning the immune response to ensure adequate protection from a variety of immune challenges

such as pathogens, non-self materials or modified or injured host cells, and dysregulation of this coordinated multifaceted response by toxicants (such as nZnO) or abiotic stressors might negatively affect the organism's health and disease resistance.

2.2. Bivalves immunity as a target for environmental nanoparticles

Hemocytes of bivalves are among the earliest responders to environmental stressors including metal pollutants and abiotic stressors [89-92]. This makes the immune system sensitive to environmental stressors and a main target for metal-containing nanoparticles including nZnO. Investigation of the functional and molecular traits directly related to the immune function and regulation of the signaling and effector immune pathways is essential to for understanding the mechanisms and implications of potential immunotoxicity of nanoparticles in marine organisms and its modulation by the abiotic environmental factors such as temperature and salinity. In this study we investigated the immune-related functional traits including hemocyte count (THC), hemocyte mortality (HM), adhesion capacity (AD), phagocytosis (Pha) and neutral red uptake (NRU) and determined the transcriptional response of genes related to immune recognition (Toll-like receptors including TLRb and TLRc, and complement components C1 and C3q) and immune effectors (antimicrobial peptides myticin, mytilin and defensin, cytokines TNF and TGF- β , and innate immune signal transduction adaptors MyD88a and MyD88c) under combined exposures to nanopollutants (nZnO) and abiotic (temperature or salinity) stress in the mussels *M. edulis*.

Studies in bivalves including marine mussels found negative impacts of high concentrations (generally in mg l⁻¹ range) of nanoparticles including nZnO on hemocytes viability, abundance [45, 48, 54, 175, 176], phagocytosis and ROS production [54, 175-177]. For instance, increases in the hemocyte mortality and decreases in the hemocytes abundance were found in the marine mussels *M. edulis*, *M. coruscus* and *Perna viridis* exposed to 2.5–10 mg l⁻¹ of nZnO [48, 54] and

2.5–10 mg l⁻¹ of nTiO₂ [175, 176]. Suppression of phagocytosis in the mussels' hemocytes was observed under exposures to high concentrations of nanoparticles, such as 5–50 mg l⁻¹ polystyrene nanoparticles or 2.5–10 mg l⁻¹ nTiO₂ and nZnO [54, 175-177]. Other studies in aquatic invertebrates including bivalves showed induction of the TLRs involved in the immune recognition by NPs [149-151] including nZnO [171, 178]. These findings indicate that depending on the species and exposure scenario, nZnO can have immunosuppressive and immunostimulatory effects in the mussels, and the reasons for these variable responses to nZnO are not well understood. Furthermore, the potential immunotoxic effects of the low, environmentally relevant concentrations of nanopollutants including nZnO have not been extensively studied in marine organisms. Recent studies using low concentration (in ug l⁻¹ range) of nanoparticles showed an increase of hemocytes mortality as well as the increase of phagocytosis and lysosomal abundance in mussels *M. edulis* exposed to 100 ug l⁻¹ nZnO [48], induction of hemocyte proliferation in clams *Ruditapes philippinarum* exposed to 10 ug l⁻¹ nZnO [53] and upregulation of transcriptional immune responses in multiple immune-related genes in hemocytes including mytilin and defensin in the mussels *M. galloprovincialis* exposed to 10-100 µg l⁻¹ nTiO₂ [179], defensin in mussels *M. edulis* exposed to 100 ug l⁻¹ nZnO [48] and C3q in the mussels *M. galloprovincialis* exposed to 100 µg l⁻¹ nCeO₂ [171]. Impaired immune defense caused by NPs and other stressors including warming and salinity stress may have broad ecological and biological consequences affecting the morbidity and mortality of the mussels due to the injuries, parasites and pathogens [180]. Therefore, understanding of the potential interactive immune effect of nanomaterials exposures (such as nZnO at low environmentally relevant concentrations) and elevated temperatures and salinity variations are of great significance for evaluating the ecological risks of nanomaterials under environmentally realistic scenarios found in polluted coastal environments [62, 181].

2.3. Hypotheses and approach to the study of nZnO immunotoxicity

We aimed to investigate the combined effects of environmental relevant concentrations of nZnO and elevated temperatures or salinity variations on the immune responses in the hemocytes of the blue mussels *M. edulis* from the Baltic Sea.

We tested the following hypotheses:

- Exposure to nZnO will negatively affect the expression of immune-related genes and the immune-related functions of mussels' hemocytes.
- Warming or low salinity stress will negatively affect the hemocytes immune responses of *M. edulis*.
- The immunotoxic effects of nZnO might be modified by the elevated temperatures or salinity variations.
- The negative effect of warming on immune responses would be exacerbated by summer due to high temperature.

To test these hypotheses, we conducted two experimental series using the experimental design described in section 1.2. Hemocytes were collected from mussels exposed for 21 days to different experimental treatments (Figures 2 and 3) for determination of functional traits (THC, HM, AD, Pha and NRU) and immune-related genes expression including myticin, mytilin, defensin, C1, C3q, TNF, TGF- β , TLRb, TLRc, MyD88a and MyD88c (Table 1). The details of the results and discussion of this study is provided in the chapters 7.1 and 7.2 describing two publications that resulted from this work [48, 182].

Table 1. A summary of the immune-related parameters used in the present study.

Biomarkers	Description	Functions
HM	The percentage of dead circulating hemocytes	An index of the hemocytes vitality and health
THC	The total number of circulating hemocytes	An index of hemocytes abundance and the immune system health
AD	The ability of hemocytes to adhere to surface	An important index of hemocytes protective function such as ability to encapsulate foreign materials
Pha	A type of endocytosis	An defense function internalizing pathogens and foreign materials and targeting them for destruction in the lysosomes
NRR	Uptake of the neutral red by the hemocytes	A marker for the total lysosomal volume of the cell
Myticin		
Mytilin	Cysteine-rich peptides	Act as broad-spectrum antibiotics against eukaryotic, bacterial and viral pathogens
defensin		
TLRb	Key immune recognition factors	Sense the pathogen-related molecular patterns; involved in the recognition of nanoparticles
TLRc		
C1	A part of the immune complement cascade	Regulate the immune recognition cascade; enhance the ability of antibodies and phagocytic cells; promote inflammation, and attack the pathogen's cell membrane
C3q		
MyD88a	Innate immune signal transduction adaptor	Link the Toll-like receptors signaling, inflammatory cytokines and immune effectors
MyD88c		
TGF- β	Inflammatory cytokines	Regulate the inflammatory response; regulate the host defense against pathogens mediating the innate immune response
TNF		

3. Combined effects of nZnO, temperature and salinity on bioenergetics of the blue mussel *M. edulis*

3.1. Bioenergetics of the bivalves

3.1.1. Stress-induced disturbances of energy homeostasis

Bioenergetics is a series of processes involving energy fluxes in living organisms that include energy transformation and utilization [183, 184]. Energy homeostasis, which is a state of energy balance between energy acquisition and energy expenditure in living organisms, is susceptible to abiotic stress factors (including warming, salinity and pollutants) in marine ectotherms such as bivalves [183, 185, 186]. Exposure to abiotic stress factors may have a negative impact on bioenergetics of organisms by raising the energy requirements for basic maintenance functions (such as damage repair, detoxification and stress protection), and/or by decreasing the energy supply by negatively affecting food intake and metabolic conversion of food energy into ATP [186, 187]. The ability to maintain energy homeostasis is considered a major factor determining the marine ectotherms' tolerance to stressors and the sustainability of their populations under multiple stressor scenarios [183, 185, 187].

The energy dependence of all vital processes and the limitation of energy acquisition in the environment lead to trade-offs in energy allocation to different energy demanding activities in an organism. In the dynamic energy budget model [183, 185, 188], the energy acquired through food ingestion is integrated in a pool from which it is used for various energy-demanding activities including basal maintenance costs, activity, growth, reproduction/development and storage (Figure 4). Among these activities, basal maintenance has a top priority in energy allocation [183]. The basal maintenance cost includes the energy consumption to maintain cellular homeostasis and basic systemic activities (such as excretion, ventilation or circulation) essential for survival. Therefore, if the energy supply drops or is only sufficient to maintain the basal maintenance cost, other energy demanding activities including growth, reproduction/development and storage will be delayed or stopped [183, 185, 188, 189]. Upon exposure to stress the basal maintenance costs of the organism increase and the energy homeostasis between the energy acquisition and energy expenditure as well as the energy allocation to different activities of the organism are affected, thereby directly affecting the performance of organisms [74, 119, 183, 185]. Thus, the study of the bioenergetics

under stress exposures provides a good tool to link the molecular and cellular stress mechanisms with fitness-related performance of organisms, and thus to the population level consequences of multiple stress factors including elevated temperature, salinity variations and nanopollutants.

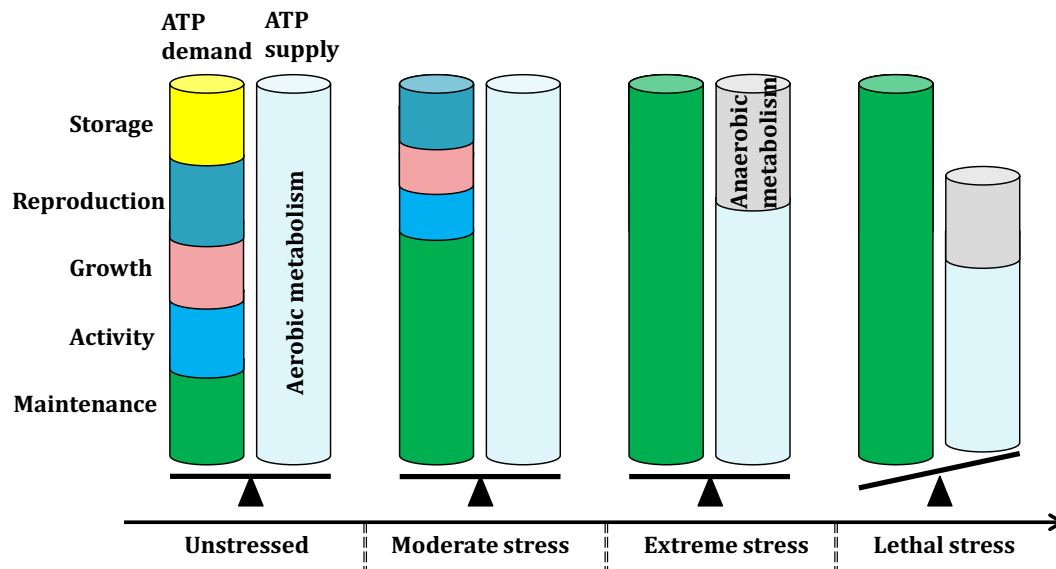


Figure 4. Conceptual diagram of energy limited stress tolerance. The X axis is the level of environmental stress and the Y axis is the aerobic scope for energy demand (left columns of each stress level) and energy supply (right columns of each stress level) (modified after Sokolova, 2013).

3.1.2. The role of energy fluxes in stress tolerance and cellular energy allocation as an index of energy status

According to previous studies on energy-based stress classification [183, 185], the overall breadth of environmental conditions experienced by the organisms can be divided into four ranges of environmental factors corresponding to unstressed conditions, moderate stress, extreme sublethal stress and lethal stress (Figure 4 and 5). Under the unstressed (normal) conditions, the energy balance is positive and ATP supply via aerobic metabolism is sufficiently high to cover the costs of all energy demanding activities of the organism including basal maintenance, mechanical work (such as locomotion or burrowing), growth, reproduction as well as deposit an excess amount of energy in storage [185]. Under these conditions, the basal metabolic costs are minimal, and the amount of energy available for other fitness function is maximal for the given life stage (Figure 4 and 5). Under the moderate stress conditions, the energy allocation to the basal maintenance costs increases to meet energy requirements for damage repair

and anti-stress responses. Sometimes aerobic metabolism is also impaired by the stressor, which together with the higher energy demand for basal maintenance leads to trade-offs with other essential energy demanding activities and a decrease of energy reserves (Figure 4 and 5). Under extreme sublethal stress conditions, available energy is fully invested in basal maintenance costs to allow short-term survival of organisms. The energy allocation to other energy demanding activities (such as growth and reproduction) disappears except for a low level of basic activities (such as foraging) that must be maintained to ensure survival. Under these conditions, anaerobic metabolism might be engaged to compensate for insufficient aerobic ATP supply. Thus, survival of the organism under extreme stress conditions is time-limited and the long-term sustainable survival of the population is impossible due to the lack of energy for growth and reproduction. As the stress intensifies situation (owing to increased deviation of the abiotic factor from the optimum and/or prolonged stress exposure), the energy balance of the organism is disrupted, which eventually leads to death (lethal stress level). The transition from moderate to extreme stress conditions can be marked by the onset of anaerobic metabolism participating in the ATP provision to compensate for the insufficient energy supply of aerobic metabolism [190, 191]. This energy-based stress classification allows comparing the effects of various stress factors on the organisms, focuses on the physiological effects related to fitness and survival, and thus can directly indicate the implications of multiple stress exposures for the survival and reproduction of the population.

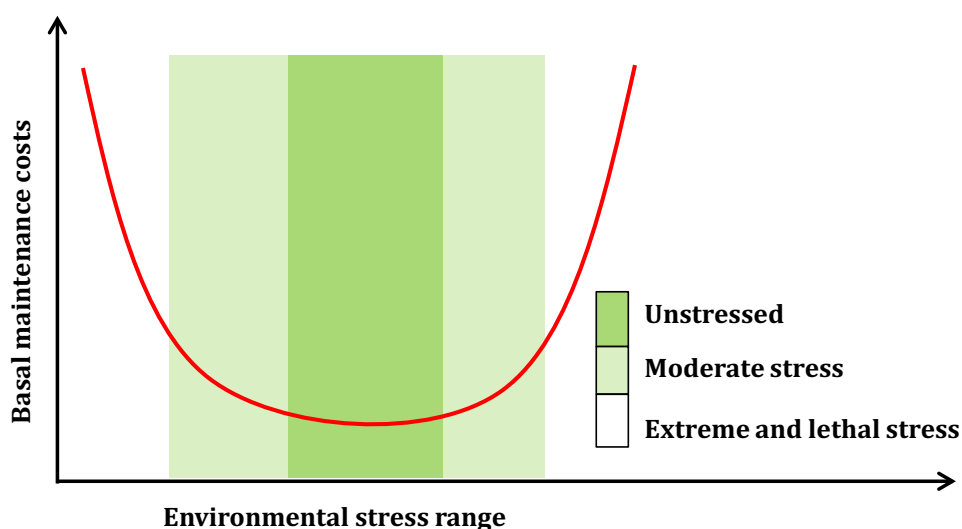


Figure 5. Conceptual diagram of the relationship between the level of environmental stress and the basal maintenance costs of the organism (modified after Sokolova, 2021).

Multiple approaches including production models (such as scope for growth or dynamic energy budget models) and biochemically-based indices (such as the cellular energy allocation) have been used to assess the stress-induced shifts in energy homeostasis [183, 185, 192, 193]. Cellular energy allocation (CEA) is an index of the net energy budget, which can provide quantitative data on the energetic response of organisms to stress [192]. It determines changes in the available total energy reserves (E_a) and potential energy expenditure (E_c) [194]. E_a is calculated by quantifying the total protein, carbohydrate and lipid content. E_c is determined by converting the activity of the mitochondrial electron transport system (ETS) as an index of cellular energy demand for basal maintenance into energy equivalents using oxyenthalpic equivalents for combustion of an average protein, carbohydrate and lipid mixture ($484 \text{ J mmol}^{-1} \text{ O}_2$) [195, 196].

It is worth noting that excess energy that remains after satisfying the energy demanding activities is stored in tissues as energy reserves in the forms of energy storage molecules including proteins, carbohydrates and lipids [185]. These energy-rich compounds play an important role in buffering energy homeostasis *in vivo*, and can be used as energy supply during periods of decreased food availability or increased energy demands, for example during reproduction [197-199]. Furthermore, total energy reserves also play a crucial role in supplying for the increased energy demand caused by environmental stress exposure. Abiotic stress often results in increased energy costs for damage repair and stress protection [185, 187, 200], and thus can lead to depletion of tissue energy reserves in aquatic organisms. The depletion of the total energy storage is an early sign that the organism is in a state of stress (caused by toxicity) before other basic energy demanding activities (such as immunity, respiration or growth) are impaired [201]. The continuing depletion of the energy reserves indicates that the organism transits into the extreme stress range, leading to the decline of performance, fitness and eventually death.

3.2. Effect of nanoparticles on bioenergetics of the bivalves

Bioenergetics of marine bivalves can be negatively affected by environmental pollutants including metals or metal-containing nanoparticles [185]. Exposure to pollutants usually results in elevated energy costs for protein synthesis required for damage repair, anti-stress responses as well as detoxification [185, 187]. In addition, immune stress, oxidative damage, apoptosis and inflammatory reactions caused by nanoparticles [48, 202, 203] can lead to higher energy costs for basal maintenance [204]. The increased

energy demand of marine bivalves exposed to nanoparticle pollutants may exceed the organism's ability to absorb and transform energy affecting their health and survival. Elevated energy demand caused by nanoparticle exposures might exhaust the energy storages of the organisms especially when the feeding activities are weakened [205-209]. As a result, exposure to nanoparticles can negatively affect the energy homeostasis of aquatic bivalves. Earlier studies on Ag and TiO₂ nanoparticles lend support to this notion showing inhibited feeding activities, reduced food absorption efficiency, suppressed digestive functions and narrowed the aerobic range for growth in nanoparticle-exposed aquatic bivalves (such as mussels and clams) [205-209].

Environmental temperature and salinity are important factors affecting energy homeostasis of marine ectotherms [186, 187]. In bivalves, energy metabolism and the availability of energy storage (particularly lipids and carbohydrates) can be affected by environmental temperature [50, 210-212] and salinity [85, 122, 213, 214] due to the impaired cellular metabolism, inhibition of food intake and the increased costs of intracellular osmotic adjustment caused by salinity variations. Thus, a decrease of lipids or carbohydrates was observed in the marine bivalves *M. edulis* [212] and freshwater bivalves *U. tumidus* [50] exposed to warming conditions. A depletion of lipids and carbohydrates was also found in the oysters *Crassostrea virginica* exposed to salinity stress [214]. Furthermore, studies in freshwater bivalves *U. tumidus* found that the bioenergetics status of this species was negatively affected by nZnO exposures (as indicated by the reduction of energy storage in soft tissues) and that the nZnO-induced disturbance of energy metabolism was modulated by environmental temperature [50]. However, to the best of our knowledge, there are no studies on the bioenergetics results of salinity-nZnO interactions or temperature-nZnO interactions in marine bivalves.

3.3. Hypotheses and approaches to study the combined effects of nanopollutants and abiotic stressors on bioenergetics

The aim of this part of my research project was to assess the bioenergetics responses to nZnO pollution under different temperature and salinity regimes in the blue mussels *M. edulis*.

We tested the following hypotheses:

- nZnO exposures will lead to disturbance of energy homeostasis of the mussels reflected in a decrease of energy reserves and/or suppressed ETS activity.

- The bioenergetics stress of nZnO might be aggravated by elevated temperature or salinity stress.
- The negative effect of warming on bioenergetics in summer would be more serious than the warming effect in winter.
- The negative effect of nZnO on bioenergetics might be stronger than the effect to dissolved Zn.

Table 2. A summary of the parameters and their functions related to bioenergetics responses and bioaccumulation of nZnO in the present study.

Biomarkers	Description	Functions
Zn content	Zn accumulation	An index of acclimated Zn concentration in the soft body of mussels
MTs	markers for intracellular Zn in the mussels	Play an important role in the binding of free intracellular metals including Zn ²⁺ and in protection against oxidative stress as ROS scavengers
Proteins	Proteins content	Major contributors to the energy storage in bivalves and used as a last-resort fuel during extreme energy demand
Carbohydrates	Carbohydrates content	Mostly represents glycogen, the major rapidly mobilized energy buffer in marine mollusks
Lipids	Lipids content	Major contributors to the energy storage in marine mollusks
ETS	The energy consumption at a mitochondrial level	Reflects the amount and functional activity of the mitochondria and can serve as an index of both the tissue energy demand and ATP synthesis capacity
Ea	The total amount of available energy	Energy reserves provide better insight into the adaptability of organisms towards toxic substances before these substances start to hamper other biological activities such as growth, respiration, and reproduction
CEA	An integrative index of the energy status	An integrated index reflecting balance between cellular energy demand and supply that can be used to quantify an organism's energetic response to stress

To test these hypotheses, we used the same experimental design as for the study of immunotoxicity (see section 1.2). Mussels were exposed for 21 days to different combinations of nZnO (or dissolved Zn), temperature and salinity conditions (Figures 2 and 3). The tissue levels of proteins, lipids and carbohydrates, total energy reserves (Ea), electron transport system (ETS) activity, and cellular energy allocation (CEA) were determined in the whole soft tissue of the mussels *M. edulis* (Table 2). Zn accumulation and tissue levels of metallothioneins (MTs) (Table 2) were measured to assess the bioavailability and accumulation of Zn in different exposures. The details of the results of these studies are provided in the chapters 7.3 [181] and 7.4 [215] of this dissertation.

4. Interactive effects of nZnO and temperature on cellular stress responses of the mussels *M. edulis*

4.1. Molecular and cellular stress responses of the bivalves

The cellular stress response encompasses molecular changes that occur in the cells responding to an adverse physiological or environmental stimulus, such as warming, low pH, low oxygen level, exposure to toxins, mechanical damage or viral infections [216, 217]. Upon exposure to stress, the physiological homeostasis of tissue is in danger and the cellular stress responses are activated to ensure protection and mitigate damage [216]. The processes involved in the cellular stress response range from activating pathways that promote survival to the pathways triggering programmed cell death that eliminate damaged cells [216-218]. The initial cellular response to environmental or intracellular stress stimulus evolved to help cells resist stressors and recover from damage by activating a certain protective cellular mechanism such as antioxidant defense or molecular chaperones. If the stressful stimulus is too strong to maintain the protective response, the death signaling pathways are activated to ensure removal of the irreparably damaged cells and prevent uncontrolled spilling of cellular content that can otherwise lead to inflammation and damage surrounding cells [216, 217].

To better understand the toxic mechanisms of nanoparticles under the conditions of natural environmental variability, it is especially important to investigate the potential hazards of nanoparticles based on the cellular stress response pathways. These pathways can be tested more reliably, easily and often in a non-invasive manner compared with the traditional toxicological approaches [219, 220]. Studies on the toxic

mechanisms of nanoparticles in mammals and various aquatic organisms have found that the key cellular stress responses to nanoparticles toxicity involve stimulation of oxidative stress, activation of apoptosis pathways, and promotion of inflammatory responses that might cause the injury of target tissues and culminate in disease, morbidity or mortality [48, 53, 74, 219-223]. Therefore, we focused on the cellular stress responses involved in oxidative stress, inflammation and apoptosis to assess the environmentally-dependent mechanisms of nZnO cytotoxicity in the mussels *M. edulis*.

4.2. The oxidative stress response

Oxidative stress is an imbalance between antioxidants and ROS in the cells. Cells produce ROS (such as superoxide, hydrogen peroxide or singlet oxygen) during normal intracellular metabolic processes by mitochondria and glycolysis [224, 225]. The ROS play important signaling role in the cell but in excess can be damaging to the proteins, lipids and DNA and are thus tightly controlled by the cellular antioxidant system including non-enzymatic antioxidants (vitamin C or β -carotene) and enzymes such as catalase and superoxide dismutases (SODs) that neutralize ROS [216]. Normally, cells are able to maintain a balance of pro-oxidant free radicals and antioxidants. There are several factors that can trigger oxidative stress, among them toxins including metals, nanomaterials, environmental stressors, as well as pathological conditions and metabolic misbalance [216, 226]. When the natural antioxidant defense capacity of the cells is overwhelmed, sustained oxidative stress may lead to DNA, protein and lipid damage, and in extreme cases can induce cell death [226-228].

Oxidative stress is considered the main toxicity mechanism of nZnO and a key hallmark of nZnO-induced damage [39, 229, 230]. The contents of protein carbonyl (PC) and lipid peroxides (LPO) are reliable indicators of the protein and lipid oxidation induced by ROS [231, 232] and can provide evidence for the potential extent of oxidative damage caused by nZnO [53]. The increased LPO and PC content was observed in various aquatic organisms including mussels exposed to nZnO [59, 233-236], indicating that the LPO and PC content are sensitive indicators of oxidative stress induced by nanoparticles. Therefore, the oxidative stress response to nZnO in the present study was determined by measuring the PC and LPO content in the blue mussels.

4.3. Apoptosis regulation

Apoptosis, a form of programmed cell death [237], is a highly controlled and regulated

biological process activated by intrinsic (e.g. oxidative stress) or extrinsic (e.g. death receptor) pathways in bivalves [137]. Unlike necrosis, which is a form of pathological cell death that induces inflammation [238, 239], apoptosis permits degradation of the damaged or superfluous cells without impairing neighboring tissues since apoptotic bodies can be phagocytized without eliciting an inflammatory response [240, 241]. Among all forms of cell death (apoptosis, autophagy, necrosis and other forms), apoptosis exhibits the most obviously distinguishing morphological characteristics and molecular pathways evolutionarily conserved among distantly related organisms [242, 243], and plays an indispensable role in development, senescence, and disease [242]. However, defective apoptosis, including apoptosis inhibition and hyperactive apoptosis, can lead to inflammatory and immune response, cause tissue damage, and contribute to diseases such as cancer [244].

Apoptotic signal can be triggered by numerous cellular stress stimuli through intrinsic apoptotic pathways, including oxidative stress and immune response, as well as abiotic external stressors such as warming, hypoxia, and exposure to metal-containing pollutants [137, 245, 246]. Earlier research on different organisms including bivalves have shown pro-apoptotic effects of nanoparticles including nZnO as indicated by upregulated the expression of apoptosis-related genes p53 and caspase 3 [42, 43, 247-249] and decreased the expression of an anti-apoptotic gene Bcl-2 [248, 249]. Therefore, here we focused on expression of apoptosis-related genes including caspase 3 (the main executor caspase in the apoptotic cascade [137, 250]), the pro-apoptotic protein p53 (the Guardian-of-Genome protein that induces apoptosis if DNA damage reaches levels beyond the capability of the cellular repair systems [251]), anti-apoptotic regulator protein Bcl-2, and various stress-inducible molecules including MAPK-related proteins p38 and JNK (that play a key role in transducing signals in response to environmental or cellular stresses and/or inflammatory stimulation in animals [252-254]). Earlier studies on various animals and our present results showed that nZnO exposure stimulated the mRNA expression of the apoptotic proteins caspase 3 [42, 247] and the pro-apoptotic protein p53 [43, 247], inhibit the expression of anti-apoptotic genes Bcl-2 [248, 249], and activated JNK and p38 MAPK pathway [230, 255-257]. These results support the notion that the induction of apoptosis might be a common response to nZnO exposures and highlight the importance of apoptosis as a toxic mechanism of nZnO.

4.4. Inflammatory responses

Inflammation is the immune system's response to a variety of injurious stimuli, including damaged cells, pathogens and environmental factors such as irradiation, warming and toxic materials [258]. Inflammation is considered a vital defense mechanism involving inflammatory cells, molecular effectors and inflammatory signaling pathways, most commonly MAPK, NF- κ B, and JAK-STAT pathways [259, 260]. Generally, during the acute inflammatory response induced by harmful stimuli, a series of cellular and molecular events and their interactions can effectively reduce cell or tissue damage [261]. This process helps restore tissue homeostasis, initiate healing and resolve acute inflammation [260]. However, uncontrolled acute inflammation may become chronic, potentially leading to disease or tissue damage [262].

Inflammation is a common response to nanopollutants including nZnO in animals including mice [263], human cells [264] and bivalves [42, 264-266]. Involvement of the inflammatory response was indicated by the upregulated transcriptional levels of inflammatory cytokines including TGF- β and NF- κ B in the digestive gland of the mussels exposed to 100 $\mu\text{g l}^{-1}$ nZnO [42]. These data indicated that inflammatory response might be induced by nanoparticles in marine bivalves and warranted inclusion of inflammatory markers (the transcription levels of the marker genes of inflammatory cytokine pathway involving tumor necrosis factor (TNF- α), transforming growth factor-beta (TGF- β), the nuclear factor κ B (NF- κ B) and an inflammation-regulating enzyme COX [267, 268]) for cellular stress assessment of the mussels in our present study. Furthermore, because the robustness and flexibility of the cellular stress response mechanisms are not well understood under the conditions of natural environment changes [26, 47], we explored the potential modulating effects of temperature on the oxidative stress, apoptosis and inflammation responses to nZnO in the mussels *M. edulis*.

4.5. Hypotheses and approaches to study the cellular stress response

The aim of this part was to determine the involvement of cellular stress responses related to oxidative stress, apoptosis and inflammation in nZnO toxicity under different temperature regimes in the gill and the digestive gland of the mussels *M. edulis*.

We tested the following hypotheses:

- Exposure to nZnO will lead to oxidative stress and induce apoptosis and inflammation in the gill and digestive gland.
- The toxic effects of nZnO will be reduced by mild warming in winter but aggravated by more extreme thermal stress in summer.
- The effect of nZnO on cellular stress responses in the mussels' digestive gland might be stronger than that the effects on the gill, because of the digestive glands are the main organ for the nanoparticle accumulation in mollusks [87, 88].

Table 3. A summary of the parameters and their functions related to molecular and cellular stress responses in the present study.

Biomarkers	Related-cellular stress response	Functions
LPO	Oxidative stress	Oxidative damage to lipids
PC		Oxidative damage to proteins
p53	Apoptosis	The main pro-apoptotic protein, the Guardian-of-Genome protein
Caspase 3		The main executor caspase in the apoptotic cascade
Bcl-2		Anti-apoptotic regulator protein, apoptosis inhibitor
p38	Apoptosis and inflammation	Stress-inducible molecule, transducing signals in response to stresses and/or inflammatory stimulation
JNK		Stress-inducible molecule, transducing signals in response to stresses and/or inflammatory stimulation
TGF- β	Inflammation	Regulation of inflammatory processes
NF- κ B		Regulation of inflammation processes
COX		Inflammation-regulating enzyme

To test these hypotheses, we conducted 21-day exposures to different concentrations of nZnO and dissolved Zn under different thermal regimes (shown in [Figure 2](#)) and collected the gill and digestive gland tissues for determination of the oxidative stress,

apoptosis and inflammation-related traits. The oxidative stress indicators (PC and LPO) and transcription pattern of marker genes in the pathways related to cell survival and proliferation (caspase 3, Bcl-2, p53, p38 and JNK) and inflammation (COX, NF- κ B, and TGF- β) were determined (Table 3). The details of the results of these experiments are provided in the Chapter 7.5 [269] of this dissertation.

5. Summary and discussion

Overall, our study indicates that nZnO exposures strongly affect the immune response in hemocytes, lead to disturbances in energy homeostasis in the whole soft tissue, and induce cellular stress response including oxidative stress, apoptosis and inflammation in the gill or digestive gland in the mussels *M. edulis*. These adverse outcome pathways induced by nZnO in the mussels *M. edulis* are generally modulated by other abiotic stressors including the elevated temperature, the season and salinity variations (Figure 6).

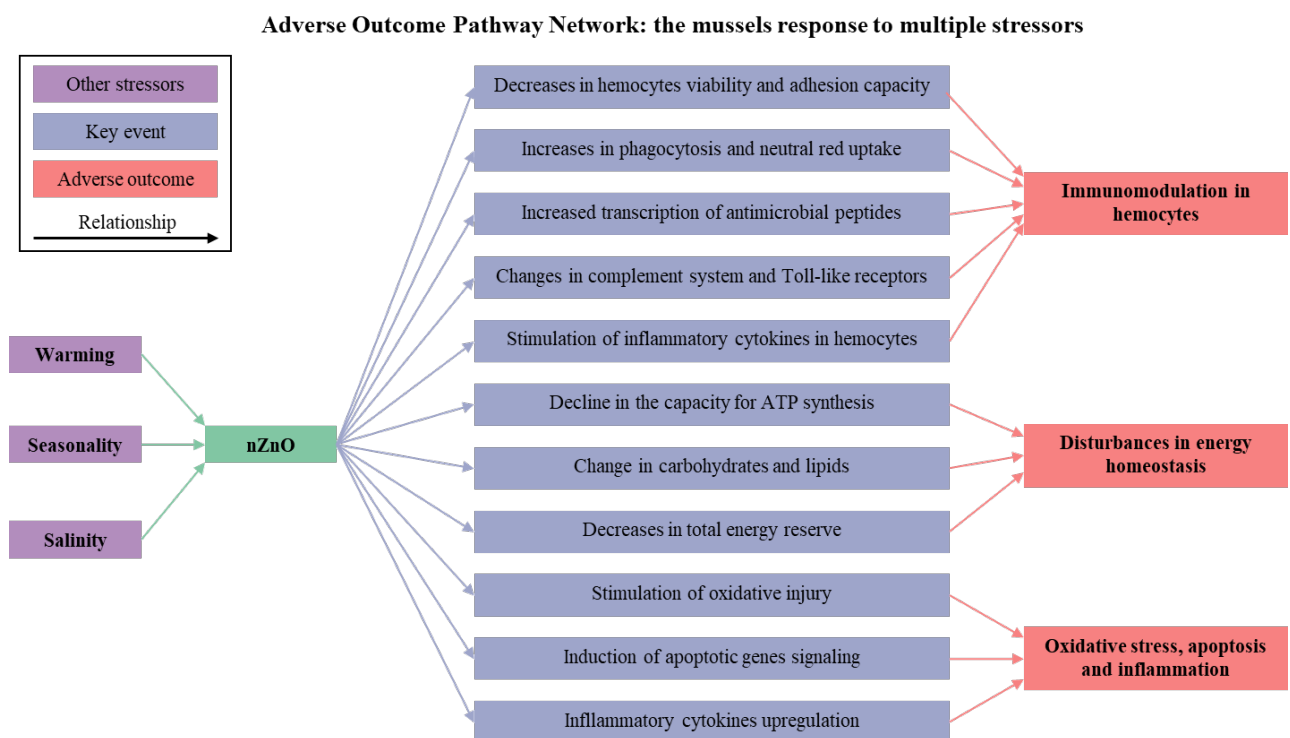


Figure 6. The combined effects of nZnO and other abiotic stressors on the marine mussels *M. edulis*. The green arrows point to the environmental stressors that influence the toxic effect of nZnO. The blue arrows point to the key events in nZnO exposures in *M. edulis*. The red arrows indicate the adverse outcomes in nZnO exposures in *M. edulis*.

5.1. Immunotoxic mechanisms of nZnO in the context of environmental variability

5.1.1. Temperature-Zn interactions

Our study showed that nZnO exposures strongly affect the expression of immune-related genes and the immune-related functions of mussels' hemocytes, and that the immunomodulatory effects of nZnO are modulated by the elevated temperatures and the season. Generally, high concentration ($100 \mu\text{g l}^{-1}$) of nZnO exposure lead to upregulation in phagocytosis indicating that nZnO particles might be recognized as non-self by the hemocytes of *M. edulis*. Furthermore, high concentration of nZnO induced inflammatory-related transcriptomic response of the hemocytes of the winter mussels indicating a coordinated immune and inflammatory response to nZnO. The immune responses of hemocytes to nZnO were qualitatively similar but stronger than the responses to the equivalent concentrations of dissolved Zn indicating that Zn^{2+} release from nZnO is not likely to fully explain the immunomodulatory effects of nZnO.

Notably, $+5 \text{ }^\circ\text{C}$ warming in summer (but not in winter) resulted in dysregulation of the expression of multiple immune-related genes including TLRs, complement system proteins as well as AMPs in the hemocytes of the mussels. This indicates that additional warming in summer might increase susceptibility of mussels to sensitivity to the pathogens (particular abundant in seawater in the summer months) and have detrimental effects on the immunity and disease resistance of the mussels. Therefore, our findings indicate that the combined exposures to elevated temperatures and nZnO might have different effects on the immune responses of bivalves depending on the seasonality and might have implication for the abilities of bivalves from nanomaterials-polluted areas to cope with the pathogen-induced summer mortality events [182].

5.1.2. Salinity-Zn interactions

nZnO and salinity variations had strong impacts on the functional and transcriptional immune responses of the mussels *M. edulis*. Similar to the findings of temperature-nZnO interactions, our study indicates that immunotoxic effects of nZnO are considerably stronger than those of equivalent concentrations of dissolved Zn, and are modulated by the environmental salinity regimes. nZnO exposures stimulated phagocytosis and lysosomal volume regardless of the exposure salinity indicating that phagocytosis might be an important uptake mechanism and a marker for nZnO in the hemocytes of the

mussels. Under the normal salinity (15) conditions, nZnO suppressed the expression of the TLRs and the complement system proteins as well as decreased the hemocyte viability and adhesion indicating that the impaired ability to recognize pathogens and initiate immune defense cascades. Exposure to the fluctuating salinity (5-15) reversed the transcriptomic responses of *M. edulis* hemocytes to nZnO [48].

Notably, low salinity (5) had strong immunosuppressive effect in *M. edulis* that largely obscured the effects of nZnO. The low-salinity regime (5) chosen for this study is close to the lower salinity tolerance limit for the blue mussels *M. edulis* [213, 270]. Our study suggest that the compromised immune defenses of the mussels *M. edulis* may contribute to the inability of the blue mussels populations to survive in the seawaters below the so called horohalinic zone (salinity 5-8) [271]. This immunocompromised status might also facilitate contribute pathogens invasion in these areas, especially since many pathogens thrive in the brackish waters [124, 272, 273].

5.2. Metabolic disturbance as a mechanism of nZnO toxicity in different environmental contexts

5.2.1. Temperature-Zn interactions

Our study showed that high concentrations (100 $\mu\text{g l}^{-1}$) of nZnO have negative impacts on bioenergetics of the marine mussels *M. edulis*. However, these negative impacts were not particularly strong and the response of parameters was not uniform, depending on season and temperature, as reflected in depletion of carbohydrates and energy reserves in winter mussels, and decrease in lipids, energy reserves and ETS activity in summer mussels. In winter mussels, warming (15 °C) led to an increase in protein content, lipid content, and total energy reserves. In contrast, in summer mussels, warming (20 °C) led to a reduction in the carbohydrates, lipids and total energy reserves as well as suppressed ETS activity. Furthermore, our study showed that elevated temperature combined with nZnO exposure might negatively affect the bioenergetics and energy reserve of the mussels in summer (but not in winter) in the lab condition. Summer is a crucial period for the Baltic Sea mussels *M. edulis* populations when reproduction and larval settlement occurs [69, 85], so that disturbance of energy homeostasis caused by warming and nZnO pollution might have implication for the population recruitment during this sensitive period. Interestingly, experimental 5°C warming had different effects in summer and in winter, leading to enhanced nZnO toxicity in summer and

alleviating it in winter. Our findings demonstrate that moderate warming in winter (but not in summer) might partially compensate for the impaired bioenergetics induced by nZnO exposures in the mussels from temperate areas (such as the Baltic Sea). Given the significant effects of ambient temperature and season on the toxicity of nZnO, it is important to consider the interactive effects of multiple abiotic stress (such as pH, temperature, and salinity) on the energetics of sentinel marine bivalve for the assessment of the toxicity impacts of nZnO. Furthermore, it would be interesting to determine whether the bioenergetic impairment at elevated temperatures (20 °C and above) might contribute to setting limits of the thermal tolerance of the Baltic Sea *M. edulis* populations [181].

5.2.2. Salinity-Zn interactions

In our present study, salinity variations strongly affected metabolic homeostasis of the mussels and affected biochemical and physiological responses to nZnO and Zn²⁺. Generally, exposure to fluctuating salinity (5-15) appeared bioenergetically less stressful than constant hypoosmotic stress (low salinity 5) in the mussels. This indicates that even short-term (24 hours) recovery might be enough to restore the energy homeostasis in the mussels *M. edulis*. Furthermore, exposure to nZnO (100 µg l⁻¹) generally did not result in strong disturbances in energy homeostasis regardless of the salinity variations in the mussels. This is similar to the findings of our present study on temperature-nZnO interactions showing relatively mild disturbance of energy homeostasis induced by the environmental relevant concentration of nZnO (100 µg l⁻¹). It is worth noting that our experiments on temperature-nZnO interactions were conducted in October at 10 °C and in June at 15 °C for the winter and summer mussels, respectively, whereas the experiments on salinity-nZnO interactions were conducted in February at 10 °C. Taken together, these findings indicate that in the absence of additional temperature stress, nZnO does not cause severe energy deficiency in the mussels regardless of the season. Exposure to equivalent concentrations of dissolved Zn (100 µg l⁻¹) suppressed the mitochondrial ATP synthesis capacity and coupling as well as anaerobic metabolism, and modified the free amino acids (FAAs) profiles in *M. edulis*. These findings indicate that nZnO is metabolically less damaging to the mussels *M. edulis* than Zn²⁺. Notably, the effects of nZnO and Zn²⁺ on metabolic responses in the mussels became increasingly difficult to detect with increasing salinity stress. These findings suggest that environmental salinity variations must be considered in the energy metabolism-related

biomarker-based assessment of the effects of pollutants including nanomaterials on coastal species such as the Baltic Sea mussels [215].

5.3. Cellular stress response in temperature-dependent nZnO toxicity mechanisms

In our present study, nZnO exposure induced oxidative injury to proteins and lipids and led to an increase in the transcript levels of apoptotic genes p53, caspase 3, p38 and JNK indicating that oxidative stress and pro-apoptotic responses as a toxic mechanism of in *M. edulis*. Furthermore, similar to the earlier findings in *M. edulis* exposed to 100 $\mu\text{g l}^{-1}$ nZnO that showed an increase of the transcript levels of inflammatory cytokines TGF- β and NF- κB in the digestive gland [42] and TGF- β and TNF in the hemocytes [182], our present study found a modest (but not statistically significant) increase in TGF- β and NF- κB mRNA expression in the mussels exposed to 100 $\mu\text{g l}^{-1}$ nZnO. These findings show that the inflammation can be induced by nZnO in marine bivalves *M. edulis* but does not appear a key consistent response to nZnO exposures in the studied range of nZnO concentrations (0-100 $\mu\text{g l}^{-1}$). Furthermore, the multi-biomarker analysis show that the toxic effect of nZnO is stronger than the effect to dissolved Zn in the mussels indicating differences of the toxic mechanisms of nZnO and dissolved Zn. The effects of nZnO on cellular stress responses in the mussels' digestive gland are stronger than that the effect on the gill, which supports the view that digestive glands are the main organ for toxicity of nanomaterials in mollusks [87, 88]. Therefore, digestive glands can serve as a tissue of choice for biomarker-based monitoring of the toxic effects of nanopollutants in mussels. Our present study shows that in the mussels *M. edulis*, the oxidative injury and apoptotic- and inflammatory-related transcriptional responses to nZnO are strongly affected by warming and the season, so that no single biomarker could be shown to consistently respond to nZnO in all experimental treatments. These findings imply that multiple biomarkers covering key biomarkers of the putative adverse outcome pathways (especially oxidative stress and apoptosis) are needed to assess nanoparticles toxicity to marine bivalves under the variable environmental conditions of coastal habitats such as the Baltic Sea [269].

Overall, our study suggests that the biomarkers for the assessment of immunotoxicity, bioenergetics and cellular stress response of nanoparticles including nZnO must be calibrated in the environmentally-relevant contexts, because the biomarker baselines may vary with salinity and temperature (our present study) and other environmental

factors [50, 76, 78, 274, 275]. These findings have important implications for environmental risk assessment of nanomaterials, for the establishing of the environmental context-specific biomarker baselines for the coastal nanopollution monitoring and for understanding of the interactive effects of multiple stressors on keystone marine bivalves [48].

6. References

- [1] Cloern JE, Abreu PC, Carstensen J, Chauvaud L, Elmgren R, Grall J, et al. Human activities and climate variability drive fast-paced change across the world's estuarine–coastal ecosystems. *Global Change Biology*. 2016 22:513-29.
- [2] Borgwardt F, Robinson L, Trauner D, Teixeira H, Nogueira AJA, Lillebø AI, et al. Exploring variability in environmental impact risk from human activities across aquatic ecosystems. *Science of the Total Environment*. 2019 652:1396-408.
- [3] Garner KL, Keller AA. Emerging patterns for engineered nanomaterials in the environment: a review of fate and toxicity studies. *Journal of Nanoparticle Research*. 2014 16:28.
- [4] Williams RJ, Harrison S, Keller V, Kuenen J, Lofts S, Praetorius A, et al. Models for assessing engineered nanomaterial fate and behaviour in the aquatic environment. *Current Opinion in Environmental Sustainability*. 2019 36:105-15.
- [5] Linders T, Infantes E, Joyce A, Karlsson T, Ploug H, Hassellöv M, et al. Particle sources and transport in stratified Nordic coastal seas in the Anthropocene. *Elem Sci Anth*. 2018 6:29.
- [6] Reusch TBH, Dierking J, Andersson HC, Bonsdorff E, Carstensen J, Casini M, et al. The Baltic Sea as a time machine for the future coastal ocean. *Science Advances*. 2018 4:eaar8195.
- [7] Stigebrandt A. Physical Oceanography of the Baltic Sea. In: Wulff FV, Rahm LA, Larsson P, editors. *A Systems Analysis of the Baltic Sea*. Berlin, Heidelberg: Springer Berlin Heidelberg; 2001, p. 19-74.
- [8] Jansson BO. The Baltic — A Systems Analysis of a Semi-enclosed Sea. In: Charnock H, Deacon G, editors. *Advances in Oceanography*. Boston, MA: Springer US; 1978, p. 131-83.
- [9] Hell B, Öiås H. A new bathymetry model for the baltic sea. *International Hydrographic Review*. 2014 November:21-32.
- [10] Jurasinski G, Janssen M, Voss M, Böttcher ME, Brede M, Burchard H, et al. Understanding the Coastal Ecocline: Assessing Sea–Land Interactions at Non-tidal, Low-Lying Coasts Through Interdisciplinary Research. *Frontiers in Marine Science*. 2018 5.
- [11] Snoeijs-Leijonmalm P, Schubert H, Radziejewska T. *Biological Oceanography of the Baltic Sea*. Springer, Dordrecht (Eds). 2017.
- [12] HELCOM. Hydrography and oxygen in the deep sea basins. 2016.
- [13] Andersson A, Meier HEM, Ripszam M, Rowe O, Wikner J, Haglund P, et al. Projected future climate change and Baltic Sea ecosystem management. *AMBIO*. 2015 44:345-56.
- [14] Tovar-Sánchez A, Sánchez-Quiles D, Basterretxea G, Benedé JL, Chisvert A, Salvador A, et al. Sunscreen Products as Emerging Pollutants to Coastal Waters. *PLoS ONE*. 2013 8:e65451.
- [15] Moreno A, Amelung B. Climate change and tourist comfort on Europe's beaches in summer: A reassessment. *Coastal management*. 2009 37:550-68.
- [16] Garnaga G. Integrated assessment of pollution in the Baltic Sea. *Ekologija*. 2012 58.
- [17] Bondarenko O, Juganson K, Ivask A, Kasemets K, Mortimer M, Kahru A. Toxicity of Ag, CuO and ZnO nanoparticles to selected environmentally relevant test organisms and mammalian cells in vitro: a critical review. *Archives of Toxicology*. 2013 87:1181-200.
- [18] Sathe P, Laxman K, Myint MTZ, Dobretsov S, Richter J, Dutta J. Bioinspired nanocoatings for biofouling prevention by photocatalytic redox reactions. *Scientific reports*. 2017 7:12.
- [19] Read DS, Matzke M, Gweon HS, Newbold LK, Heggelund L, Ortiz MD, et al. Soil pH effects on the interactions between dissolved zinc, non-nano- and nano-ZnO with soil bacterial communities. *Environmental Science and Pollution Research*. 2016 23:4120-8.
- [20] Piccinno F, Gottschalk F, Seeger S, Nowack B. Industrial production quantities and uses of ten engineered nanomaterials in Europe and the world; 2011.
- [21] Stoller M, Ochando-Pulido J. ZnO Nano-Particles Production Intensification by Means of a Spinning Disk Reactor. *Nanomaterials*. 2020 10:1321.
- [22] Narayanan PM, Wilson WS, Abraham AT, Sevanan M. Synthesis, characterization, and antimicrobial activity of zinc oxide nanoparticles against human pathogens. *BioNanoScience*. 2012 2:329-35.
- [23] Beegam A, Prasad P, Jose J, Oliveira M, Costa FG, Soares AMVM, et al. Environmental Fate of Zinc Oxide Nanoparticles: Risks and Benefits. In: Soloneski S, Larramendy M, editors. *Toxicology - New Aspects to This Scientific Conundrum*: InTech; 2016.
- [24] Martínez-Carmona M, Gun'ko Y, Vallet-Regí M. ZnO Nanostructures for Drug Delivery and Theranostic Applications. *Nanomaterials (Basel, Switzerland)*. 2018 8:268.
- [25] Gottschalk F, Lassen C, Kjoelholt J, Christensen F, Nowack B. Modeling Flows and Concentrations of Nine Engineered Nanomaterials in the Danish Environment. *International journal of environmental research*

- and public health. 2015 12:5581-602.
- [26] Yung MMN, Mouneyrac C, Leung KMY. Ecotoxicity of Zinc Oxide Nanoparticles in the Marine Environment. In: Bhushan B, editor. Encyclopedia of Nanotechnology. Dordrecht: Springer Netherlands; 2014, p. 1-17.
- [27] Hong H, Adam V, Nowack B. Form-Specific and Probabilistic Environmental Risk Assessment of Three Engineered Nanomaterials (nano-Ag, nano-TiO₂ and nano-ZnO) in European Freshwaters. Environmental Toxicology and Chemistry. 2021 n/a.
- [28] Dumont E, Johnson AC, Keller VDJ, Williams RJ. Nano silver and nano zinc-oxide in surface waters – Exposure estimation for Europe at high spatial and temporal resolution. Environmental Pollution. 2015 196:341-9.
- [29] Gottschalk F, Sun T, Nowack B. Environmental concentrations of engineered nanomaterials: Review of modeling and analytical studies. Environmental Pollution. 2013 181:287-300.
- [30] Coll C, Notter D, Gottschalk F, Sun TY, Som C, Nowack B. Probabilistic environmental risk assessment of five nanomaterials (nano-TiO₂, nano-Ag, nano-ZnO, CNT, and fullerenes). Nanotoxicology. 2016 10:436-44.
- [31] EPA U. National Recommended Water Quality Criteria EPA-822-R-02-047. Office of Science and Technology. 2002.
- [32] Siddiqi KS, ur Rahman A, Tajuddin, Husen A. Properties of Zinc Oxide Nanoparticles and Their Activity Against Microbes. Nanoscale research letters. 2018 13:141.
- [33] Munn S, Aschberger K, Olsson H, Pakalin S, Pellegrini G, Vegro S, et al. European Union Risk Assessment Report - Zinc Metal. Publications Office of the European Union. 2010 JRC61245:1-697.
- [34] Falfushynska H, Gnatyshyna L, Horyn O, Sokolova I, Stoliar O. Endocrine and cellular stress effects of zinc oxide nanoparticles and nifedipine in marsh frogs *Pelophylax ridibundus*. Aquatic Toxicology. 2017 185:171-82.
- [35] Falfushynska H, Gnatyshyna L, Yurchak I, Sokolova I, Stoliar O. The effects of zinc nanooxide on cellular stress responses of the freshwater mussels *Unio tumidus* are modulated by elevated temperature and organic pollutants. Aquatic Toxicology. 2015 162:82-93.
- [36] Shaw BJ, Handy RD. Physiological effects of nanoparticles on fish: a comparison of nanometals versus metal ions. Environ Int. 2011 37:1083-97.
- [37] Gagné F, Auclair J, Turcotte P, Gagnon C, Peyrot C, Wilkinson K. The influence of surface waters on the bioavailability and toxicity of zinc oxide nanoparticles in freshwater mussels. Comparative Biochemistry and Physiology Part C: Toxicology & Pharmacology. 2019 219:1-11.
- [38] Gagné F, Auclair J, Peyrot C, Wilkinson KJ. The influence of zinc chloride and zinc oxide nanoparticles on air-time survival in freshwater mussels. Comparative Biochemistry and Physiology Part C: Toxicology & Pharmacology. 2015 172-173:36-44.
- [39] Xia T, Kovochich M, Liong M, Mädler L, Gilbert B, Shi H, et al. Comparison of the mechanism of toxicity of zinc oxide and cerium oxide nanoparticles based on dissolution and oxidative stress properties. ACS Nano. 2008 2:2121-34.
- [40] Xiao Y, Vijver MG, Chen G, Peijnenburg WJGM. Toxicity and Accumulation of Cu and ZnO Nanoparticles in *Daphnia magna*. Environmental Science & Technology. 2015 49:4657-64.
- [41] Nel A, Xia T, Madler L, Li N. Toxic Potential of Materials at the Nanolevel. Science. 2006 311:622-7.
- [42] Falfushynska HI, Wu F, Ye F, Kasianchuk N, Dutta J, Dobretsov S, et al. The effects of ZnO nanostructures of different morphology on bioenergetics and stress response biomarkers of the blue mussels *Mytilus edulis*. Science of The Total Environment. 2019 694:133717.
- [43] Li J, Schiavo S, Xiangli D, Rametta G, Miglietta ML, Oliviero M, et al. Early ecotoxic effects of ZnO nanoparticle chronic exposure in *Mytilus galloprovincialis* revealed by transcription of apoptosis and antioxidant-related genes. Ecotoxicology. 2018 27:369-84.
- [44] Yung MMN, Kwok KWH, Djuricic AB, Giesy JP, Leung KMY. Influences of temperature and salinity on physicochemical properties and toxicity of zinc oxide nanoparticles to the marine diatom *Thalassiosira pseudonana*. Scientific reports. 2017 7.
- [45] Katsumiti A, Arostegui I, Oron M, Gilliland D, Valsami-Jones E, Cajaraville MP. Cytotoxicity of Au, ZnO and SiO₂ NPs using in vitro assays with mussel hemocytes and gill cells: Relevance of size, shape and additives. Nanotoxicology. 2016 10:185-93.
- [46] Czyżowska A, Barbasz A. A review: zinc oxide nanoparticles – friends or enemies? International Journal of Environmental Health Research. 2020:1-17.
- [47] Ma H, Williams PL, Diamond SA. Ecotoxicity of manufactured ZnO nanoparticles – A review. Environmental Pollution. 2013 172:76-85.

- [48] Wu F, Falfushynska H, Dellwig O, Piontkivska H, Sokolova IM. Interactive effects of salinity variation and exposure to ZnO nanoparticles on the innate immune system of a sentinel marine bivalve, *Mytilus edulis*. *Science of the Total Environment*. 2020 712:136473.
- [49] Hou J, Wu Y, Li X, Wei B, Li S, Wang X. Toxic effects of different types of zinc oxide nanoparticles on algae, plants, invertebrates, vertebrates and microorganisms. *Chemosphere*. 2018 193:852-60.
- [50] Falfushynska HI, Gnatyshyna LL, Ivanina AV, Khoma VV, Stoliar OB, Sokolova IM. Bioenergetic responses of freshwater mussels *Unio tumidus* to the combined effects of nano-ZnO and temperature regime. *Science of The Total Environment*. 2019 650:1440-50.
- [51] Goncalves RA, de Oliveira Franco Rossetto AL, Nogueira DJ, Vicentini DS, Matias WG. Comparative assessment of toxicity of ZnO and amine-functionalized ZnO nanorods toward *Daphnia magna* in acute and chronic multigenerational tests. *Aquat Toxicol*. 2018 197:32-40.
- [52] Kaya H, Aydin F, Gurkan M, Yilmaz S, Ates M, Demir V, et al. A comparative toxicity study between small and large size zinc oxide nanoparticles in tilapia (*Oreochromis niloticus*): Organ pathologies, osmoregulatory responses and immunological parameters. *Chemosphere*. 2016 144:571-82.
- [53] Marisa I, Matozzo V, Munari M, Binelli A, Parolini M, Martucci A, et al. In vivo exposure of the marine clam *Ruditapes philippinarum* to zinc oxide nanoparticles: responses in gills, digestive gland and haemolymph. *Environmental Science and Pollution Research*. 2016 23:15275-93.
- [54] Wu FL, Cui SK, Sun M, Xie Z, Huang W, Huang XZ, et al. Combined effects of ZnO NPs and seawater acidification on the haemocyte parameters of thick shell mussel *Mytilus coruscus*. *Science of The Total Environment*. 2018 624:820-30.
- [55] Fabrega J, Tantra R, Amer A, Stolpe B, Tomkins J, Fry T, et al. Sequestration of Zinc from Zinc Oxide Nanoparticles and Life Cycle Effects in the Sediment Dweller Amphipod *Corophium volutator*. *Environmental Science & Technology*. 2012 46:1128-35.
- [56] Hanna SK, Miller RJ, Muller EB, Nisbet RM, Lenihan HS. Impact of Engineered Zinc Oxide Nanoparticles on the Individual Performance of *Mytilus galloprovincialis*. *Plos One*. 2013 8:e61800.
- [57] Muller EB, Hanna SK, Lenihan HS, Miller R, Nisbet RM. Impact of engineered zinc oxide nanoparticles on the energy budgets of *Mytilus galloprovincialis*. *Journal of Sea Research*. 2014 94:29-36.
- [58] Buffet PE, Amiard-Triquet C, Dybowska A, Risso-de Faverney C, Guibbolini M, Valsami-Jones E, et al. Fate of isotopically labeled zinc oxide nanoparticles in sediment and effects on two endobenthic species, the clam *Scrobicularia plana* and the ragworm *Hediste diversicolor*. *Ecotoxicology and Environmental Safety*. 2012 84:191-8.
- [59] Trevisan R, Delapiedra G, Mello DF, Arl M, Schmidt EC, Meder F, et al. Gills are an initial target of zinc oxide nanoparticles in oysters *Crassostrea gigas*, leading to mitochondrial disruption and oxidative stress. *Aquatic Toxicology*. 2014 153:27-38.
- [60] Rocha TL, Gomes T, Sousa VS, Mestre NC, Bebianno MJ. Ecotoxicological impact of engineered nanomaterials in bivalve molluscs: An overview. *Marine Environmental Research*. 2015 111:74-88.
- [61] Heinlaan M, Muna M, Knobel M, Kistler D, Odzak N, Kuhnel D, et al. Natural water as the test medium for Ag and CuO nanoparticle hazard evaluation: An interlaboratory case study. *Environmental Pollution*. 2016 216:689-99.
- [62] Holmstrup M, Bindesbol AM, Oostingh GJ, Duschl A, Scheil V, Kohler HR, et al. Interactions between effects of environmental chemicals and natural stressors: A review. *Science of The Total Environment*. 2010 408:3746-62.
- [63] Liu H, Zhang H, Wang J, Wei J. Effect of temperature on the size of biosynthesized silver nanoparticle: Deep insight into microscopic kinetics analysis. *Arabian Journal of Chemistry*. 2020 13:1011-9.
- [64] Yung MMN, Wong SWY, Kwok KWH, Liu FZ, Leung YH, Chan WT, et al. Salinity-dependent toxicities of zinc oxide nanoparticles to the marine diatom *Thalassiosira pseudonana*. *Aquatic Toxicology*. 2015 165:31-40.
- [65] Singh P, Arif Y, Siddiqui H, Sami F, Zaidi R, Azam A, et al. Nanoparticles enhances the salinity toxicity tolerance in *Linum usitatissimum* L. by modulating the antioxidative enzymes, photosynthetic efficiency, redox status and cellular damage. *Ecotoxicology and Environmental Safety*. 2021 213:112020.
- [66] Auffan M, Matson CW, Rose J, Arnold M, Proux O, Fayard B, et al. Salinity-dependent silver nanoparticle uptake and transformation by Atlantic killifish (*Fundulus heteroclitus*) embryos. *Nanotoxicology*. 2014 8:167-76.
- [67] Mos B, Kaposi KL, Rose AL, Kelaher B, Dworjanyn SA. Moderate ocean warming mitigates, but more extreme warming exacerbates the impacts of zinc from engineered nanoparticles on a marine larva. *Environmental Pollution*. 2017 228:190-200.
- [68] Cabral H, Fonseca V, Sousa T, Costa Leal M. Synergistic Effects of Climate Change and Marine Pollution: An Overlooked Interaction in Coastal and Estuarine Areas. *International journal of environmental*

- research and public health. 2019 16:2737.
- [69] Kijewski T, Śmietanka B, Zbawicka M, Gosling E, Hummel H, Wenne R. Distribution of *Mytilus* taxa in European coastal areas as inferred from molecular markers. *Journal of Sea Research*. 2011 65:224-34.
- [70] Mathiesen SS, Thyrring J, Hemmer-Hansen J, Berge J, Sukhotin A, Leopold P, et al. Genetic diversity and connectivity within *Mytilus spp.* in the subarctic and Arctic. *Evolutionary Applications*. 2017 10:39-55.
- [71] Beyer J, Green NW, Brooks S, Allan IJ, Ruus A, Gomes T, et al. Blue mussels (*Mytilus edulis* spp.) as sentinel organisms in coastal pollution monitoring: A review. *Marine Environmental Research*. 2017 130:338-65.
- [72] Bricker S, Lauenstein G, Maruya K. NOAA's Mussel Watch Program: Incorporating contaminants of emerging concern (CECs) into a long-term monitoring program. *Marine Pollution Bulletin*. 2014 81:289-90.
- [73] Wijsman JWM, Troost K, Fang J, Roncarati A. Global Production of Marine Bivalves. Trends and Challenges. In: Smaal AC, Ferreira JG, Grant J, Petersen JK, Strand Ø, editors. *Goods and Services of Marine Bivalves*. Cham: Springer International Publishing; 2019, p. 7-26.
- [74] Falfushynska H, Sokolov EP, Haider F, Oppermann C, Kragl U, Ruth W, et al. Effects of a common pharmaceutical, atorvastatin, on energy metabolism and detoxification mechanisms of a marine bivalve *Mytilus edulis*. *Aquatic Toxicology*. 2019 208:47-61.
- [75] González-Fernández C, Albentosa M, Sokolova I. Interactive effects of nutrition, reproductive state and pollution on molecular stress responses of mussels, *Mytilus galloprovincialis* Lamarck, 1819. *Marine Environmental Research*. 2017 131:103-15.
- [76] Blanco-Rayón E, Guilhermino L, Irazola M, Ivanina AV, Sokolova IM, Izagirre U, et al. The influence of short-term experimental fasting on biomarker responsiveness in oil WAF exposed mussels. *Aquatic Toxicology*. 2019 206:164-75.
- [77] Marigómez I, Múgica M, Izagirre U, Sokolova IM. Chronic environmental stress enhances tolerance to seasonal gradual warming in marine mussels. *Plos One*. 2017 12:e0174359.
- [78] Múgica M, Sokolova IM, Izagirre U, Marigómez I. Season-dependent effects of elevated temperature on stress biomarkers, energy metabolism and gamete development in mussels. *Marine Environmental Research*. 2015 103:1-10.
- [79] Strohmeier T, Strand Ø, Alunno-Bruscia M, Duinker A, Cranford PJ. Variability in particle retention efficiency by the mussel *Mytilus edulis*. *Journal of Experimental Marine Biology and Ecology*. 2012 412:96-102.
- [80] Møhlenberg F, Riisgård HU. Efficiency of particle retention in 13 species of suspension feeding bivalves. *Ophelia*. 1978 17:239-46.
- [81] Canesi L, Ciacci C, Fabbri R, Marcomini A, Pojana G, Gallo G. Bivalve molluscs as a unique target group for nanoparticle toxicity. *Mar Environ Res*. 2012 76:16-21.
- [82] Shang Y, Lan Y, Liu Z, Kong H, Huang X, Wu F, et al. Synergistic Effects of Nano-ZnO and Low pH of Sea Water on the Physiological Energetics of the Thick Shell Mussel *Mytilus coruscus*. *Frontiers in Physiology*. 2018 9:757-.
- [83] Stuckas H, Knöbel L, Schade H, Breusing C, Hinrichsen H-H, Bartel M, et al. Combining hydrodynamic modelling with genetics: can passive larval drift shape the genetic structure of Baltic *Mytilus* populations? *Molecular Ecology*. 2017 26:2765-82.
- [84] Jansson A-M, Kautsky N. QUANTITATIVE SURVEY OF HARD BOTTOM COMMUNITIES IN A BALTIC ARCHIPELAGO. In: Keegan BF, Ceidigh PO, Boaden PJS, editors. *Biology of Benthic Organisms*: Pergamon; 1977, p. 359-66.
- [85] Gosling EM. *The Mussel Mytilus : ecology, physiology, genetics, and culture*. Amsterdam, New York: Elsevier; 1992.
- [86] Joubert Y, Pan J-F, Buffet P-E, Pilet P, Gilliland D, Valsami-Jones E, et al. Subcellular localization of gold nanoparticles in the estuarine bivalve *Scrobicularia plana* after exposure through the water. *Gold Bulletin*. 2013 46:47-56.
- [87] Al-Sid-Cheikh M, Rouleau C, Pelletier E. Tissue distribution and kinetics of dissolved and nanoparticulate silver in Iceland scallop (*Chlamys islandica*). *Marine Environmental Research*. 2013 86:21-8.
- [88] Hull MS, Chaurand P, Rose J, Auffan M, Bottero J-Y, Jones JC, et al. Filter-Feeding Bivalves Store and Biodeposit Colloidally Stable Gold Nanoparticles. *Environmental Science & Technology*. 2011 45:6592-9.
- [89] Perez DG, Fontanetti CS. Hemocytical responses to environmental stress in invertebrates: a review. *Environmental Monitoring and Assessment*. 2010 177:437-47.
- [90] Jenny MJ, Ringwood AH, Lacy ER, Lewitus AJ, Kempton JW, Gross PS, et al. Potential Indicators of stress response Identified by Expressed Sequence Tag Analysis of hemocytes and Embryos From the American

- Oyster, *Crassostrea virginica*. *Marine Biotechnology*. 2002 4:81-93.
- [91] Lacoste A, Malham SK, Gélébart F, Cueff A, Poulet SA. Stress-induced immune changes in the oyster *Crassostrea gigas*. *Developmental & Comparative Immunology*. 2002 26:1-9.
- [92] Roch P. Various Aspects of Bivalve Mollusk Immunity. *Bulletin De La Societe Zoologique De France*. 1999 124:313-24.
- [93] Schiedek D, Sundelin B, Readman JW, Macdonald RW. Interactions between climate change and contaminants. *Marine Pollution Bulletin*. 2007 54:1845-56.
- [94] IPCC. Climate change 2014: Synthesis report. In: Contribution of Working Groups I, II and III to the Fifth Assessment Report of the Intergovernmental Panel on Climate Change. 2014.
- [95] IPCC. Special Report on the Ocean and Cryosphere in a Changing Climate. [H.-O. Pörtner, D.C. Roberts, V. Masson-Delmotte, P. Zhai, M. Tignor, E. Poloczanska, K. Mintenbeck, M. Nicolai, A. Okem, J. Petzold, B. Rama, N. Weyer (eds.)]. Cambridge University Press, Cambridge, United Kingdom and New York, NY, USA, In press. 2019.
- [96] Kniebusch M, Meier HEM, Neumann T, Börgel F. Temperature Variability of the Baltic Sea Since 1850 and Attribution to Atmospheric Forcing Variables. *Journal of Geophysical Research: Oceans*. 2019 124:4168-87.
- [97] Boukadida K, Banni M, Gourves PY, Cachot J. High sensitivity of embryo-larval stage of the Mediterranean mussel, *Mytilus galloprovincialis* to metal pollution in combination with temperature increase. *Marine Environmental Research*. 2016 122:59-66.
- [98] Wang YJ, Hu MH, Shin PKS, Cheung SG. Immune responses to combined effect of hypoxia and high temperature in the green-lipped mussel *Perna viridis*. *Marine Pollution Bulletin*. 2011 63:201-8.
- [99] Jansen JM, Hummel H, Bonga SW. The respiratory capacity of marine mussels (*Mytilus galloprovincialis*) in relation to the high temperature threshold. *Comparative Biochemistry and Physiology a-Molecular & Integrative Physiology*. 2009 153:399-402.
- [100] Portner HO, Langenbuch M, Michaelidis B. Synergistic effects of temperature extremes, hypoxia, and increases in CO₂ on marine animals: From Earth history to global change. *Journal of Geophysical Research-Oceans*. 2005 110.
- [101] Velez C, Figueira E, Soares A, Freitas R. Effects of seawater temperature increase on economically relevant native and introduced clam species. *Marine Environmental Research*. 2017 123:62-70.
- [102] Wang YJ, Li LS, Hu MH, Lu WQ. Physiological energetics of the thick shell mussel *Mytilus coruscus* exposed to seawater acidification and thermal stress. *Science of The Total Environment*. 2015 514:261-72.
- [103] Attig H, Kamel N, Sforzini S, Dagnino A, Jamel J, Boussetta H, et al. Effects of thermal stress and nickel exposure on biomarkers responses in *Mytilus galloprovincialis* (Lam). *Marine Environmental Research*. 2014 94:65-71.
- [104] Banni M, Hajer A, Sforzini S, Oliveri C, Boussetta H, Viarengo A. Transcriptional expression levels and biochemical markers of oxidative stress in *Mytilus galloprovincialis* exposed to nickel and heat stress. *Comparative Biochemistry and Physiology C-Toxicology & Pharmacology*. 2014 160:23-9.
- [105] Hu MH, Li LS, Sui YM, Li J, Wang YJ, Lu WQ, et al. Effect of pH and temperature on antioxidant responses of the thick shell mussel *Mytilus coruscus*. *Fish & Shellfish Immunology*. 2015 46:573-83.
- [106] Nardi A, Mincarelli LF, Benedetti M, Fattorini D, d'Errico G, Regoli F. Indirect effects of climate changes on cadmium bioavailability and biological effects in the Mediterranean mussel *Mytilus galloprovincialis*. *Chemosphere*. 2017 169:493-502.
- [107] Mackenzie BR, Schiedek D. Daily ocean monitoring since the 1860s shows record warming of northern European seas. *Global Change Biology*. 2007 13:1335-47.
- [108] Bagwe R, Beniash E, Sokolova IM. Effects of cadmium exposure on critical temperatures of aerobic metabolism in eastern oysters *Crassostrea virginica* (Gmelin, 1791). *Aquatic Toxicology*. 2015 167:77-89.
- [109] Cherkasov AS, Taylor C, Sokolova IM. Seasonal variation in mitochondrial responses to cadmium and temperature in eastern oysters *Crassostrea virginica* (Gmelin) from different latitudes. *Aquatic Toxicology*. 2010 97:68-78.
- [110] Ioannou S, Anestis A, Pörtner HO, Michaelidis B. Seasonal patterns of metabolism and the heat shock response (HSR) in farmed mussels *Mytilus galloprovincialis*. *Journal of Experimental Marine Biology and Ecology*. 2009 381:136-44.
- [111] Katsikatsou M, Anestis A, Pörtner H-O, Vratsistas A, Aligizaki K, Michaelidis B. Field studies and projections of climate change effects on the bearded horse mussel *Modiolus barbatus* in the Gulf of Thermaikos, Greece. *Mar Ecol Prog Ser*. 2012 449:183-96.
- [112] Cao A, Novás A, Ramos-Martínez JI, Barcia R. Seasonal variations in haemocyte response in the mussel

- Mytilus galloprovincialis* Lmk. Aquaculture. 2007 263:310-9.
- [113] Sokolova IM, Lannig G. Interactive effects of metal pollution and temperature on metabolism in aquatic ectotherms: implications of global climate change. *Climate Research*. 2008 37:181-201.
- [114] Hallman TA, Brooks ML. Metal-mediated climate susceptibility in a warming world: Larval and latent effects on a model amphibian. *Environmental Toxicology and Chemistry*. 2016 35:1872-82.
- [115] Heugens EHW, Jager T, Creyghton R, Kraak MHS, Hendriks AJ, Van Straalen NM, et al. Temperature-Dependent Effects of Cadmium on *Daphnia magna*: Accumulation versus Sensitivity. *Environmental Science & Technology*. 2003 37:2145-51.
- [116] Lai RWS, Yung MMN, Zhou G-J, He YL, Ng AMC, Djurišić AB, et al. Temperature and salinity jointly drive the toxicity of zinc oxide nanoparticles: a challenge to environmental risk assessment under global climate change. *Environmental Science: Nano*. 2020 7:2995-3006.
- [117] McLusky DS, Elliott M. *The Estuarine Ecosystem. Ecology, Threats and Management*. Third edition ed: Oxford University Press; 2004.
- [118] Pierce DW, Gleckler PJ, Barnett TP, Santer BD, Durack PJ. The fingerprint of human-induced changes in the ocean's salinity and temperature fields. *Geophysical Research Letters*. 2012 39:L21704.
- [119] Haider F, Sokolov EP, Sokolova IM. Effects of mechanical disturbance and salinity stress on bioenergetics and burrowing behavior of the soft-shell clam *Mya arenaria*. *Journal of Experimental Biology*. 2018 221.
- [120] Sokolov EP, Sokolova IM. Compatible osmolytes modulate mitochondrial function in a marine osmoconformer *Crassostrea gigas* (Thunberg, 1793). *Mitochondrion*. 2019 45:29-37.
- [121] Zhao X, Yu H, Kong L, Li Q. Transcriptomic responses to salinity stress in the Pacific oyster *Crassostrea gigas*. *Plos One*. 2012 7:e46244-e.
- [122] Berger VJ, Kharazova AD. Mechanisms of salinity adaptations in marine molluscs. In: Naumov AD, Hummel H, Sukhotin AA, Ryland JS, editors. *Interactions and Adaptation Strategies of Marine Organisms*. Dordrecht: Springer Netherlands; 1997, p. 115-26.
- [123] Malagoli D, Casarini L, Sacchi S, Ottaviani E. Stress and immune response in the mussel *Mytilus galloprovincialis*. *Fish & Shellfish Immunology*. 2007 23:171-7.
- [124] Casas SM, Figueras A, Ordás MC, Reece KS, Villalba A. Perkinsosis in molluscs: A review. *Aquatic Living Resources*. 2004 17:411-32.
- [125] Corporeau C, Auffret M. In situ hybridisation for flow cytometry: a molecular method for monitoring stress-gene expression in hemolymph cells of oysters. *Aquatic Toxicology*. 2003 64:427-35.
- [126] Rivera-Ingraham GA, Barri K, Boël M, Farcy E, Charles A-L, Geny B, et al. Osmoregulation and salinity-induced oxidative stress: is oxidative adaptation determined by gill function? *Journal of Experimental Biology*. 2016 219:80-9.
- [127] Wang J, Wang W-x. Salinity influences on the uptake of silver nanoparticles and silver nitrate by marine medaka (*Oryzias melastigma*): Salinity influences on silver nanoparticle uptake by marine medaka. *Environmental Toxicology and Chemistry*. 2014 33:632-40.
- [128] Park J, Kim S, Yoo J, Lee J-S, Park J-W, Jung J. Effect of salinity on acute copper and zinc toxicity to *Tigriopus japonicus*: The difference between metal ions and nanoparticles. *Marine Pollution Bulletin*. 2014 85:526-31.
- [129] Khlebovich VV. Acclimation of animal organisms: basic theory and applied aspects. *Biology Bulletin Reviews*. 2017 7:279-86.
- [130] Thompson EL, Taylor DA, Nair SV, Birch G, Coleman R, Raftos DA. Optimal acclimation periods for oysters in laboratory-based experiments. *Journal of Molluscan Studies*. 2012 78:304-7.
- [131] Burge CA, Closek CJ, Friedman CS, Groner ML, Jenkins CM, Shore-Maggio A, et al. The Use of Filter-feeders to Manage Disease in a Changing World. *Integrative and Comparative Biology*. 2016 56:573-87.
- [132] Mydlarz LD, Jones LE, Harvell CD. Innate Immunity, Environmental Drivers, and Disease Ecology of Marine and Freshwater Invertebrates. *Annual Review of Ecology, Evolution, and Systematics*. 2006 37:251-88.
- [133] Song L, Wang L, Qiu L, Zhang H. Bivalve Immunity. In: Söderhäll K, editor. *Invertebrate Immunity*. Boston, MA: Springer US; 2010, p. 44-65.
- [134] Canesi L, Procházková P. Chapter 7 - The Invertebrate Immune System as a Model for Investigating the Environmental Impact of Nanoparticles. In: Boraschi D, Duschl A, editors. *Nanoparticles and the Immune System*. San Diego: Academic Press; 2014, p. 91-112.
- [135] Allam B, Raftos D. Immune responses to infectious diseases in bivalves. *Journal of Invertebrate Pathology*. 2015 131:121-36.
- [136] Hughes FM, Foster B, Grewal S, Sokolova IM. Apoptosis as a host defense mechanism in *Crassostrea virginica* and its modulation by *Perkinsus marinus*. *Fish & Shellfish Immunology*. 2010 29:247-57.
- [137] Sokolova IM. Apoptosis in molluscan immune defense. *Invertebrate Survival Journal*. 2009 6:49-58.

- [138] Kwon H, Bang K, Cho S. Characterization of the Hemocytes in Larvae of *Protaetia brevitarsis seulensis*: Involvement of Granulocyte-Mediated Phagocytosis. *Plos One*. 2014 9:e103620.
- [139] Canesi L, Gallo G, Gavioli M, Pruzzo C. Bacteria-hemocyte interactions and phagocytosis in marine bivalves. *Microscopy Research and Technique*. 2002 57:469-76.
- [140] Hegaret H, Wikfors GH, Soudant P. Flow cytometric analysis of haemocytes from eastern oysters, *Crassostrea virginica*, subjected to a sudden temperature elevation II. Haemocyte functions: aggregation, viability, phagocytosis, and respiratory burst. *Journal of Experimental Marine Biology and Ecology*. 2003 293:249-65.
- [141] Chu FE. Defense mechanisms of marine bivalves. *Recent advances in marine biotechnology*. 2000.
- [142] Buggé DM, Hégaret H, Wikfors GH, Allam B. Oxidative burst in hard clam (*Mercenaria mercenaria*) haemocytes. *Fish Shellfish Immunol*. 2007 23:188-96.
- [143] Olafsen JA. Role of lectins (C-reactive protein) in defense of marine bivalves against bacteria. *Adv Exp Med Biol*. 1995 371a:343-8.
- [144] Batista FM, Boudry P, Dos Santos A, Renault T, Ruano F. Infestation of the cupped oysters *Crassostrea angulata*, *C. gigas* and their first-generation hybrids by the copepod *Mycicola ostreae*: differences in susceptibility and host response. *Parasitology*. 2009 136:537-43.
- [145] Janeway CA, Jr., Medzhitov R. Innate immune recognition. *Annu Rev Immunol*. 2002 20:197-216.
- [146] Medzhitov R, Janeway CA, Jr. Decoding the patterns of self and nonself by the innate immune system. *Science*. 2002 296:298-300.
- [147] Ward AE, Rosenthal BM. Evolutionary responses of innate immunity to adaptive immunity. *Infection Genetics and Evolution*. 2014 21:492-6.
- [148] Zhang LL, Li L, Guo XM, Litman GW, Dishaw LJ, Zhang GF. Massive expansion and functional divergence of innate immune genes in a protostome. *Scientific reports*. 2015 5.
- [149] Kedmi R, Ben-Arie N, Peer D. The systemic toxicity of positively charged lipid nanoparticles and the role of Toll-like receptor 4 in immune activation. *Biomaterials*. 2010 31:6867-75.
- [150] Turabekova M, Rasulev B, Theodore M, Jackman J, Leszczynska D, Leszczynski J. Immunotoxicity of nanoparticles: a computational study suggests that CNTs and C-60 fullerenes might be recognized as pathogens by Toll-like receptors. *Nanoscale*. 2014 6:3488-95.
- [151] Yang H, Fung SY, Xu SY, Sutherland DP, Kollmann TR, Liu MY, et al. Amino Acid-Dependent Attenuation of Toll-like Receptor Signaling by Peptide-Gold Nanoparticle Hybrids. *Acs Nano*. 2015 9:6774-84.
- [152] Ricklin D, Reis ES, Mastellos DC, Gros P, Lambris JD. Complement component C3-The "Swiss Army Knife" of innate immunity and host defense. *Immunological Reviews*. 2016 274:33-58.
- [153] Volanakis JE. Participation of C3 and its ligands in complement activation. *Current Topics in Microbiology and Immunology*. 1990 153:1-21.
- [154] Mayilyan KR, Kang YH, Dodds AW, Sim RB. The Complement System in Innate Immunity. In: Heine H, editor. *Innate Immunity of Plants, Animals, and Humans*. Berlin, Heidelberg: Springer Berlin Heidelberg; 2008, p. 219-36.
- [155] Christophides GK, Zdobnov E, Barillas-Mury C, Birney E, Blandin S, Blass C, et al. Immunity-related genes and gene families in *Anopheles gambiae*. *Science*. 2002 298:159-65.
- [156] Chen YX, Xu KD, Li JJ, Wang X, Ye YY, Qi PZ. Molecular characterization of complement component 3 (C3) in *Mytilus coruscus* improves our understanding of bivalve complement system. *Fish & Shellfish Immunology*. 2018 76:41-7.
- [157] Dong WQ, Chen YX, Lu WX, Wu B, Qi PZ. Transcriptome analysis of *Mytilus coruscus* hemocytes in response to *Vibrio alginolyticus* infection. *Fish & Shellfish Immunology*. 2017 70:560-7.
- [158] Peng MX, Niu DH, Chen ZY, Lan TY, Dong ZG, Tran TN, et al. Expression of a novel complement C3 gene in the razor clam *Sinonovacula constricta* and its role in innate immune response and hemolysis. *Developmental and Comparative Immunology*. 2017 73:184-92.
- [159] Peng MX, Niu DH, Wang F, Chen ZY, Li JL. Complement C3 gene: Expression characterization and innate immune response in razor clam *Sinonovacula constricta*. *Fish & Shellfish Immunology*. 2016 55:223-32.
- [160] Wang LL, Zhang H, Wang LL, Zhang DX, Lv Z, Liu ZQ, et al. The RNA-seq analysis suggests a potential multi-component complement system in oyster *Crassostrea gigas*. *Developmental and Comparative Immunology*. 2017 76:209-19.
- [161] Venier P, Domeneghetti S, Sharma N, Pallavicini A, Gerdol M. Chapter 7 - Immune-Related Signaling in Mussel and Bivalves. In: Ballarin L, Cammarata M, editors. *Lessons in Immunity*: Academic Press; 2016, p. 93-105.
- [162] Qiu L, Song L, Xu W, Ni D, Yu Y. Molecular cloning and expression of a Toll receptor gene homologue from Zhikong Scallop, *Chlamys farreri*. *Fish Shellfish Immunol*. 2007 22:451-66.

- [163] Canesi L, Betti M, Ciacci C, Citterio B, Pruzzo C, Gallo G. Tyrosine kinase-mediated cell signalling in the activation of *Mytilus* hemocytes: possible role of STAT-like proteins. *Biol Cell*. 2003 95:603-13.
- [164] Yu M, Zheng L, Wang X, Wu M, Qi M, Fu W, et al. Comparative transcriptomic analysis of surf clams (*Paphia undulate*) infected with two strains of *Vibrio* spp. reveals the identity of key immune genes involved in host defense. *Bmc Genomics*. 2019 20:988.
- [165] Montagnani C, Labreuche Y, Escoubas JM. Cg-IkappaB, a new member of the IkappaB protein family characterized in the pacific oyster *Crassostrea gigas*. *Dev Comp Immunol*. 2008 32:182-90.
- [166] Birrer SC, Reusch TBH, Roth O. Salinity change impairs pipefish immune defence. *Fish & Shellfish Immunology*. 2012 33:1238-48.
- [167] Gu J, Dai SY, Liu HT, Cao QQ, Yin SW, Lai KP, et al. Identification of immune-related genes in gill cells of Japanese eels (*Anguilla japonica*) in adaptation to water salinity changes. *Fish & Shellfish Immunology*. 2018 73:288-96.
- [168] Schmitz M, Baekelandt S, Bequet S, Kestemont P. Chronic hyperosmotic stress inhibits renal Toll-Like Receptors expression in striped catfish (*Pangasianodon hypophthalmus*, Sauvage) exposed or not to bacterial infection. *Developmental and Comparative Immunology*. 2017 73:139-43.
- [169] Yao C-L, Somero GN. The impact of acute temperature stress on hemocytes of invasive and native mussels (*Mytilus galloprovincialis* and *Mytilus californianus*): DNA damage, membrane integrity, apoptosis and signaling pathways. *Journal of Experimental Biology*. 2012 215:4267-77.
- [170] Yang Y, Yu H, Li H, Wang A, Yu H-y. Effect of high temperature on immune response of grass carp (*Ctenopharyngodon idellus*) by transcriptome analysis. *Fish & Shellfish Immunology*. 2016 58:89-95.
- [171] Auguste M, Balbi T, Montagna M, Fabbri R, Sendra M, Blasco J, et al. In vivo immunomodulatory and antioxidant properties of nanoceria (nCeO(2)) in the marine mussel *Mytilus galloprovincialis*. *Comparative Biochemistry and Physiology C-Toxicology & Pharmacology*. 2019 219:95-102.
- [172] Balbi T, Smerilli A, Fabbri R, Ciacci C, Montagna M, Grasselli E, et al. Co-exposure to n-TiO₂ and Cd²⁺ results in interactive effects on biomarker responses but not in increased toxicity in the marine bivalve *M. galloprovincialis*. *Science of The Total Environment*. 2014 493:355-64.
- [173] Shi W, Han Y, Guo C, Zhao XG, Liu SX, Su WH, et al. Immunotoxicity of nanoparticle nTiO(2) to a commercial marine bivalve species, *Tegillarca granosa*. *Fish & Shellfish Immunology*. 2017 66:300-6.
- [174] Xu MS, Wu J, Ge DL, Wu CW, Chi CF, Lv ZM, et al. A novel toll-like receptor from *Mytilus coruscus* is induced in response to stress. *Fish & Shellfish Immunology*. 2018 78:331-7.
- [175] Huang XZ, Lin DH, Ning K, Sui YM, Hu MH, Lu WQ, et al. Hemocyte responses of the thick shell mussel *Mytilus coruscus* exposed to nano-TiO₂ and seawater acidification. *Aquatic Biology*. 2016 180:1-10.
- [176] Wang YJ, Hu MH, Li QZ, Li JL, Lin DH, Lu WQ. Immune toxicity of TiO₂ under hypoxia in the green-lipped mussel *Perna viridis* based on flow cytometric analysis of hemocyte parameters. *Science of The Total Environment*. 2014 470:791-9.
- [177] Canesi L, Ciacci C, Bergami E, Monopoli MP, Dawson KA, Papa S, et al. Evidence for immunomodulation and apoptotic processes induced by cationic polystyrene nanoparticles in the hemocytes of the marine bivalve *Mytilus*. *Mar Environ Res*. 2015 111:34-40.
- [178] Lu YL, Zhang AG, Li CH, Zhang P, Su XR, Li Y, et al. The link between selenium binding protein from *Sinonovacula constricta* and environmental pollutions exposure. *Fish & Shellfish Immunology*. 2013 35:271-7.
- [179] Barmo C, Ciacci C, Canonico B, Fabbri R, Cortese K, Balbi T, et al. In vivo effects of n-TiO₂ on digestive gland and immune function of the marine bivalve *Mytilus galloprovincialis*. *Aquatic Toxicology*. 2013 132:9-18.
- [180] Renault T. Immunotoxicological effects of environmental contaminants on marine bivalves. *Fish & Shellfish Immunology*. 2015 46:88-93.
- [181] Wu F, Sokolov EP, Dellwig O, Sokolova IM. Season-dependent effects of ZnO nanoparticles and elevated temperature on bioenergetics of the blue mussel *Mytilus edulis*. *Chemosphere*. 2021 263:127780.
- [182] Wu F, Sokolova IM. Immune responses to ZnO nanoparticles are modulated by season and environmental temperature in the blue mussels *Mytilus edulis*. *Science of The Total Environment*. 2021 801:149786.
- [183] Sokolova I. Bioenergetics in environmental adaptation and stress tolerance of aquatic ectotherms: linking physiology and ecology in a multi-stressor landscape. *Journal of Experimental Biology*. 2021 224.
- [184] Skulachev V, Bogachev AV, Kasparinsky FO. Principles of Bioenergetics. Berlin, Heidelberg, Germany: Springer-Verlag. 2013.
- [185] Sokolova IM, Frederich M, Bagwe R, Lannig G, Sukhotin AA. Energy homeostasis as an integrative tool for assessing limits of environmental stress tolerance in aquatic invertebrates. *Marine Environmental Research*. 2012 79:1-15.

- [186] Sokolova IM, Sukhotin AA, Lannig G. Stress effects on metabolism and energy budgets in mollusks. In: Abele, D, Zenteno-Savin, T, Vazquez-Medina, J (Eds), *Oxidative Stress in Aquatic Ecosystems* Blackwell Wiley, Boston etc. 2011:pp. 263- 80.
- [187] Sokolova IM. Energy-Limited Tolerance to Stress as a Conceptual Framework to Integrate the Effects of Multiple Stressors. *Integrative and Comparative Biology*. 2013 53:597-608.
- [188] Kooijman SALM, Kooijman SALM. *Dynamic energy and mass budgets in biological systems*: Cambridge university press; 2000.
- [189] Rombough P. Energy partitioning during fish development: additive or compensatory allocation of energy to support growth? *Functional Ecology*. 1994:178-86.
- [190] Pörtner H-O. Climate variations and the physiological basis of temperature dependent biogeography: systemic to molecular hierarchy of thermal tolerance in animals. *Comparative Biochemistry and Physiology Part A: Molecular & Integrative Physiology*. 2002 132:739-61.
- [191] Pörtner H-O. Oxygen-and capacity-limitation of thermal tolerance: a matrix for integrating climate-related stressor effects in marine ecosystems. *Journal of Experimental Biology*. 2010 213:881-93.
- [192] Smolders R, Bervoets L, De Coen W, Blust R. Cellular energy allocation in zebra mussels exposed along a pollution gradient: linking cellular effects to higher levels of biological organization. *Environ Pollut*. 2004 129:99-112.
- [193] Bartlett JK, Maher WA, Purss MBJ. Cellular energy allocation analysis of multiple marine bivalves using near infrared spectroscopy. *Ecological Indicators*. 2018 90:247-56.
- [194] DeCoen WM, Janssen CR. The use of biomarkers in *Daphnia magna* toxicity testing .2. Digestive enzyme activity in *Daphnia magna* exposed to sublethal concentrations of cadmium, chromium and mercury. *Chemosphere*. 1997 35:1053-67.
- [195] Gnaiger E. Calculation of Energetic and Biochemical Equivalents of Respiratory Oxygen Consumption. In: Gnaiger E, Forstner H, editors. *Polarographic Oxygen Sensors*. Berlin, Heidelberg: Springer Berlin Heidelberg; 1983, p. 337-45.
- [196] Verslycke T, Roast SD, Widdows J, Jones MB, Janssen CR. Cellular energy allocation and scope for growth in the estuarine mysid *Neomysis integer* (Crustacea : Mysidacea) following chlorpyrifos exposure: a method comparison. *Journal of Experimental Marine Biology and Ecology*. 2004 306:1-16.
- [197] Krams IA, Krams R, Jöers P, Munkevics M, Trakimas G, Luoto S, et al. Developmental speed affects ecological stoichiometry and adult fat reserves in *Drosophila melanogaster*. *Animal Biology*. 2020 71:1-20.
- [198] Levy SF, Ziv N, Siegal ML. Bet hedging in yeast by heterogeneous, age-correlated expression of a stress protectant. *PLoS biology*. 2012 10:e1001325.
- [199] Ratcliff WC, Denison RF. Individual-level bet hedging in the bacterium *Sinorhizobium meliloti*. *Current Biology*. 2010 20:1740-4.
- [200] Berenbaum MR, Zangerl AR. Costs of Inducible Defense: Protein Limitation, Growth, and Detoxification in *Parnip Webworms*. *Ecology*. 1994 75:2311-7.
- [201] Smolders R, De Boeck G, Blust R. Changes in cellular energy budget as a measure of whole effluent toxicity in zebrafish (*Danio rerio*). *Environmental Toxicology and Chemistry*. 2003 22:890-9.
- [202] Ansar S, Abudawood M, Hamed SS, Aleem MM. Exposure to Zinc Oxide Nanoparticles Induces Neurotoxicity and Proinflammatory Response: Amelioration by Hesperidin. *Biological Trace Element Research*. 2017 175:360-6.
- [203] Attia H, Nounou H, Shalaby M. Zinc Oxide Nanoparticles Induced Oxidative DNA Damage, Inflammation and Apoptosis in Rat's Brain after Oral Exposure. *Toxics*. 2018 6.
- [204] Wang H, Ye JP. Regulation of energy balance by inflammation: Common theme in physiology and pathology. *Reviews in Endocrine & Metabolic Disorders*. 2015 16:47-54.
- [205] Hu M, Lin D, Shang Y, Hu Y, Lu W, Huang X, et al. CO₂-induced pH reduction increases physiological toxicity of nano-TiO₂ in the mussel *Mytilus coruscus*. *Scientific Reports*. 2017 7:40015-.
- [206] Shang Y, Wu F, Wei S, Guo W, Chen J, Huang W, et al. Specific dynamic action of mussels exposed to TiO₂ nanoparticles and seawater acidification. *Chemosphere*. 2020 241:125104.
- [207] Kong H, Wu F, Jiang X, Wang T, Hu M, Chen J, et al. Nano-TiO₂ impairs digestive enzyme activities of marine mussels under ocean acidification. *Chemosphere*. 2019 237:124561.
- [208] Saidani W, Sellami B, Khazri A, Mezni A, Dellali M, Joubert O, et al. Metal accumulation, biochemical and behavioral responses on the Mediterranean clams *Ruditapes decussatus* exposed to two photocatalyst nanocomposites (TiO₂ NPs and AuTiO₂NPs). *Aquatic Toxicology*. 2019 208:71-9.
- [209] Saggese I, Sarà G, Dondero F. Silver Nanoparticles Affect Functional Bioenergetic Traits in the Invasive Red Sea Mussel *Brachidontes pharaonis*. *BioMed research international*. 2016 2016:1872351-.

- [210] Andrade M, De Marchi L, Pretti C, Chiellini F, Morelli A, Figueira E, et al. The impacts of warming on the toxicity of carbon nanotubes in mussels. *Marine Environmental Research*. 2019 145:11-21.
- [211] Scott-Fordsmand JJ, Weeks JM. Biomarkers in earthworms. In: Ware GW, editor. *Reviews of Environmental Contamination and Toxicology*, Vol 165; 2000, p. 117-59.
- [212] Clements JC, Hicks C, Tremblay R, Comeau LA. Elevated seawater temperature, not pCO₂, negatively affects post-spawning adult mussels (*Mytilus edulis*) under food limitation. *Conservation physiology*. 2018 6:cox078-cox.
- [213] Riisgård HU, Lüskow F, Pleissner D, Lundgreen K, López MÁP. Effect of salinity on filtration rates of mussels *Mytilus edulis* with special emphasis on dwarfed mussels from the low-saline Central Baltic Sea. *Helgoland Marine Research*. 2013 67:591-8.
- [214] Dickinson GH, Ivanina AV, Matoo OB, Portner HO, Lannig G, Bock C, et al. Interactive effects of salinity and elevated CO₂ levels on juvenile eastern oysters, *Crassostrea virginica*. *Journal of Experimental Biology*. 2012 215:29-43.
- [215] Noor MN, Wu F, Sokolov EP, Falfushynska H, Timm S, Haider F, et al. Salinity-dependent effects of ZnO nanoparticles on bioenergetics and intermediate metabolite homeostasis in a euryhaline marine bivalve, *Mytilus edulis*. *Sci Total Environ*. 2021 774:145195.
- [216] Fulda S, Gorman AM, Hori O, Samali A. Cellular Stress Responses: Cell Survival and Cell Death. *International Journal of Cell Biology*. 2010 2010:214074.
- [217] Díaz-Hung M-L, Martínez G, Hetz C. Chapter Two - Emerging roles of the unfolded protein response (UPR) in the nervous system: A link with adaptive behavior to environmental stress? In: Kepp O, Galluzzi L, editors. *International Review of Cell and Molecular Biology*: Academic Press; 2020, p. 29-61.
- [218] Welch WJ. How cells respond to stress. *Sci Am*. 1993 268:56-64.
- [219] Halappanavar S, van den Brule S, Nymark P, Gaté L, Seidel C, Valentino S, et al. Adverse outcome pathways as a tool for the design of testing strategies to support the safety assessment of emerging advanced materials at the nanoscale. *Particle and Fibre Toxicology*. 2020 17:16.
- [220] Gerloff K, Landesmann B, Worth A, Munn S, Palosaari T, Whelan M. The Adverse Outcome Pathway approach in nanotoxicology. *Computational Toxicology*. 2017 1:3-11.
- [221] Luo Z, Li Z, Xie Z, Sokolova IM, Song L, Peijnenburg WJGM, et al. Rethinking Nano-TiO₂ Safety: Overview of Toxic Effects in Humans and Aquatic Animals. *Small*. 2020 16:2002019.
- [222] Castro-Bugallo A, González-Fernández Á, Guisande C, Barreiro A. Comparative Responses to Metal Oxide Nanoparticles in Marine Phytoplankton. *Archives of Environmental Contamination and Toxicology*. 2014 67:483-93.
- [223] Schiavo S, Oliviero M, Miglietta M, Rametta G, Manzo S. Genotoxic and cytotoxic effects of ZnO nanoparticles for *Dunaliella tertiolecta* and comparison with SiO₂ and TiO₂ effects at population growth inhibition levels. *Science of The Total Environment*. 2016 550:619-27.
- [224] Schulze-Osthoff K, Bakker AC, Vanhaesebroeck B, Beyaert R, Jacob WA, Fiers W. Cytotoxic activity of tumor necrosis factor is mediated by early damage of mitochondrial functions. Evidence for the involvement of mitochondrial radical generation. *Journal of Biological Chemistry*. 1992 267:5317-23.
- [225] Van Herreweghe F, Mao J, Chaplen FWR, Grooten J, Gevaert K, Vandekerckhove J, et al. Tumor necrosis factor-induced modulation of glyoxalase I activities through phosphorylation by PKA results in cell death and is accompanied by the formation of a specific methylglyoxal-derived AGE. *Proceedings of the National Academy of Sciences*. 2002 99:949.
- [226] Trachootham D, Lu W, Ogasawara MA, Valle NR-D, Huang P. Redox Regulation of Cell Survival. *Antioxidants & Redox Signaling*. 2008 10:1343-74.
- [227] Hoeijmakers JHJ. Genome maintenance mechanisms for preventing cancer. *Nature*. 2001 411:366-74.
- [228] Genestra M. Oxyl radicals, redox-sensitive signalling cascades and antioxidants. *Cellular Signalling*. 2007 19:1807-19.
- [229] Vandebriel RJ, De Jong WH. A review of mammalian toxicity of ZnO nanoparticles. *Nanotechnology, science and applications*. 2012 5:61-71.
- [230] Wang J, Deng X, Zhang F, Chen D, Ding W. ZnO nanoparticle-induced oxidative stress triggers apoptosis by activating JNK signaling pathway in cultured primary astrocytes. *Nanoscale research letters*. 2014 9:117-.
- [231] Fernando N, Wickremesinghe S, Niloofa R, Rodrigo C, Karunanayake L, de Silva HJ, et al. Protein Carbonyl as a Biomarker of Oxidative Stress in Severe Leptospirosis, and Its Usefulness in Differentiating Leptospirosis from Dengue Infections. *Plos One*. 2016 11:e0156085.
- [232] Grotto D, Maria LS, Valentini J, Paniz C, Schmitt G. Importance of the lipid peroxidation biomarkers and methodological aspects FOR malondialdehyde quantification. *Química Nova* [online]. 2009 v. 32, n. 1:pp. 169-74.

- [233] Gagné F, Turcotte P, Auclair J, Gagnon C. The effects of zinc oxide nanoparticles on the metallome in freshwater mussels. *Comparative biochemistry and physiology Toxicology & pharmacology : CBP*. 2013 158.
- [234] Ates M, Daniels J, Arslan Z, Farah IO, Rivera HF. Comparative evaluation of impact of Zn and ZnO nanoparticles on brine shrimp (*Artemia salina*) larvae: effects of particle size and solubility on toxicity. *Environmental Science: Processes & Impacts*. 2013 15:225-33.
- [235] Ali D, Alarifi S, Kumar S, Ahamed M, Siddiqui M. Oxidative stress and genotoxic effect of zinc oxide nanoparticles in freshwater snail *Lymnaea luteola* L. *Aquat Toxicol*. 2012 124-125:83-90.
- [236] Fahmy S, Abdel-Ghaffar F, Bakry F, Sayed D. Ecotoxicological Effect of Sublethal Exposure to Zinc Oxide Nanoparticles on Freshwater Snail *Biomphalaria alexandrina*. *Archives of Environmental Contamination and Toxicology*. 2014 67.
- [237] Samali A, Zhivotovsky B, Jones D, Nagata S, Orrenius S. Apoptosis: Cell death defined by caspase activation. *Cell Death & Differentiation*. 1999 6:495-6.
- [238] Berenbom M, Chang PI, Betz HE, Stowell RE. Chemical and enzymatic changes associated with mouse liver necrosis in vitro. *Cancer Research*. 1955 15:1.
- [239] Trauth BC, Klas C, Peters AMJ, Matzku S, Möller P, Falk W, et al. Monoclonal Antibody-Mediated Tumor Regression by Induction of Apoptosis. *Science*. 1989 245:301-5.
- [240] Kerr JFR, Wyllie AH, Currie AR. Apoptosis: A Basic Biological Phenomenon with Wideranging Implications in Tissue Kinetics. *British Journal of Cancer*. 1972 26:239-57.
- [241] Kerr JFR. Shrinkage necrosis: A distinct mode of cellular death. *The Journal of Pathology*. 1971 105:13-20.
- [242] Lockshin RA, Zakeri Z. Cell death in health and disease. *Journal of Cellular and Molecular Medicine*. 2007 11:1214-24.
- [243] Samali A, Gorman AM, Cotter TG. Apoptosis-the story so far. *Experientia*. 1996 52:933-41.
- [244] Poon IKH, Lucas CD, Rossi AG, Ravichandran KS. Apoptotic cell clearance: basic biology and therapeutic potential. *Nature reviews Immunology*. 2014 14:166-80.
- [245] Xu X, Lai Y, Hua Z-C. Apoptosis and apoptotic body: disease message and therapeutic target potentials. *Bioscience Reports*. 2019 39.
- [246] Brown DA, Yang N, Ray SD. Apoptosis. In: Wexler P, editor. *Encyclopedia of Toxicology (Third Edition)*. Oxford: Academic Press; 2014, p. 287-94.
- [247] Du J, Cai J, Wang S, You H. Oxidative stress and apoptosis to zebrafish (*Danio rerio*) embryos exposed to perfluorooctane sulfonate (PFOS) and ZnO nanoparticles. *Int J Occup Med Environ Health*. 2017 30:213-29.
- [248] Bai DP, Zhang XF, Zhang GL, Huang YF, Gurunathan S. Zinc oxide nanoparticles induce apoptosis and autophagy in human ovarian cancer cells. *Int J Nanomedicine*. 2017 12:6521-35.
- [249] El-Shorbagy HM, Eissa SM, Sabet S, El-Ghor AA. Apoptosis and oxidative stress as relevant mechanisms of antitumor activity and genotoxicity of ZnO-NPs alone and in combination with N-acetyl cysteine in tumor-bearing mice. *Int J Nanomedicine*. 2019 14:3911-28.
- [250] Kiss T. Apoptosis and its functional significance in molluscs. *Apoptosis*. 2010 15:313-21.
- [251] Singh N, Manshian B, Jenkins GJS, Griffiths SM, Williams PM, Maffei TGG, et al. NanoGenotoxicology: The DNA damaging potential of engineered nanomaterials. *Biomaterials*. 2009 30:3891-914.
- [252] Kyriakis JM, Avruch J. Mammalian MAPK signal transduction pathways activated by stress and inflammation: a 10-year update. *Physiol Rev*. 2012 92:689-737.
- [253] Owens DM, Keyse SM. Differential regulation of MAP kinase signalling by dual-specificity protein phosphatases. *Oncogene*. 2007 26:3203-13.
- [254] Chuang S-M, Wang I-C, Yang J-L. Roles of JNK, p38 and ERK mitogen-activated protein kinases in the growth inhibition and apoptosis induced by cadmium. *Carcinogenesis*. 2000 21:1423-32.
- [255] Qu M, Li D, Zhao Y, Yuan Y, Wang D. Exposure to low-dose nanopolystyrene induces the response of neuronal JNK MAPK signaling pathway in nematode *Caenorhabditis elegans*. *Environmental Sciences Europe*. 2020 32:58.
- [256] Zhao X, Rao Y, Liang J, Lin S, Wang X, Li Z, et al. Silver Nanoparticle-Induced Phosphorylation of Histone H3 at Serine 10 Involves MAPK Pathways. *Biomolecules*. 2019 9:78.
- [257] Kang SJ, Kim BM, Lee YJ, Hong SH, Chung HW. Titanium dioxide nanoparticles induce apoptosis through the JNK/p38-caspase-8-Bid pathway in phytohemagglutinin-stimulated human lymphocytes. *Biochemical and Biophysical Research Communications*. 2009 386:682-7.
- [258] Medzhitov R. Inflammation 2010: new adventures of an old flame. *Cell*. 2010 140:771-6.
- [259] Nathan C, Ding A. Nonresolving inflammation. *Cell*. 2010 140:871-82.
- [260] Chen L, Deng H, Cui H, Fang J, Zuo Z, Deng J, et al. Inflammatory responses and inflammation-associated

- diseases in organs. *Oncotarget*. 2018 9:7204-18.
- [261] Ferrero-Miliani L, Nielsen OH, Andersen PS, Girardin SE. Chronic inflammation: importance of NOD2 and NALP3 in interleukin-1beta generation. *Clinical and experimental immunology*. 2007 147:227-35.
- [262] Zhou Y, Hong Y, Huang H. Triptolide Attenuates Inflammatory Response in Membranous Glomerulo-Nephritis Rat via Downregulation of NF-κB Signaling Pathway. *Kidney Blood Press Res*. 2016 41:901-10.
- [263] Cho WS, Duffin R, Howie SEM, Scotton CJ, Wallace WAH, MacNee W, et al. Progressive severe lung injury by zinc oxide nanoparticles; the role of Zn²⁺ dissolution inside lysosomes. *Particle and Fibre Toxicology*. 2011 8.
- [264] Chang H, Ho CC, Yang CS, Chang WH, Tsai MH, Tsai HT, et al. Involvement of MyD88 in zinc oxide nanoparticle-induced lung inflammation. *Experimental and Toxicologic Pathology*. 2013 65:887-96.
- [265] Martínez-Gutierrez F, Thi EP, Silverman JM, de Oliveira CC, Svensson SL, Vanden Hoek A, et al. Antibacterial activity, inflammatory response, coagulation and cytotoxicity effects of silver nanoparticles. *Nanomedicine*. 2012 8:328-36.
- [266] Roma J, Matos AR, Vinagre C, Duarte B. Engineered metal nanoparticles in the marine environment: A review of the effects on marine fauna. *Marine Environmental Research*. 2020 161:105110.
- [267] Letterio JJ, Roberts AB. Regulation of immune responses by TGF-beta. *Annu Rev Immunol*. 1998 16:137-61.
- [268] Hoesel B, Schmid JA. The complexity of NF-κB signaling in inflammation and cancer. *Molecular Cancer*. 2013 12:86.
- [269] Wu F, Sokolov EP, Khomich A, Fettekenhauer C, Schnell G, Seitz H, et al. Interactive effects of ZnO nanoparticles and temperature on molecular and cellular stress responses of the blue mussel *Mytilus edulis*. *Science of The Total Environment*. 2022 818:151785.
- [270] van der Gaag M, van der Velde G, Wijnhoven S, Leuven RSEW. Salinity as a barrier for ship hull-related dispersal and invasiveness of dreissenid and mytilid bivalves. *Marine Biology*. 2016 163:147-.
- [271] Attrill MJ, Rundle SD. Ecotone or Ecocline: Ecological Boundaries in Estuaries. *Estuarine, Coastal and Shelf Science*. 2002 55:929-36.
- [272] Telesh IV, Schubert H, Skarlato SO. Revisiting Remane's concept: evidence for high plankton diversity and a protistan species maximum in the horohalinicum of the Baltic Sea. *Marine Ecology Progress Series*. 2011 421:1-11.
- [273] Oliver JD. *Vibrio vulnificus*. In: F. L. Thompson, B. Austin, (ed.) *JS, editors. The Biology of Vibrios*. Washington, DC.: American Society for Microbiology 2006, p. 349-66.
- [274] Hamer B, Jaksic Z, Pavicic-Hamer D, Peric L, Medakovic D, Ivankovic D, et al. Effect of hypoosmotic stress by low salinity acclimation of Mediterranean mussels *Mytilus galloprovincialis* on biological parameters used for pollution assessment. *Aquat Toxicol*. 2008 89:137-51.
- [275] Blanco-Rayón E, Ivanina AV, Sokolova IM, Marigómez I, Izagirre U. Food-type may jeopardize biomarker interpretation in mussels used in aquatic toxicological experimentation. *PLoS ONE*. 2019 14:e0220661.

7. Appendix

My contributions to the publications included in this thesis.

Publication 1: Wu, FL and Sokolova I. M. (2021). Science of the Total Environment 801, 149786.

“Immune responses to ZnO nanoparticles are modulated by season and environmental temperature in the blue mussels Mytilus edulis”

The experiments and manuscript writing were mostly done by me. My overall contribution is approximately 80%.

Publication 2: Wu, FL, Falfushynska, H, Dellwig, O., Piontkivska, H. and Sokolova, I. M. (2020). Science of The Total Environment 712, 136473.

“Interactive effects of salinity variation and exposure to ZnO nanoparticles on the innate immune system of a sentinel marine bivalve, Mytilus edulis”

I performed approximately half of the experiments (including exposures and assays) and wrote large sections of the manuscript. My overall contribution is about 55%.

Publication 3: Wu, FL, Sokolov, E. P, Dellwig, O. and Sokolova, I. M. (2021). Chemosphere 263, 127780.

“Season-dependent effects of ZnO nanoparticles and elevated temperature on bioenergetics of the blue mussel Mytilus edulis”

In this work, I did a large part of the experiments and manuscript writing. My overall contribution to this work is approximately 80%.

Publication 4: Noor, M. N, Wu, FL, Sokolov, E. P, Falfushynska, H, Timm, S, Haider, F. and Sokolova, I. M. (2021). Science of The Total Environment 774, 145195.

“Salinity-dependent effects of ZnO nanoparticles on bioenergetics and intermediate metabolite homeostasis in a euryhaline marine bivalve, Mytilus edulis”

I have contributed to the assessments of CEA and the manuscript preparation. My overall contribution is approximately 20%.

Publication 5: Wu, FL, Sokolov, E. P., Khomich, A., Fettkenhauer, C., Schnell, G., Seitz, H. and Sokolova, I. M. (2021). Science of The Total Environment 818, 151785.

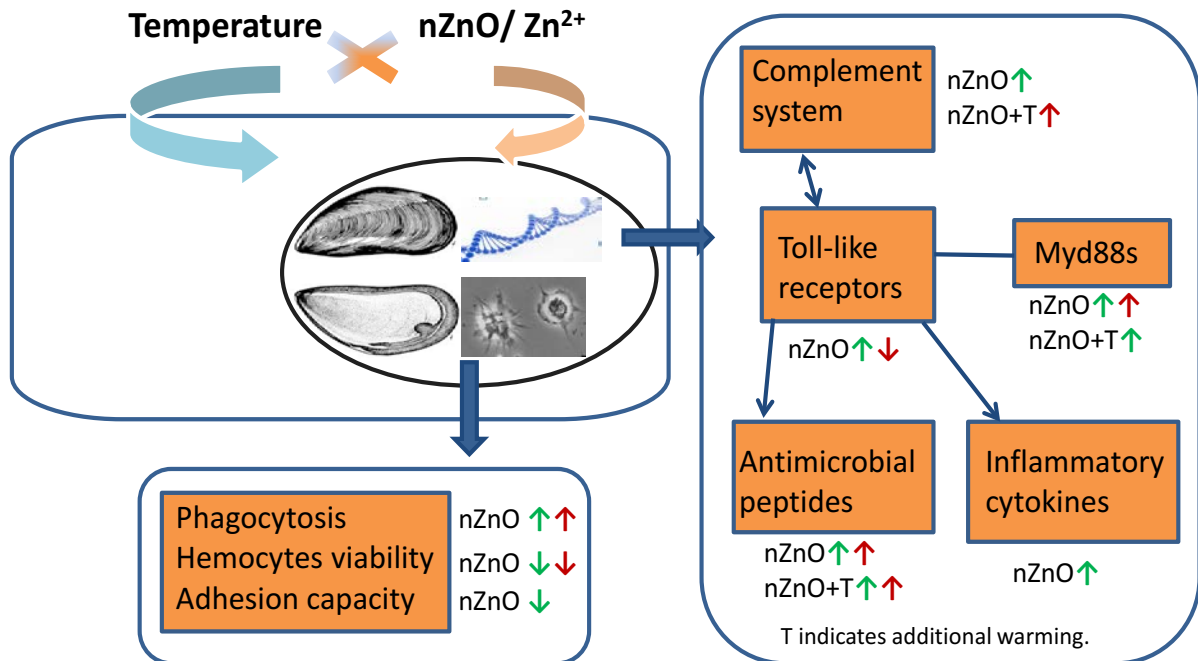
“Interactive effects of ZnO nanoparticles and temperature on molecular and cellular stress responses of the blue mussel Mytilus edulis”

In this work, I performed most experiments and manuscript writing, and co-supervised a guest researcher (Mr. Khomich) who contribute to assessment of molecular stress markers. My overall contribution to this work is about 75%.

7.1. Immune responses to ZnO nanoparticles are modulated by season and environmental temperature in the blue mussels *Mytilus edulis*

Wu FL and Sokolova I. M. (2021). Science of the Total Environment 801, 149786.

DOI: <https://doi.org/10.1016/j.scitotenv.2021.149786>





Immune responses to ZnO nanoparticles are modulated by season and environmental temperature in the blue mussels *Mytilus edulis*

Fangli Wu^a, Inna M. Sokolova^{a,b,*}

^a Department of Marine Biology, Institute for Biological Sciences, University of Rostock, Rostock, Germany

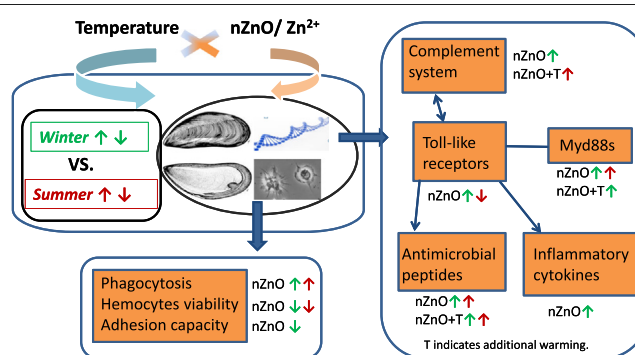
^b Department of Maritime Systems, Interdisciplinary Faculty, University of Rostock, Rostock, Germany



HIGHLIGHTS

- In winter mussels, nZnO induced a strong transcriptomic response and stimulated phagocytosis.
- In summer mussels, the immune cell responses to nZnO were blunted.
- The transcriptional responses to dissolved Zn were weaker than the responses to nZnO.
- Warming leads to dysregulation of the transcriptomic response in summer but not in winter.
- Warming suppressed the nZnO-induced transcriptional upregulation in summer but not in winter.

GRAPHICAL ABSTRACT



ARTICLE INFO

Article history:

Received 26 May 2021

Received in revised form 22 July 2021

Accepted 16 August 2021

Available online 20 August 2021

Editor: Lotfi Aleya

Keywords:

Warming

nZnO

Mussel

Hemocyte

Immune response

Seasonality

mRNA expression

ABSTRACT

Increased production and release of ZnO nanoparticles (nZnO) can cause toxic effects on marine ecosystems and aquatic organisms. However, nZnO toxicity and its modulation by common environmental stressors such as temperature are not yet fully understood. We examined the responses of immune cells (hemocytes) of the blue mussels (*Mytilus edulis*) exposed to different concentrations (0, 10, 100 $\mu\text{g l}^{-1}$) of nZnO or dissolved zinc combined with two temperatures (ambient (10 °C in winter and 15 °C in summer) and warming (+5 °C above ambient temperature)) in winter and summer for 21 days. In winter mussels, exposure to nZnO induced a strong transcriptomic response in multiple immune and inflammation-related genes, stimulated phagocytosis and hemocyte mortality yet suppressed adhesion capacity of hemocytes. In summer mussels, the immune cell responses to nZnO were blunted. The transcriptional responses of hemocytes to dissolved Zn were qualitatively similar but weaker than the responses to nZnO. In the absence of the toxic stress, +5 °C warming lead to dysregulation of the transcription of key immune-related genes in the summer but not the winter mussels. Seasonal warm acclimatization and additional warming in summer suppressed the nZnO-induced transcriptional upregulation of antimicrobial peptides, Toll-like receptors and the complement system. These findings demonstrate that nZnO act as an immunogen in *M. edulis* and indicate that +5 °C warming might have detrimental effect on innate immunity of the temperate mussel populations in summer when exposure to pathogens is especially high.

Capsule: ZnO nanoparticles act as an immunotoxicant inducing a strong immune response in the mussels which is dysregulated by warming in summer but not in winter.

© 2021 Elsevier B.V. All rights reserved.

* Corresponding author at: Department of Marine Biology, Institute for Biological Sciences, University of Rostock, Rostock, Germany.
E-mail address: inna.sokolova@uni-rostock.de (I.M. Sokolova).

1. Introduction

Engineered nanoparticles (with at least one dimension <100 nm) are contaminants of emerging concern (CECs) in the coastal and marine environments and a potential threat to humans and coastal ecosystems (Garner and Keller, 2014; Williams et al., 2019). Zinc oxide nanoparticles (nZnO) are commonly used in antifouling, antimicrobial substances and UV screens (Read et al., 2016; Williams et al., 2019). Quantitative assessment of nZnO in the marine environment is complicated by the lack of the analytical approaches to measure ZnO in complex environmental matrices such as the sea water or sediment, but predicted environmental concentrations (PECs) of nZnO reach hundreds ng l⁻¹ in the European natural surface water (Coll et al., 2016; Dumont et al., 2015; Gottschalk et al., 2013; Hong et al., 2021) and up to 100 µg kg⁻¹ in the sediment (Gottschalk et al., 2013; Yung et al., 2014). Recent studies showed negative impacts of high nZnO concentrations (0.1–4 mg l⁻¹) on physiological performance of benthic marine organisms including suppression of growth (Hanna et al., 2013; Muller et al., 2014), reproduction (Fabrega et al., 2012) and immune response (Wu et al., 2020; Wu et al., 2018), as well as disturbances in bioenergetics and redox status (Trevisan et al., 2014; Wu et al., 2021). However, immunotoxic effects of nZnO have not yet been extensively studied in marine organisms, especially in the context of natural variability of other abiotic stressors common in the coastal environments.

Innate immunity is the most important defense of marine bivalves against pathogens, parasites and tissue injury (Mydlarz et al., 2006). Blood cells (hemocytes) play a key role in the innate immune defense of molluscs as they encapsulate or destroy pathogens and foreign bodies, produce antimicrobial peptides and reactive intermediates involved in the pathogen killing, and participate in tissue healing and shell repair (Allam and Raftos, 2015; Hughes et al., 2010; Kwon et al., 2014; Sokolova, 2009). Hemocytes are among the earliest responders to environmental insults including toxins and abiotic stressors in marine bivalves (Jenny et al., 2002; Lacoste et al., 2002; Perez and Fontanetti, 2010; Roch, 1999). This makes the immune system of bivalves an important target for toxicity of CECs including nZnO. Studies in marine bivalves including mussels showed that exposures to ZnO nanoparticles can decrease total hemocyte counts, phagocytosis capacity and oxidative burst of hemocytes (Wu et al., 2018), induce DNA damage (Katsumiti et al., 2016; Marisa et al., 2016), and suppress the expression of the immune related genes (Wu et al., 2020).

Temperature is an important abiotic factor that influences ectotherms' performance through the direct effects on biological rates and stability of macromolecules (Schiedek et al., 2007). In temperate shallow coasts including the Baltic Sea, temperature varies on seasonal and diurnal basis, combined with the long-term warming trend due to the global climate change (Mackenzie and Schiedek, 2007). In northern and central Europe, the mean air temperature is predicted to increase by 5–8 °C by the end of this century (IPCC, 2014). Temperature could influence nanoparticles' toxicity in aquatic organisms (Falfushynska et al., 2015; Falfushynska et al., 2019a; Yung et al., 2017) and has an important immunomodulatory effect in marine organisms (Beaudry et al., 2016; Malagoli et al., 2007; Matozzo et al., 2012; Rahman et al., 2019). The effects of the temperature on the immune parameters of bivalves vary from stimulating to suppressing depending on the thermal tolerance of a species and the degree of the deviation of the temperature from the species-specific temperature optimum (Beaudry et al., 2016; Malagoli et al., 2007; Matozzo et al., 2012; Rahman et al., 2019). In freshwater bivalves such as the swollen river mussel, *Unio tumidus*, temperature was found to modulate the immunotoxicity of nZnO (Falfushynska et al., 2015). Furthermore, the temperature-dependent biological responses to nanoparticles might vary seasonally as was shown in springtails *Folsomia candida* (Zhang and Filser, 2020) and the blue mussels *Mytilus edulis* (Wu et al., 2021). Impairment of the immune functions caused by the nanoparticles and elevated temperature can have wide-ranging ecological consequences potentially affecting

the morbidity and mortality caused by pathogens, parasites or injury (Renault, 2015). Therefore, understanding of the potential combined effects of nanomaterials and warming (such as occurs seasonally or due to the climate change) is of great significance for assessing the ecological risks of nanopollutants in marine environments (Holmstrup et al., 2010; Wu et al., 2021).

In this work, we determined the combined effects of seasonality (winter and summer), warming (+5 °C above ambient temperature) and exposure to different concentrations of nZnO (or dissolved Zn as a positive control for the effects of Zn²⁺ release) on innate immune response in the hemocytes of *M. edulis* from the Baltic Sea. Mussels of the genus *Mytilus* are important biological indicator species in temperate ecosystems worldwide and, as filter-feeders, are sensitive to nanoparticle toxicity (Beyer et al., 2017). We hypothesized that nZnO will negatively affect the innate immune response in the mussels and that the negative effects of nZnO on immunity will be modulated by warming and seasonality. We determined the total hemocytes count, hemocytes mortality, adhesion capacity, phagocytosis and lysosomal status in hemocytes of *M. edulis* exposed for 21 days to different combinations of temperature and nZnO. Molecular immune profile of the hemocytes was assessed by mRNA expression of the key immune-related genes including the pathogen recognition factors (Toll-like receptor b and c), antimicrobial peptides (myticin, mytilin and defensin), complement systems (C1 and C3q), inflammatory cytokines (TNF and TGF-β), and MyD88 innate immune signal transduction adaptors (MyD88a and MyD88c). Our study shows that the effects of the nanopollutants such as nZnO on the innate immunity of the mussels are temperature- and season-dependent and provides new insights into the potential effects of nZnO on immunocompetence of the mussels in polluted temperate coasts.

2. Materials and methods

2.1. Mussel collection and exposures

The samples analyzed here were collected in the same experiment as described elsewhere (Wu et al., 2021). The details of the mussel collection and maintenance, experimental exposures, as well as determination of Zn concentrations in the seawater and the mussels' body are provided in our earlier report (Wu et al., 2021). Briefly, the adult *M. edulis* (shell length, 56 ± 6 mm) were collected in late October 2018 (winter experiment: the average seawater temperature ~ 10 °C) and June 2019 (summer experiment: the average seawater temperature ~ 15 °C) from the same site at a water depth of about 1 m near coastlines of Warnemünde, Germany (54°10'49.602"N, 12°05'21.991"E) (Supplementary Fig. 1). The study site is characterized by low pollution levels. The two collection periods corresponded to the reproductive rest (October) and spawning (June) in the Baltic Sea *Mytilus* spp. (Benito et al., 2019; Kautsky, 1982). Habitat salinity at the collection site was 10–16 (practical salinity units).

The experimental exposures followed the protocols described in Wu et al. (2021). Briefly, after the two-week preliminary acclimation (salinity 15 and the season-specific control temperature of 10 °C and 15 °C for the winter and summer mussels, respectively), the mussels were exposed for 21 days to different temperatures, nZnO and dissolved Zn levels. Within each season, the mussels were divided into ten treatments and exposed to ambient (10 °C in winter and 15 °C in summer similar to the temperature at the time of collection) or elevated (by 5 °C) temperature combined with different concentrations (0, 10, 100 µg l⁻¹) of nZnO or dissolved zinc using a static-renewal design. For each treatment, three replicate tanks, each containing 20 mussels in 6 l of seawater was used. The mussels were fed every two days with a commercial blend of live algae containing *Nannochloropsis oculata*, *Phaeodactylum* sp. and *Chlorella* sp. (Premium Reef Blend, CoralSands, Wiesbaden, Germany) per manufacturer's instructions. Artificial seawater (Instant Ocean®) was used in this study

and supplemented with 20% of the filtered natural Baltic seawater (salinity ~12) to achieve salinity 15.

During each water change, fresh nZnO suspensions were made from the same stock and sonicated prior to addition to the experimental tanks. Following addition of nZnO or dissolved Zn (as ZnSO₄), the water in experimental tanks was vigorously mixed to ensure chemicals' distribution. Further details of the mussels' maintenance and exposures are provided in the supplementary materials (SI Appendix). Preparation and characterization of nZnO and ZnSO₄ were described elsewhere [(Falfushynska et al., 2019b), see SI Appendix for the detailed information]. The average particle size and zeta-potential of nZnO used in these experiments was 30 nm and -9.6 mV, respectively (Supplementary Figs. 1 and 3). The size of the nanoparticle aggregates has been determined as the hydrodynamic diameter (~817 nm at salinity 15) by Dynamic Light Scattering (DLS) (Supplementary Fig. 3). Pilot studies showed that the dissolved Zn concentrations in the seawater in nZnO exposures were not significantly above the normal seawater background indicating that there was no considerable dissolution of nZnO during exposures, likely due to frequent water change (data not shown). Total Zn concentrations (including dissolved and particulate Zn) and Zn accumulation in the mussels from the same exposures as used in the present study are reported elsewhere (Wu et al., 2021). No mortality of the mussels occurred during the experiment.

Elevated temperatures (by 5 °C) were chosen to represent the predicted warming condition in natural habitats of the Baltic Sea mussels *Mytilus* spp. according to the near-future (2100) climate change scenarios (IPCC, 2014). As the predicted no observed effect concentration (PENC) for nZnO is 0.2–5 µg l⁻¹ (Chen et al., 2018a; Coll et al., 2016; Hong et al., 2021), we selected two nZnO levels (10 µg l⁻¹ as low concentration and 100 µg l⁻¹ as high concentration) for hazard assessment to detect sub-lethal physiological effects. Exposure to 10 µg l⁻¹ and 100 µg l⁻¹ of dissolved zinc was used as a positive control to test whether the toxic effects of nZnO might be due to the potential release of Zn²⁺ due to the nanoparticles dissolution. The durations of the preliminary acclimation (14 days) and experimental exposures (21 days) were considered sufficient to reach physiological steady-state in the mussels (Berger, 1986; Khlebovich, 2017). After 21 days of experimental exposures, mussels were dissected and hemolymph was collected for further analyses of the functional traits and immune gene expression in hemocytes.

2.2. Hemolymph collection

Hemolymph was collected from the posterior adductor muscle of mussels using a 1.0 ml syringe with a 21 gauge needle. All samples were mixed with 1 ml ice cold sterile-filtered artificial seawater and stored on ice to minimize aggregation of hemocytes. To reduce the variability among biological replicates and obtain sufficient material for all analyses, each biological replicate represented pooled hemolymph from six mussels (0.6–1.0 ml hemolymph per mussel) from the same replicate tank. A total of three biological replicates was used to measure functional traits and gene expression of hemocytes. For the functional traits measurements, hemolymph samples were used immediately after collection. For mRNA expression measurements, hemolymph was centrifuged for 10 min at 1000 ×g, the hemocyte pellet was washed once with ice-cold filtered seawater and kept at -80 °C for further analysis.

2.3. Functional traits

Total hemocytes count (HC) was determined using a Brightline hemocytometer (Sigma Aldrich, St. Louis, MO, USA) and expressed as the amount of cells per ml haemolymph. Hemocyte mortality (HM) was determined using Trypan Blue exclusion assay and expressed in the percentage of the blue-stained (dead) hemocytes relative to the total hemocyte count in each sample. Adhesion capacity (AD) of hemocytes

was measured by a 12-well plate (Costar, Corning) as the percentage of adhered hemocytes in the hemocyte population of 10⁶ cells per well. Five technical replicates were done for each biological replicate to measure HC, HM and AD, and the values of five technical replicates were averaged. Other details of analyses can be found elsewhere (Wu et al., 2020).

Phagocytosis rate (Pha) was measured as the number of engulfed zymosan particles per cell (Coles et al., 1995). Briefly, suspension of Neutral Red-stained, heat-stabilized zymosan (Sigma Aldrich, St. Louis, MO, USA) was added to hemocytes at the final concentration of 200 zymosan particles per hemocyte. Hemocytes were incubated for 30 min at room temperature, centrifuged 10 min at 1000 ×g, resuspended in 2 ml ice cold ASW to remove free and surface-attached zymosan particles, and centrifuged again for 10 min at 1000 ×g to collect the hemocytes. For calibration, a cell-free solution with the known number of the zymosan particles was used. The Neutral Red dye was extracted from the hemocyte samples and the standards by incubation in 0.1 ml acetic acid (1% in 50% ethanol) for 5 min. The absorbance was determined at 550 nm by a 96-well plate on a SpectraMax ID3 Multi-Mode Microplate Reader (Molecular Devices, USA).

Neutral red uptake (NRU) was measured in hemocytes and was expressed in absorbance units (AU) per 10⁶ hemocytes. Briefly, hemolymph samples were centrifuged for 10 min at 600 ×g, 4 °C and resuspended in 2 ml of HEPES-buffer containing 20 mM 4-(2-hydroxyethyl)-1-piperazineethanesulfonic acid (HEPES), 436 mM NaCl, 53 mM MgSO₄, 10 mM KCl, 10 mM CaCl₂, pH 7.3 (Marchi et al., 2004). Hemocytes were washed three times by centrifugation-resuspension and resuspended in 0.2 ml HEPES-buffer at the concentration of 10⁷ cells ml⁻¹. Hemocyte suspension (1 ml containing 10⁷ cells) was added to 0.5 ml of physiological saline with 0.004% w/v Neutral Red, incubated for 2 h and centrifuged 10 min at 600 ×g. Hemocytes were washed twice to remove the free dye, and resuspended in 1 ml HEPES-buffer. The dye was extracted from the cell suspensions with 0.2 ml an acetic acid-ethanol mixture (1:1 v/v). Absorbance was measured at 550 nm using a 96-well plate on a SpectraMax iD3 Multi-Mode Microplate Reader (Molecular Devices, USA).

2.4. mRNA expressions of key immune-related genes

For analysis of the transcript levels of immune-related genes (Table 1), total RNA was isolated from hemocytes, and cDNA synthesis and quantitative PCR were conducted as described elsewhere (Wu et al., 2020). The primer sequences and the details of the mRNA expression analyses are provided in Table 1 and SI Appendix, respectively. The apparent amplification efficiency was calculated for each primer pair, and the expression of the target genes was normalized against the expression of the eukaryotic elongation factor eEF1 (Pfaffl, 2001). The results was expressed as fold change in mRNA expression in the treated group relative to the mRNA expression in the respective control group (no Zn additions and ambient temperature corresponding to 10 °C in winter and 15 °C in summer).

2.5. Statistics

The effects of Zn treatment, temperature regime and their interactions on the studied traits were tested separately for each season by two-way analysis of variance (ANOVA). Further, the interactive effects of Zn treatment and season at a common temperature (15 °C) were tested by two-way ANOVA. Prior to analyses, data were checked for normality and homogeneity of variances using the Shapiro-Wilks and Levene's tests, respectively. Data deviating from the normal distribution were Box-Cox transformed. The significant effects of Zn treatments were analyzed using Tukey's Honest Significant Difference (HSD) test within each temperature regime, and the effects of temperature were analyzed by a Student's *t*-test within each Zn treatment. The principal component analysis (PCA) and discriminant analysis (DA) were carried out on the

Table 1

Primer sequences for the target and housekeeping genes used for qPCR.

NCBI accession numbers of the sequences used for primer design are given. When no sequence information was available for *M. edulis*, we used homologous sequences from closely related *Mytilus* species (*M. galloprovincialis*, or *M. coruscus*) to generate primers. For TGF- β we used earlier published primers from *M. coruscus* (Qi et al., 2019). Gene abbreviations: TLRb - Toll-like receptor b; TLRc - Toll-like receptor c; C1 - C1 complement domain-containing protein; C3q - Complement component C3-like protein; MyD88a - Myeloid differentiation primary response gene 88 a; Myd88c - Myeloid differentiation primary response gene 88 c; TNF - Tumor necrosis factor; TGF- β - Transforming growth factor-beta; eEF1 - Eukaryotic elongation factor 1 α .

Gene	Forward primer (5'-3')	Reverse primer (5'-3')	NCBI accession #	T _{read}
Myticin	CAGAGGCAAGTTGTGCTTCC	GGAATGCTCACTGGAACAACG	AF177540	77 °C
Mytilin	GGCGTGTACTGCAAAATGT	TGTTCCGTTTCTCTGTGGG	AF162336	78 °C
Defensin	CAGCAAATGCAAGGGAGGT	TGGCGCAATCCAAC TAGA	JN935272	79 °C
TLRb	TGATTGGCCGTAGAGGAGC	CATACACAGTGTCTCGCT	JX173687	77 °C
TLRc	ATCCCGAGAAGTATCGCTGC	CAAAAGGGGACAGCGATCA	JX173688	76 °C
C1	GGCATTAAACATCAGGAGCG	TACGTCCCTTACGTGGAGC	HQ664950	76 °C
C3q	TGATTTGTCGGGGAAAGTGG	GCAGACCTGCCTGTTCTTCT	KP125947	79 °C
MyD88a	AGGATTCGAGGACAGCGAAG	GGCCAAACCAATCTCGTTC	JX112712.1	74 °C
Myd88c	TCTTGCTGGAGGGGCAAAAT	GCACCTGGCGTAATGATTG	KC357782.1	75 °C
TNF	ATGTGCCAATCCCTGTCT	TCTGCTGTACCTGTTACC	KC994893	75 °C
TGF- β	TGCGGGTAAACCAAGACCA	TCCTGGCGGCTCAATTAC	-	76 °C
eEF1	GACAGCAAAAACGACCCACC	TTCTCCAGGGTGGTTCAGGA	AF063420	77 °C

normalized data. Further details of the statistical tests are described in SI Appendix. The analyses were performed using SPSS 18.0 and GraphPad Prism 6.0. The results were expressed as the means \pm the standard error (SE) and the effects were considered significant at $P < 0.05$.

3. Results

In winter mussels' hemocytes, the ANOVA results showed significant effects of Zn exposure \times temperature interactions ($P < 0.05$) for HM, Pha, NRU and the transcript levels of defensin and Myd88c (SI Appendix, Supplementary Table 1A). In summer mussels' hemocytes, the Zn exposure \times temperature interactions were significant ($P < 0.05$) for Pha, NRU and the transcript levels of most studied genes except defensin, C3q and Myd88a (SI Appendix, Supplementary Table 1B). At a common temperature of 15 °C, significant effects of season and the interactions between season and Zn treatment were found for Pha, NRU and the expressions of most of the studied genes ($P < 0.05$) (SI Appendix, Supplementary Table 2).

3.1. Hemocytes functions

No significant effects of nZnO or dissolved zinc were observed on the total hemocyte counts (Fig. 1A, B). Within each season, warming had no significant effect on the total hemocyte counts (Fig. 1A, B). Generally, hemocyte mortality increased with increasing of nZnO or dissolved zinc concentrations at all temperature \times season combinations (Fig. 1C, D). Within each season, warming had no significant effect on the hemocyte mortality (Fig. 1C, D).

In winter mussels, a slight but statistically significant ($P < 0.05$) decrease was observed in adhesion capacity when the mussels were exposed to high nZnO at 10 °C or 15 °C, whereas dissolved zinc exposure had no significant effect on this trait (Fig. 1E). In the winter Zn²⁺ exposed mussels, elevated temperature (15 °C) improved the adhesion capacity of hemocytes (Fig. 1E). No significant effects of the warming, nZnO or dissolved zinc groups were observed on the hemocyte adhesion capacity in the summer mussels (Fig. 1F).

Exposure to nZnO (10 or 100 $\mu\text{g l}^{-1}$) and dissolved Zn (100 $\mu\text{g l}^{-1}$ only) stimulated phagocytosis in all temperature \times season combinations except for the winter mussels at 15 °C (Fig. 2A, B). In control mussels, elevated temperatures stimulated phagocytosis (Fig. 2A, B). Warming also stimulated phagocytosis in the nZnO-exposed summer mussels, whereas this trend was reversed in the winter (Fig. 2A, B).

Exposure to 10 or 100 $\mu\text{g l}^{-1}$ of nZnO significantly increased the neutral red uptake (NRU) of the hemocytes in the winter and summer (Fig. 2C, D). A similar trend was found in the mussels exposed to 100 $\mu\text{g l}^{-1}$ Zn²⁺ in all temperature \times season combinations except for the winter mussels at 15 °C (Fig. 2C, D). In the control and nZnO-

exposed mussels, elevated temperature increased the NRU regardless of the season (Fig. 2C, D). In the mussels exposed to dissolved Zn, a similar effect of warming was observed in summer but not in winter (Fig. 2C, D).

3.2. Immune gene expression

3.2.1. Winter mussels

At 10 °C, nZnO exposure increased the transcript levels of most studied immune-related genes in the mussels' hemocytes (Figs. 3–5A, C, E, G). At 10 °C, the increases of the mRNA levels in the hemocytes of the mussels exposed to 100 $\mu\text{g l}^{-1}$ nZnO (relative to the respective controls) were: \sim 8.0, 3.3 and 3.2-fold for mytilin, myticin and defensin; \sim 5.3 and 3.4-fold for TLRb and TLRc; \sim 6.3 and 11.1-fold for TNF and TGF- β ; \sim 6.7 and 10.0-fold for C1 and C3q; and \sim 4.3 and 2.9-fold for MyD88a and MyD88c, respectively. At 10 °C, the mRNA levels of mytilin (\sim 3.6-fold), TNF (\sim 3.5-fold), TGF- β (\sim 4.7-fold), C1 (\sim 2.8-fold), C3q (\sim 3.7-fold), MyD88a (\sim 2.1-fold) and MyD88c (\sim 1.8-fold) were also significantly elevated in the hemocytes of the mussels exposed to 100 $\mu\text{g l}^{-1}$ dissolved Zn (Figs. 3A, 4E, G and 5A, C, E and G). Expressions of other studied immune-related genes were not significantly affected by dissolved Zn²⁺ exposures at 10 °C (Figs. 3–5A, C, E, and G).

Elevated temperature (15 °C) had no significant influence on the transcript levels of the immune-related genes in the control winter mussels (Figs. 3–5A, C, E, and G). Similar to the pattern observed at 10 °C, exposure to nZnO at 15 °C upregulated the immune gene expression in the hemocytes (Fig. 3–5A, C, E, and G). At 15 °C, the relative increases of the transcript levels of the immune-related genes in the mussels exposed to 100 $\mu\text{g l}^{-1}$ nZnO (relative to the respective controls) were: \sim 3.8, 3.0 and 16.1-fold for mytilin, myticin and defensin; \sim 6.1 and 3.7-fold for TLRb and TLRc; \sim 5.7 and 3.0-fold for TNF and TGF- β ; \sim 5.6 and 7.6-fold for C1 and C3q; and \sim 6.4 and 5.5-fold for MyD88a and MyD88c, respectively. Effects of the dissolved Zn at 15 °C were weaker than those of the corresponding nZnO concentrations, and a significant increase in the mRNA expression (\sim 1.6–3.7-fold above the control) were only found in some immune-related genes of the mussels exposed to 100 $\mu\text{g l}^{-1}$ dissolved Zn (Figs. 3–5A, C, E, and G).

3.2.2. Summer mussels

The transcriptional response to nZnO of most studied immune-related genes (except defensin) was dampened in the summer mussels. Thus, at the ambient summer temperature (15 °C), exposure to 100 $\mu\text{g l}^{-1}$ nZnO increased the transcript levels of defensin and MyD88c (by \sim 7.5 and 3.7-fold, respectively) and decreased the transcript levels of TLRc by \sim 2.3-fold, relative to the control baseline (Figs. 3F, 4D and 5H). Transcript levels of MyD88c were also \sim 3.1-fold

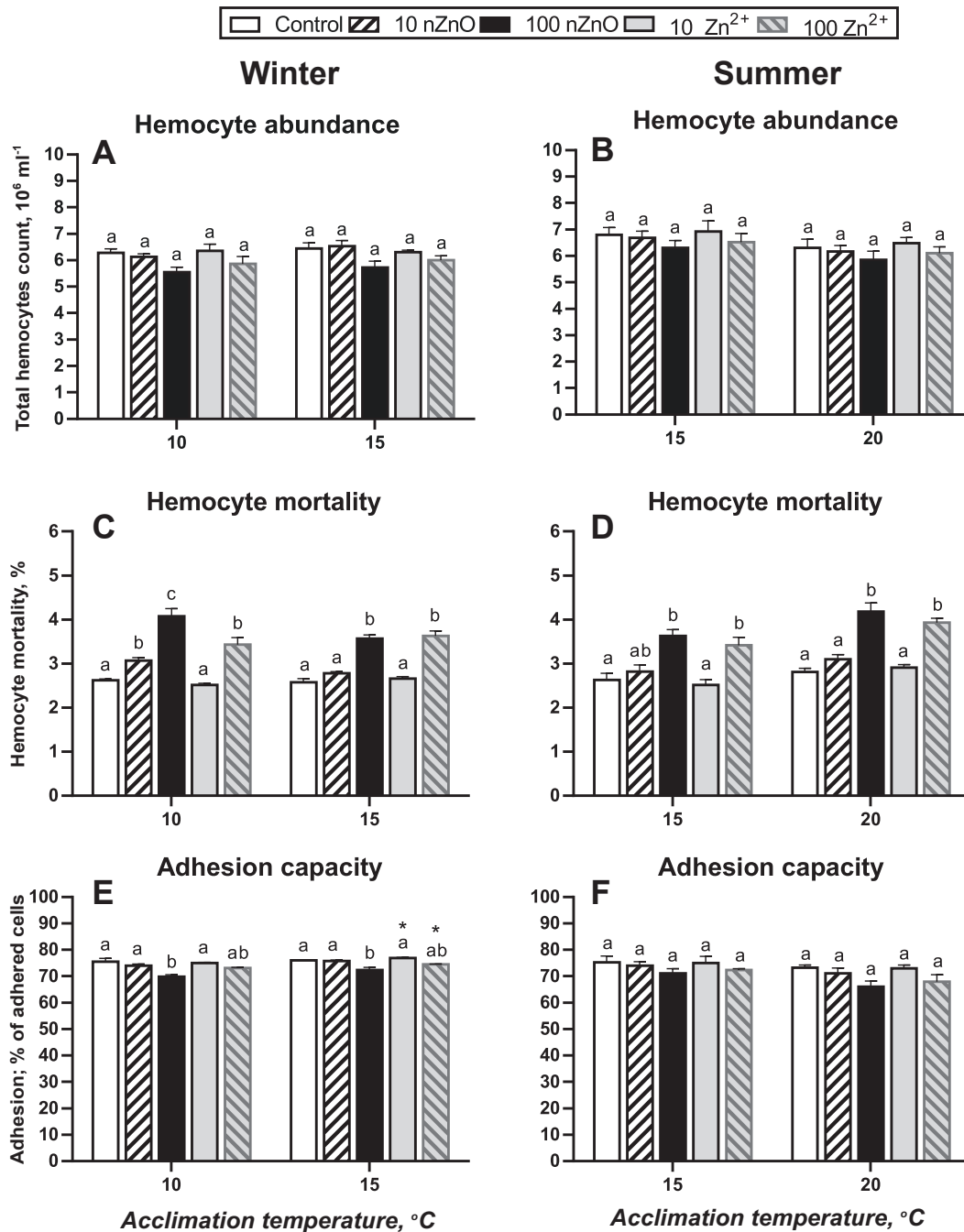


Fig. 1. Functional parameters of hemocytes of *M. edulis* in response to nZnO/Zn²⁺ and temperature exposures.

A, C, E – Winter; B, D, F – Summer; Total hemocytes count (A, B) was expressed as the amount of cells per ml haemolymph; Mortality (C, D) was evaluated as the percentage of the blue-stained hemocytes relative to the total hemocyte count; Adhesion capacity (E, F) was expressed in the percentage of adhered hemocytes in the total hemocyte population (10⁶ cells). Different letters indicate significant differences among nZnO or Zn²⁺ treatments within fixed temperature level (Tukey HSD test, $P < 0.05$), and asterisks indicate significant differences between two temperatures within the same Zn treatment group (t -test, $P < 0.05$). $N = 3$. (For interpretation of the references to colour in this figure legend, the reader is referred to the web version of this article.)

elevated in the hemocytes of the mussels exposed to 10 $\mu\text{g l}^{-1}$ nZnO (Fig. 5H). mRNA expressions of other immune-related genes were not significantly affected by 10 $\mu\text{g l}^{-1}$ or 100 $\mu\text{g l}^{-1}$ of nZnO. Exposure to 10 $\mu\text{g l}^{-1}$ of dissolved Zn suppressed the transcript levels of myticin, mytilin and defensin by ~2.3, 3.1 and 6.8-fold, respectively (Fig. 3B, D, F), whereas exposure to high dissolved Zn elevated the mRNA levels of defensin and C1 (by ~4.9 and 3.4-fold, respectively) and suppressed the mRNA levels of TLRb, TLRc and TGF- β (by ~3.4, 12.6 and 16.9-fold, respectively) (Figs. 3F, 4B, D, H and 5B).

Elevated temperature (20 °C) suppressed mRNA expression of defensin (by ~4.6-fold), TGF- β (by ~9.2-fold) and the complement system C1 (by ~3.9-fold) and upregulated MyD88c (by ~4.1-fold) in the summer control mussels (Figs. 3F, 4H and 5B, H). Transcript levels of other studied immune-related genes were not affected by warming (Figs. 3–5 B, D, F and H). Co-exposure to the elevated temperature (20 °C) and nZnO generally enhanced the transcriptional response of the immune-related genes compared to the responses observed at 15 °C (Figs. 3B, D, F, 4B, H and 5B). At 20 °C, exposure to dissolved Zn

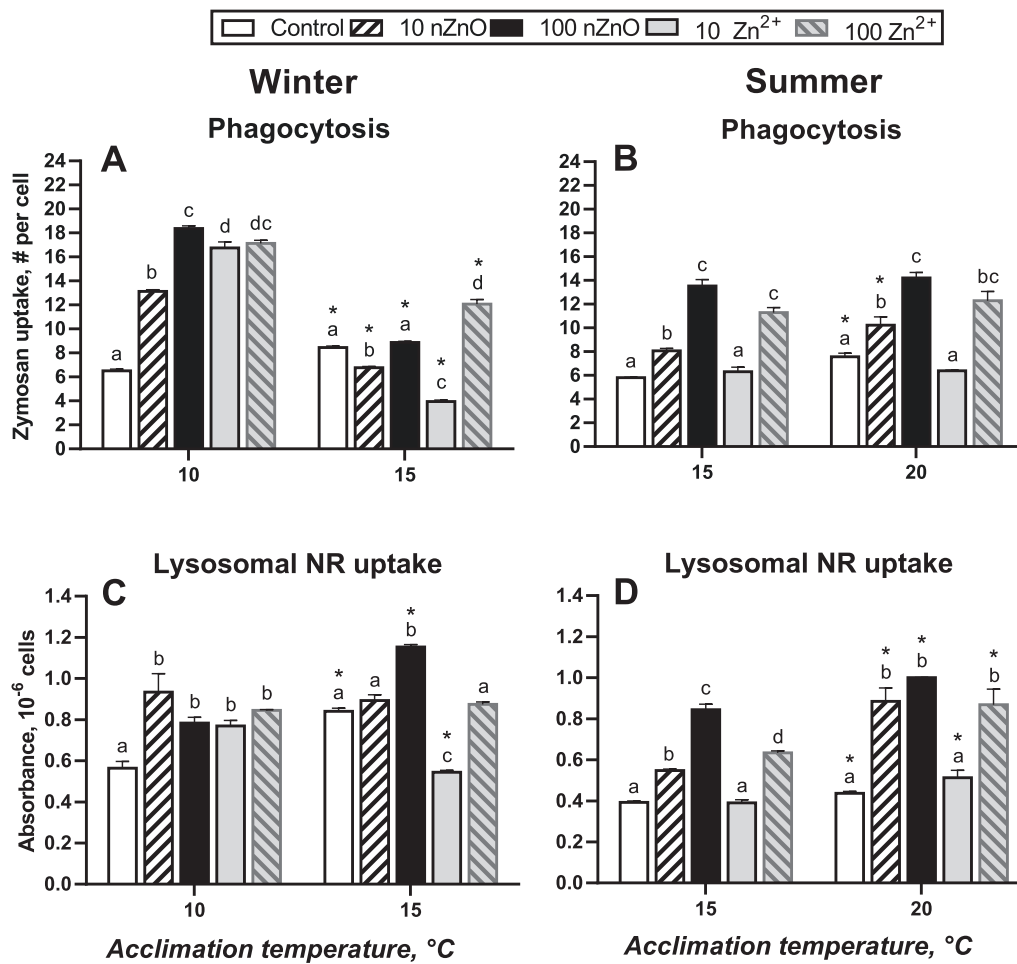


Fig. 2. Functional parameters of hemocytes of *M. edulis* in response to nZnO/Zn²⁺ and temperature exposures.

A, C – Winter; B, D – Summer; Phagocytosis (A, B) was evaluated as the number of ingested zymosan particles per cell; Neutral red uptake (C, D) was expressed in absorbance units (AU) per 10⁶ hemocytes. Different letters indicate significant differences among nZnO or Zn²⁺ treatments within fixed temperature level (Tukey HSD test, $P < 0.05$), and asterisks indicate significant differences between two temperatures within the same Zn treatment group (t -test, $P < 0.05$). $N = 3$. (For interpretation of the references to colour in this figure legend, the reader is referred to the web version of this article.)

had no significant influence on the expression of most of the immune-related genes except for defensin (suppressed by 10 $\mu\text{g l}^{-1}$ Zn²⁺ and up-regulated by 100 $\mu\text{g l}^{-1}$ Zn²⁺) and TGF- β (upregulated by 10 $\mu\text{g l}^{-1}$ Zn²⁺) (Figs. 3–5B, D, F and H).

3.3. Principal component (PCA) and discriminant analysis (DA)

The PCA and DA analyses based on the integrated biomarker profile showed a strong differentiation of the groups acclimated to the high concentration of nZnO from all other groups, as well as clear separation of the elevated temperature and ambient temperature groups in both winter and summer mussels (Figs. 6 and 7).

3.3.1. Winter mussels

In winter mussels, PC1 explained 67.3% of the overall variance and was the main axis associated with Zn exposure (Fig. 6A). The group exposed to the high (100 $\mu\text{g l}^{-1}$) concentration of nZnO was separated from all other groups along the PC1 axis and was associated with the high loadings of mytilin, myticin, TLRb, TLRc, C1, C3q, and TGF- β (Fig. 6B). The position of the control samples overlapped with the groups exposed to the low concentration of dissolved Zn, whereas the groups exposed to low concentration of nZnO or high concentration of dissolved Zn occupied intermediate positions between the controls and the group exposed to high nZnO concentration. In winter mussels, PC2 accounted for 10.1% of the overall variance and presented a

temperature specific response since the groups exposed to the elevated temperature (15 °C) were separated from the ambient winter temperature (10 °C) along this axis (Fig. 6A) associated with high loadings of phagocytosis rate and mRNA expression of defensin (Fig. 6B; Supplementary Table 3).

The DA analysis showed high Mahalanobis distances between the controls and the groups exposed to high concentration of nZnO as well as between the controls and those exposed to 100 $\mu\text{g l}^{-1}$ dissolved Zn (Fig. 6C). The traits that significantly contributed to the discriminant model in the winter mussels included TLRb, C1, C3q, TGF- β , hemocyte mortality, phagocytosis and NRU ($P < 0.05$) (SI Appendix, Supplementary Table 4).

3.3.2. Summer mussels

In summer mussels, PC 1 (34.2% variation) separated the groups exposed to high concentration of nZnO and all other groups (Fig. 7A) and had high loadings of mytilin, defensin, myticin, and MyD88a, hemocyte mortality, phagocytosis and NRU. The PC2 (20.9% variation) separated the elevated temperature (20 °C)-exposed mussels from the ambient temperature (15 °C) group (Fig. 6A) and had high loadings of NRU and mRNA expression of TLRb (Fig. 7B; SI Appendix, Supplementary Table 5).

The DA analysis showed high Mahalanobis distances between the controls and the groups exposed to high concentration of nZnO as well as the controls and the groups exposed to high concentration of

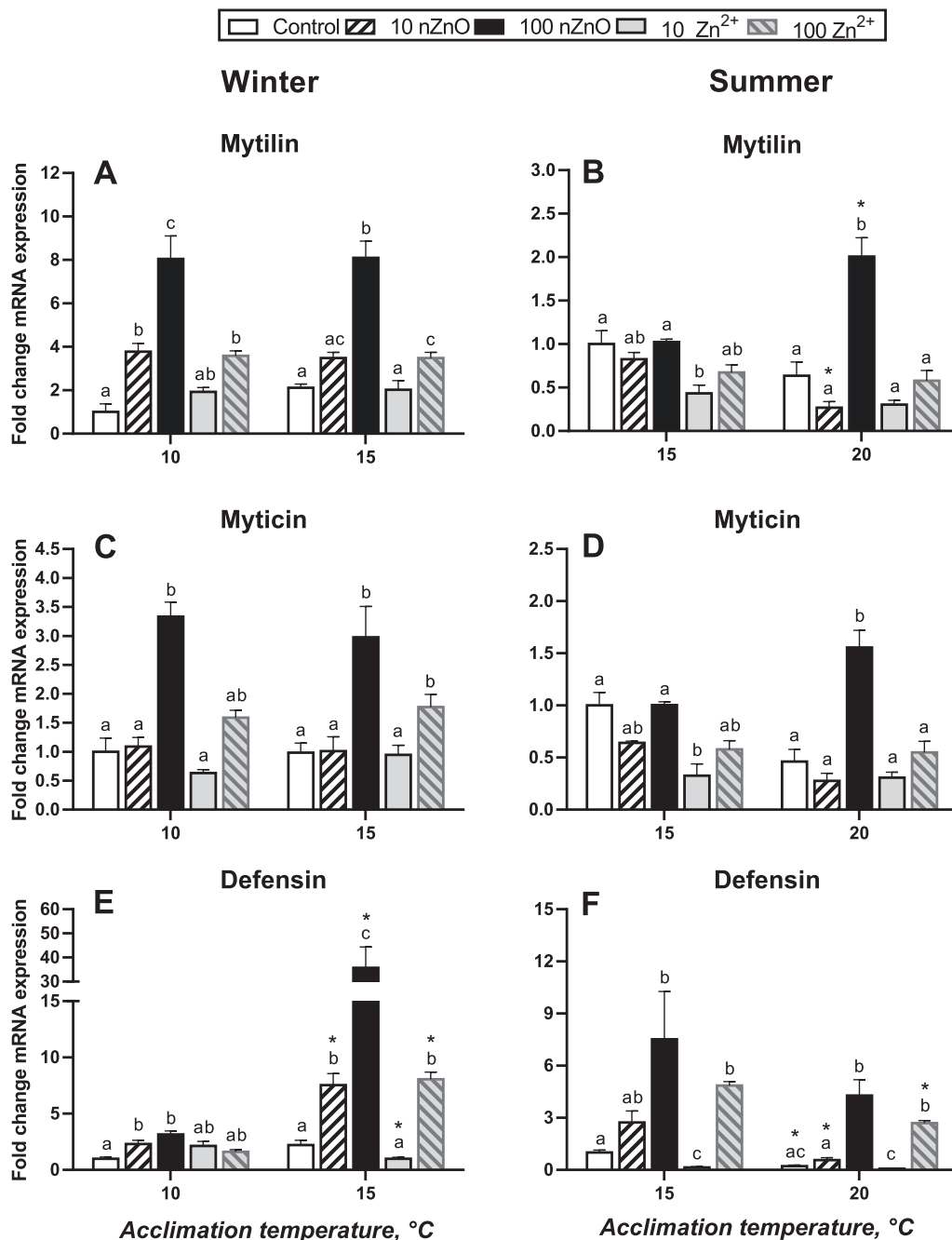


Fig. 3. Immune-related gene expression of hemocytes of *M. edulis* in response to nZnO/Zn²⁺ and temperature exposures.

A, C, E – Winter; B, D, F – Summer; Mytilin (A, B); Myticin (C, D); Defensin (E, F). The results were expressed as fold change in mRNA expression in the treated group relative to the mRNA expression in the respective control group (no Zn additions and ambient temperature corresponding to 10 °C in winter and 15 °C in summer). Different letters indicate significant differences among nZnO or Zn²⁺ treatments within fixed temperature level (Tukey HSD test, $P < 0.05$), and asterisks indicate significant differences between two temperatures within the same Zn treatment group (t-test, $P < 0.05$). $N = 3$.

dissolved Zn (Fig. 7C). The traits that significantly contributed to the discriminant model in the summer mussels ($P < 0.05$) included mRNA expression of the defensin and C1, and hemocyte mortality (SI Appendix, Supplementary Table 6).

4. Discussion

Our study showed that nZnO strongly affects the immune-related functional and transcriptional responses of the mussels' hemocytes, and that the immunomodulatory effects of nZnO are modified by the season and the ambient temperature (SI Appendix, Supplementary Table 7).

4.1. Effect of nZnO on hemocytes functional traits

The number of circulating hemocytes is an important index of the immune health in bivalves that depends on the dynamic balance between hemocyte mortality, hematopoiesis, and infiltration (Allam and Raftos, 2015; Pila et al., 2016). Exposures to high concentrations (100 $\mu\text{g l}^{-1}$) of nZnO or dissolved zinc increased mortality of mussels' hemocytes regardless of the temperature or the season. Similar increases in hemocyte mortality were observed in bivalves *M. edulis*, *M. coruscus* and *Perna viridis* under nZnO (Wu et al., 2020; Wu et al., 2018) and nTiO₂ exposures (Huang et al., 2016; Wang et al., 2014).

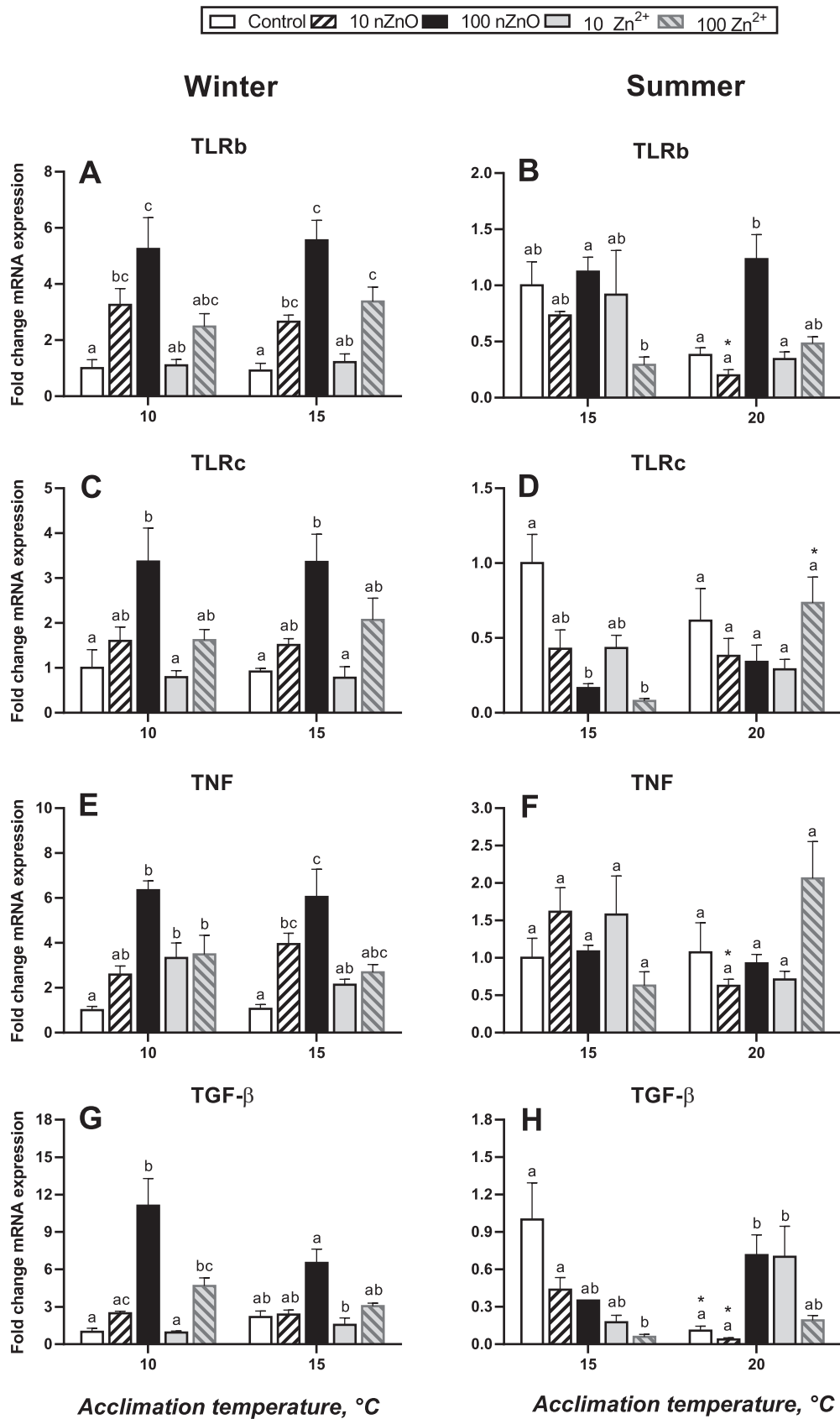


Fig. 4. Immune related-gene expression of hemocytes of *M. edulis* in response to nZnO/Zn²⁺ and temperature exposures. A, C, E, G – Winter; B, D, F, H – Summer; TLRb (A, B); TLRc (C, D); TNF (E, F); TGF-β (G, H). The results were expressed as fold change in mRNA expression in the treated group relative to the mRNA expression in the respective control group (no Zn additions and ambient temperature corresponding to 10 °C in winter and 15 °C in summer). Different letters indicate significant differences among nZnO or Zn²⁺ treatments within fixed temperature level (Tukey HSD test, *P* < 0.05), and asterisks indicate significant differences between two temperatures within the same Zn treatment group (*t*-test, *P* < 0.05). *N* = 3.

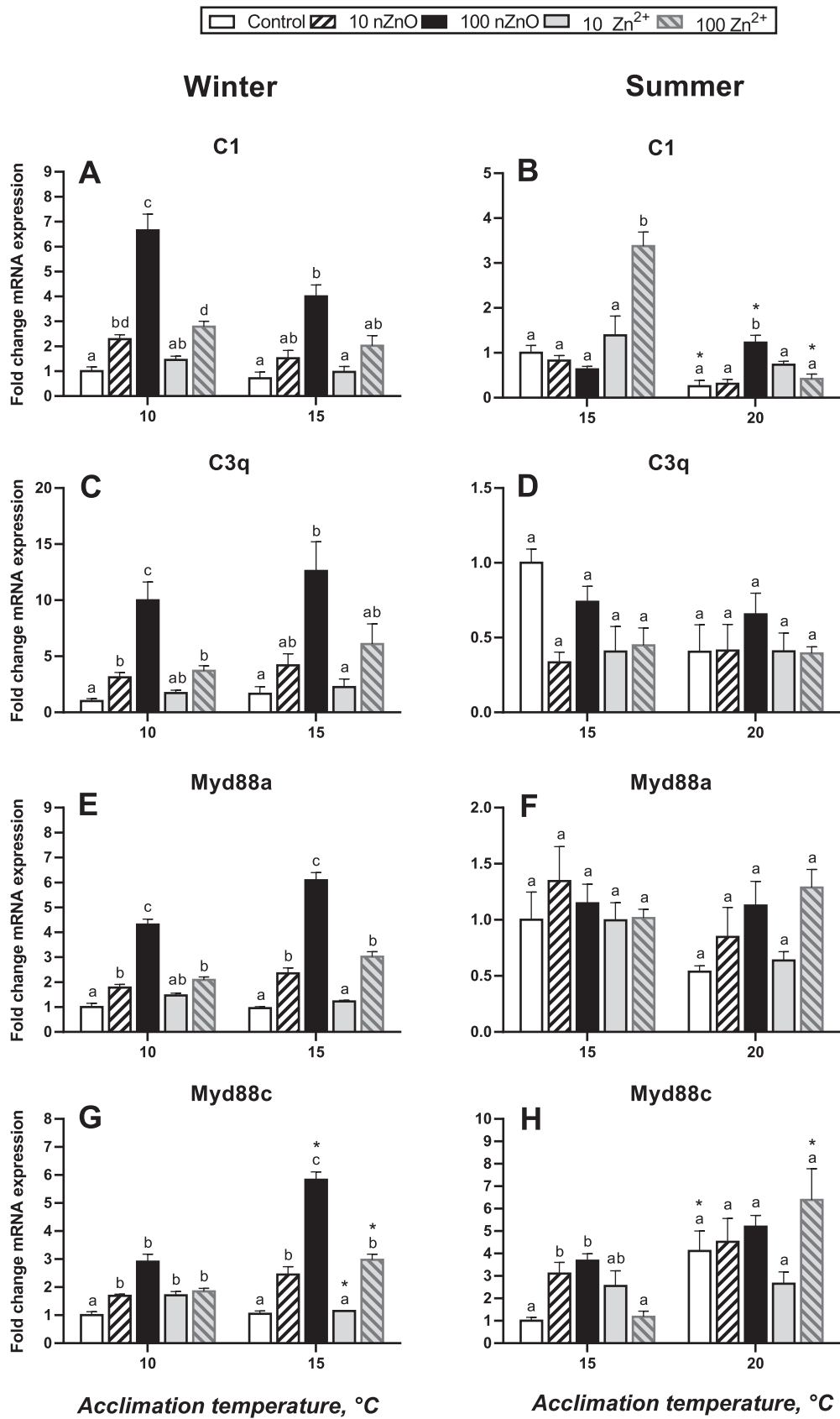


Fig. 5. Immune-related gene expression of hemocytes of *M. edulis* in response to nZnO/Zn²⁺ and temperature exposures. A, C, E, G – Winter; B, D, F, H – Summer; C1 (A, B); C3q (C, D); MyD88a (E, F); MyD88c (G, H). The results were expressed as fold change in mRNA expression in the treated group relative to the mRNA expression in the respective control group (no Zn additions and ambient temperature corresponding to 10 °C in winter and 15 °C in summer). Different letters indicate significant differences among nZnO or Zn²⁺ treatments within fixed temperature level (Tukey HSD test, P < 0.05), and asterisks indicate significant differences between two temperatures within the same Zn treatment group (t-test, P < 0.05). N = 3.

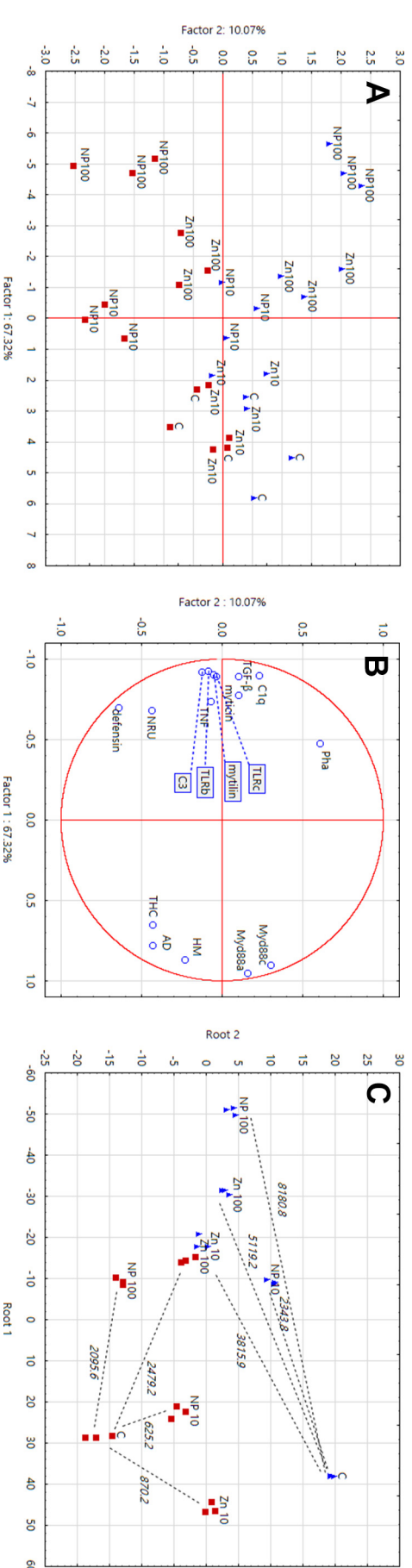


Fig. 6. Biplots originating from principal component analysis (PCA) and discriminant analysis (DA) integrating all measured biomarkers of winter mussels *M. edulis* in response to $nZnO/Zn^{2+}$ and temperature exposures. A – the position of samples from different combinations of Zn exposure and temperature groups in the plane of the two first principal components; B – the variable-based plot showing the associations of the respective biomarkers with the two first principal components; for the points located too closely to each other (TLRb, TLRc, mytilin and C1) the labels are shown connected with lines to the respective points; C – a discriminant analysis biplot of the different Zn exposures based on the multibiomarker profiles. Numbers next to the lines indicate the Mahalanobis distance between the respective groups. Experimental treatment groups: the blue triangles (Δ) – normal temperature; the red squares (\square) – elevated temperature; C – control (no Zn addition); 10 NP – 10 $\mu g\ l^{-1}\ nZnO$; 100 NP – 100 $\mu g\ l^{-1}\ nZnO$; 10 Zn – 10 $\mu g\ l^{-1}\ Zn^{2+}$; 100 Zn – 100 $\mu g\ l^{-1}\ Zn^{2+}$. (For interpretation of the references to colour in this figure legend, the reader is referred to the web version of this article.)

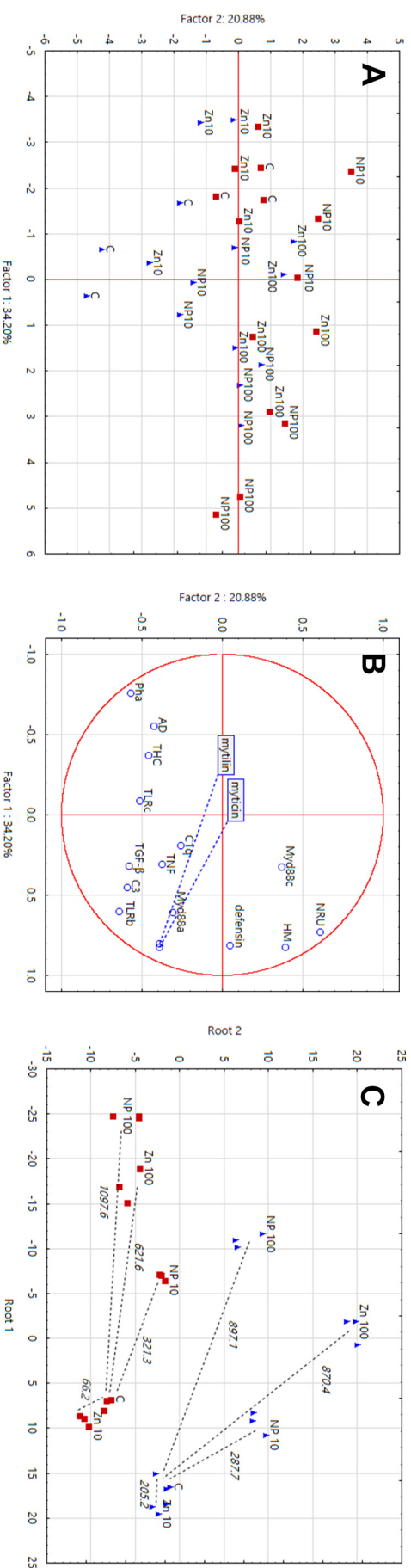


Fig. 7. Biplots originating from principal component analysis (PCA) and discriminant analysis (DA) integrating all measured biomarkers of summer mussels *M. edulis* in response to nZnO/Zn²⁺ and temperature exposures. A – the position of samples from different combinations of Zn exposure and temperature groups in the plane of the two first principal components; B – the variable-based plot showing the associations of the respective biomarkers with the two first principal components; for the points located too closely to each other (mytilin and mytilin) the labels are shown connected with lines to the respective points; C – a discriminant analysis biplot of the different Zn exposures based on the multibiomarker profiles. Numbers next to the lines indicate the Mahalanobis distance between the respective groups. Experimental treatment groups: the blue triangles (Δ) – normal temperature; the red squares (□) – elevated temperature; C – control (no Zn addition); 10 NP – 10 μg l⁻¹ nZnO; 100 NP – 100 μg l⁻¹ nZnO; 100 NP – 100 μg l⁻¹ nZnO; 10 Zn – 10 μg l⁻¹ Zn²⁺; 100 Zn – 100 μg l⁻¹ Zn²⁺. (For interpretation of the references to colour in this figure legend, the reader is referred to the web version of this article.)

Despite elevated mortality, the total hemocyte count of *M. edulis* did not change in response to the nZnO or dissolved Zn exposures. Similarly, exposure of the Baltic Sea *M. edulis* to 100 $\mu\text{g l}^{-1}$ nZnO under the normal (15) or fluctuating (5–15) salinity had no impact on the total hemocyte count (Wu et al., 2020). These findings suggest that mussels can compensate for increased hemocytes mortality caused by nZnO by increased hematopoiesis and/or recruitment of the resident hemocytes from other compartments.

Hemocyte adhesion capacity (AD) is essential for the protective functions such as encapsulation of the foreign bodies and wound healing in bivalves (Holmblad and Soderhall, 1999; Ivanina et al., 2018). In our present study, a significant decrease of AD was found in winter mussels *M. edulis* under high concentration of nZnO (100 $\mu\text{g l}^{-1}$). A similar albeit not statistically significant trend was found in the summer mussels. A decrease in the AD was earlier reported in the blue mussels *M. edulis* exposed to high concentrations of nZnO (100 $\mu\text{g l}^{-1}$) under different salinity regimes (Wu et al., 2020). The mechanism of the inhibition of AD caused by nZnO might be related to changes in the function and abundance of the adhesion-related molecules such as integrins (Holmblad and Soderhall, 1999) or by induction of apoptosis by nZnO exposure (Falfushynska et al., 2015; Li et al., 2018) that might contribute to the loss of the hemocyte attachment. Unlike nZnO, exposure to dissolved Zn had no significant influence on the AD of the hemocytes of the mussels in our present study. These results are consistent with the earlier reports that found no effect of dissolved metals including Zn^{2+} (Wu et al., 2020), Cd^{2+} and Cu^{2+} (Ivanina et al., 2014; Ivanina et al., 2016) on the adhesion capacity of bivalve hemocytes.

Phagocytosis plays an important defense function in marine bivalves internalizing pathogens and foreign materials and targeting them for destruction in the lysosomes (Canesi et al., 2002; Hegaret et al., 2003). Exposure to 10–100 $\mu\text{g l}^{-1}$ nZnO stimulated phagocytosis in the hemocytes of *M. edulis*. This stimulation indicated that ZnO nanoparticles might be recognized as non-self-material and engulfed by the mussel hemocytes (Canesi et al., 2012). The nZnO-induced increase in phagocytosis was accompanied by an increase in the lysosomal volume of hemocytes showed by the enhanced NRU. Earlier studies in the mammalian cell cultures and bivalve hemocytes also reported an increase in the lysosomal volume in response to nanomaterial exposures (Halamoda Kenzaoui et al., 2012; Huang et al., 2015; Wang et al., 2018a; Wang et al., 2018b; Zhou et al., 2018).

Overall, our present study shows that modulation of the studied functional traits and viability of the mussel hemocytes by nZnO exposures was consistent across experimental temperatures in both studied seasons. These changes (elevated mortality, enhanced phagocytosis and NRU, and suppressed adhesion capacity) might thus be considered a signature of nZnO-induced immunotoxicity. Except for mortality that similarly increased in nZnO- and Zn^{2+} -exposed mussels, other studied traits (including phagocytosis, NRU and AD) were considerably less sensitive to dissolved Zn than to nZnO indicating that Zn^{2+} release is unlikely to fully explain the observed immunomodulatory effects of ZnO nanoparticles.

4.2. Season-dependent transcriptional immune responses to nZnO

Exposure to nZnO induced a strong transcriptomic response in various immune-related genes in the hemocytes of *M. edulis* collected in the winter, both at the ambient (10 °C) and the elevated (15 °C) temperatures. The transcriptional profile of hemocytes of nZnO-exposed winter mussels indicated overall stimulation of the pathogen recognition, humoral defense and inflammatory pathways by the nanoparticles. Thus, mRNA levels of the Toll-like receptors TLRb and c were upregulated by nZnO in the winter mussels. The Toll-like receptors are key immune recognition factors that sense the pathogen-related molecular patterns (Ward and Rosenthal, 2014; Zhang et al., 2015). In aquatic organisms including molluscs, the Toll-like receptors are involved in the recognition of nanoparticles (Kedmi et al., 2010; Turabekova et al., 2014; Yang et al.,

2015) and stimulated by nZnO and dissolved metals (Auguste et al., 2019; Lu et al., 2013). The upregulation of the mussels' TLRs by nZnO observed in our present study might thus explain the elevated expression of humoral defense mechanisms (such as antimicrobial peptides) and inflammatory pathways (discussed below) which are regulated by Toll-like receptors (Doyle et al., 2004; Engström, 1999).

The antimicrobial peptides (AMPs) myticin, mytilin and defensin were strongly transcriptionally stimulated by nZnO exposure in the winter mussels. AMPs are cysteine-rich peptides that act as broad-spectrum antibiotics against eukaryotic, bacterial and viral pathogens in marine bivalves (Balseiro et al., 2011; Domeneghetti et al., 2015; Hubert et al., 1996; Mitta et al., 1999; Schmitt et al., 2012). Similar to our present findings, earlier research showed transcriptional upregulation defensin in the blue mussels exposed to 100 $\mu\text{g l}^{-1}$ nZnO albeit this effect was observed only under the normal (15) salinity regime but not at the low (5) or fluctuating (5–15) salinity (Wu et al., 2020). Defensin expression was the most sensitive to nZnO exposure of all studied AMPs regardless of the acclimation temperature (this study) and salinity (Wu et al., 2020). Elevated mRNA expression of mytilin and defensin was also observed in *M. galloprovincialis* exposed to 10–100 $\mu\text{g l}^{-1}$ nTiO₂ (Barmo et al., 2013). Thus, the present study and published research (Barmo et al., 2013; Ciacci et al., 2011; Wu et al., 2020) indicate that nZnO interactions with the mussels cells activates signal transduction pathways similar to the known AMP inducers such as bacteria, fungi or viruses.

Inflammation is a common cellular response to nanopollutants including nZnO-as demonstrated in bivalves (Falfushynska et al., 2019b), human cell cultures (Chang et al., 2013) and mice (Cho et al., 2011). Consistent with this notion, our present study showed upregulated transcript levels of inflammatory cytokines including the tumor necrosis factor (TNF- α) and transforming growth factor-beta (TGF- β) in nZnO-exposed winter mussels. nZnO exposures also stimulated the mRNA expression of TGF- β and the nuclear factor κB (NF- κB), a key inflammation regulator, in the *M. edulis* exposed to nZnO (Falfushynska et al., 2019b), supporting pro-inflammatory action of nZnO. Furthermore, nZnO exposure activated the downstream components of the complement system (including the classical (C1) and alternative (C3q) pathways) in the winter mussels, consistent with the notion of the complement system activation by the inflammatory cytokines TNF- α and TGF- β (Markiewski and Lambris, 2007). The complement system regulates the immune recognition cascade to recognize and opsonize foreign bodies and altered-self particles such as infected or dying host cells (Mayilyan et al., 2008; Ricklin et al., 2016; Volanakis, 1990). In marine bivalves, the complement system components including C1 and C3q are stimulated by bacterial pathogens or toxic stress (Chen et al., 2018b; Dong et al., 2017; Peng et al., 2017; Peng et al., 2016; Wang et al., 2017). Our present findings of upregulation of the complement system molecules by nZnO are consistent with the earlier reports of the induction of the expression of C3q by metals and metal-containing nanoparticles (including nCeO₂ and Cu²⁺) in bivalves (Auguste et al., 2019; Chen et al., 2018b). This indicates that the immune system of mussels might recognize and opsonize the nanoparticles as foreign materials, leading to enhanced phagocytosis of nanoparticles. Furthermore, transcriptional upregulation of the MyD88 factors (MyD88a and MyD88c) which link the Toll-like receptors signaling with inflammatory and immune effectors (Bouallegui, 2019; Muzio et al., 2013; Wesche et al., 2013) went hand-in-hand with an increase in the mRNA level of the TLRs, inflammatory cytokines, AMPs, and the complement system indicating a coordinated inflammatory and immune response to nZnO in the winter mussels at all experimental temperatures.

In summer mussels, the immune responses to nZnO were blunted, especially at the ambient (15 °C) temperature. This was reflected in the PCA analysis that showed that PC1 (the axis that separated the control from nZnO-exposed groups) explained ~34% of the overall variance in summer mussels compared to ~67% in the winter mussels. The nZnO-induced increase in phagocytosis rates was considerably less pronounced in the summer mussels compared to their winter counterparts,

regardless of the acclimation temperature. The transcriptional response to nZnO was also blunted or reversed in the summer mussels. Thus, unlike in the winter mussels, no ZnO-induced transcriptional upregulation of mytilin, myticin, MyD88a or the complement system proteins C1 and C3q was found in the summer mussels at 15 °C. The mRNA expression of the inflammatory cytokines was suppressed (TGF- β) or remained unchanged (TNF- α) in the nZnO-exposed summer mussels at 15 °C. Likewise, the transcript levels of the Toll-like receptors were unchanged (TLRb) or suppressed (TLRc) in the summer mussels at 15 °C. This blunted immune response to nZnO in the summer mussels is unlikely to be a direct consequence of the temperature because the winter mussels retained a strong immune response to nZnO at 15 °C. Interestingly, warming to 20 °C partially restored the transcriptomic response to nZnO in the hemocytes of the summer mussels; however, this effect was evident only for some genes (including AMPs, TLRb, C1 and TGF- β) and the degree of the transcriptional induction by nZnO remained lower than in the winter. The causes of the observed decrease in the immune sensitivity to nZnO in the summer mussels are presently unknown and require further investigation. One possible mechanism might include a trade-off between reproduction and immunity in summer mediated by the competing energy demands of these processes as shown in bivalves (Brokordt et al., 2019; Di and Baozhong, 2021) and other invertebrates (Schwenke et al., 2016). Such trade-off might limit the energy investment into the immune defense during the reproductive period in summer mussels leading to a dampened response to nanopollutants.

4.3. Conclusions and outlook

The present study demonstrated that nZnO strongly affect the immune-related functional and transcriptional responses of the hemocytes of a sentinel mussel *M. edulis*, and that the immunomodulatory effects of nZnO are modified by the season and the ambient temperature. Generally, exposure to nZnO induced a strong transcriptomic response in multiple immune and inflammation-related genes and stimulated phagocytosis (indicating that nZnO particles might be recognized as non-self by the mussel hemocytes) in the winter *M. edulis* indicating a coordinated inflammatory and immune response to nZnO. In addition, these transcriptional immune responses to nZnO were considerably stronger than those induced by the comparable concentrations of dissolved Zn suggesting that Zn²⁺ release is not likely to fully explain the immunostimulatory effects of nZnO. Notably, seasonal warm acclimatization and additional warming in summer (but not in winter) mitigated or suppressed the nZnO-induced transcriptional upregulation of AMPs, TLRs and the complement system proteins indicating that elevated summer temperatures might reduce sensitivity to the pathogen- and non-self-recognition in the mussels. The findings suggest that the combined exposures to nZnO and warming have different effects on the innate immunity of the mussels depending on the season, which might have implications for the ability of mussels from nanoparticle-polluted habitats to cope with the elevated levels of the pathogen exposure common in summer.

CRedit authorship contribution statement

Fangli Wu: Conceptualization, Data curation, Formal analysis, Funding acquisition, Investigation, Methodology, Visualization, Writing – original draft, Writing – review & editing. **Inna M. Sokolova:** Conceptualization, Funding acquisition, Methodology, Supervision, Project administration, Writing – review & editing.

Declaration of competing interest

The authors declare that they have no known competing financial interests or personal relationships that could have appeared to influence the work reported in this paper.

Acknowledgements

This work was in part supported by the Research Training Group 'Baltic TRANSCOAST' funded by the DFG (Deutsche Forschungsgemeinschaft) under grant number GRK 2000 to IMS and the China Scholarship Council (CSC) to FW. We thank Fei Ye and Joydeep Dutta (KTH Royal Institute of Technology, Sweden) for their assistance with the nanoparticle characterization. The project metadata are submitted to PANGAEA® Data Publisher open access database.

Appendix A. Supplementary data

Supplementary data to this article can be found online at <https://doi.org/10.1016/j.scitotenv.2021.149786>.

References

- Allam, B., Raftos, D., 2015. Immune responses to infectious diseases in bivalves. *J. Invertebr. Pathol.* 131, 121–136.
- Auguste, M., Balbi, T., Montagna, M., Fabbri, R., Sendra, M., Blasco, J., Canesi, L., 2019. In vivo immunomodulatory and antioxidant properties of nanoceria (nCeO₂) in the marine mussel *Mytilus galloprovincialis*. *Comp. Biochem. Physiol., Part C: Toxicol. Pharmacol.* 219, 95–102.
- Balseiro, P., Falco, A., Romero, A., Dios, S., Martinez-Lopez, A., Figueras, A., Estepa, A., Novoa, B., 2011. *Mytilus galloprovincialis* myticin C: a chemotactic molecule with antiviral activity and immunoregulatory properties. *PLoS One* 6.
- Barmo, C., Ciacci, C., Canonico, B., Fabbri, R., Cortese, K., Balbi, T., Marcomini, A., Pojana, G., Gallo, G., Canesi, L., 2013. In vivo effects of n-TiO₂ on digestive gland and immune function of the marine bivalve *Mytilus galloprovincialis*. *Aquat. Toxicol.* 132, 9–18.
- Beaudry, A., Fortier, M., Masson, S., Auffret, M., Brousseau, P., Fournier, M., 2016. Effect of temperature on immunocompetence of the blue mussel (*Mytilus edulis*). *J. Xenobiotics* 6, 5889.
- Benito, D., Ahvo, A., Nuutinen, J., Bilbao, D., Saenz, J., Etxebarria, N., Lekube, X., Izagirre, U., Lehtonen, K.K., Marigómez, I., et al., 2019. Influence of season-dependent ecological variables on biomarker baseline levels in mussels (*Mytilus trossulus*) from two Baltic Sea subregions. *Sci. Total Environ.* 689, 1087–1103.
- Berger, V.J., 1986. Adaptations of Marine Molluscs to Changes of Environmental Salinity. Nauka, Leningrad 216 pp.
- Beyer, J., Green, N.W., Brooks, S., Allan, I.J., Ruus, A., Gomes, T., Brate, I.L.N., Schoyen, M., 2017. Blue mussels (*Mytilus edulis* spp.) as sentinel organisms in coastal pollution monitoring: a review. *Mar. Environ. Res.* 130, 338–365.
- Bouallegui, Y., 2019. Immunity in mussels: an overview of molecular components and mechanisms with a focus on the functional defenses. *Fish Shellfish Immunol.* 89, 158–169.
- Brokordt, K., Defranchi, Y., Espósito, I., Cárcamo, C., Schmitt, P., Mercado, L., de la Fuente-Ortega, E., Rivera-Ingraham, G.A., 2019. Reproduction immunity trade-off in a mollusk: hemocyte energy metabolism underlies cellular and molecular immune responses. *Front. Physiol.* 10.
- Canesi, L., Gallo, G., Gavioli, M., Pruzzo, C., 2002. Bacteria-hemocyte interactions and phagocytosis in marine bivalves. *Microsc. Res. Tech.* 57, 469–476.
- Canesi, L., Ciacci, C., Fabbri, R., Marcomini, A., Pojana, G., Gallo, G., 2012. Bivalve molluscs as a unique target group for nanoparticle toxicity. *Mar. Environ. Res.* 76, 16–21.
- Chang, H., Ho, C.C., Yang, C.S., Chang, W.H., Tsai, M.H., Tsai, H.T., Lin, P.P., 2013. Involvement of MyD88 in zinc oxide nanoparticle-induced lung inflammation. *Exp. Toxicol. Pathol.* 65, 887–896.
- Chen, G., Peijnenburg, W.J.G.M., Xiao, Y., Vijver, M.G., 2018a. Developing species sensitivity distributions for metallic nanomaterials considering the characteristics of nanomaterials, experimental conditions, and different types of endpoints. *Food Chem. Toxicol.* 112, 563–570.
- Chen, Y.X., Xu, K.D., Li, J.J., Wang, X., Ye, Y.Y., Qi, P.Z., 2018b. Molecular characterization of complement component 3 (C3) in *Mytilus coruscus* improves our understanding of bivalve complement system. *Fish Shellfish Immunol.* 76, 41–47.
- Cho, W.S., Duffin, R., Howie, S.E.M., Scotton, C.J., Wallace, W.A.H., MacNee, W., Bradley, M., Megson, I.L., Donaldson, K., 2011. Progressive severe lung injury by zinc oxide nanoparticles; the role of Zn₂ dissolution inside lysosomes. *Part. Fibre Toxicol.* 8.
- Ciacci, C., Barmo, C., Fabbri, R., Canonico, B., Gallo, G., Canesi, L., 2011. Immunomodulation in *Mytilus galloprovincialis* by non-toxic doses of hexavalent chromium. *Fish Shellfish Immunol.* 31, 1026–1033.
- Coles, J.A., Farley, S.R., Pipe, R.K., 1995. Alteration of immune response of the common marine mussel *Mytilus edulis* resulting from exposure to cadmium. *Dis. Aquat. Org.* 22, 59–65.
- Coll, C., Notter, D., Gottschalk, F., Sun, T.Y., Som, C., Nowack, B., 2016. Probabilistic environmental risk assessment of five nanomaterials (nano-TiO₂, nano-ag, nano-ZnO, CNT, and fullerenes). *Nanotoxicology* 10, 436–444.
- Di, W., Baozhong, L., 2021. Transcriptomic Analysis of the Reproductive Effects on Immunity in the Clam *Meretrix petechialis* During the Breeding Season. *Research Square Preprint*. <https://doi.org/10.21203/rs.3.rs-62336/v1>.
- Domeneghetti, S., Franzoi, M., Damiano, N., Norante, R., El Haifawy, N.M., Mammi, S., Marin, O., Bellanda, M., Venier, P., 2015. Structural and antimicrobial features of peptides related to myticin C, a special defense molecule from the Mediterranean mussel *Mytilus galloprovincialis*. *J. Agric. Food Chem.* 63, 9251–9259.

- Dong, W.Q., Chen, Y.X., Lu, W.X., Wu, B., Qi, P.Z., 2017. Transcriptome analysis of *Mytilus coruscus* hemocytes in response to *Vibrio alginolyticus* infection. *Fish Shellfish Immunol.* 70, 560–567.
- Doyle, S.E., O'Connell, R.M., Miranda, G.A., Vaidya, S.A., Chow, E.K., Liu, P.T., Suzuki, S., Suzuki, N., Modlin, R.L., Yeh, W.-C., et al., 2004. Toll-like receptors induce a phagocytic gene program through p38. *J. Exp. Med.* 199, 81–90.
- Dumont, E., Johnson, A.C., Keller, V.D.J., Williams, R.J., 2015. Nano silver and nano zinc-oxide in surface waters – exposure estimation for Europe at high spatial and temporal resolution. *Environ. Pollut.* 196, 341–349.
- Engström, Y., 1999. Induction and regulation of antimicrobial peptides in *Drosophila*. *Dev. Comp. Immunol.* 23, 345–358.
- Fabrega, J., Tantra, R., Amer, A., Stolpe, B., Tomkins, J., Fry, T., Lead, J.R., Tyler, C.R., Galloway, T.S., 2012. Sequestration of zinc from zinc oxide nanoparticles and life cycle effects in the sediment dweller amphipod *Corophium volutator*. *Environ. Sci. Technol.* 46, 1128–1135.
- Falfushynska, H., Gnatyshyna, L., Yurchak, I., Sokolova, I., Stoliar, O., 2015. The effects of zinc nanooxide on cellular stress responses of the freshwater mussels *Unio tumidus* are modulated by elevated temperature and organic pollutants. *Aquat. Toxicol.* 162, 82–93.
- Falfushynska, H.I., Gnatyshyna, L.L., Ivanina, A.V., Khoma, V.V., Stoliar, O.B., Sokolova, I.M., 2019a. Bioenergetic responses of freshwater mussels *Unio tumidus* to the combined effects of nano-ZnO and temperature regime. *Sci. Total Environ.* 650, 1440–1450.
- Falfushynska, H.I., Wu, F., Ye, F., Kasianchuk, N., Dutta, J., Dobretsov, S., Sokolova, I.M., 2019b. The effects of ZnO nanostructures of different morphology on bioenergetics and stress response biomarkers of the blue mussels *Mytilus edulis*. *Sci. Total Environ.* 694, 133717.
- Garner, K.L., Keller, A.A., 2014. Emerging patterns for engineered nanomaterials in the environment: a review of fate and toxicity studies. *J. Nanopart. Res.* 16, 28.
- Gottschalk, F., Sun, T., Nowack, B., 2013. Environmental concentrations of engineered nanomaterials: review of modeling and analytical studies. *Environ. Pollut.* 181, 287–300.
- Halamoda Kenzaoui, B., Chapuis Bernasconi, C., Guney-Ayra, S., Juillerat-Jeanerret, L., 2012. Induction of oxidative stress, lysosome activation and autophagy by nanoparticles in human brain-derived endothelial cells. *Biochem. J.* 441, 813–821.
- Hanna, S.K., Miller, R.J., Muller, E.B., Nisbet, R.M., Lenihan, H.S., 2013. Impact of engineered zinc oxide nanoparticles on the individual performance of *Mytilus galloprovincialis*. *PLoS One* 8, 7.
- Hegaret, H., Wikfors, G.H., Soudant, P., 2003. Flow cytometric analysis of haemocytes from eastern oysters, *Crassostrea virginica*, subjected to a sudden temperature elevation II. Haemocyte functions: aggregation, viability, phagocytosis, and respiratory burst. *J. Exp. Mar. Biol. Ecol.* 293, 249–265.
- Holmblad, T., Soderhall, K., 1999. Cell adhesion molecules and antioxidative enzymes in a crustacean, possible role in immunity. *Aquaculture* 172, 111–123.
- Holmström, M., Bindsbol, A.M., Oostingh, G.J., Duschl, A., Scheil, V., Kohler, H.R., Loureiro, S., Soares, A., Ferreira, A.L.G., Kienle, C., et al., 2010. Interactions between effects of environmental chemicals and natural stressors: a review. *Sci. Total Environ.* 408, 3746–3762.
- Hong, H., Adam, V., Nowack, B., 2021. Form-specific and probabilistic environmental risk assessment of three engineered nanomaterials (nano-Ag, nano-TiO₂ and nano-ZnO) in European freshwaters. *Environ. Toxicol. Chem.* 00, 1–11. <https://doi.org/10.1002/etc.5146>.
- Huang, D., Zhou, H., Gao, J., 2015. Nanoparticles modulate autophagic effect in a dispersity-dependent manner. *Sci. Rep.* 5, 14361.
- Huang, X.Z., Lin, D.H., Ning, K., Sui, Y.M., Hu, M.H., Lu, W.Q., Wang, Y.J., 2016. Hemocyte responses of the thick shell mussel *Mytilus coruscus* exposed to nano-TiO₂ and seawater acidification. *Aquat. Biol.* 180, 1–10.
- Hubert, F., Noel, T., Roch, P., 1996. A member of the arthropod defensin family from edible Mediterranean mussels (*Mytilus galloprovincialis*) (vol 240, pg 304, 1996). *Eur. J. Biochem.* 240, 302–306.
- Hughes, F.M., Foster, B., Grewal, S., Sokolova, I.M., 2010. Apoptosis as a host defense mechanism in *Crassostrea virginica* and its modulation by *Perkinsus marinus*. *Fish Shellfish Immunol.* 29, 247–257.
- IPCC, 2014. Climate change 2014: synthesis report. Contribution of Working Groups I, II and III to the Fifth Assessment Report of the Intergovernmental Panel on Climate Change.
- Ivanina, A.V., Hawkins, C., Sokolova, I.M., 2014. Immunomodulation by the interactive effects of cadmium and hypercapnia in marine bivalves *Crassostrea virginica* and *Mercenaria mercenaria*. *Fish Shellfish Immunol.* 37, 299–312.
- Ivanina, A.V., Hawkins, C., Sokolova, I.M., 2016. Interactive effects of copper exposure and environmental hypercapnia on immune functions of marine bivalves *Crassostrea virginica* and *Mercenaria mercenaria*. *Fish Shellfish Immunol.* 49, 54–65.
- Ivanina, A.V., Borah, B.M., Vogts, A., Malik, I., Wu, J.Y., Chin, A.R., Almarza, A.J., Kumta, P., Piontkivska, H., Beniash, E., et al., 2018. Potential trade-offs between biomineralization and immunity revealed by shell properties and gene expression profiles of two closely related *Crassostrea* species. *J. Exp. Biol.* 221.
- Jenny, M.J., Ringwood, A.H., Lacy, E.R., Lewitus, A.J., Kempton, J.W., Gross, P.S., Warr, G.W., Chapman, R.W., 2002. Potential indicators of stress response identified by expressed sequence tag analysis of hemocytes and embryos from the American oyster, *Crassostrea virginica*. *Mar. Biotechnol.* 4, 81–93.
- Katsumiti, A., Arostegui, I., Oron, M., Gilliland, D., Valsami-Jones, E., Cajaraville, M.P., 2016. Cytotoxicity of Au, ZnO and SiO₂ NPs using in vitro assays with mussel hemocytes and gill cells: relevance of size, shape and additives. *Nanotoxicology* 10, 185–193.
- Kautsky, N., 1982. Quantitative studies on gonad cycle, fecundity, reproductive output and recruitment in a Baltic *Mytilus edulis* population. *Mar. Biol.* 68, 143–160.
- Kedmi, R., Ben-Arie, N., Peer, D., 2010. The systemic toxicity of positively charged lipid nanoparticles and the role of toll-like receptor 4 in immune activation. *Biomaterials* 31, 6867–6875.
- Khlebovich, V.V., 2017. Acclimation of animal organisms: basic theory and applied aspects. *Biol. Bull. Rev.* 7, 279–286.
- Kwon, H., Bang, K., Cho, S., 2014. Characterization of the hemocytes in larvae of *Protoctea brevitarsis seulensis*: involvement of granulocyte-mediated phagocytosis. *PLoS One* 9, e103620.
- Lacoste, A., Malham, S.K., Gélébart, F., Cuffe, A., Poulet, S.A., 2002. Stress-induced immune changes in the oyster *Crassostrea gigas*. *Dev. Comp. Immunol.* 26, 1–9.
- Li, J., Schiavo, S., Xiangli, D., Rametta, G., Miglietta, M.L., Oliviero, M., Changwen, W., Manzo, S., 2018. Early ecotoxic effects of ZnO nanoparticle chronic exposure in *Mytilus galloprovincialis* revealed by transcription of apoptosis and antioxidant-related genes. *Ecotoxicology* 27, 369–384.
- Lu, Y.L., Zhang, A.G., Li, C.H., Zhang, P., Su, X.R., Li, Y., Mu, C.K., Li, T.W., 2013. The link between selenium binding protein from *Sinonovacula constricta* and environmental pollutants exposure. *Fish Shellfish Immunol.* 35, 271–277.
- Mackenzie, B.R., Schiedek, D., 2007. Daily Ocean monitoring since the 1860s shows record warming of northern European seas. *Glob. Chang. Biol.* 13, 1335–1347.
- Malagoli, D., Casarini, L., Sacchi, S., Ottaviani, E., 2007. Stress and immune response in the mussel *Mytilus galloprovincialis*. *Fish Shellfish Immunol.* 23, 171–177.
- Marchi, B., Burlando, B., Moore, M.N., Viarengo, A., 2004. Mercury- and copper-induced lysosomal membrane destabilisation depends on [Ca²⁺]_i dependent phospholipase A₂ activation. *Aquat. Toxicol.* 66, 197–204.
- Marisa, I., Matozzo, V., Munari, M., Binelli, A., Parolini, M., Martucci, A., Franceschinis, E., Brianese, N., Marin, M.G., 2016. In vivo exposure of the marine clam *Ruditapes philippinarum* to zinc oxide nanoparticles: responses in gills, digestive gland and haemolymph. *Environ. Sci. Pollut. Res.* 23, 15275–15293.
- Markiewski, M.M., Lambris, J.D., 2007. The role of complement in inflammatory diseases from behind the scenes into the spotlight. *Am. J. Pathol.* 171, 715–727.
- Matozzo, V., Chinellato, A., Munari, M., Finos, L., Bressan, M., Marin, M.G., 2012. First evidence of immunomodulation in bivalves under seawater acidification and increased temperature. *PLoS One* 7, e33820.
- Mayilyan, K.R., Kang, Y.H., Dodds, A.W., Sim, R.B., 2008. The complement system in innate immunity. In: Heine, H. (Ed.), *Innate Immunity of Plants, Animals, and Humans*. Springer Berlin Heidelberg, Berlin, Heidelberg, pp. 219–236.
- Mitta, G., Hubert, F., Noel, T., Roch, P., 1999. Myticin, a novel cysteine-rich antimicrobial peptide isolated from haemocytes and plasma of the mussel *Mytilus galloprovincialis*. *Eur. J. Biochem.* 265, 71–78.
- Muller, E.B., Hanna, S.K., Lenihan, H.S., Miller, R., Nisbet, R.M., 2014. Impact of engineered zinc oxide nanoparticles on the energy budgets of *Mytilus galloprovincialis*. *J. Sea Res.* 94, 29–36.
- Muzio, M., Ni, J., Feng, P., Dixit, V.M., 2013. IRAK (Pelle) family member IRAK-2 and MyD88 as proximal mediators of IL-1 signaling (Reprinted from science, vol 278, pg 1612–1615, 1997). *J. Immunol.* 190, 16–19.
- Mydlarz, L.D., Jones, L.E., Harvell, C.D., 2006. Innate immunity, environmental drivers, and disease ecology of marine and freshwater invertebrates. *Annu. Rev. Ecol. Evol. Syst.* 37, 251–288.
- Peng, M.X., Niu, D.H., Wang, F., Chen, Z.Y., Li, J.L., 2016. Complement C3 gene: expression characterization and innate immune response in razor clam *Sinonovacula constricta*. *Fish Shellfish Immunol.* 55, 223–232.
- Peng, M.X., Niu, D.H., Chen, Z.Y., Lan, T.Y., Dong, Z.G., Tran, T.N., Li, J.L., 2017. Expression of a novel complement C3 gene in the razor clam *Sinonovacula constricta* and its role in innate immune response and hemolysis. *Dev. Comp. Immunol.* 73, 184–192.
- Perez, D.G., Fontanetti, C.S., 2010. Hemocytal responses to environmental stress in invertebrates: a review. *Environ. Monit. Assess.* 177, 437–447.
- Pfaffl, M.W., 2001. A new mathematical model for relative quantification in real-time RT-PCR. *Nucleic Acids Res.* 29, 2002–2007.
- Pila, E.A., Sullivan, J.T., Wu, X.Z., Fang, J., Rudko, S.P., Gordy, M.A., Hanington, P.C., 2016. Haematopoiesis in molluscs: a review of haemocyte development and function in gastropods, cephalopods and bivalves. *Dev. Comp. Immunol.* 58, 119–128.
- Qi, P., Huang, H., Guo, B., Liao, Z., Liu, H., Tang, Z., He, Y., 2019. A novel interleukin-1 receptor-associated kinase-4 from thick shell mussel *Mytilus coruscus* is involved in inflammatory response. *Fish Shellfish Immunol.* 84, 213–222.
- Rahman, M.A., Henderson, S., Miller-Ezzy, P., Li, X.X., Qin, J.G., 2019. Immune response to temperature stress in three bivalve species: Pacific oyster *Crassostrea gigas*, Mediterranean mussel *Mytilus galloprovincialis* and mud cockle *Katelysia rhytiphora*. *Fish Shellfish Immunol.* 86, 868–874.
- Read, D.S., Matzke, M., Gweon, H.S., Newbold, L.K., Heggelund, L., Ortiz, M.D., Lahive, E., Spurgeon, D., Svendsen, C., 2016. Soil pH effects on the interactions between dissolved zinc, non-nano- and nano-ZnO with soil bacterial communities. *Environ. Sci. Pollut. Res.* 23, 4120–4128.
- Renault, T., 2015. Immunotoxicological effects of environmental contaminants on marine bivalves. *Fish Shellfish Immunol.* 46, 88–93.
- Ricklin, D., Reis, E.S., Mastellos, D.C., Gros, P., Lambris, J.D., 2016. Complement component C3—the “Swiss Army Knife” of innate immunity and host defense. *Immunol. Rev.* 274, 33–58.
- Roch, P., 1999. Various aspects of bivalve mollusk immunity. *Bull. Soc. Zool. Fr.* 124, 313–324.
- Schiedek, D., Sundelin, B., Readman, J.W., Macdonald, R.W., 2007. Interactions between climate change and contaminants. *Mar. Pollut. Bull.* 54, 1845–1856.
- Schmitt, P., Rosa, R.D., Duprethuy, M., de Lorgethuy, J., Bacher, E., Destoumieux-Garzon, D., 2012. The antimicrobial defense of the Pacific oyster, *Crassostrea gigas*. How diversity may compensate for scarcity in the regulation of resident/pathogenic microflora. *Front. Microbiol.* 3.

- Schwenke, R.A., Lazzaro, B.P., Wolfner, M.F., 2016. Reproduction-immunity trade-offs in insects. *Annu. Rev. Entomol.* 61, 239–256.
- Sokolova, I.M., 2009. Apoptosis in molluscan immune defense. *Invertebr. Surviv. J.* 6, 49–58.
- Trevisan, R., Delapiedra, G., Mello, D.F., Arl, M., Schmidt, E.C., Meder, F., Monopoli, M., Carginin-Ferreira, E., Bouzon, Z.L., Fisher, A.S., et al., 2014. Gills are an initial target of zinc oxide nanoparticles in oysters *Crassostrea gigas*, leading to mitochondrial disruption and oxidative stress. *Aquat. Toxicol.* 153, 27–38.
- Turabekova, M., Rasulev, B., Theodore, M., Jackman, J., Leszczynska, D., Leszczynski, J., 2014. Immunotoxicity of nanoparticles: a computational study suggests that CNTs and C-60 fullerenes might be recognized as pathogens by toll-like receptors. *Nanoscale* 6, 3488–3495.
- Volanakis, J.E., 1990. Participation of C3 and its ligands in complement activation. *Curr. Top. Microbiol. Immunol.* 153, 1–21.
- Wang, Y.J., Hu, M.H., Li, Q.Z., Li, J.L., Lin, D.H., Lu, W.Q., 2014. Immune toxicity of TiO₂ under hypoxia in the green-lipped mussel *Perna viridis* based on flow cytometric analysis of hemocyte parameters. *Sci. Total Environ.* 470, 791–799.
- Wang, L.L., Zhang, H., Wang, L.L., Zhang, D.X., Lv, Z., Liu, Z.Q., Wang, W.L., Zhou, Z., Qiu, L.M., Wang, H., et al., 2017. The RNA-seq analysis suggests a potential multi-component complement system in oyster *Crassostrea gigas*. *Dev. Comp. Immunol.* 76, 209–219.
- Wang, B., Zhang, J., Chen, C., Xu, G., Qin, X., Hong, Y., Bose, D.D., Qiu, F., Zou, Z., 2018a. The size of zinc oxide nanoparticles controls its toxicity through impairing autophagic flux in A549 lung epithelial cells. *Toxicol. Lett.* 285, 51–59.
- Wang, F., Salvati, A., Boya, P., 2018b. Lysosome-dependent cell death and deregulated autophagy induced by amine-modified polystyrene nanoparticles. *Open Biol.* 8, 170271.
- Ward, A.E., Rosenthal, B.M., 2014. Evolutionary responses of innate immunity to adaptive immunity. *Infect. Genet. Evol.* 21, 492–496.
- Wesche, H., Henzel, W.J., Shillinglaw, W., Li, S.Y., Cao, Z.D., 2013. MyD88: an adapter that recruits IRAK to the IL-1 receptor complex (Reprinted from *immunity*, vol 7, pg 837–847, 1997). *J. Immunol.* 190, 5–15.
- Williams, R.J., Harrison, S., Keller, V., Kuenen, J., Lofts, S., Praetorius, A., Svendsen, C., Vermeulen, L.C., van Wijnen, J., 2019. Models for assessing engineered nanomaterial fate and behaviour in the aquatic environment. *Curr. Opin. Environ. Sustain.* 36, 105–115.
- Wu, F.L., Cui, S.K., Sun, M., Xie, Z., Huang, W., Huang, X.Z., Liu, L.P., Hu, M.H., Lu, W.Q., Wang, Y.J., 2018. Combined effects of ZnO NPs and seawater acidification on the haemocyte parameters of thick shell mussel *Mytilus coruscus*. *Sci. Total Environ.* 624, 820–830.
- Wu, F., Falfushynska, H., Dellwig, O., Piontkivska, H., Sokolova, I.M., 2020. Interactive effects of salinity variation and exposure to ZnO nanoparticles on the innate immune system of a sentinel marine bivalve, *Mytilus edulis*. *Sci. Total Environ.* 712.
- Wu, F.L., Sokolov, E.P., Dellwig, O., Sokolova, I.M., 2021. Season-dependent effects of ZnO nanoparticles and elevated temperature on bioenergetics of the blue mussel *Mytilus edulis*. *Chemosphere* 263, 127780.
- Yang, H., Fung, S.Y., Xu, S.Y., Sutherland, D.P., Kollmann, T.R., Liu, M.Y., Turvey, S.E., 2015. Amino acid-dependent attenuation of toll-like receptor signaling by peptide-gold nanoparticle hybrids. *ACS Nano* 9, 6774–6784.
- Yung, M.M.N., Mouneyrac, C., Leung, K.M.Y., 2014. Ecotoxicity of zinc oxide nanoparticles in the marine environment. In: Bhushan, B. (Ed.), *Encyclopedia of Nanotechnology*. Springer, Netherlands, Dordrecht, pp. 1–17.
- Yung, M.M.N., Kwok, K.W.H., Djuricic, A.B., Giesy, J.P., Leung, K.M.Y., 2017. Influences of temperature and salinity on physicochemical properties and toxicity of zinc oxide nanoparticles to the marine diatom *Thalassiosira pseudonana*. *Sci. Rep.* 7.
- Zhang, X., Filser, J., 2020. Seasonal Effects on the Outcome of Reproduction Tests With Silver Nanoparticles, Silver Nitrate and the Collembola *Folsomia Candida*.
- Zhang, L.L., Li, L., Guo, X.M., Litman, G.W., Dishaw, L.J., Zhang, G.F., 2015. Massive expansion and functional divergence of innate immune genes in a protostome. *Sci. Rep.* 5.
- Zhou, H., Gong, X., Lin, H., Chen, H., Huang, D., Li, D., Shan, H., Gao, J., 2018. Gold nanoparticles impair autophagy flux through shape-dependent endocytosis and lysosomal dysfunction. *J. Mater. Chem. B* 6, 8127–8136.

Supporting Information for “Immune responses to ZnO nanoparticles are modulated by environmental temperature in the blue mussels *Mytilus edulis*”

Fangli Wu¹, Inna M. Sokolova^{1,2*}

¹Department of Marine Biology, Institute for Biological Sciences, University of Rostock, Rostock, Germany

²Department of Maritime Systems, Interdisciplinary Faculty, University of Rostock, Rostock, Germany

*Corresponding author: Inna Sokolova, inna.sokolova@uni-rostock.de

This PDF file includes:

Supplementary text: Description of experimental procedures

Supplementary Figure 1 and 2

Supplementary Table 1 to 7

Supplementary References

Characterization of ZnO nanoparticles

Dispersion of ZnO nanoparticles (nZnO) (particle size <100 nm (TEM), average particle size 30.1 ± 0.4 nm, pH 7.5 ± 1.5 , hydrodynamic size $\sim 817 \pm 174$ nm and zeta-potential -9.6 mV at salinity 15) were purchased from Sigma-Aldrich Sweden AB (Stockholm, Sweden). High resolution transmission electron microscopy of nZnO showed a lattice spacing of 2.45 Å and 2.60 Å corresponding to the (101) and (002) lattice planes of typical wurtzite zinc oxide crystals ([Supplementary Figure 1 was published as \(Falfushynska et al., 2019\)](#)).

Animal collection and maintenance

The wild blue mussels *M. edulis* (shell length, 56 ± 6 mm) were collected near Rostock, Germany ($54^{\circ}10'49.602''\text{N}$, $12^{\circ}05'21.991''\text{E}$) in late October 2018 (winter experiment: the average seawater temperature ~ 10 °C) and June 2019 (summer experiment: the average seawater temperature ~ 15 °C). All mussels used in the experiments were adults, and the two collection periods corresponded to the reproductive rest (October) and spawning (June) in the Baltic Sea *Mytilus* spp. (Benito et al., 2019; Kautsky, 1982). Habitat salinity at the collection site was 10-16. The mussels with no shell damage were selected and the shell surface was cleaned from epibionts. Prior to the experiments, the mussels were kept for two weeks in recirculated temperature-controlled aquaria at salinity 15 and the temperature similar to that at the time of collection (10 °C and 15 °C for the winter and summer mussels, respectively). Two weeks is considered sufficient time for acclimation to environmental shifts in temperate marine bivalves (Berger, 1986; Khlebovich, 2017).

Experimental exposures

After two-week preliminary acclimation, the mussels were randomly divided into ten treatment groups and exposed for 21 days to different temperatures and concentrations of nZnO or dissolved Zn. Within each season, two factors were tested in a fully crossed

design with two temperature levels (10 and 15 °C as ambient and elevated temperature in the winter, and 15 and 20 °C as ambient and elevated temperature in the summer) and five Zn treatments: no Zn addition as a control, nZnO at the concentrations of 10 $\mu\text{g l}^{-1}$ Zn and 100 $\mu\text{g l}^{-1}$ Zn, and 10 $\mu\text{g l}^{-1}$ and 100 $\mu\text{g l}^{-1}$ of dissolved Zn (added as ZnSO_4). A static renewal design was used with the water change every two days in all experimental treatments. For each treatment, three replicate tanks, each containing 20 mussels in 6 l of seawater was used. Fresh aliquots of nZnO suspension or ZnSO_4 solution were added during every water change to maintain nZnO or Zn^{2+} levels. The mussels were fed ~2 h before the water change with a commercial blend of live algae containing *Nannochloropsis oculata*, *Phaeodactylum* sp. and *Chlorella* sp. (Premium Reef Blend, CoralSands, Wiesbaden, Germany) per manufacturer's instructions. No mortality of the mussels occurred during the experiment. Measurements on functional traits and gene expression of hemocytes were conducted after 21 days of the experimental exposures.

mRNA expression of key immune-related genes

Total RNA was extracted from the hemocytes using TRIzol reagent (Thermo Fisher Scientific, Berlin, Germany) and purified from the possible DNA contamination with TURBO DNA-free Kit (Thermo Fisher Scientific, Berlin, Germany). cDNA was synthesized from 2.0 μg of purified RNA by High Capacity cDNA Reverse Transcription Kit (Thermo Fisher Scientific, Berlin, Germany) according to the manufacturer's instructions. qRT-PCR was performed using StepOnePlus™ Real-Time PCR System Thermal Cycling Block (Applied Biosystems, Thermo Fisher Scientific, Berlin, Germany) and Biozym Blue S'Green qPCR Mix Separate ROX kit (Biozym Scientific GmbH, Hessisch Oldendorf, Germany) according to the manufacturer's instructions. The cycling parameters were as follows: 95 °C for 2 min to activate the polymerase followed by 40 cycles of 15 s at 95 °C and 30 s at 60 °C. Signal readout was conducted at the primer-specific reading temperature at the end of each cycle ([Supplementary Table 1](#)). In each run, serial dilutions of a cDNA standard were

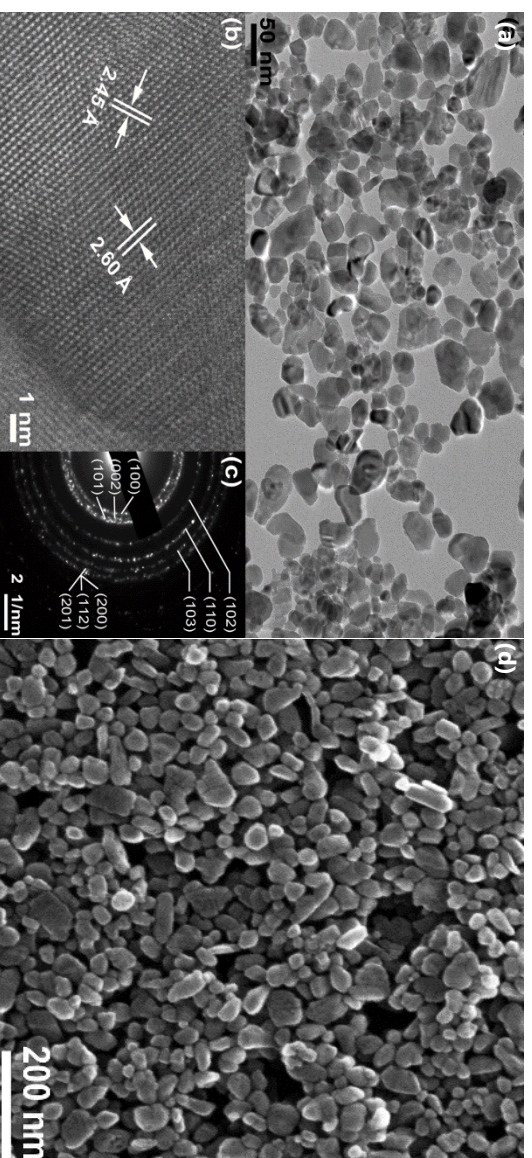
amplified to determine amplification efficiency (Pfaffl, 2001). In a pilot analysis, we tested three housekeeping genes (the eukaryotic elongation factor 1 (eEF1), tubulin and β -actin) and chose the least variable eEF1 for normalization of the target gene expression.

Statistical analysis

Pilot analysis showed no effects of replicate tanks or individual gender on the studied traits ($P > 0.05$); therefore, individual mussels were randomly used for subsequent analysis. The effects of Zn treatment, temperature regime and their interactions on the studied traits were tested separately for each season by two-way analysis of variance (ANOVA). Furthermore, the interactive effects of Zn treatment and season at a common temperature (15 °C) were tested by the two-way ANOVA. The factor “Zn treatment” had five levels (control – no Zn addition, 10 $\mu\text{g l}^{-1}$ nZnO, 100 $\mu\text{g l}^{-1}$ nZnO, 10 $\mu\text{g l}^{-1}$ dissolved Zn or 100 $\mu\text{g l}^{-1}$ dissolved Zn). The factor “Temperature” had two levels (ambient temperature and elevated temperature). The factor “Season” had two levels (winter and summer). Prior to analyses, data were checked for normality and homogeneity of variances using the Shapiro–Wilk's and Levene's tests, respectively. Data deviating from the normal distribution were Box-Cox transformed. The significant effects of Zn treatments were analyzed using Tukey's Honest Significant Difference (HSD) test within each temperature regime, and the effects of temperature were analyzed by a Student's *t* test within each Zn treatment. Finally, normalized, Box-Cox transformed data were subjected to the principal component analysis (PCA) to reduce the dimensionality of the dataset. Discriminant analysis with stepwise module was performed to assess the ability of the studied biomarkers to distinguish between the different treatment groups. The analyses were performed using SPSS 18.0 and GraphPad Prism 6.0. The results were expressed as the means \pm the standard error (SE) and the significant effects were considered at $P < 0.05$.

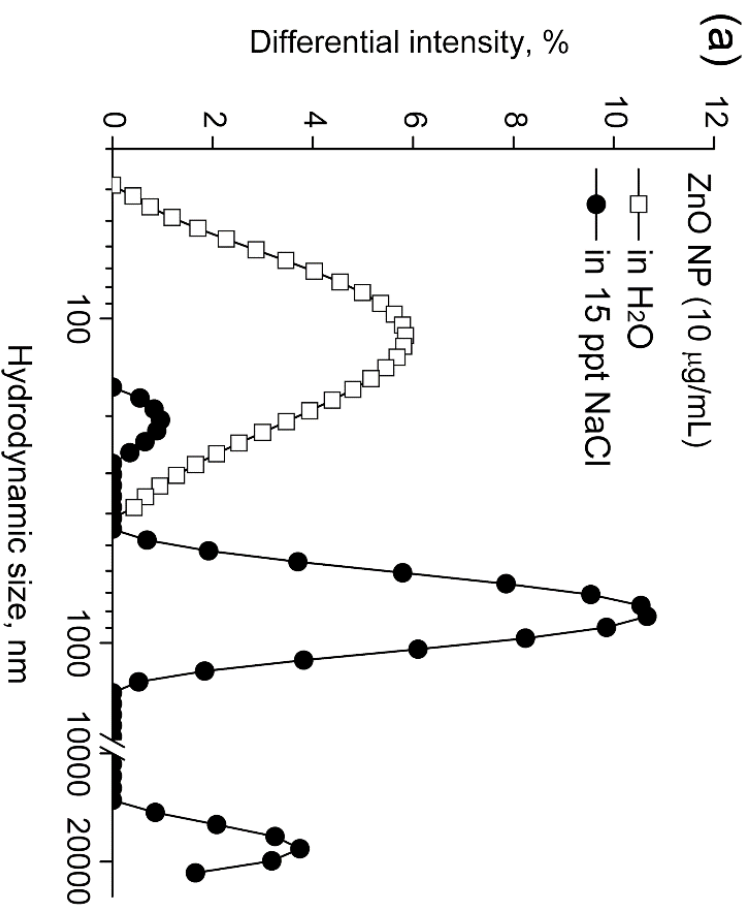


Supplementary Figure 1. Map showing the sampling site in the present work.



Supplementary Figure 2. Images of nZnO used in the present work.

(a) Transmission electron micrographs (TEM) of nZnO, (b) high resolution imaging of a single nZnO, (c) selected area diffraction (SAED) pattern from nZnO, and (d) scanning electron micrograph (SEM) of nZnO. Same batch of nanoparticles was used in our present study as the earlier published work from our laboratory (Falfushynska et al., 2019). This figure has been published in the Science of the Total Environment (Falfushynska et al., 2019), copyright Elsevier (2019), and is reproduced with a kind permission of the copyright holder.



Supplementary Figure 3. Distribution of intensity-weighted hydrodynamic particle size of nZnO dispersed in distilled water (H₂O) or in the water of salinity 15 (15 ppt NaCl). Same batch of nanoparticles was used in our present study as the earlier published work from our laboratory (Falfushynska et al., 2019). This figure has been published in the Science of the Total Environment (Falfushynska et al., 2019), copyright Elsevier (2019), and is reproduced with a kind permission of the copyright holder.

Supplementary Table 1. Two-way ANOVA analysis of the hemocyte immune related biomarkers of *M. edulis* in response to Zn treatment and temperature. Temperature: 10 and 15 °C in winter; 15 and 20 °C in summer. Zn treatment: control, 10 µg l⁻¹ nZnO, 100 µg l⁻¹ nZnO, 10 µg l⁻¹ Zn²⁺, and 100 µg l⁻¹ Zn²⁺. Degrees of freedom (d.f.) for the error were 20 for all studied traits. F and P values are given. Significant effects are highlighted in bold.

A. Winter:

Source	F	P	F	P	F	P	F	P	F	P	F	P	F	P			
	Total hemocytes		Hemocyte		Adhesion		Phagocytosis		Neutral red		Mytilin		Defensin				
	df		df		df		df		df		df		df				
Temperature	1	1.757	0.200	1.933	0.180	15.420	0.001	1700.125	<0.001	13.139	0.002	0.151	0.702	69.767	<0.001	2.312	0.144
Zn	4	5.366	0.004	91.370	<0.001	18.445	<0.001	281.784	<0.001	33.209	<0.001	14.873	<0.001	35.068	<0.001	30.102	0.000
T * Zn	4	0.326	0.857	5.015	0.006	0.657	0.629	255.935	<0.001	26.886	<0.001	0.521	0.721	17.071	<0.001	1.206	0.339
	df		TLRb		TLRc		TNF		TGF-β		CI		C3q		Myd88a		Myd88c
Temperature	1	0.103	0.751	0.071	0.793	0.106	0.748	0.084	0.776	11.301	0.003	2.248	0.149	3.096	0.094	6.992	0.016
Zn	4	18.776	<0.001	9.956	<0.001	17.822	<0.001	22.239	<0.001	23.242	<0.001	17.467	<0.001	69.251	<0.001	48.129	<0.001
T * Zn	4	0.297	0.877	0.090	0.985	1.013	0.424	2.674	0.062	0.029	0.998	0.067	0.991	2.224	0.103	6.397	0.002

B. Summer

Source	F	P	F	P	F	P	F	P	F	P	F	P	F	P	F	P	
	Total hemocytes count		Hemoocyte mortality		Adhesion capacity		Phagocytosis		Neutral red uptake		Myricin		Defensin		Mytilin		
Temperature	1	6.21	0.022	20.157	<0.001	7.027	0.015	25.307	<0.001	78.003	<0.001	2.69	0.117	27.345	<0.001	2.058	0.167
Zn treatment	4	1.274	0.313	33.91	<0.001	3.185	0.035	132.1	<0.001	104.004	<0.001	15.667	<0.001	65.011	<0.001	15.444	<0.001
T * Zn	4	0.009	1	0.666	0.623	0.234	0.916	4.479	0.01	4.371	0.011	4.525	0.009	2.161	0.111	6.162	0.002
	df	TLRb		TLRc		TNF		TGF- β		C1		C3q		Myd88a		Myd88c	
Temperature	1	8.606	0.008	0.702	0.412	0.166	0.688	0.55	0.467	27.704	<0.001	0.802	0.381	3.17	0.09	24.435	<0.001
Zn treatment	4	6.401	0.002	3.294	0.032	0.043	0.996	4.763	0.007	6.518	0.002	1.285	0.309	1.592	0.215	2.163	0.11
T * Zn	4	4.469	0.01	3.771	0.019	3.092	0.039	11.078	<0.001	11.91	<0.001	1.237	0.327	1.012	0.425	3.089	0.039

Supplementary Table 2. Two-way ANOVA analyses of the hemocyte immune related biomarkers of *M. edulis* in response to Zn treatment and season at 15 °C. Season: summer and winter; Zn treatment: control, 10 µg l⁻¹ nZnO, 100 µg l⁻¹ nZnO, 10 µg l⁻¹ Zn²⁺, and 100 µg l⁻¹ Zn²⁺. Degrees of freedom (d.f.) for the error were 20 for all studied traits. F and P values are given. Significant effects are highlighted in bold.

Source	F	P	F	P	F	P	F	P	F	P	F	P	F	P			
df	Total hemocytes		Hemocyte		Adhesion		Phagocytosis		Neutral red		Myticin		Defensin		Mytilin		
Season	1	7.2	0.014	0.328	0.573	3.129	0.092	27.576	<0.001	991.618	<0.001	229.312	<0.001	39.042	<0.001	302.447	<0.001
Zn	4	2.188	0.107	32.975	<0.001	3.016	0.042	182.662	<0.001	332.032	<0.001	8.683	<0.001	55.572	<0.001	13.095	<0.001
Season * Zn	4	0.265	0.897	0.515	0.725	0.079	0.988	45.645	<0.001	29.919	<0.001	3.285	0.032	2.73	0.058	4.631	0.008
	df	TLRb		TLRc		TNF		TGF-β		C1		C3q		Myd88a		Myd88c	
Season	1	12.58	0.002	105.382	<0.001	0.444	0.513	250.66	<0.001	37.458	<0.001	0.337	0.568	25.11	<0.001	5.296	0.032
Zn	4	5.595	0.003	3.498	0.025	4.753	0.007	10.823	<0.001	5.837	0.003	3.121	0.038	11.003	<0.001	21.836	<0.001
Season * Zn	4	7.402	0.001	15.174	<0.001	5.451	0.004	7.303	0.001	9.683	<0.001	4.988	0.006	7.375	0.001	6.918	0.001

Supplementary Table 3. Factor loadings for the first two principal components of the hemocyte immune related biomarkers of *M. edulis* exposed to different combinations of Zn treatment and temperature in winter experiment.

Traits with high loadings (>0.6 absolute value) are highlighted in bold.

Variable	Factor 1	Factor 2
myticin	-0.777594	0.104831
defensin	-0.700428	-0.638741
mytilin	-0.907058	-0.048371
C3q	-0.923982	-0.120416
C1	-0.902486	0.235919
TLRb	-0.925914	-0.082939
TLRc	-0.892925	-0.035642
Myd88a	0.951597	0.163116
Myd88c	0.898893	0.303907
TNF	-0.735963	-0.068937
TGF- β	-0.892616	0.103405
THC	0.652556	-0.425704
HM	0.868813	-0.228470
AD	0.775229	-0.430053
Pha	-0.476323	0.609991
NRU	-0.685521	-0.432782

Supplementary Table 4. Discriminant Function Stepwise Analysis of the hemocyte immune related biomarkers of *M. edulis* exposed to different combinations of Zn treatment and temperature in winter experiment.

Values that significantly discriminate studied groups (P<0.05) are shown in red. Wilks' Lambda: < 0.00001, F_{144.55}=9.3949, P< 0.001.

	Wilks' Lambda	Partial Lambda	F-remove (2,16)	P-value	1-Toler. (R-Sqr.)
myticin	< 0.00001	0.152169	3.09535	0.113127	0.910858
defensin	< 0.00001	0.165958	2.79202	0.135333	0.825207
mytilin	< 0.00001	0.226025	1.90238	0.247862	0.851729
C3q	< 0.00001	0.058918	8.87377	0.013511	0.993535
C1	< 0.00001	0.039774	13.41215	0.005314	0.987808
TLRb	< 0.00001	0.073989	6.95303	0.022963	0.986717
TLRc	< 0.00001	0.404938	0.81640	0.627981	0.923372
Myd88a	< 0.00001	0.467074	0.63388	0.740005	0.957009
Myd88c	< 0.00001	0.576290	0.40847	0.884950	0.910290
TNF	< 0.00001	0.348123	1.04031	0.511279	0.854776
TGF-β	< 0.00001	0.097049	5.16895	0.042592	0.945328
THC	< 0.00001	0.155495	3.01726	0.118334	0.886754
HM	< 0.00001	0.054389	9.65898	0.011193	0.913739
AD	< 0.00001	0.693165	0.24592	0.967023	0.388615
Pha	< 0.00001	0.007286	75.69109	0.000083	0.787703
NRU	< 0.00001	0.076795	6.67869	0.025019	0.797043

Supplementary Table 5. Factor loadings for the first two principal components of the hemocyte immune related biomarkers of *M. edulis* exposed to different combinations of Zn treatment and temperature in summer experiment.

Traits with high loadings (>0.6 absolute value) are highlighted in bold.

Variable	Factor 1	Factor 2
myticin	0.822661	-0.388978
defensin	0.813485	0.048489
mytilin	0.798346	-0.387835
C3q	0.449974	-0.591043
C1	0.191503	-0.254088
TLRb	0.599250	-0.641294
TLRc	-0.088354	-0.512388
Myd88a	0.605434	-0.307367
Myd88c	0.321042	0.374773
TNF	0.304007	-0.373353
TGF- β	0.314540	-0.579497
THC	-0.373946	-0.457358
HM	0.819825	0.394540
AD	-0.557151	-0.424172
Pha	-0.761862	-0.566196
NRU	0.725308	0.611041

Supplementary Table 6. Discriminant Function Stepwise Analysis of the hemocyte immune related biomarkers of *M. edulis* exposed to different combinations of Zn treatment and temperature in summer experiment.

Values that significantly discriminate studied groups ($P < 0.05$) are shown in red. Wilks' Lambda: < 0.00001 , $F_{144,55} = 6.0721$, $P < 0.001$.

	Wilks' Lambda	Partial Lambda	F-remove (2,16)	P-value	1-Toler. (R-Sqr.)
myticin	< 0.00001	0.206398	2.13611	0.208715	0.975610
defensin	< 0.00001	0.060014	8.70162	0.014108	0.916832
mytilin	< 0.00001	0.244716	1.71465	0.286696	0.955701
C3q	< 0.00001	0.191106	2.35149	0.179674	0.920898
C1	< 0.00001	0.093935	5.35870	0.039581	0.739575
TLRb	< 0.00001	0.339511	1.08078	0.492778	0.799669
TLRc	< 0.00001	0.108750	4.55301	0.054888	0.925041
Myd88a	< 0.00001	0.637287	0.31620	0.936247	0.692463
Myd88c	< 0.00001	0.143129	3.32596	0.099474	0.894294
TNF	< 0.00001	0.530708	0.49126	0.832945	0.761359
TGF- β	< 0.00001	0.329647	1.12975	0.471416	0.468691
THC	< 0.00001	0.114818	4.28303	0.061862	0.914436
HM	< 0.00001	0.047123	11.23386	0.007968	0.919353
AD	< 0.00001	0.237450	1.78412	0.271446	0.825325
Pha	< 0.00001	0.200995	2.20847	0.198293	0.731853
NRU	< 0.00001	0.123846	3.93029	0.072969	0.710302

Supplementary Table 7. A summary table indicating changes in the studied immune-related biomarkers in *M. edulis*.

Changes in a trait compared to the respective control (not exposed to nZnO or dissolved Zn at the same respective acclimation temperature) are indicated as follows: upward arrow (↑) and orange color – increase, downward arrow (↓) and blue color – decrease, tilde (~) – no significant change. W10 and W15 – winter mussels acclimated at 10 and 15 °C, respectively; S15 and S20 - summer mussels acclimated at 15 and 20 °C, respectively.

A. Functional traits of the hemocytes.

Source	Total hemocytes count				Hemocyte mortality				Adhesion capacity				Phagocytosis				Neutral red uptake				
	W10	W15	S15	S20	W10	W15	S15	S20	W10	W15	S15	S20	W10	W15	S15	S20	W10	W15	S15	S20	
10 µg l ⁻¹ nZnO	~	~	~	~	↑	~	~	~	~	~	~	~	↑	↓	↑	↑	↑	~	~	↑	↑
100 µg l ⁻¹ nZnO	~	~	~	~	↑	↑	↑	↑	↓	↓	~	~	↑	~	↑	↑	↑	↑	↑	↑	↑
10 µg l ⁻¹ Zn ²⁺	~	~	~	~	~	~	~	~	~	~	~	~	~	~	↓	~	↑	↓	~	~	~
100 µg l ⁻¹ Zn ²⁺	~	~	~	~	↑	↑	↑	↑	~	~	~	~	↑	↑	↑	↑	↑	~	~	↑	↑

Supplementary References

Benito, D., Ahvo, A., Nuutinen, J., Bilbao, D., Saenz, J., Etxebarria, N., Lekube, X., Izagirre, U., Lehtonen, K. K., Marigómez, I. et al. (2019). Influence of season-depending ecological variables on biomarker baseline levels in mussels (*Mytilus trossulus*) from two Baltic Sea subregions. *Science of The Total Environment* **689**, 1087-1103.

Berger, V. J. (1986). Adaptations of marine molluscs to changes of environmental salinity. Leningrad: "Nauka". 216 pp.

Coles, J. A., Farley, S. R. and Pipe, R. K. (1995). Alteration of immune response of the common marine mussel *Mytilus edulis* resulting from exposure to cadmium. *Diseases of Aquatic Organisms* **22**, 59-65.

Falfushynska, H. I., Wu, F., Ye, F., Kasianchuk, N., Dutta, J., Dobretsov, S. and Sokolova, I. M. (2019). The effects of ZnO nanostructures of different morphology on bioenergetics and stress response biomarkers of the blue mussels *Mytilus edulis*. *Science of The Total Environment* **694**, 133717.

Kautsky, N. (1982). Quantitative studies on gonad cycle, fecundity, reproductive output and recruitment in a baltic *Mytilus edulis* population. *Marine biology* **68**, 143-160.

Khlebovich, V. V. (2017). Acclimation of animal organisms: basic theory and applied aspects. *Biology Bulletin Reviews* **7**, 279-286.

Marchi, B., Burlando, B., Moore, M. N. and Viarengo, A. (2004). Mercury- and copper-induced lysosomal membrane destabilisation depends on $[Ca^{2+}]_i$ dependent phospholipase A2 activation. *Aquatic Toxicology* **66**, 197-204.

Pfaffl, M. W. (2001). A new mathematical model for relative quantification in real-time RT-PCR. *Nucleic Acids Research* **29**, 2002-2007.

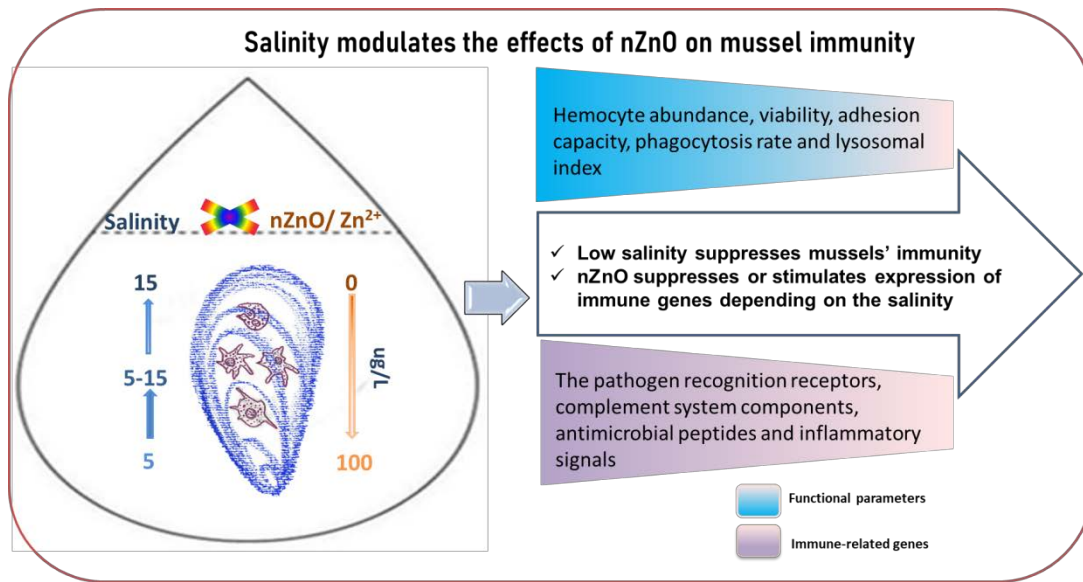
Qi, P., Huang, H., Guo, B., Liao, Z., Liu, H., Tang, Z. and He, Y. (2019). A novel interleukin-1 receptor-associated kinase-4 from thick shell mussel *Mytilus coruscus* is involved in inflammatory response. *Fish & Shellfish Immunology* **84**, 213-222.

Wu, F. L., Falfushynska, H., Dellwig, O., Piontkivska, H. and Sokolova, I. M. (2020). Interactive effects of salinity variation and exposure to ZnO nanoparticles on the innate immune system of a sentinel marine bivalve, *Mytilus edulis*. *Science of The Total Environment* **712**.

7.2. Interactive effects of salinity variation and exposure to ZnO nanoparticles on the innate immune system of a sentinel marine bivalve, *Mytilus edulis*

Wu, F, Falfushynska, H, Dellwig, O, Piontkivska, H. and Sokolova, I. M. (2020). Science of The Total Environment 712.

DOI: <https://doi.org/10.1016/j.scitotenv.2019.136473>





Interactive effects of salinity variation and exposure to ZnO nanoparticles on the innate immune system of a sentinel marine bivalve, *Mytilus edulis*

Fangli Wu^{a,1}, Halina Falfushynska^{a,b,1}, Olaf Dellwig^c, Helen Piontkivska^d, Inna M. Sokolova^{a,e,*}

^a Department of Marine Biology, Institute for Biological Sciences, University of Rostock, Rostock, Germany

^b Department of Human Health, Physical Rehabilitation and Vital Activity, Ternopil V. Hnatiuk National Pedagogical University, Ternopil, Ukraine

^c Department of Marine Geology, Leibniz Institute for Baltic Sea Research Warnemünde, Rostock, Germany

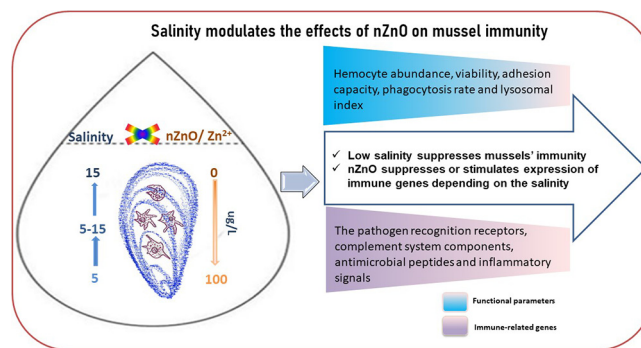
^d Department of Biological Sciences, Kent State University, Kent, OH, USA

^e Department of Maritime Systems, Interdisciplinary Faculty, University of Rostock, Rostock, Germany

HIGHLIGHTS

- Interactive effects of salinity stress and nZnO were investigated in the blue mussels.
- Exposure to nZnO stimulated phagocytosis but suppressed hemocyte viability and adhesion.
- Low salinity (5) had a major immunosuppressive effect overriding the effects of nZnO.
- Nano-ZnO exposure at salinity 15 decreased expression of the pattern recognition receptors and the complement system.
- The immunosuppressive molecular effects of nZnO were reversed at the fluctuating salinity (5–15).

GRAPHICAL ABSTRACT



ARTICLE INFO

Article history:

Received 11 November 2019

Received in revised form 26 December 2019

Accepted 31 December 2019

Available online 07 January 2020

Editor: Jay Gan

ABSTRACT

ZnO nanoparticles (nZnO) are released into the coastal environment from multiple sources, yet their toxicity to marine organisms is not well understood. We investigated the interactive effects of salinity (normal 15, low 5, and fluctuating 5–15) and nZnO (100 $\mu\text{g l}^{-1}$) on innate immunity of the blue mussels *Mytilus edulis* from a brackish area of the Baltic Sea. Exposure to ionic Zn (100 $\mu\text{g l}^{-1}$) was used to test whether the toxic effects of nZnO can be attributed to the potential release of Zn^{2+} . Functional parameters and the expression of key immune-related genes were investigated in the mussels exposed to nZnO or ionic Zn under different salinity regimes for 21 days. nZnO exposures elevated hemocyte mortality, suppressed adhesion, stimulated phagocytosis, and led to an apparent increase in lysosomal volume. At salinity 15, nZnO suppressed the mRNA expression of the Toll-like receptors TLRa, b and c, C-lectin, and the complement system component C3q indicating impaired ability for pathogen recognition. In contrast, the mRNA levels of an antimicrobial peptide defensin increased during nZnO exposure at salinity 15. At fluctuating salinity (5–15), nZnO exposure increased expression of multiple immune-related genes in hemocytes including the complement system components C1 and C3q, and the Toll-like receptors TLRa, b and c. Low salinity (5) had strong immunosuppressive effects on the functional and molecular immune traits of *M. edulis* that overshadowed the effects of nZnO. The salinity-dependent modulation of immune response to nZnO cannot be attributed to the differences in the aggregation or solubility of nZnO, and likely reflects the interaction of the toxic effects of nanoparticles and physiological effects of the osmotic stress. These findings

* Corresponding author at: Department of Marine Biology, Institute for Biological Sciences, University of Rostock, Rostock, Germany.

E-mail address: inna.sokolova@uni-rostock.de (I.M. Sokolova).

¹ These authors contributed equally to the work.

have implications for the environmental risk assessment of nanomaterials and the development of the context-specific biomarker baselines for coastal pollution monitoring.

© 2018 Elsevier B.V. All rights reserved.

1. Introduction

Engineered nanomaterials (i.e. materials containing particles with one or more dimensions <100 nm) including ZnO nanoparticles (nZnO) are increasingly used in industrial applications, energy production, medicine, and personal care products (Williams et al., 2019). A broad use of ZnO nanoparticles as antimicrobials, UV screens, catalysts, and antifouling agents results in the massive release of nZnO into the environment and raises concerns about its environmental and human health hazards (Bondarenko et al., 2013; Sathe et al., 2017; Williams et al., 2019). Quantification of nZnO in the marine environment is complicated by the lack of the analytical approaches to measure nZnO in complex environmental matrices such as the sea water or sediment, but the modeling-based estimates predict the levels from hundreds nanograms per liter up to 900 $\mu\text{g l}^{-1}$ nZnO in the surface waters and >100 $\mu\text{g kg}^{-1}$ in the sediment (Coll et al., 2016; Yung et al., 2014). nZnO is recognized as an ecotoxic agent by the European Chemicals Agency (ECHA) based on extrapolations from the toxicity of dissolved Zn and bulk ZnO (Munn et al., 2010). The toxic mechanisms of nZnO are not yet fully understood, but there is increasing evidence that nZnO toxicity is different from that of ionic Zn or the bulk ZnO (Falfushynska et al., 2017; Falfushynska et al., 2015; Falfushynska et al., 2019a; Shaw and Handy, 2011; Yung et al., 2014). Therefore, understanding of the sublethal effects of nanoparticulate pollutants (such as nZnO) on keystone marine organisms is essential for the assessment of the unintended impacts of nanotechnologies on coastal ecosystems.

Recent studies in marine organisms show that nZnO exposure can influence growth and metabolism (Fabrega et al., 2012; Hanna et al., 2013), stimulate antioxidant and detoxification mechanisms (Buffet et al., 2012), impair feeding and locomotion (Buffet et al., 2012) and negatively affect reproduction (Fabrega et al., 2012). However, the potential immunotoxicity of nZnO in marine organisms remains underexplored. This is an important gap in our knowledge, because studies in humans and mammalian models show that the innate immune system is a key target for nZnO toxicity (Ignacio et al., 2014; Roy et al., 2014; Zhang et al., 2017). In marine invertebrates (including bivalves), the multifunctional macrophage-like cells called hemocytes play a central role in the immune response (Allam and Raftos, 2015; Mydlarz et al., 2006; Zheng et al., 2005). Hemocytes participate in the destruction of the pathogens through phagocytosis, oxidative burst and apoptosis, and produce the opsonizing molecules and antimicrobial peptides (Allam and Raftos, 2015; Hughes et al., 2010; Sokolova, 2009). ZnO nanoparticles are acutely cytotoxic to bivalve hemocytes during in vitro exposures (Katsumiti et al., 2016). Furthermore, in vivo exposures of the thick shelled mussels *Mytilus coruscus* to high concentrations of nZnO (2.5–10 mg l^{-1}) negatively affect hemocyte survival, phagocytosis and lysosomal abundance, and increase the baseline production of reactive oxygen species (ROS) (Wu et al., 2018). In the carpet clams *Ruditapes philippinarum*, nZnO exposure induced DNA damage in circulating hemocytes and led to hemocyte proliferation (Katsumiti et al., 2016; Marisa et al., 2016). Other metal-containing nanoparticles (such as nano-TiO₂) can also have negative impacts on the immune parameters including suppression of phagocytosis and viability of bivalve hemocytes (Huang et al., 2016; Marisa et al., 2015; Wang et al., 2014). Given the high likelihood of nanoparticle exposures in coastal environments, it is essential to assess the impacts of environmentally relevant levels of emerging nanoparticle pollutants on the innate immune defense of keystone marine organisms such as marine bivalves.

The aim of our present study was to investigate the effects of exposure to waterborne nZnO (100 $\mu\text{g l}^{-1}$ Zn) on the immune parameters of the blue mussels *M. edulis* acclimated to different salinity regimes. The blue mussels (*Mytilus* spp.) are economically and ecologically important species in temperate to subarctic coastal ecosystems (Kijewski et al., 2011; Mathiesen et al., 2017) and common sentinel organisms for environmental monitoring and ecosystem health assessment (Beyer et al., 2017; Bricker et al., 2014). Salinity is an important environmental factor in shallow marine habitats, including estuaries, coastal lagoons, and semi-enclosed seas (such as the Baltic Sea) where salinity can fluctuate due to freshwater run-off, precipitation, and evaporation (McLusky and Elliott, 2004; Pierce et al., 2012). Salinity can affect stability, aggregation, and bioavailability of the nanoparticles (Yung et al., 2017), thus potentially modulating the toxic impacts of nZnO. Furthermore, salinity variation strongly affects physiology, metabolism, and osmotic balance of marine bivalves (Berger and Kharazova, 1997) and can affect their immune functions and host-pathogen interactions (Casas et al., 2004; Corporeau and Auffret, 2003; Malagoli et al., 2007). This creates a physiological basis for potential interactions between salinity and nZnO-induced stress on the immunity of bivalves in coastal environments with variable salinities.

We hypothesized that exposure to nZnO will negatively affect the immune-related functions and suppress expression of immune-related genes in hemocytes of the mussels, and that the immunotoxic effects of nZnO might be exacerbated by osmotic stress due to the low or variable salinity. To test these hypotheses, we acclimated the blue mussels *M. edulis* for 21 days under the control (salinity 15), low (salinity 5) and fluctuating (15–5) salinity regimes in the presence or absence of nZnO and determined the functional traits (mortality, phagocytosis and adhesion capacity) as well as the mRNA expression of key immune-related genes in mussel hemocytes including the complement systems, recognition factors (Toll-like receptors and the membrane-bound C-lectin), MYD88 innate immune signal transduction adaptors, and antimicrobial peptides myticin, mytilin and defensin. This study provides new insights into the potential mechanisms of nZnO-induced immunomodulation in the mussels and demonstrates the important role of the salinity regime in determining the cellular immune response to nanoparticle pollutants.

2. Materials and methods

2.1. Animal collection and maintenance

Mussels were collected near Warnemünde, Germany (54°10' 49.602"N, 12°05'21.991"E). The Baltic populations of *Mytilus* represent *M. edulis* × *M. trossulus* hybrids, and the population at the study site has ~70% nuclear and 100% mitochondrial genetic background of *M. edulis* (Stuckas et al., 2017). Therefore, we designated the experimental animals *M. edulis*. The mussels were transported to the University of Rostock within 2 h of collection in a cooler lined with the seawater-soaked paper towels. The shells were cleaned from epibionts, and the mussels were kept in aerated, temperature-controlled recirculated aquaria with a multi-step filtration system including UV-water treatment, protein skimmer, and a moving bed biofilter. Mussels were maintained for a week at salinity 15 (practical salinity scale) and temperature 10 °C. These conditions were close to the salinity (12) and temperature (7 °C) in the mussels' habitat at the time of collection. Therefore, salinity 15 was considered normal (control) salinity in this study.

After the preliminary acclimation, the mussels were randomly assigned to one of the nine experimental groups and exposed for 21 days to the different combinations of salinity and Zn exposure regimes. The duration of experimental exposures (21 days) was chosen because in temperate marine bivalves, 2–3 weeks are required to reach a new physiological steady-state after an environmental shift (Khlebovich, 1981; Khlebovich, 2017; Thompson et al., 2012). Experimental exposures followed a full factorial design with three salinity regimes (normal salinity 15, fluctuating salinity 5–15, or low salinity 5) and three levels of Zn exposure (no Zn addition as a control, nZnO or ionic Zn at the nominal concentrations of $100 \mu\text{g l}^{-1}$ Zn). In the fluctuating salinity, the square salinity wave was applied as follows: 22 h at salinity 15, 2 h at salinity 10, 22 h at salinity 5, and 2 h at salinity 10, repeated for three weeks. Ionic Zn treatments were included to test whether the observed effects of nZnO can be ascribed to the release of Zn^{2+} . Each of the nine experimental treatment groups was randomly subdivided and placed into five replicate tanks per treatment, each tank containing 12 mussels in 1 l of seawater. Experimental seawater was prepared with the Instant Ocean® sea salt dissolved in distilled water and supplemented with 10% of the filtered natural Baltic seawater (salinity 9–12) to achieve the target salinities.

A static renewal design was used with the water change and nZnO or ZnSO_4 additions (depending on the treatment) every two days. Commercial ZnO nanoparticles (nZnO) (average particle size 30 nm) were purchased from Sigma-Aldrich Sweden AB (Stockholm, Sweden). The suspensions of nanoparticles ($10 \mu\text{g ml}^{-1}$) had the following characteristics in the exposure media: at salinity 5, the hydrodynamic size with a major peak at 854 ± 172 nm, a minor peak $188 \text{ nm} \pm 28$ nm, and zeta-potential of 2.9 mV; at salinity 15, the hydrodynamic size with a major peak at 817 ± 174 nm, and a minor peak at 211 ± 24 nm, zeta-potential -9.6 mV (Supplementary Fig. 1). Suspensions of nZnO were added to experimental water to achieve the nominal concentration of $100 \mu\text{g l}^{-1}$ Zn during every water change and maintained in suspension by vigorous aeration. For ionic Zn exposures, $100 \mu\text{g l}^{-1} \text{Zn}^{2+}$ (as ZnSO_4) were added during every water change.

Mussels were exposed for 21 days to different conditions in 12: 12 light: dark period. All exposures were conducted at 10 ± 1 °C. During preliminary acclimation and experimental exposures, mussels were fed before every water change with a commercial blend of live algae containing *Nannochloropsis oculata*, *Phaeodactylum* sp. and *Chlorella* sp. (Premium Reef Blend, CoralSands, Wiesbaden, Germany) per manufacturer's instructions. No mortality of the mussels occurred during the experimental exposures except for the mussels under low salinity condition where 5% (three out of 60) mussels died after 21 days.

2.2. Zn concentrations in the seawater and mussels' body

Water samples (14.5 ml) were collected from experimental tanks before each water change and stored at +4 °C. Prior to analysis, the seawater samples were acidified with trace-metal grade HNO_3 to ensure dissolution of nZnO. Whole soft body of the mussels was homogenized under the liquid nitrogen, and 200–300 mg of the soft tissue powder was dried out in an incubator at 70 °C. The dry tissue was digested with 1 ml of 30% hydrogen peroxide, incubated at 70 °C overnight to evaporate hydrogen peroxide, and digested in 1 ml of 65% HNO_3 (trace metal grade) at 70 °C for 24 h. The digested tissue samples were filtered through $0.45 \mu\text{m}$ filters and stored at +4 °C until further analysis.

Zn concentration in seawater samples was measured using quadrupole inductively coupled plasma mass spectrometry (ICP-MS) (iCAP Q; Thermo Fisher Scientific) coupled to a seaFAST matrix removal and preconcentration module (Elemental Scientific), with the latter using a chelating resin (Dellwig et al., 2019; Lagerström et al., 2013; Sohrin et al., 2008). Helium served as a collision gas to avoid polyatomic interferences and indium was used as an internal standard to compensate for instrumental fluctuations. The seawater samples were diluted ten times

with 2 vol% HNO_3 (sub-boiled) and measured against an external calibration ranging from 0.01 to $10 \mu\text{g Zn l}^{-1}$. Precision and trueness were checked with the international seawater reference material NASS-7 (NRCC) and were 7.4% and 2.4%, respectively.

Zn concentrations in the acid digestions of the mussel soft tissues were measured by inductively coupled plasma - optical emission spectrometry (ICP-OES) (iCAP 7400 Duo, Thermo Fisher Scientific; Zn wavelengths 202.5 nm, 206.2 nm, 213.8 nm) in axial mode using external calibration (0.005 – 2 mg l^{-1}) and scandium (227.3 nm) as an internal standard. The final dilution factor (2 vol% HNO_3) of the original acid digestions for ICP-OES measurement was 12.5. Precision and trueness were checked with the international reference material SGR-1b (USGS) and were 1.1% and 5.0%, respectively.

2.3. Hemolymph collection

After 21 days of experimental exposures, mussels were dissected on ice, and hemolymph was collected from the posterior adductor muscle using a 1.0 ml plastic syringe with a 21 gauge needle. All samples were mixed with 1 ml ice cold filtered artificial seawater (ASW) and stored on ice to prevent aggregation of hemocytes. Each biological replicate represented pooled hemolymph from six mussels (0.6–1.0 ml per mussel) to reduce individual variation. For the functional traits analysis, the freshly collected hemocytes were used immediately. For mRNA expression analyses, hemolymph samples were centrifuged for 10 min at $1000 \times g$. The hemocyte pellet was washed once with ice-cold filtered ASW and stored at -80 °C until RNA extraction. A total of three biological replicates was used to assess abundance, mortality, and functional traits of hemocytes, and a total of six replicates was used for gene expression analyses.

2.4. Hemocyte count and mortality

Total hemocytes count was determined using a Brightline hemocytometer (Sigma Aldrich, St. Louis, MO, USA). Hemocyte mortality was determined using Trypan Blue exclusion assay. Briefly, hemolymph and 0.4% Trypan Blue solution were mixed (8:2 v/v) and incubated for 3 min. Unstained (live) and blue-stained (dead) cells were counted using a Brightline hemocytometer. Hemocyte mortality was evaluated as the percentage of the blue-stained hemocytes relative to the total hemocyte count.

2.5. Adhesion capacity

Hemocytes (10^6 cells) were placed in 1 ml of filtered ASW in the wells of a 12-well plate (Costar, Corning) and incubated for 2 h at room temperature. After the incubation, the ASW was collected and the wells were surface-washed with 1 ml of ice cold ASW to collect the non-adhered hemocytes. The samples were centrifuged for 10 min at $1000 \times g$, resuspended in 1 ml of ice cold ASW, and the non-adhered hemocytes were counted using a BrightLine hemocytometer. The adhesion capacity was expressed as the percentage of adhered hemocytes in the total hemocyte population in each sample.

2.6. Phagocytosis

Phagocytosis assay was performed using a modified procedure described elsewhere (Coles et al., 1995). Suspension of Neutral Red-stained, heat-stabilized zymosan (Sigma Aldrich, St. Louis, MO, USA) was added to hemocytes at the final concentration of 200 zymosan particles per hemocyte. Hemocytes were incubated for 30 min at room temperature, centrifuged 10 min at $1000 \times g$, resuspended in 2 ml ice cold ASW to remove free and surface-attached zymosan, and centrifuged again for 10 min at $1000 \times g$ to collect the hemocytes. The hemocyte pellet was resuspended in 0.1 ml acetic acid (1% in 50% ethanol) and incubated for 5 min to extract Neutral Red from the engulfed

zymosan particles. The Neutral Red dye was also extracted from the cell-free suspensions with the known amounts of the zymosan particles and used as standards for calibration. The optical densities of the sample and standard extracts were read at 550 nm using a 96-well plate on a SpectraMax iD3 Multi-Mode Microplate Reader (Molecular devices, USA). Results were expressed as the number of ingested zymosan particles per cell.

2.7. Neutral red uptake assay

Hemolymph samples were centrifuged for 10 min at 600 ×g, 4°C and resuspended in 2 ml of HEPES-buffer containing 20 mM 4-(2-hydroxyethyl)-1-piperazineethanesulfonic acid (HEPES), 436 mM NaCl, 53 mM MgSO₄, 10 mM KCl, 10 mM CaCl₂, pH 7.3 (Marchi et al., 2004). Hemocytes were washed by centrifugation-resuspension three times and resuspended in 0.2 ml HEPES-buffer at the concentration of 10⁷ cells ml⁻¹. Hemocyte suspension (1 ml containing 10⁷ cells) was added to 0.5 ml of physiological saline with 0.004% w/v Neutral Red, incubated for 2 h and centrifuged 10 min at 600 ×g. Hemocytes were washed twice to remove the free dye, and resuspended in 1 ml HEPES-buffer. The dye was extracted from the cell suspension with 0.2 ml an acetic acid–ethanol mixture (1:1 v/v). Absorbance was measured at 550 nm using a 96-well plate on a SpectraMax iD3 Multi-Mode Microplate Reader (Molecular Devices, USA). The Neutral Red Uptake (NRU) of hemocytes was expressed as absorbance units (AU) per 10⁶ hemocytes.

2.8. mRNA expression of target genes

Total RNA was extracted from the hemocytes using TRIzol reagent (Thermo Fisher Scientific, Berlin, Germany) according to the manufacturer’s protocol. RNA samples were purified from possible DNA contamination with TURBO DNA-free Kit (Thermo Fisher Scientific, Berlin, Germany). cDNA was synthesized from 1.5 µg of total RNA using High Capacity cDNA Reverse Transcription Kit (Thermo Fisher Scientific, Berlin, Germany) following the manufacturer’s instructions. qRT-PCR was performed using StepOnePlus™ Real-Time PCR System Thermal Cycling Block (Applied Biosystems, Thermo Fisher Scientific, Berlin, Germany) and Biozym Blue S’Green qPCR Mix Separate ROX kit (Biozym Scientific GmbH, Hessisch Oldendorf, Germany). Reaction mixture containing 10 µl of 2× qPCR S’Green BlueMix and ROX additive mixture, 1.6 µl of each forward and reverse primer (to the final concentration of 0.4 µM) (Table), 4.8 µl PCR grade water and 2 µl of cDNA were added to the wells of 96 well PCR plates, sealed (RT-PCR Seal foil, Roth, Karlsruhe, Germany) and briefly spun to eliminate air bubbles. The cycling

parameters were as follows: 95 °C for 10 min to activate the polymerase followed by 40 cycles of 15 s at 95 °C and 60 s at 60 °C. Signal readout was conducted at the primer-specific reading temperature (Table 1) selected so as to melt the primer dimers but not the amplification product. Following amplification, a melt curve analysis was performed to ensure that a single PCR product was amplified. In each run, serial dilutions of a cDNA standard were amplified to determine amplification efficiency (Pfaffl, 2001). In a pilot analysis, we tested three housekeeping genes (the eukaryotic elongation factor 1 (eEF1), tubulin and β-actin) and chose eEF1 that showed the least variation among and within the experimental groups for normalization of the target gene expression. The apparent amplification efficiency was calculated for each primer pair, and the expression of the target genes was normalized against the expression of the eukaryotic elongation factor eEF1 as described elsewhere (Pfaffl, 2001).

2.9. Statistics

Data were tested for the normality and homogeneity of variances using Kolmogorov-Smirnov and Levine test, respectively. Outliers detected by box-and-whiskers plots were removed from the subsequent analysis. Not-normally distributed data were subjected to Box-Cox transformation. The effects of salinity regime, Zn treatment and their interaction on the studied traits were tested using factorial ANOVA with salinity and Zn exposure as fixed factors (Supplementary Table 1). The factor “Salinity regime” had three levels (normal salinity NS, fluctuating salinity FS and low salinity LS). The factor “Zn treatment” had three levels (control – no Zn addition, 100 µg l⁻¹ nZnO, or 100 µg l⁻¹ ionic Zn). Tukey’s Honest Significant Differences (HSD) test was used to assess the differences between the pairs of means of interest.

Normalized, Box-Cox transformed data were subjected to the principal component analysis (PCA) with NIPALS algorithm to reduce the dimensionality of the data set and identify the patterns of biomarker responses among different experimental conditions. The integrated biomarker response (IBR) index was calculated using CALculate IBR Interface (Calibri, <https://liec-univ-lorraine.shinyapps.io/calibri/>) for each treatment group as described elsewhere (Devin et al., 2014). Because IBR software accepts a maximum of eight traits, we calculated the IBR for mRNA expression of the eight target genes with the highest variability among the treatment groups. All other statistical analyses were conducted using IBM® SPSS® Statistics ver. 22.0.0.0 (IBM Corp., Armonk, NY, USA) and GraphPad Prism ver. 7.02 (GraphPad Software Inc., La Jolla, CA, USA) software. The results are expressed as the means ± the standard error (SE) unless noted otherwise. The effects were considered significant if the probability of the Type I error (P) was <0.05.

Table 1
Primer sequences for the target and housekeeping genes used for qPCR. Abbreviations: C1 - C1 complement domain-containing protein; C3q - complement component C3-like protein; C-lectin - membrane-bound C-type lectin, TLR - Toll-like receptors, MyD88 - myeloid differentiation primary response gene 88, HSP70-70 kDa heat shock protein; JNK - c-Jun N-terminal kinase; eEF1 - eukaryotic elongation factor 1α. NCBI accession numbers of the sequences used for primer design are given. Because *M. edulis* does not yet have a completely sequenced genome assembly, we used homologous sequences from either *M. galloprovincialis* or *M. edulis* to generate primers.

Gene	Forward primer (3'-5')	Reverse primer (3'-5')	NCBI accession #	T _{read}
C1	GGCATTAACATCAGGCAGCG	TACGTCCTTTACGTGGAGC	HQ664950	76 °C
C3q	TGATTTGCCGGGAAGTGG	GCAGACCTGCCTGTTCTCT	KP125947	79 °C
C-lectin	ACTGGACGGTAGCTGTTTG	TGTAGCGCCGGATAAAGCAT	KP125930	74 °C
Defensin	CAGCAAATTTCAAGGGAGGT	TGGCGCAAATCCAAC TAGA	JN935272	79 °C
Myticin	CAGAGGCAAGTTGCTCTCC	GGAATGCTCACTGGAACAACG	AF177540	77 °C
Mytilin B	GGCGTTGCTACTGCAAAATGT	TGTTCGGTTTCTCTGTGGG	AF162336	78 °C
TLRa	ACCCCAAACATACGACGCT	CTATGCAGGCCCCAGGTATG	KC344669	72 °C
TLRb	TGATTGGCCGTAGAGGAGC	CATACACAGTGTCTCGCCT	JX173687	77 °C
TLRc	ATCCCGAGAAGTATCGCTGC	CAAAAAGGGGGACAGCGATCA	JX173688	76 °C
MyD88a	AGGATTCGAGGACAGCGAAG	GGCCAAACCATTCTCGTTG	JX112712.1	74 °C
Myd88c	TCTTGCTGGAGGGGAAAAT	GCACCTGGCGCTAATGATTG	KC357782.1	75 °C
HSP70	GGAGAGAAAGTCCAAGGGAGG	TTCGCTCCTTTCTGTGGGAG	AF172607	75 °C
JNK	CCTTTTATGGCAGCAGCGTG	AAAATCCAGTGCCCGATGGT	MH603332.1	76 °C
eEF1	GACAGCAAAAACGACCACC	TTCTCCAGGTGGTTCAGGA	AF063420	77 °C

3. Results

3.1. Zn concentrations in seawater and the soft body of mussels

The total Zn concentration in the seawater was 3.7 ± 0.5 , 88.1 ± 3.6 , and $80.2 \pm 2.2 \mu\text{g l}^{-1}$ in the control, Zn^{2+} , and nZnO exposures, respectively ($N = 12$). Free Zn^{2+} concentration of the nZnO exposed water (determined in the samples filtered through $0.2 \mu\text{m}$ filters prior to the acid dissolution of nZnO) was not significantly different from the control ($P > 0.05$) indicating a minimal release of Zn^{2+} from nZnO.

Zn content of the soft tissues of the mussels was not affected by the acclimation salinity or nZnO exposure, whereas exposure to ionic Zn led to accumulation of Zn in the soft body (Fig. 1A).

3.2. Hemocyte abundance and viability

Hemocyte abundance decreased in the mussels exposed to low but not the fluctuating salinity regime (Fig. 1B). Within the low salinity-acclimated group, the hemocyte abundance was further decreased by exposure to nZnO (Fig. 1B). Exposure to nZnO or ionic Zn had no effect on the hemocyte count in the mussels acclimated to the normal or fluctuating salinity (Fig. 1B).

Mortality of the hemocytes was significantly elevated ($P < 0.05$) in the mussels exposed to nZnO, regardless of the acclimation salinity, as well as in all groups of the mussels maintained under the low salinity regime (Fig. 1C). Exposure to ionic Zn had no effect on the hemocyte viability within the respective salinity groups (Fig. 1C).

3.3. Hemocyte functions

Adhesion capacity of the hemocytes was suppressed in the mussels exposed to nZnO in all acclimation salinity regimes, as well as in all groups of the mussels maintained under the constant low salinity (Fig. 1D). Exposure to ionic Zn had no effect on the hemocyte adhesion capacity, regardless of the salinity exposure (Fig. 1D).

Exposure to nZnO and ionic Zn significantly increased phagocytosis rates in the mussel hemocytes ($P < 0.05$) except for ionic Zn-exposed group at low salinity (Fig. 1E). The stimulating effects of nZnO on phagocytosis were stronger than those of ionic Zn (Fig. 1E). Exposure to the fluctuating and low salinity led to a significant increase in the phagocytosis rate of the mussel hemocytes, with a stronger effect of the constant low salinity than the fluctuating salinity regime (Fig. 1E).

NRU increased in response to nZnO and ionic Zn exposures under all salinity regimes (Fig. 1F). An increase in NRU was stronger in the hemocytes of the mussels exposed to nZnO compared with those exposed to ionic Zn (Fig. 1F). Acclimation at the fluctuating or low salinity also led to a modest but significant increase in the NRU of the hemocytes (Fig. 1F).

3.4. Immune gene expression: normal salinity

At salinity 15, exposure to nZnO and ionic Zn suppressed expression of C3q (by ~ 1.7 -fold), TLRb (by ~ 3.4 – 3.6 -fold), TLRc (by ~ 2 -fold), and C-lectin (by ~ 79 -fold in the nZnO group and by ~ 1.8 -fold in the ionic Zn-exposed group) in *M. edulis* hemocytes (Figs. 2B, D, E and 3B). Transcript levels of C1 decreased by ~ 1.8 -fold in the nZnO-exposed mussels under the normal salinity regime but not in their counterparts exposed to ionic Zn (Fig. 2A). Expression of MyD88a and MyD88c was suppressed by ~ 1.6 -fold in the hemocytes of the mussels exposed to ionic Zn (but not nZnO) at the normal salinity (Fig. 3A). Defensin mRNA levels increased by ~ 3.3 -fold in nZnO-exposed mussels (but not in those exposed to ionic Zn) at salinity 15 (Fig. 3E). The mRNA levels of TLRa, myticin and mytilin were not affected by nZnO or ionic Zn exposure at salinity 15 (Figs. 2C and 3C, D).

3.5. Immune gene expression: fluctuating salinity

Acclimation at the fluctuating salinity (5–15) in clean ASW (without addition of nZnO or ionic Zn) led to transcriptional downregulation of TLRb by ~ 2.6 -fold and C-lectin by ~ 12.2 -fold (Fig. 2D and F), as well as a modest but significant decrease (by ~ 1.3 – 1.6 -fold) in mRNA levels of C3q, TLRc and MyD88c (Figs. 2B, E and 3B). The mRNA expression of the C1q, TLRa, MyD88a, myticin, mytilin and defensin were not affected by acclimation at the fluctuating salinity (Figs. 2A, C and 3A, C, D, E).

Exposure to nZnO at the fluctuating salinity upregulated the transcript levels of C1q (by ~ 4.0 -fold), C3q (by ~ 2.1 -fold), TLRa, TLRb, and TLRc (by ~ 1.9 , 2.0 and 3.7 -fold, respectively) in the mussel hemocytes (Fig. 2A–E). The mRNA levels of C-lectin and defensin decreased by ~ 6.0 -fold in the hemocytes of the mussels exposed to nZnO at the fluctuating salinity (Figs. 2F and 3E). Exposure to nZnO had no effect on the hemocyte mRNA levels of MyD88a, MyD88c, myticin, and mytilin at the fluctuating salinity (Fig. 3A–D). Exposure to ionic Zn at the fluctuating salinity had no effect on mRNA levels of most of the studied immune-related genes except for C-lectin that increased by ~ 7.8 -fold (Fig. 2F), and mytilin and defensin that decreased by ~ 1.5 and 1.9 -fold, respectively (Fig. 3C, E).

3.6. Immune gene expression: low salinity

Acclimation at the low salinity (5) without addition of nZnO or ionic Zn resulted in suppression of the transcript levels of the most studied immune-related genes in the mussel hemocytes including the complement systems C1q and C3q (by ~ 3.7 and 7.5 -fold, respectively), TLR pathway (with ~ 2.2 , 4.2 and 30.0 -fold decrease in mRNA of TLRa, b and c, respectively), MyD88c (by ~ 2.6 -fold), myticin (by ~ 2.3 -fold), mytilin (by ~ 2.2 -fold), and defensin (by ~ 1.9 -fold) (Figs. 2A–E and 3B–E). Expression of MyD88a was elevated (by ~ 2.7 -fold) in the hemocytes of the mussels acclimated to the low salinity (Fig. 3B), whereas the mRNA levels of C-lectin did not change in response to the low salinity acclimation (Fig. 2F).

At the low salinity, exposure to nZnO upregulated the mRNA expression of TLRc and MyD88c (by ~ 6.4 and 2.0 -fold, respectively) (Figs. 2E and 3B) and downregulated the mRNA levels of C-lectin (by ~ 24 -fold) and MyD88a (by ~ 2.0 -fold) (Figs. 2F and 3A). The hemocyte transcript levels of the complement system components (C1q and C3q), TLRa, TLRc, myticin and mytilin were not affected by nZnO exposures in the low salinity-acclimated mussels (Figs. 2A, B, C, E and 3C, D). Exposure to ionic Zn upregulated the transcript levels of C1q (by ~ 2.4 -fold), TLRb and TLRc (by ~ 3.0 and 9.6 -fold, respectively) and MyD88c (by ~ 1.9 -fold) in the hemocytes of the low salinity-acclimated mussels (Figs. 2A, D, E and 3B). The mRNA levels of C-lectin and defensin decreased by ~ 3.7 and 8.9 -fold, respectively, in the hemocytes of Zn^{2+} -exposed mussels at the low salinity (Figs. 2F and 3E), whereas the levels of C3q, TLRa, MyD88a, myticin, and mytilin mRNA did not change (Figs. 2B, 3A, C, D).

3.7. Biomarker profile integration

The principal components analysis (PCA) identified three principal components (PC) with the eigenvalues > 2 jointly explaining 71% of the variation in the data set (Supplementary Table 2). The first PC (36% of the variation) had high positive loadings (> 0.6) of the complement system genes (C1q and C3q), mytilin, TLRa, TLRc and HSP70, and a high negative loading of MyD88a. The PC2 (20% of the variation) had a high positive loading of myticin and high negative loadings of the NRU and phagocytosis activity. The PC3 (15% of the variation) had a high positive loading of defensin mRNA levels and a high negative loading of TLRb.

In the plane of the two 1st PCs, the control and ionic Zn-exposed groups from the normal or fluctuating salinity grouped closely together, with elevated expression of myticin, defensin, MyD88c and TLRb as

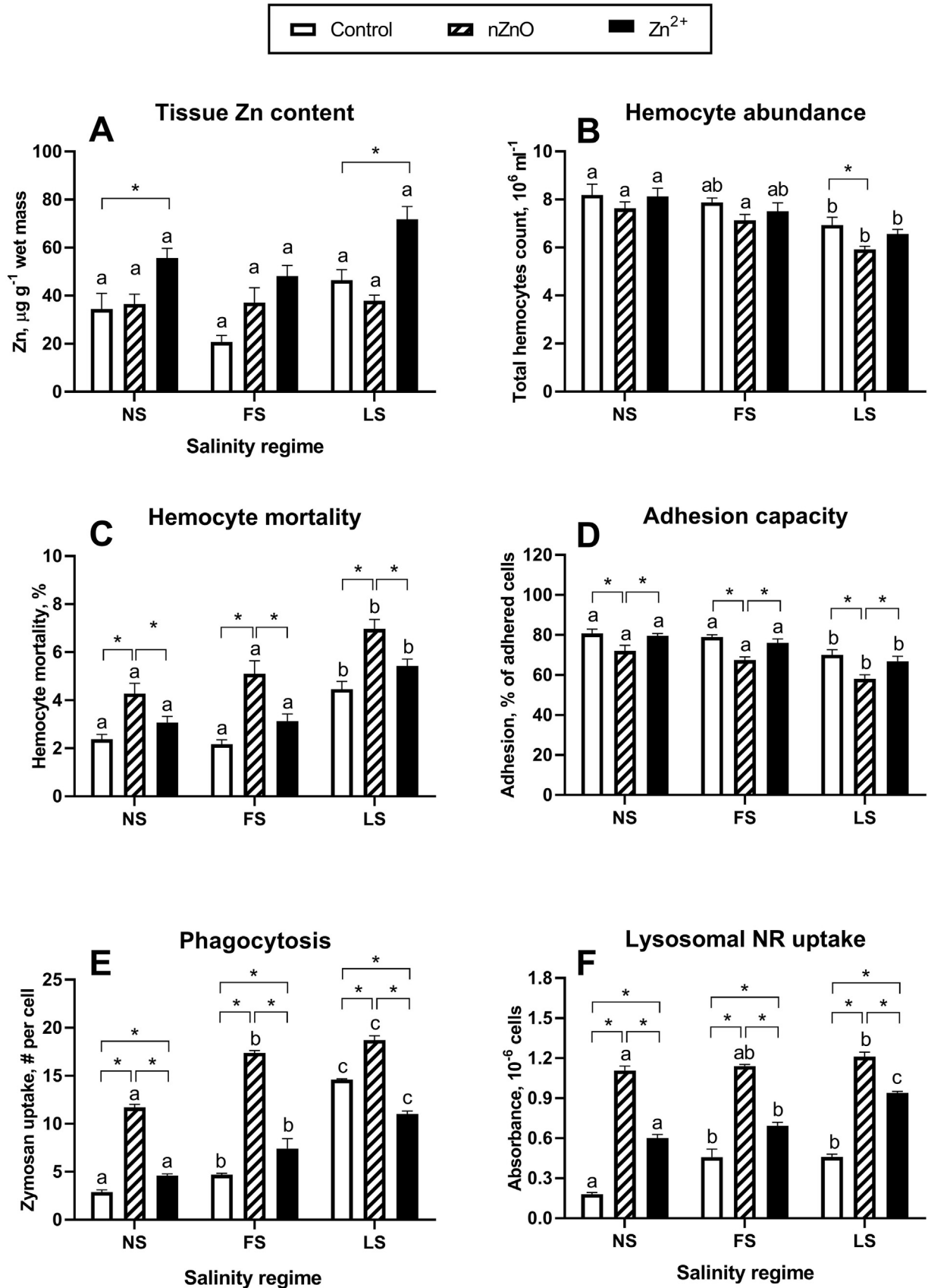


Fig. 1. Hemocyte functional parameters of *M. edulis* exposed to nine combinations of nZnO or Zn²⁺ (0, 100 µg l⁻¹) and salinity (5, 5–15, and 15) during 21 days. A – Zn content of the soft tissues; B – total hemocytes count (10⁶ ml⁻¹); C – hemocyte mortality (%); D – adhesion capacity (%); E – phagocytosis (Zymosan particles per cells); F – neutral red uptake (10⁻⁶ cells). Asterisks indicate significant differences among nZnO or Zn²⁺ treatments within fixed salinity level (Tukey HSD test, *P* < 0.05), and different letters indicate significant differences between three salinity levels within fixed nZnO or Zn²⁺ concentration (Tukey HSD test, *P* < 0.05), *N* = 3.

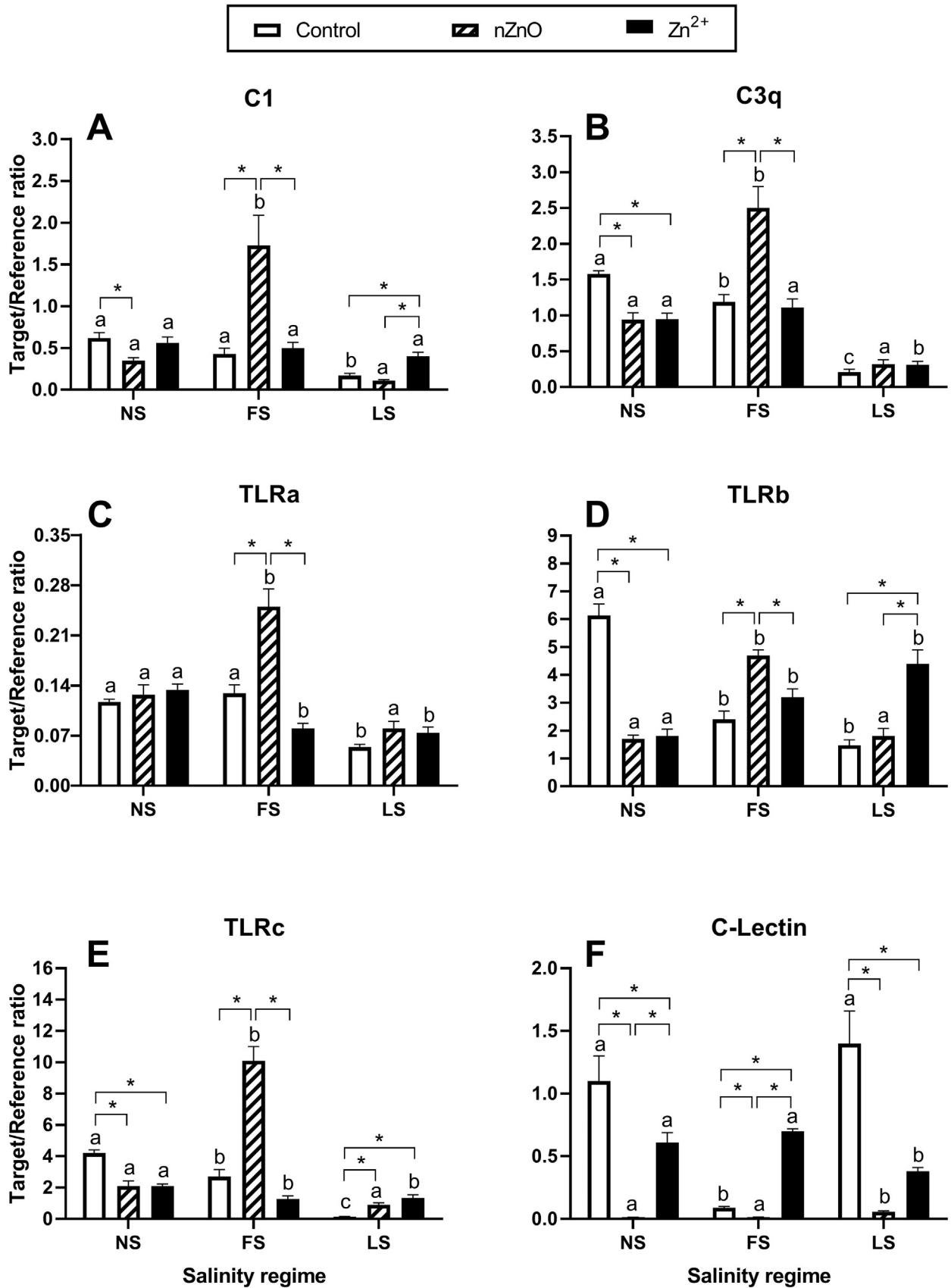


Fig. 2. Expression of mRNA of the complement systems and pathogen recognition factors in hemocytes of *M. edulis* exposed to nine combinations of nZnO or Zn²⁺ (0, 100 μg l⁻¹) and salinity (5, 5–15 and 15) during 21 days. A – C1 complement domain-containing protein; B – complement component C3-like protein; C – Toll-like receptor a; D – Toll-like receptor b; E – Toll-like receptor c; F – membrane bound C-type lectin. Asterisks indicate significant differences among nZnO or Zn²⁺ treatments within fixed salinity level (Tukey HSD test, *P* < 0.05), and different letters indicate significant differences between three salinity levels within fixed nZnO or Zn²⁺ concentration (Tukey HSD test, *P* < 0.05), *N* = 6.

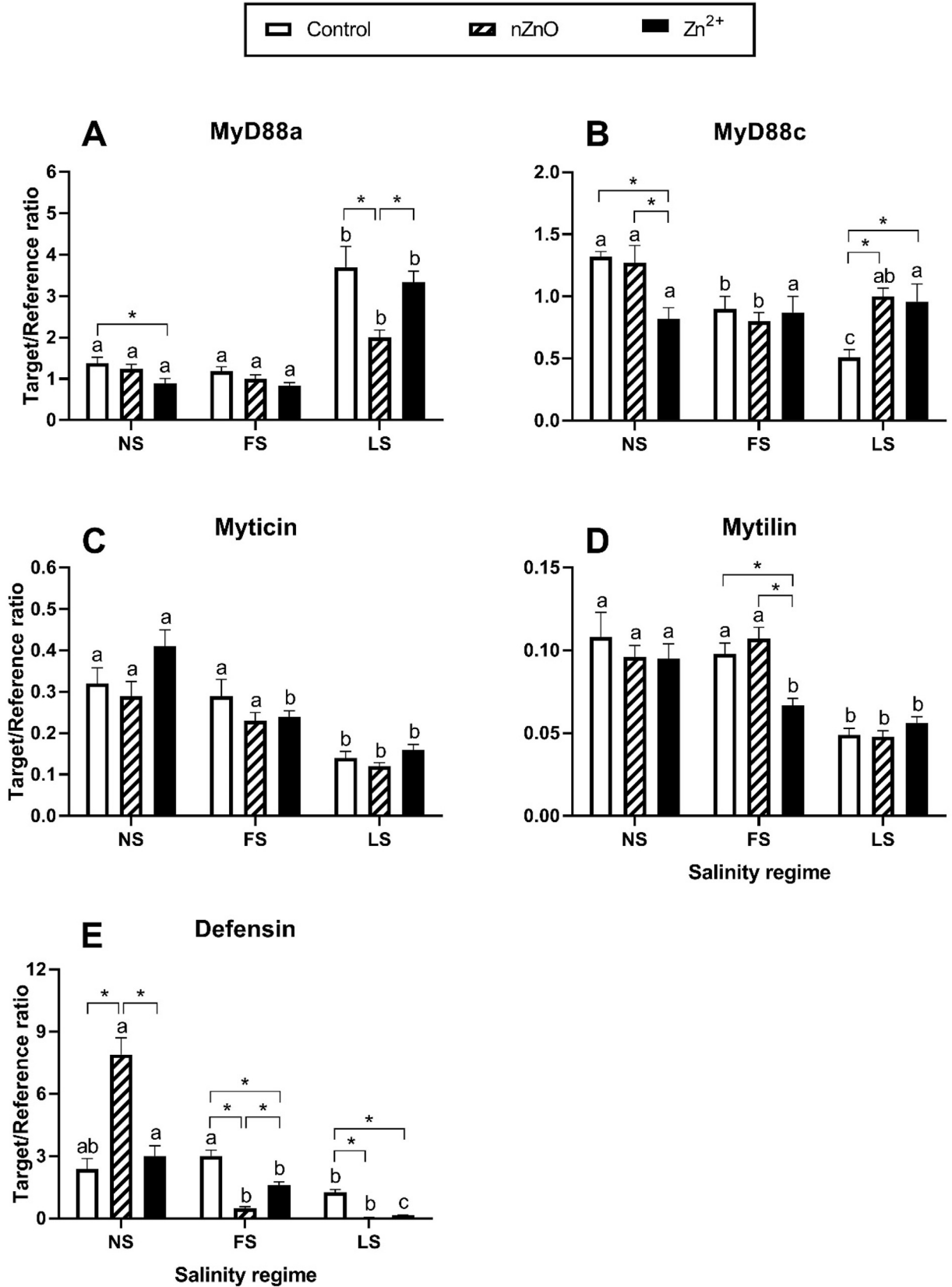


Fig. 3. Expression of mRNA of the MYD88 innate immune signal transduction adaptors and antimicrobial peptides in hemocytes of *M. edulis* exposed to nine combinations of nZnO or Zn²⁺ (0, 100 $\mu\text{g l}^{-1}$) and salinity (5, 5–15 and 15) during 21 days. A – myeloid differentiation primary response gene 88 a; B – myeloid differentiation primary response gene 88 c; C – myticin; D – mytilin; E – defensin. Asterisks indicate significant differences among nZnO or Zn²⁺ treatments within fixed salinity level (Tukey HSD test, $P < 0.05$), and different letters indicate significant differences between three salinity levels within fixed nZnO or Zn²⁺ concentration (Tukey HSD test, $P < 0.05$), $N = 6$.

associated marker traits (Fig. 5). The nZnO exposed groups acclimated at the normal and fluctuating salinity separated from the respective control and ionic Zn-exposed groups along the PC2 axis that correlated with the elevated phagocytosis rate, high NRU values and HSP70 expression. All low salinity acclimated groups were grouped together in the bottom left quadrant of the PC plane, with the elevated expression of MyD88a as an associated marker (Fig. 5).

Under the normal salinity regime, the integrated biomarker response (IBR) values (calculated based on the eight biomarkers with the largest variation among the experimental groups including C-lectin, defensin, TLRa, TLRb, TLRc, MyD88a, Cq3 and HSP70) was high in the control group (median 5.16), and decreased in the nZnO and ionic Zn exposed groups (medians 3.02 and 1.39, respectively). In the hemocytes of the mussels from the fluctuating salinity, the IBR values were low in the control and ionic Zn exposed groups (medians 1.39 and 1.15, respectively) and elevated in the nZnO-exposed group (median 8.48). In the low salinity acclimated mussels, the IBR was low in all groups (median of 0.52, 0.17 and 1.08 in the control, nZnO, and ionic Zn-exposed groups, respectively).

4. Discussion

Our study shows that ambient salinity and ZnO nanoparticles have strong impacts on the immune-related functions and gene expression profile in hemocytes of a euryhaline marine bivalve *M. edulis*. The effects of nZnO on the mussels' immunity are modulated by salinity and can range from suppressive to stimulatory, depending on the salinity regime. The immunomodulatory effects of nZnO and ionic Zn in mussels occurred despite the lack (during the nZnO exposures) or minimal (ionic Zn exposures) accumulation of Zn in the soft tissues of the mussels. Earlier studies indicate that mussels tightly regulate their tissue Zn content (Chan, 1988), and that Zn accumulation only occurs during prolonged exposures to high concentrations of ionic Zn or nZnO (≥ 200 – $500 \mu\text{g l}^{-1}$) (Chan, 1988; Hanna et al., 2013; Muller et al., 2014). Our present findings are consistent with this notion and show that physiological effects of exposure to low concentrations of nZnO and ionic Zn ($100 \mu\text{g l}^{-1}$) in the mussels are independent of the bioaccumulation of Zn in the mussels' soft bodies.

4.1. Interactive effects of salinity and nZnO on hemocyte abundance, viability and functions

The immune system of bivalves relies heavily on circulating hemocytes for immune surveillance. Abundance of the circulating hemocytes is determined by the balance between hemocyte mortality, hematopoiesis, and mobilization of the hemocytes to and from various body compartments (Allam and Raftos, 2015; Pila et al., 2016). Our present study shows that exposure to $100 \mu\text{g l}^{-1}$ nZnO significantly increased mortality of the mussels' hemocytes regardless of the salinity regime. Similarly, increased hemocyte mortality was found in the Korean mussel *M. coruscus* and the green-lipped mussel *Perna viridis* exposed to nTiO₂ (Huang et al., 2016; Wang et al., 2014) and in *M. coruscus* exposed to nZnO (Wu et al., 2018). Notably, the blue mussels *M. edulis* were able to compensate for the negative effects of nZnO on hemocyte viability at the normal and fluctuating salinity so that the abundance of circulating hemocytes remained at the normal level. This might reflect elevated hematopoiesis and/or recruitment of the resident hemocytes from the tissues of nZnO-exposed mussels. At the low salinity, however, the combined osmotic and nZnO stress exceeded this compensatory capacity, and the abundance of the circulating hemocytes decreased. A similar decline in the hemocyte abundance was found in the mussels *M. coruscus* and *P. viridis* exposed to high concentrations (2.5 – 10 mg l^{-1}) of TiO₂ or ZnO nanoparticles (Huang et al., 2016; Wang et al., 2014; Wu et al., 2018). Elevated hemocyte mortality likely reflects nZnO-induced apoptosis in the mussels' cells (Falfushynska et al., 2019b). It is worth noting that even though free metal ions are

toxic to the bivalve hemocytes (Anderson, 1993; Bruneau et al., 2015; Cheng, 1988; Cherkasov et al., 2007; Foster et al., 2011; Ivanina et al., 2014; Sheir and Handy, 2010), Zn²⁺ release is unlikely to explain the increase in the hemocyte mortality of nZnO-exposed mussels in our present study. Exposure to ionic Zn ($100 \mu\text{g l}^{-1}$) had no effect on the viability of abundance of the hemocytes (this study) and did not stimulate apoptosis in the mussels' cells (Falfushynska et al., 2019b).

Low salinity and nZnO exposure negatively affected the adhesion capacity of the mussels' hemocytes, with apparently additive effects of these two stressors on hemocytes' adhesion. Adhesion plays an important role in the innate immunity (Holmblad and Soderhall, 1999; Ivanina et al., 2018), and suppression of the adhesive capacity by nZnO might negatively impact the protective functions. The mechanisms of nZnO-induced suppression of the adhesive capacity of the mussels' hemocytes are not known but might involve impairment of the cytoskeleton and/or a decrease in the abundance or function of the adhesion proteins in the cell membrane. Apoptosis caused by nZnO (Falfushynska et al., 2015; Li et al., 2018) may also contribute to the decreased adhesion capacity of the mussel hemocytes since apoptotic cells tend to round up and detach (Elmore, 2007; Palamà et al., 2016). Notably, exposure to ionic Zn ($100 \mu\text{g l}^{-1}$) had no effect on the adhesion capacity of the mussels' hemocytes. This is consistent with the earlier reports that showed no effect of dissolved metals such as Cd²⁺ ($50 \mu\text{g l}^{-1}$) and Cu²⁺ ($50 \mu\text{g l}^{-1}$) on the adhesion capacity of hemocytes of marine bivalves *Crassostrea virginica* and *Mercenaria mercenaria* (Ivanina et al., 2014; Ivanina et al., 2016).

Phagocytosis is another key defense mechanism in the innate immunity of the bivalves (Canesi et al., 2002). Bivalve hemocytes can effectively clear pathogens by phagocytosis followed by cytotoxic reactions such as the oxidative burst, release of antimicrobial peptides and lysosomal degradation (Canesi et al., 2002; Hegaret et al., 2003). The pathogens and foreign materials are internalized inside endocytic vesicles of hemocytes, which fuse with early endosomes maturing into the lysosomes (Cooper, 2000). In vitro studies with bivalve hemocytes showed that these cells can also phagocytose nanoparticles and their aggregates (Canesi et al., 2012). Our present study demonstrated an increase in the phagocytic activity in the hemocytes of nZnO-exposed *M. edulis* associated with an increase in the lysosomal abundance (indicated by the higher NRU). Exposure to ionic Zn also had a stimulatory effect on phagocytosis of the hemocytes albeit weaker than nZnO. This was an unexpected finding because earlier studies showed suppression of phagocytosis of the hemocytes exposed to nanoparticles in vivo and in vitro (Canesi et al., 2015; Huang et al., 2016; Wang et al., 2014; Wu et al., 2018). These differences might be attributed to the different concentrations and/or types of the nanoparticles used in our present study ($100 \mu\text{g l}^{-1}$ nZnO) and the earlier published research (that used 2.5 – 10 mg l^{-1} nTiO₂ and nZnO, or 5 – 50 mg l^{-1} of polystyrene nanoparticles) (Canesi et al., 2015; Huang et al., 2016; Wang et al., 2014; Wu et al., 2018). Further studies are needed to assess the variability of the phagocytic responses to nZnO exposure in different species of marine bivalves across a wide range of nZnO concentrations to resolve this question.

Neutral Red is a supravital dye, which selectively accumulates in the lysosomes by the active (ATP-dependent) transport (Repetto et al., 2008). The uptake of the neutral red occurs only in the live cells (Repetto et al., 2008) and depends on the total lysosomal volume of the cells (Winckler, 1974). Typically, exposure to the pollutants leads to the loss of the cell viability and thus a decrease in the Neutral Red uptake (Bunderson-Schelvan et al., 2017; Moore et al., 2006; Repetto et al., 2008; Wang et al., 2018b). In our present study, an opposite trend has been found with increasing Neutral Red uptake in the hemocytes of the mussels exposed to nZnO and, to a lesser degree, ionic Zn. This trend cannot be explained by increased cell viability since the hemocyte viability decreased during nZnO and ionic Zn exposures of *M. edulis*. The most parsimonious explanation is an increase in the lysosomal volume possibly reflecting lysosomal proliferation or stimulation of autophagy

by nZnO and ionic Zn. Recent studies show that nanoparticle exposures can increase the number of lysosomes and lead to lysosomal enlargement in different cell types (Halameda Kenzaoui et al., 2012; Huang et al., 2015; Wang et al., 2018a; Wang et al., 2018c; Zhou et al., 2018). Future studies are needed to test whether similar lysosomal proliferation and/or lysosomal enlargement occurs in the hemocytes of *M. edulis* exposed to nZnO or ionic Zn. Overall, our study indicates that the Neutral Red viability assay should be interpreted with caution during long-term chronic exposures to the toxicants that can potentially affect lysosomal proliferation, as it does not always correlate with the cell viability.

4.2. Effects of salinity and nZnO on the immune gene expression profiles

Acclimation salinity strongly modified the molecular responses of the hemocytes to nZnO and ionic Zn exposures in *M. edulis*. A possible explanation of the modulatory effects of salinity immunotoxicity of nZnO might be the direct effects of salinity on the physicochemical properties of nZnO such as aggregation, dissolution or sedimentation (Yung et al., 2017; Yung et al., 2015). Generally, lower salinity and lower ionic strength decreases the aggregation and the rate of sedimentation of nZnO (Bian et al., 2011; Keller et al., 2010; Yung et al., 2017). However, in salinities 12–32 the change in the aggregate size of nZnO was modest with the mean aggregate size of ~750 nm at salinity 12 and ~800 nm at salinity 32 (Yung et al., 2017). In the range of salinities used in our present work (5–15), the changes in the nZnO aggregation were negligible (Supplementary Fig. 1) and unlikely to explain the salinity-dependent differences in the hemocyte responses to nZnO.

Environmental salinity may also affect the bioavailability of Zn^{2+} added as $ZnSO_4$ or released by dissolution of nZnO in the experimental exposures. Typically, low salinity increases bioavailability of Zn^{2+} and therefore its toxicity for marine organisms (Park et al., 2014; Yung et al., 2017; Yung et al., 2015). Recent studies showed the significant effects of salinity on Zn^{2+} release only at the high concentrations of nZnO (3–50 $mg\ l^{-1}$) but not at the lower nZnO levels (0.5–1 $mg\ l^{-1}$) (Yung et al., 2017). In our present study, release of ionic Zn from nZnO was minimal regardless of the experimental salinity. Therefore, bioavailability of free Zn^{2+} is not likely to explain the differences in immune cell responses to nZnO exposures at different salinities. This conclusion is supported by the finding that hemocytes' responses to ionic Zn were not enhanced at low salinity in *M. edulis*. Taken together, these data indicate that the interactive effects of salinity and Zn exposures on the molecular responses of the hemocytes are mediated by the effects of salinity on mussels' physiology rather than the direct effects on the physicochemical properties of nZnO or bioavailability of Zn^{2+} .

Expression of immune recognition factors (including Toll-like receptors, the complement system and C-lectin) was suppressed by nZnO exposure in the mussels acclimated at the salinity 15. This suppression was significant for the Toll-like receptors TLRb and c, the complement components C1q and C3q and C-lectin. The Toll-like receptors (TLRs) and C-lectins belong to the transmembrane receptors family of the pattern recognition receptors (PRRs) that recognize the pathogen-associated molecular pattern of viruses and bacteria (TLRs) or eukaryotic pathogens such as protists and parasitic helminths (C-lectins) (Ward and Rosenthal, 2014; Zhang et al., 2015). Furthermore, C-lectins contribute to the immune memory and immune priming in mollusks (Wang et al., 2013). It has been proposed that PRRs including the Toll-like receptors can recognize nanoparticles in bivalves (Kedmi et al., 2010; Turabekova et al., 2014; Yang et al., 2015). Although the exact mechanism of this interaction is unknown, PRRs in animals are affected by nanoparticles and metal stress (Auguste et al., 2019; Lu et al., 2013; Shi et al., 2017). Thus, the TLRs expression was significantly downregulated in hemocytes of the mussel *M. galloprovincialis* exposed to nCeO₂ (Auguste et al., 2019) and nTiO₂ (Balbi et al., 2014), in the ark clam *Tegillarca granosa* exposed to nTiO₂ (Shi et al., 2017), as well as in rats exposed to gold nanoparticles (Yang et al., 2015). These results and

our present findings indicate that different types of nanoparticles (nZnO, nCeO₂, nTiO₂ and nano-gold) share suppression of PRRs as a common immunotoxic mechanism and thus might decrease sensitivity to pathogen challenges, at least under some salinity conditions. Notably, exposure to ionic Zn at salinity 15 also led to a modest but statistically significant suppression of mRNA levels for TLRb, TLRc, C3q and C-lectin in *M. edulis*. In contrast, the expression of Toll-like receptors was significantly increased upon exposure to Cu^{2+} and Pb^{2+} in *M. coruscus* (Xu et al., 2018). The difference of in the transcriptional responses of PRRs to NPs and ionic metals might indicate involvement of different binding sites for these pollutants. However, the underlying mechanisms of metal and nanoparticles interactions with PRRs are still not known and require further investigation.

The complement system represents the next step in the immune recognition cascade which recognizes and opsonizes foreign and altered-self particles such as invading microorganisms or dying, infected and damaged host cells (Mayilyan et al., 2008). The complement system plays an important role in the first line of immune defense (Ricklin et al., 2016; Volanakis, 1990) and is stimulated by toxic insults or bacterial PAMPs in marine bivalves (Chen et al., 2018; Dong et al., 2017; Peng et al., 2017; Peng et al., 2016; Wang et al., 2017). Therefore, decreased expression levels of the key immune recognition factors in nZnO-exposed (and to a lesser degree, ionic Zn-exposed) mussels can impair their ability to detect a broad range of immune threats including bacteria, viruses and eukaryotic pathogens and might have negative implications for the downstream steps of the immune cascade. However, these immunosuppressive effects of nZnO and ionic Zn on the pathogen recognition were found only in salinity 15. Furthermore, earlier studies showed an induction of the complement component 3 (C3q) expression in the gills of *M. coruscus* after stimulation with Cu^{2+} (Chen et al., 2018) and in the hemocytes *M. galloprovincialis* exposed to 100 $\mu g\ l^{-1}$ nCeO₂ (Auguste et al., 2019). This indicates that the complement system response to the metal or metal-containing nanoparticles might be toxicant- and salinity-specific.

Exposure to the fluctuating salinity regime (5–15) had little effect on the expression of the immune recognition genes in *M. edulis* except TLRb and C-lectin that decreased by ~2.6-fold ~12.2-fold, respectively. However, co-exposure to nZnO (but not the ionic Zn) and fluctuating salinity strongly upregulated mRNA expression of all studied Toll-like receptors and the complement components C1q and C3q. The only exception to this pattern was the expression of C-lectin where nZnO exposure led to a further decline of already suppressed C-lectin mRNA levels at the fluctuating salinity. The suppressive effects of the fluctuating salinity on C-lectin transcript levels were reversed by exposure to ionic Zn. These findings indicate that nZnO can antagonize the immunosuppressive effects of the fluctuating salinity with regard to the recognition factors for bacterial and viral pathogens such as the Toll-like receptors and the complement system. However, the recognition ability for eukaryotic pathogens (such as fungi, protists or parasitic helminths) that critically depends on the function of the membrane-bound lectins (Llibre et al., 2016; van Die and Cummings, 2017; Vautier et al., 2012) may be impaired by nZnO.

In *M. edulis*, acclimation at the low salinity (5) had negative effect on mRNA expression of all studied immune-related genes except C-lectin and MyD88c. Combined with a decrease in the hemocyte viability and abundance, these changes might result in general immunosuppression in *M. edulis* under hypoosmotic stress. These findings agree with the studies in mussels and oysters that showed compromised immune status at low salinity including a decrease in hemocyte abundance, viability, production of bacteriotoxic reactive oxygen species and lysosomal activity (Bussell et al., 2008; Gagnaire et al., 2006; Matozzo and Marin, 2011; Wang et al., 2012). The immunosuppression by osmotic stress has been also found in a marine pipefish *Syngnathus typhle* exposed to low salinity (Birrer et al., 2012) and in the freshwater fish *Anguilla japonica* and *Pangasianodon hypophthalmus* exposed to high salinity (Gu et al., 2018) (Schmitz et al., 2017). In fish, exposure to suboptimal or

supraoptimal salinity negatively affected expression of the Toll-like receptors and the complement system C3q (Birrner et al., 2012; Gu et al., 2018; Schmitz et al., 2017), similar to our present findings in the mussels. IBR and PCA analyses indicate that hypoosmotic stress has a dominant impact on immunity-related biomarkers in *M. edulis* overriding the impacts of nZnO and ionic Zn exposures. Thus, grouping of the experimental treatment groups in the plane of the 1st two principal components indicates similarity of the biomarker profiles in all low salinity acclimated mussels, regardless of the Zn treatment (Fig. 4). Furthermore, IBR values of immune biomarkers were lowest in the mussels acclimated to the low salinity (IBR 0.17–1.08) compared with their counterparts maintained under the normal (IBR 1.39–5.16) or fluctuating (IBR 1.15–8.48) salinity. The immunosuppressive effects of low salinity might be attributed to the shifts in the osmotic balance in the mussels' hemolymph (Liu et al., 2008) and/or to suppressed metabolism under salinity stress (Wang et al., 2012). Immunosuppressive effects of hypoosmotic stress were not evident in the fluctuating salinity regime suggesting that 22 h recovery at salinity 15 was sufficient to prevent the negative immune effects of hypoosmotic stress in *M. edulis*.

Unlike the immune recognition factors, expression levels of key immune activators, the myeloid differentiation factors 88 MyD88a and MyD88c (Goldstein, 2004; Guo et al., 2018; Janssens and Beyaert, 2002; Ning et al., 2015) were less sensitive to osmotic and nZnO-induced stress in the mussels' hemocytes. MyD88s are important adaptor molecules in the Toll-like receptors and members of the interleukin-1 receptor signaling pathway (Muzio et al., 2013; Wesche et al., 2013) that transmit signals culminating in activation of the nuclear factor- κ B (NF- κ B) and induction of the inflammatory cytokines (Kumar et al., 2009). In mollusks, exposure to viral and bacterial PAMPs typically leads to the elevated expression of MyD88s, which might decrease susceptibility to microbial pathogens (Guo et al., 2018; Lee et al., 2011; Ning et al., 2015; Priyathilaka et al., 2018). Inflammation is a common response to nanoparticle exposure as shown in the mussels *M. edulis* and *M. galloprovincialis* exposed to nZnO and nano-silver, respectively (Bouallegui et al., 2017; Falfushynska et al., 2019b) and in nZnO-exposed mice (Cho et al., 2011). In mammals, MyD88-dependent inflammatory signaling pathway is sensitive to nZnO as shown by the

suppressed expression of MyD88 and the intestinal pro-inflammatory cytokines and chemokines in ZnO-supplemented piglets (Hu et al., 2014). In the lung epithelial cell culture, nZnO induced MyD88-dependent pro-inflammatory cytokines, and this effect was stronger than the effect of ionic Zn (Chang et al., 2013). Our present study showed a decrease in MyD88a and MyD88c expression in hemocytes of ionic Zn-exposed mussels at the normal (but not at the low or fluctuating) salinity. Although this change was statistically significant ($P < 0.05$), it remains unclear whether a small (~1.6-fold) decrease in the transcript levels of MyD88 factors is biologically meaningful. Exposure to nZnO did not affect the transcript levels of MyD88 factors in the mussels kept at the normal and fluctuating salinities. At the low salinity, the nZnO-induced changes in the expression levels of MyD88a and MyD88c had opposite directions (~2.0-fold decrease and ~1.9-fold increase, respectively) indicating a possible compensation mechanism. Interestingly, exposure of *M. edulis* to ZnO nanoparticles ($10\text{--}100\ \mu\text{g l}^{-1}$ Zn) led to a strong upregulation of NF- κ B mRNA expression, consistent with the notion that nZnO does not inhibit the inflammatory signaling pathways (such as those regulated by MyD88) in the mussels (Falfushynska et al., 2019b).

Antimicrobial peptides (AMPs) such as defensin, myticin and mytilin play an important role in elimination of viral, bacterial and fungal pathogens by permeating the cell membranes, disrupting DNA or RNA biosynthesis, or inducing catastrophic ATP loss in the pathogens (Diamond et al., 2009). The antimicrobial peptides can also regulate cytokine production as well as recruitment, activity and proliferation of the innate immune cells (Diamond et al., 2009; Singh et al., 2014). Defensins, myticins and mytilins are small cysteine-rich peptides that can disrupt the membrane of Gram-positive and Gram-negative bacteria and eukaryotic microbes (Balseiro et al., 2011; Mitta et al., 1999; Rosa et al., 2011; Schmitt et al., 2012; Seo et al., 2005). In marine bivalves, these AMPs are highly inducible by the pathogens and their PAMPs including bacteria, viruses and protozoans (Balseiro et al., 2011; Domeneghetti et al., 2015; Hubert et al., 1996; Mitta et al., 1999; Schmitt et al., 2012). Our present study showed that myticin and mytilin mRNA expression is suppressed by acclimation at the constantly low salinity (5) but insensitive to nZnO exposure or the

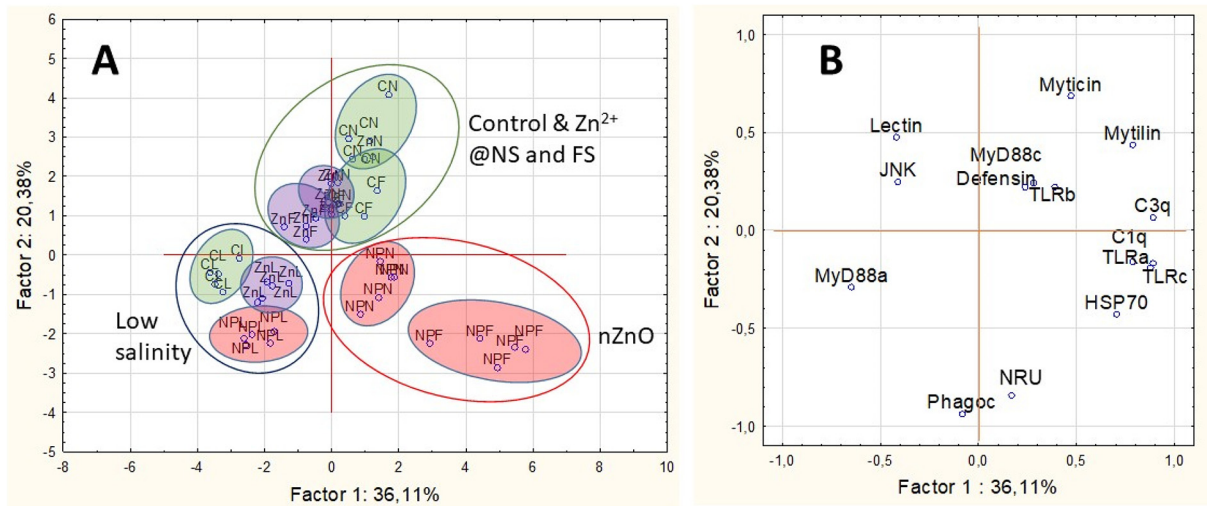


Fig. 4. Principal component analysis of the biochemical and molecular biomarkers of *M. edulis* exposed to nine combinations of nZnO or Zn²⁺ ($0, 100\ \mu\text{g l}^{-1}$) and salinity (5, 5–15 and 15). Biomarker abbreviations: Phagoc – phagocytosis (Zyosan particles per cell); NRU – neutral red uptake (10^{-6} cells); MyD88a – myeloid differentiation primary response gene 88 a; MyD88c – myeloid differentiation primary response gene 88 c; C1q – C1q complement domain-containing protein; C3q – complement component C3-like protein; TLRa – Toll-like receptor a; TLRb – Toll-like receptor b; TLRc – Toll-like receptor c; Lectin – membrane bound C-type lectin; HSP70 – 70 kDa heat shock protein; JNK – c-Jun N-terminal kinase. In addition to the immune-related biomarkers, two general cellular stress biomarkers (mRNA expression of the heat shock protein HSP70 and c-Jun terminal kinase JNK) were used in the PCA analysis (means shown in Supplementary Fig. 2). Experimental treatment groups: LS – low salinity (5); NPs – nZnO; CN – control and normal salinity (15); ZnN – ionic Zn and normal salinity (15); NPN – nZnO and normal salinity (15); CF – control and fluctuating salinity (5–15); ZnF – ionic Zn and fluctuating salinity (5–15); NPF – nZnO and fluctuating salinity (5–15); CL – control and low salinity (5); ZnL – ionic Zn and low salinity (5); NPL – nZnO and low salinity (5). (For interpretation of the references to colour in this figure legend, the reader is referred to the web version of this article.)

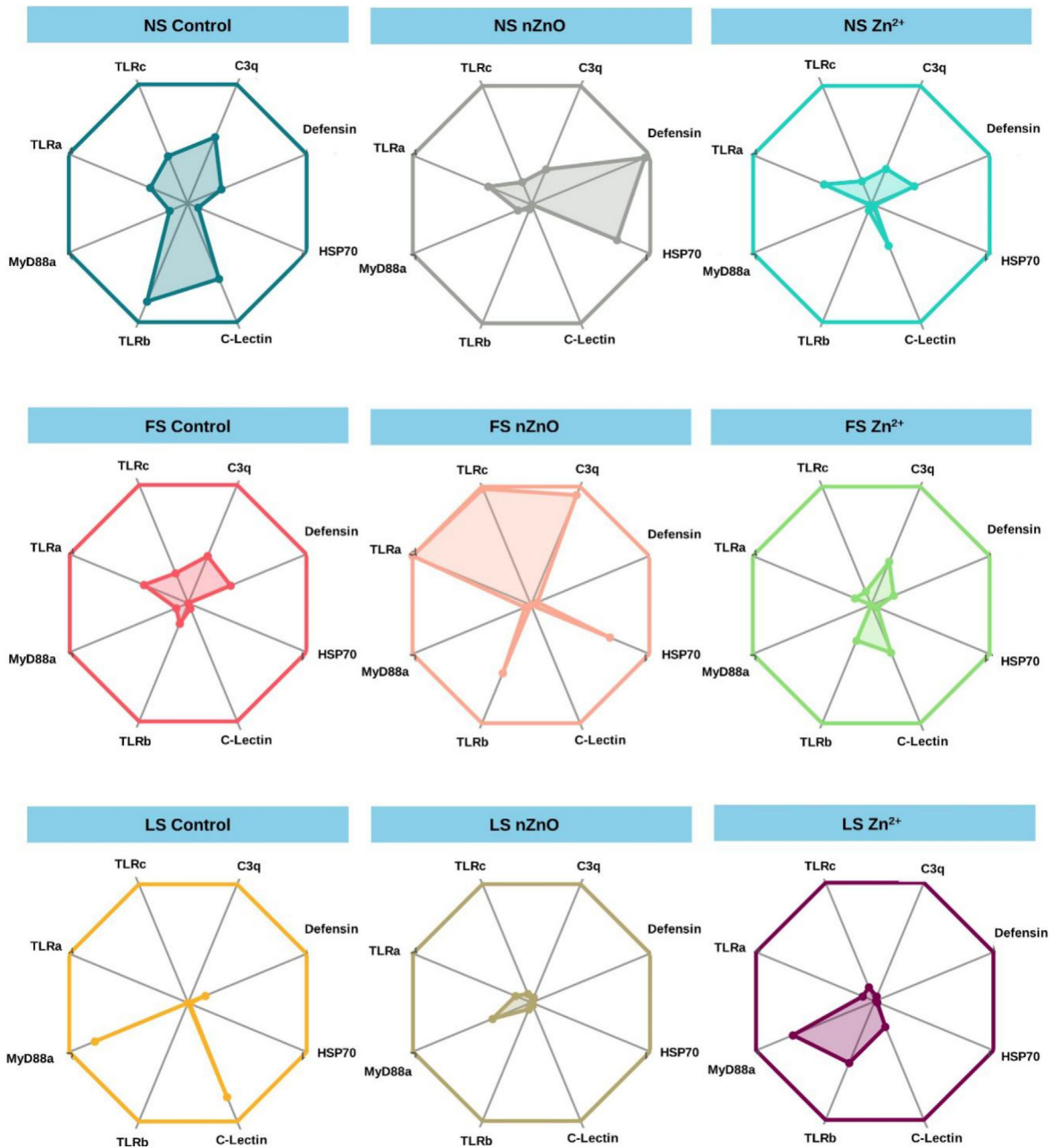


Fig. 5. Integrated biomarker radar plot for immune-related biomarkers of *M. edulis* exposed to nine combinations of nZnO or ionic Zn (0, 100 $\mu\text{g l}^{-1}$) and salinity (5, 5–15 and 15). Biomarker abbreviations: C3q – complement component C3-like protein; TLRa – Toll-like receptor a; TLRb – Toll-like receptor b, TLRc – Toll-like receptor c; MyD88 – myeloid differentiation primary response gene 88; HSP70 – 70 kDa heat shock protein; Dfnc – defensin; Lctn – membrane-bound C-type lectin. Experimental treatment groups: CNS – control and normal salinity (15); ZnNS – ionic Zn and normal salinity (15); ZnONS – nZnO and normal salinity (15); CFS – control and fluctuating salinity (5–15); ZnFS – ionic Zn and fluctuating salinity (5–15); ZnOFS – nZnO and fluctuating salinity (5–15); CLS – control and low salinity (5); ZnLS – ionic Zn and low salinity (5); ZnOLS – nZnO and low salinity (5).

fluctuating salinity stress. Similarly, exposure to 100 $\mu\text{g l}^{-1}$ of nCeO₂ had no effect on the mytilin mRNA levels in the hemocytes of *M. galloprovincialis* (Auguste et al., 2019). Unlike nZnO and nCeO₂, exposure to 10–100 $\mu\text{g l}^{-1}$ nTiO₂ led to the elevated mRNA expression of mytilin in the hemocytes of *M. galloprovincialis* (Barmo et al., 2013).

Unlike mytilin and myticin, the mRNA expression of defensin was differentially affected by nZnO depending on the salinity regime in *M. edulis*. Under the normal salinity regimes, nZnO exposure upregulated the defensin transcript in the mussels' hemocytes. A similar upregulation of the defensin mRNA was found in the hemocytes of *M. galloprovincialis* exposed to 10–100 $\mu\text{g l}^{-1}$ nTiO₂ (Barmo et al., 2013). In *M. edulis* acclimated to the low or fluctuating salinity, nZnO exposure suppressed the defensin mRNA levels. This suppression was

especially stark in the nZnO-exposed mussels at the low salinity that had the defensin transcript levels ~60-fold lower than the control (salinity 15) baseline. This is consistent with the results a field study in *M. galloprovincialis* that showed significant effects of salinity on the expression of defensin (Li et al., 2009). These findings indicate that combined salinity and nZnO stress might strongly impair the AMP-dependent pathogen killing ability of the mussels' hemocytes that represents an essential component of the innate immune defense. It is worth noting that defensin appears to be the most sensitive of the three studied AMP to nZnO exposures. This finding is consistent with the earlier reports that defensin is more sensitive than myticin and mytilin to toxic exposures such as hexavalent chromium and nTiO₂ in bivalves (Barmo et al., 2013; Ciacci et al., 2011).

It is worth noting that the toxic effects of ZnO nanoparticles are commonly ascribed to the toxicity of free Zn^{2+} released by the nanoparticle degradation in the environment or within the acidic environment of the lysosomes (Fairbairn et al., 2011; Franklin et al., 2007; Miao et al., 2010; Katsumiti et al., 2016). However, our present study as well as earlier research on bivalves (Falfushynska et al., 2015; Falfushynska et al., 2019a; Falfushynska et al., 2019b) and marine phytoplankton (Manzo et al., 2013; Miao et al., 2010; Peng et al., 2011) shows that the extent and the mechanisms of nZnO toxicity cannot be explained by the toxicity of ionic Zn. Generally, ZnO nanoparticles are more toxic than the equivalent amounts of ionic Zn to marine organisms. Furthermore, many molecular pathways that are strongly modulated by nZnO exposure (such as the immune recognition factors and an AMP defensin) are unresponsive to ionic Zn exposures. These differences are reflected in a stark separation of the immune biomarker profiles of nZnO-exposed and ionic Zn-exposed mussels in the PCA analysis, especially at the normal and fluctuating salinity. Earlier studies also showed that nZnO exposures have a strong pro-apoptotic and pro-inflammatory effect on the mussels' cells, unlike ionic Zn exposures that did not induce inflammation and suppressed apoptosis in the digestive gland cells of *M. edulis* (Falfushynska et al., 2019b). These findings emphasize the need for further toxicity testing and environmental risk assessment focused on the nanoparticles, as well as the need for innovative methods for detection and monitoring of the nanoparticles in the environment, because the risk assessments of nanoparticles based the toxicity of the constituent metals may potentially underestimate the environmental impact of the nanoparticles.

4.3. Conclusions and outlook

Ambient salinity and ZnO nanoparticles have strong impacts on the immune-related functions and gene expression profile in the hemocytes of marine bivalves *M. edulis*. Environmentally relevant concentrations of nZnO ($100 \mu\text{g l}^{-1}$ Zn) had stronger immunomodulatory effects in the blue mussels than the equivalent concentrations of ionic Zn. Stimulation of phagocytosis and lysosome enlargement/proliferation in response to nZnO exposure indicates that phagocytosis might be a key uptake mechanism for ZnO nanoparticles in the mussels' hemocytes. At salinity 15, nZnO suppressed the hemocyte viability, adhesion capacity and expression of the pathogen-associated pattern receptors and the complement system indicating the impaired ability to recognize pathogens and mount innate immune response. Unexpectedly, the fluctuating salinity abolished many of the negative immune effects of nZnO except the suppression of the hemocyte vitality and adhesion.

Exposure to low salinity (5) had strong immunosuppressive effects in *M. edulis* overriding the impact of nZnO. The low salinity regime chosen for our present study is close to the lower salinity tolerance limit of *M. edulis* (Riisgård et al., 2013; van der Gaag et al., 2016). Our findings suggest that immunocompromised status may contribute to the inability of *M. edulis* population to survive in the brackish waters below the so called horohalincium (salinity 5–8) zone (Attrill and Rundle, 2002). The weakened host defense may also cause advantages for invading pathogens due to the seawater freshening that results from the climate change, especially since many eukaryotic and prokaryotic pathogens thrive in the brackish water (Casas et al., 2004; Oliver, 2006; Telesh et al., 2011).

Given the significant effects of salinity changes on the toxicity of nZnO, it is important to consider combined effects of multiple environmental stressors such as temperature, salinity and pH for the assessment of the environmental impacts of metal-containing nanoparticles including nZnO. Furthermore, the immune-related biomarkers for assessment of the toxic effects of the nanoparticles must be calibrated in the environmentally-relevant contexts as the biomarker baselines may be strongly shifted by salinity (our present study) and other biotic and abiotic stressors (Blanco-Rayón et al., 2019a; Blanco-Rayón et al., 2019b; Falfushynska et al., 2019a; Hamer et al., 2008; Múgica et al.,

2015). These findings have important implications for understanding of the combined effects of multiple stressors on immune biology of key-stone marine organisms and emphasize the urgent need for establishing the nanoparticle-specific guidelines for water quality and toxicity assessment in the anthropogenically modified coastal ecosystems.

Declaration of competing interest

The authors declare that they have no known competing financial interests or personal relationships that could have appeared to influence the work reported in this paper.

Acknowledgements

This work was in part supported by the Research Training Group 'Baltic TRANSCOAST' funded by the DFG (Deutsche Forschungsgemeinschaft) under grant number GRK 2000 (www.baltic-transcoast.uni-rostock.de) to IMS, Alexander von Humboldt Foundation to HF, and the China Scholarship Council (CSC) to FW. HP was supported by Kent State University Brain Health Institute Pilot Award. We thank Fei Ye and Joydeep Dutta (KTH Royal Institute of Technology, Sweden) for their assistance with the nanoparticle characterization, and Mirza Nusrat Noor for the help with experimental exposures. The project metadata are submitted to PANGAEA® Data Publisher open access database (<https://doi.org/10.1594/PANGAEA.908851>) (Sokolova et al., 2019). This is Baltic TRANSCOAST publication no. GRK2000/0027.

Authors' contributions

FW – conceptualization, methodology, investigation, data curation, validation, visualization, formal analysis, funding acquisition, writing – original draft, writing – review & editing; HF – conceptualization, methodology, investigation, data curation, validation, formal analysis, visualization, funding acquisition, writing – original draft, writing – review & editing; OD – methodology, investigation, data curation, validation, writing – review & editing; HP – data curation, validation, formal analysis, software, writing – review & editing; IMS – conceptualization, methodology, visualization, formal analysis, supervision, resources, funding acquisition, writing – original draft, writing – review & editing.

Appendix A. Supplementary data

Supplementary data to this article can be found online at <https://doi.org/10.1016/j.scitotenv.2019.136473>.

References

- Allam, B., Raftos, D., 2015. Immune responses to infectious diseases in bivalves. *J. Invertebr. Pathol.* 131, 121–136.
- Anderson, R.S., 1993. Modulation of non-specific immunity by environmental stressors. In: Couch, J.A., Fournie, J.W. (Eds.), *Advances in Fisheries Science, Pathobiology of Marine and Estuarine Organisms*. CRC Press, London, pp. 483–510.
- Attrill, M.J., Rundle, S.D., 2002. Ecotone or ecocline: ecological boundaries in estuaries. *Estuar. Coast. Shelf Sci.* 55, 929–936.
- Auguste, M., Balbi, T., Montagna, M., Fabbri, R., Sendra, M., Blasco, J., et al., 2019. In vivo immunomodulatory and antioxidant properties of nanoceria (nCeO₂) in the marine mussel *Mytilus galloprovincialis*. *Comparative Biochemistry and Physiology C-Toxicology & Pharmacology* 219, 95–102.
- Balbi, T., Smerilli, A., Fabbri, R., Ciacci, C., Montagna, M., Grasselli, E., et al., 2014. Co-exposure to n-TiO₂ and Cd²⁺ results in interactive effects on biomarker responses but not in increased toxicity in the marine bivalve *M. galloprovincialis*. *Sci. Total Environ.* 493, 355–364.
- Balseiro, P., Falco, A., Romero, A., Dios, S., Martinez-Lopez, A., Figueras, A., et al., 2011. *Mytilus galloprovincialis* Myticin C: a chemotactic molecule with antiviral activity and immunoregulatory properties. *PLoS One* 6.
- Barmo, C., Ciacci, C., Canonico, B., Fabbri, R., Cortese, K., Balbi, T., et al., 2013. In vivo effects of n-TiO₂ on digestive gland and immune function of the marine bivalve *Mytilus galloprovincialis*. *Aquat. Toxicol.* 132, 9–18.
- Berger, V.J., Kharazova, A.D., 1997. Mechanisms of salinity adaptations in marine molluscs. *Hydrobiologia* 355, 115–126.

- Beyer, J., Green, N.W., Brooks, S., Allan, I.J., Ruus, A., Gomes, T., et al., 2017. Blue mussels (*Mytilus edulis* spp.) as sentinel organisms in coastal pollution monitoring: a review. *Mar. Environ. Res.* 130, 338–365.
- Bian, S.W., Mudunkotuwa, I.A., Rupasinghe, T., Grassian, V.H., 2011. Aggregation and dissolution of 4 nm ZnO nanoparticles in aqueous environments: influence of pH, ionic strength, size, and adsorption of humic acid. *Langmuir* 27, 6059–6068.
- Birrer, S.C., Reusch, T.B.H., Roth, O., 2012. Salinity change impairs pipefish immune defence. *Fish & Shellfish Immunology* 33, 1238–1248.
- Blanco-Rayón, E., Guilhermino, L., Irazola, M., Ivanina, A.V., Sokolova, I.M., Izagirre, U., et al., 2019a. The influence of short-term experimental fasting on biomarker responsiveness in oil WAF exposed mussels. *Aquat. Toxicol.* 206, 164–175.
- Blanco-Rayón, E., Ivanina, A.V., Sokolova, I.M., Marigómez, I., Izagirre, U., 2019b. Food-type may jeopardize biomarker interpretation in mussels used in aquatic toxicological experimentation. *PLoS One* 14, e0220661.
- Bondarenko, O., Juganson, K., Ivask, A., Kasemets, K., Mortimer, M., Kahru, A., 2013. Toxicity of Ag, CuO and ZnO nanoparticles to selected environmentally relevant test organisms and mammalian cells in vitro: a critical review. 87.
- Bouallegui, Y., Ben Younes, R., Bellamine, H., Oueslati, R., 2017. Histopathology and analyses of inflammation intensity in the gills of mussels exposed to silver nanoparticles: role of nanoparticle size, exposure time, and uptake pathways. *Toxicol. Mech. Methods* 27, 582–591.
- Bricker, S., Lauenstein, G., Maruya, K., 2014. NOAA's mussel watch program: incorporating contaminants of emerging concern (CECs) into a long-term monitoring program. *Mar. Pollut. Bull.* 81, 289–290.
- Bruneau, A., Fortier, M., Gagne, F., Gagnon, C., Turcotte, P., Tayabali, A., et al., 2015. In vitro immunotoxicology of quantum dots and comparison with dissolved cadmium and tellurium. *Environ. Toxicol.* 30 (1), 9–25 (n/a-n/a).
- Buffet, P.E., Amiard-Triquet, C., Dybowska, A., Risso-de Faverney, C., Guibolini, M., Valsami-Jones, E., et al., 2012. Fate of isotopically labeled zinc oxide nanoparticles in sediment and effects on two endobenthic species, the clam *Scrobicularia plana* and the ragworm *Hediste diversicolor*. *Ecotoxicol. Environ. Saf.* 84, 191–198.
- Bunderson-Schelvan, M., Holian, A., Hamilton Jr., R.F., 2017. Engineered nanomaterial-induced lysosomal membrane permeabilization and anti-cathepsin agents. *Journal of toxicology and environmental health. Part B, Critical reviews* 20, 230–248.
- Bussell, J.A., Gidman, E.A., Causton, D.R., Gwynn-Jones, D., Malham, S.K., Jones, M.L.M., et al., 2008. Changes in the immune response and metabolic fingerprint of the mussel, *Mytilus edulis* (Linnaeus) in response to lowered salinity and physical stress. *J. Exp. Mar. Biol. Ecol.* 358, 78–85.
- Canesi, L., Gallo, G., Gavioli, M., Pruzzo, C., 2002. Bacteria-hemocyte interactions and phagocytosis in marine bivalves. *Microsc. Res. Tech.* 57, 469–476.
- Canesi, L., Ciacci, C., Fabbri, R., Marcomini, A., Pojana, G., Gallo, G., 2012. Bivalve molluscs as a unique target group for nanoparticle toxicity. *Mar. Environ. Res.* 76, 16–21.
- Canesi, L., Ciacci, C., Bergami, E., Monopoli, M.P., Dawson, K.A., Papa, S., et al., 2015. Evidence for immunomodulation and apoptotic processes induced by cationic polystyrene nanoparticles in the hemocytes of the marine bivalve *Mytilus*. *Mar. Environ. Res.* 111, 34–40.
- Casas, S.M., Figueras, A., Ordás, M.C., Reece, K.S., Villalba, A., 2004. Perkinsosis in molluscs: a review. *Aquat. Living Resour.* 17, 411–432.
- Chan, H.M., 1988. Accumulation and tolerance to cadmium, copper, lead and zinc by the green mussel *Perna viridis*. *Mar. Ecol. Prog. Ser.* 48.
- Chang, H., Ho, C.C., Yang, C.S., Chang, W.H., Tsai, M.H., Tsai, H.T., et al., 2013. Involvement of MyD88 in zinc oxide nanoparticle-induced lung inflammation. *Exp. Toxicol. Pathol.* 65, 887–896.
- Chen, Y.X., Xu, K.D., Li, J.J., Wang, X., Ye, Y.Y., Qi, P.Z., 2018. Molecular characterization of complement component 3 (C3) in *Mytilus coruscus* improves our understanding of bivalve complement system. *Fish & Shellfish Immunology* 76, 41–47.
- Cheng, T.C., 1988. In vivo effects of heavy metals on cellular defense mechanisms of *Crassostrea virginica*: total and differential cell counts. *J. Invertebr. Pathol.* 51, 207–214.
- Cherkasov, A.S., Grewal, S., Sokolova, I.M., 2007. Combined effects of temperature and cadmium exposure on haemocyte apoptosis and cadmium accumulation in the eastern oyster *Crassostrea virginica* (Gmelin). *J. Thermal Biology* 32, 162–170.
- Cho, W.S., Duffin, R., Howie, S.E.M., Scotton, C.J., Wallace, W.A.H., MacNee, W., et al., 2011. Progressive severe lung injury by zinc oxide nanoparticles; the role of Zn²⁺ dissolution inside lysosomes. *Particle and Fibre Toxicology* 8.
- Ciacci, C., Barmo, C., Fabbri, R., Canonico, B., Gallo, G., Canesi, L., 2011. Immunomodulation in *Mytilus galloprovincialis* by non-toxic doses of hexavalent chromium. *Fish & Shellfish Immunology* 31, 1026–1033.
- Coles, J.A., Farley, S.R., Pipe, R.K., 1995. Alteration of immune response of the common marine mussel *Mytilus edulis* resulting from exposure to cadmium. *Dis. Aquat. Org.* 22, 59–65.
- Coll, C., Notter, D., Gottschalk, F., Sun, T., Som, C., Nowack, B., 2016. Probabilistic environmental risk assessment of five nanomaterials (nano-TiO₂, nano-Ag, nano-ZnO, CNT, and fullerenes). *Nanotoxicology* 10, 436–444.
- Cooper, G., 2000. *The Cell: A Molecular Approach*. 2nd edition. Sinauer Associates, Sunderland (MA) pp. Available from: <https://www.ncbi.nlm.nih.gov/books/NBK9953/>.
- Corporeau, C., Auffret, M., 2003. In situ hybridisation for flow cytometry: a molecular method for monitoring stress-gene expression in hemolymph cells of oysters. *Aquat. Toxicol.* 64, 427–435.
- Dellwig, O., Wegwerth, A., Schnetger, B., Schulz, H., Arz, H.W., 2019. Dissimilar behaviors of the geochemical twins W and Mo in hypoxic-euxinic marine basins. *Earth Sci. Rev.* 193, 1–23.
- Devin, S., Burgeot, T., Giambérini, L., Minguez, L., Pain-Devin, S., 2014. The integrated biomarker response revisited: optimization to avoid misuse. *Environ. Sci. Pollut. Res.* 21, 2448–2454.
- Diamond, G., Beckloff, N., Weinberg, A., Kisich, K.O., 2009. The roles of antimicrobial peptides in innate host defense. *Curr. Pharm. Des.* 15, 2377–2392.
- van Die, I., Cummings, R.D., 2017. The mannose receptor in regulation of helminth-mediated host immunity. *Front. Immunol.* 8, 1677.
- Domenech, S., Franzoi, M., Damiano, N., Norante, R., El Haifawy, N.M., Mammi, S., et al., 2015. Structural and antimicrobial features of peptides related to Myticin C, a special defense molecule from the Mediterranean mussel *Mytilus galloprovincialis*. *J. Agric. Food Chem.* 63, 9251–9259.
- Dong, W.Q., Chen, Y.X., Lu, W.X., Wu, B., Qi, P.Z., 2017. Transcriptome analysis of *Mytilus coruscus* hemocytes in response to *Vibrio alginolyticus* infection. *Fish & Shellfish Immunology* 70, 560–567.
- Elmore, S., 2007. Apoptosis: a review of programmed cell death. *Toxicol. Pathol.* 35, 495–516.
- Fabrega, J., Tantra, R., Amer, A., Stolpe, B., Tomkins, J., Fry, T., et al., 2012. Sequestration of zinc from zinc oxide nanoparticles and life cycle effects in the sediment dweller amphipod *Corophium volutator*. *Environmental Science & Technology* 46, 1128–1135.
- Fairbairn, E.A., Keller, A.A., Madler, L., Zhou, D.X., Pokhrel, S., Cherr, G.N., 2011. Metal oxide nanomaterials in seawater: linking physicochemical characteristics with biological response in sea urchin development. *J. Hazard. Mater.* 192, 1565–1571.
- Falfushynska, H., Gnatyshyna, L., Yurchak, I., Sokolova, I., Stoliar, O., 2015. The effects of zinc nanooxide on cellular stress responses of the freshwater mussels *Unio tumidus* are modulated by elevated temperature and organic pollutants. *Aquat. Toxicol.* 162, 82–93.
- Falfushynska, H., Gnatyshyna, L., Horyn, O., Sokolova, I., Stoliar, O., 2017. Endocrine and cellular stress effects of zinc oxide nanoparticles and nifedipine in marsh frogs *Pelophylax ridibundus*. *Aquat. Toxicol.* 185, 171–182.
- Falfushynska, H.I., Gnatyshyna, L.L., Ivanina, A.V., Khoma, V.V., Stoliar, O.B., Sokolova, I.M., 2019a. Bioenergetic responses of freshwater mussels *Unio tumidus* to the combined effects of nano-ZnO and temperature regime. *Sci. Total Environ.* 650, 1440–1450.
- Falfushynska, H.I., Wu, F., Ye, F., Kasianchuk, N., Dutta, J., Dobretsov, S., et al., 2019b. The effects of ZnO nanostructures of different morphology on bioenergetics and stress response biomarkers of the blue mussels *Mytilus edulis*. *Sci. Total Environ.* 694, 133717.
- Foster, B., Grewal, S., Graves, O., Hughes Jr., F.M., Sokolova, I.M., 2011. Copper exposure affects hemocyte apoptosis and *Perkinsus marinus* infection in eastern oysters *Crassostrea virginica* (Gmelin). *Fish & Shellfish Immunology* 31, 341–349.
- Franklin, N.M., Rogers, N.J., Apte, S.C., Batley, G.E., Gadd, G.E., Casey, P.S., 2007. Comparative toxicity of nanoparticulate ZnO, bulk ZnO, and ZnCl₂ to a freshwater microalga (*Pseudokirchneriella subcapitata*): the importance of particle solubility. *Environmental Science & Technology* 41, 8484–8490.
- van der Gaag, M., van der Velde, G., Wijnhoven, S., Leuven, R.S.E.W., 2016. Salinity as a barrier for ship hull-related dispersal and invasiveness of dreissenid and mytilid bivalves. *Mar. Biol.* 163, 147. <https://doi.org/10.1007/s00227-016-2926-7>.
- Gagnaire, B., Frouin, H., Moreau, K., Thomas-Guyon, H., Renault, T., 2006. Effects of temperature and salinity on haemocyte activities of the Pacific oyster, *Crassostrea gigas* (Thunberg). *Fish Shellfish Immunol* 20, 536–547.
- Goldstein, D.R., 2004. Toll-like receptors and other links between innate and acquired alloimmunity. *Curr. Opin. Immunol.* 16, 538–544.
- Gu, J., Dai, S.Y., Liu, H.T., Cao, Q.Q., Yin, S.W., Lai, K.P., et al., 2018. Identification of immune-related genes in gill cells of Japanese eels (*Anguilla japonica*) in adaptation to water salinity changes. *Fish & Shellfish Immunology* 73, 288–296.
- Guo, B.Y., Liu, S.B., Li, J.J., Liao, Z., Liu, H.H., Xia, H., et al., 2018. Identification and functional characterization of three myeloid differentiation factor 88 (MyD88) isoforms from thick shell mussel *Mytilus coruscus*. *Fish & Shellfish Immunology* 83, 123–133.
- Halimoda Kenzaoui, B., Chapuis Bernasconi, C., Guney-Ayra, S., Juillerat-Jeanneret, L., 2012. Induction of oxidative stress, lysosome activation and autophagy by nanoparticles in human brain-derived endothelial cells. *Biochem. J.* 441, 813–821.
- Hamer, B., Jaksic, Z., Pavic-Hamer, D., Peric, L., Medakovic, D., Ivankovic, D., et al., 2008. Effect of hypoosmotic stress by low salinity acclimation of Mediterranean mussels *Mytilus galloprovincialis* on biological parameters used for pollution assessment. *Aquat. Toxicol.* 89, 137–151.
- Hanna, S.K., Miller, R.J., Muller, E.B., Nisbet, R.M., Lenihan, H.S., 2013. Impact of engineered zinc oxide nanoparticles on the individual performance of *Mytilus galloprovincialis*. *PLoS One* 8.
- Hegaret, H., Wikfors, G.H., Soudant, P., 2003. Flow cytometric analysis of haemocytes from eastern oysters, *Crassostrea virginica*, subjected to a sudden temperature elevation II. Haemocyte functions: aggregation, viability, phagocytosis, and respiratory burst. *J. Exp. Mar. Biol. Ecol.* 293, 249–265.
- Holmblad, T., Soderhall, K., 1999. Cell adhesion molecules and antioxidative enzymes in a crustacean, possible role in immunity. *Aquaculture* 172, 111–123.
- Hu, C.H., Song, Z.H., Xiao, K., Song, J., Jiao, L.F., Ke, Y.L., 2014. Zinc oxide influences intestinal integrity, the expressions of genes associated with inflammation and TLR4-myeloid differentiation factor 88 signaling pathways in weaning pigs. *Innate Immunology* 20, 478–486.
- Huang, D., Zhou, H., Gao, J., 2015. Nanoparticles modulate autophagic effect in a dispersity-dependent manner. *Sci. Rep.* 5, 14361.
- Huang, X.Z., Lin, D.H., Ning, K., Sui, Y.M., Hu, M.H., Lu, W.Q., et al., 2016. Hemocyte responses of the thick shell mussel *Mytilus coruscus* exposed to nano-TiO₂ and seawater acidification. *Aquat. Biol.* 180, 1–10.
- Hubert, F., Noel, T., Roch, P., 1996. A member of the arthropod defensin family from edible Mediterranean mussels (*Mytilus galloprovincialis*). *Eur. J. Biochem.* 240, 302–306.
- Hughes, F.M., Foster, B., Grewal, S., Sokolova, I.M., 2010. Apoptosis as a host defense mechanism in *Crassostrea virginica* and its modulation by *Perkinsus marinus*. *Fish & Shellfish Immunology* 29, 247–257.
- Ignacio, R.M.C., Kim, C.-S., Kim, S.-K., 2014. Immunotoxicity of metal oxide nanoparticle: zinc oxide. *Molecular & Cellular Toxicology* 10, 237–244.

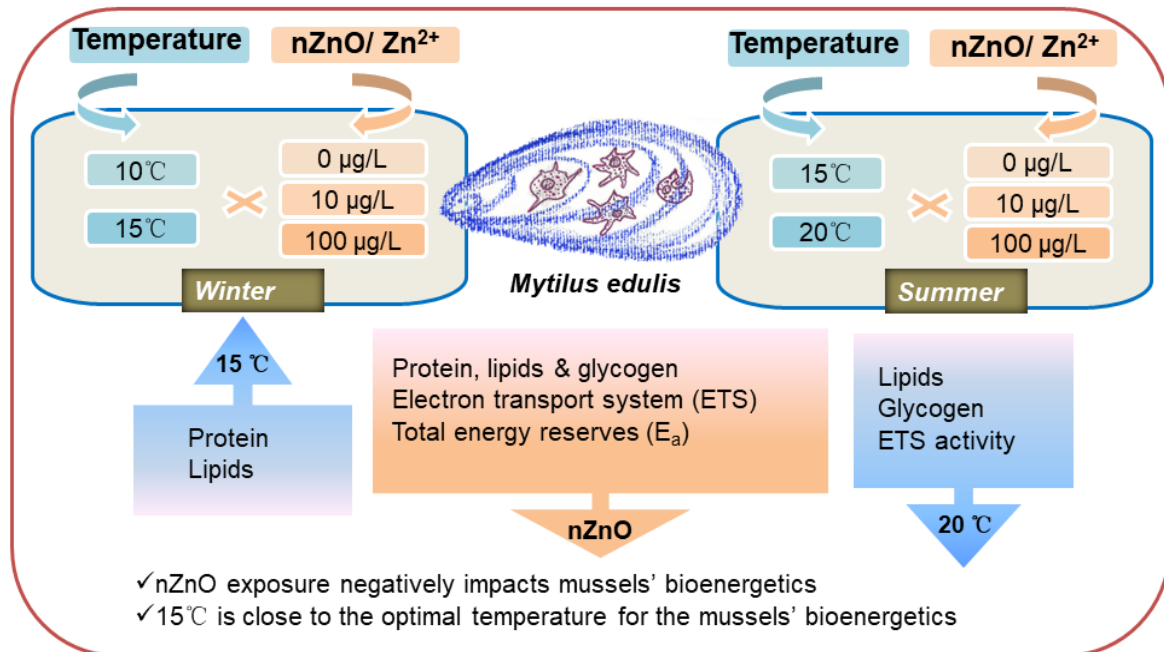
- Ivanina, A.V., Hawkins, C., Sokolova, I.M., 2014. Immunomodulation by the interactive effects of cadmium and hypercapnia in marine bivalves *Crassostrea virginica* and *Mercenaria mercenaria*. *Fish & Shellfish Immunology* 37, 299–312.
- Ivanina, A.V., Hawkins, C., Sokolova, I.M., 2016. Interactive effects of copper exposure and environmental hypercapnia on immune functions of marine bivalves *Crassostrea virginica* and *Mercenaria mercenaria*. *Fish & Shellfish Immunology* 49, 54–65.
- Ivanina, A.V., Borah, B.M., Vogts, A., Malik, I., Wu, J., Chin, A.R., et al., 2018. Potential trade-offs between biomineralization and immunity revealed by shell properties and gene expression profiles of two closely related *Crassostrea* species. *J. Exp. Biol.* 221, jeb183236.
- Janssens, S., Beyaert, R., 2002. A universal role for MyD88 in TLR/IL-1R-mediated signaling. *Trends Biochem. Sci.* 27, 474–482.
- Katsumiti, A., Arostegui, I., Oron, M., Gilliland, D., Valsami-Jones, E., Cajaraville, M.P., 2016. Cytotoxicity of Au, ZnO and SiO₂ NPs using in vitro assays with mussel hemocytes and gill cells: relevance of size, shape and additives. *Nanotoxicology* 10, 185–193.
- Kedmi, R., Ben-Arie, N., Peer, D., 2010. The systemic toxicity of positively charged lipid nanoparticles and the role of Toll-like receptor 4 in immune activation. *Biomaterials* 31, 6867–6875.
- Keller, A.A., Wang, H.T., Zhou, D.X., Lenihan, H.S., Cherr, G., Cardinale, B.J., et al., 2010. Stability and aggregation of metal oxide nanoparticles in natural aqueous matrices. *Environmental Science & Technology* 44, 1962–1967.
- Khlebovich, V.V., 1981. Acclimation of Animal Organisms. Leningrad: Nauka.
- Khlebovich, V.V., 2017. Acclimation of animal organisms: basic theory and applied aspects. *Biol. Bull. Rev.* 7, 279–286.
- Kijewski, T., Śmietanka, B., Zbawicka, M., Gosling, E., Hummel, H., Wenne, R., 2011. Distribution of *Mytilus* taxa in European coastal areas as inferred from molecular markers. *J. Sea Res.* 65, 224–234.
- Kumar, H., Kumagai, Y., Tsuchida, T., Koenig, P.A., Satoh, T., Guo, Z.J., et al., 2009. Involvement of the NLRP3 Inflammasome in innate and humoral adaptive immune responses to fungal beta-glucan. *J. Immunol.* 183, 8061–8067.
- Lagerström, M.E., Field, M.P., Séguret, M., Fischer, L., Hann, S., Sherrell, R.M., 2013. Automated on-line flow-injection ICP-MS determination of trace metals (Mn, Fe, Co, Ni, Cu and Zn) in open ocean seawater: application to the GEOTRACES program. *Mar. Chem.* 155, 71–80.
- Lee, Y., Whang, I., Umasuthan, N., De Zoysa, M., Oh, C., Kang, D.H., et al., 2011. Characterization of a novel molluscan MyD88 family protein from Manila clam, *Ruditapes philippinarum*. *Fish & Shellfish Immunology* 31, 887–893.
- Li, H., Toubiana, M., Monfort, P., Roch, P., 2009. Influence of temperature, salinity and E. coli tissue content on immune gene expression in mussel: results from a 2005–2008 survey. *Dev. Comp. Immunol.* 33, 974–979.
- Li, J., Schiavo, S., Xiangli, D., Rametta, G., Miglietta, M.L., Oliviero, M., et al., 2018. Early ecotoxic effects of ZnO nanoparticle chronic exposure in *Mytilus galloprovincialis* revealed by transcription of apoptosis and antioxidant-related genes. *Ecotoxicology* 27, 369–384.
- Liu, H., Pan, L., Fu, L., 2008. Effect of salinity on hemolymph osmotic pressure, sodium concentration and Na⁺-K⁺-ATPase activity of gill of Chinese crab, *Eriocheir sinensis*. *J. Ocean Univ. China* 7, 77–82.
- Libre, A., Klennerman, P., Willberg, C.B., 2016. Multi-functional lectin-like transcript-1: a new player in human immune regulation. *Immunol. Lett.* 177, 62–69.
- Lu, Y.L., Zhang, A.G., Li, C.H., Zhang, P., Su, X.R., Li, Y., et al., 2013. The link between selenium binding protein from *Sinonovacula constricta* and environmental pollution exposure. *Fish & Shellfish Immunology* 35, 271–277.
- Malagoli, D., Casarini, L., Sacchi, S., Ottaviani, E., 2007. Stress and immune response in the mussel *Mytilus galloprovincialis*. *Fish & Shellfish Immunology* 23, 171–177.
- Manzo, S., Miglietta, M.L., Rametta, G., Buono, S., Di Francia, G., 2013. Toxic effects of ZnO nanoparticles towards marine algae *Dunaliella tertiolecta*. *Sci. Total Environ.* 445, 371–376.
- Marchi, B., Burlando, B., Moore, M.N., Viarengo, A., 2004. Mercury- and copper-induced lysosomal membrane destabilisation depends on [Ca²⁺]_i dependent phospholipase A2 activation. *Aquat. Toxicol.* 66, 197–204.
- Marisa, I., Marin, M.G., Caicci, F., Franceschinis, E., Martucci, A., Matozzo, V., 2015. In vitro exposure of haemocytes of the clam *Ruditapes philippinarum* to titanium dioxide (TiO₂) nanoparticles: nanoparticle characterisation, effects on phagocytic activity and internalisation of nanoparticles into haemocytes. *Mar. Environ. Res.* 103, 11–17.
- Marisa, I., Matozzo, V., Munari, M., Binelli, A., Parolini, M., Martucci, A., et al., 2016. In vivo exposure of the marine clam *Ruditapes philippinarum* to zinc oxide nanoparticles: responses in gills, digestive gland and haemolymph. *Environ. Sci. Pollut. Res. Int.* 23, 15275–15293.
- Mathiesen, S.S., Thyrring, J., Hemmer-Hansen, J., Berge, J., Sukhotin, A., Leopold, P., et al., 2017. Genetic diversity and connectivity within *Mytilus* spp. in the subarctic and Arctic. *Evol. Appl.* 10, 39–55.
- Matozzo, V., Marin, M.G., 2011. Bivalve immune responses and climate changes: is there a relationship? *ISJ-Invertebr. Surviv. J.* 8, 70–77.
- Mayilyan, K.R., Kang, Y.H., Dodds, A.W., Sim, R.B., 2008. The complement system in innate immunity. In: Heine, H. (Ed.), *Innate Immunity of Plants, Animals, and Humans*. Springer Berlin Heidelberg, Berlin, Heidelberg, pp. 219–236.
- McLusky, D.S., Elliott, M., 2004. *The Estuarine Ecosystem. Ecology, Threats and Management*. Oxford University Press.
- Miao, A.J., Zhang, X.Y., Luo, Z.P., Chen, C.S., Chin, W.C., Santschi, P.H., et al., 2010. Zinc oxide-engineered nanoparticles: dissolution and toxicity to marine phytoplankton. *Environ. Toxicol. Chem.* 29, 2814–2822.
- Mitta, G., Hubert, F., Noel, T., Roch, P., 1999. Myticin, a novel cysteine-rich antimicrobial peptide isolated from haemocytes and plasma of the mussel *Mytilus galloprovincialis*. *Eur. J. Biochem.* 265, 71–78.
- Moore, M.N., Icarus Allen, J., McVeigh, A., 2006. Environmental prognostics: an integrated model supporting lysosomal stress responses as predictive biomarkers of animal health status. *Mar. Environ. Res.* 61, 278–304.
- Múgica, M., Sokolova, I.M., Izagirre, U., Marigómez, I., 2015. Season-dependent effects of elevated temperature on stress biomarkers, energy metabolism and gamete development in mussels. *Mar. Environ. Res.* 103, 1–10.
- Muller, E.B., Hanna, S.K., Lenihan, H.S., Miller, R.J., Nisbet, R.M., 2014. Impact of engineered zinc oxide nanoparticles on the energy budgets of *Mytilus galloprovincialis*. *J. Sea Res.* 94, 29–36.
- Munn, S., Aschberger, K., Olsson, H., Pakalin, S., Pellegrini, G., Vegro, S., et al., 2010. European Union Risk Assessment Report - Zinc Metal. Publications Office of the European Union, pp. 1–697 JRC61245.
- Muzio, M., Ni, J., Feng, P., Dixit, V.M., 2013. IRAK (Pelle) family member IRAK-2 and MyD88 as proximal mediators of IL-1 signaling (reprinted from science, vol 278, pg 1612–1615, 1997). *J. Immunol.* 190, 16–19.
- Mydlarz, L.D., Jones, L.E., Harvell, C.D., 2006. Innate immunity, environmental drivers, and disease ecology of marine and freshwater invertebrates. *Annu. Rev. Ecol. Evol. Syst.* 37, 251–288.
- Ning, X.H., Wang, R.J., Li, X., Wang, S.Y., Zhang, M.R., Xing, Q., et al., 2015. Genome-wide identification and characterization of five MyD88 duplication genes in Yesso scallop (*Patinopecten yessoensis*) and expression changes in response to bacterial challenge. *Fish & Shellfish Immunology* 46, 181–191.
- Oliver, J.D. *Vibrio vulnificus*. In: F. L. Thompson, B. Austin, (Ed.) *JS, editors. The Biology of Vibrios*. American Society for Microbiology Washington, DC, 2006, pp. 349–366.
- Palamà, I.E., d'Amone, S., Arcadio, V., Biasucci, M., Mezzi, A., Cortese, B., 2016. Cell mechanotactic and cytotoxic response to zinc oxide nanorods depends on substrate stiffness. *Toxicology Research* 5, 1699–1710.
- Park, J., Kim, S., Yoo, J., Lee, J.S., Park, J.W., Jung, J., 2014. Effect of salinity on acute copper and zinc toxicity to *Tigriopus japonicus*: the difference between metal ions and nanoparticles. *Mar. Pollut. Bull.* 85, 526–531.
- Peng, X.H., Palma, S., Fisher, N.S., Wong, S.S., 2011. Effect of morphology of ZnO nanostructures on their toxicity to marine algae. *Aquat. Toxicol.* 102, 186–196.
- Peng, M.X., Niu, D.H., Wang, F., Chen, Z.Y., Li, J.L., 2016. Complement C3 gene: expression characterization and innate immune response in razor clam *Sinonovacula constricta*. *Fish & Shellfish Immunology* 55, 223–232.
- Peng, M.X., Niu, D.H., Chen, Z.Y., Lan, T.Y., Dong, Z.G., Tran, T.N., et al., 2017. Expression of a novel complement C3 gene in the razor clam *Sinonovacula constricta* and its role in innate immune response and hemolysis. *Dev. Comp. Immunol.* 73, 184–192.
- Pfaffl, M.W., 2001. A new mathematical model for relative quantification in real-time RT-PCR. *Nucleic Acids Res.* 29, 2002–2007.
- Pierce, D.W., Gleckler, P.J., Barnett, T.P., Santer, B.D., Durack, P.J., 2012. The fingerprint of human-induced changes in the ocean's salinity and temperature fields. *Geophys. Res. Lett.* 39, L21704.
- Pila, E.A., Sullivan, J.T., Wu, X.Z., Fang, J., Rudko, S.P., Gordy, M.A., et al., 2016. Haematopoiesis in molluscs: a review of haemocyte development and function in gastropods, cephalopods and bivalves. *Developmental & Comparative Immunology* 58, 119–128.
- Priyathilaka, T.T., Bathige, S., Lee, S., Lee, J., 2018. Molecular identification and functional analysis of two variants of myeloid differentiation factor 88 (MyD88) from disk abalone (*Haliotis discus discus*). *Dev. Comp. Immunol.* 79, 113–127.
- Repetto, G., del Peso, A., Zurita, J.L., 2008. Neutral red uptake assay for the estimation of cell viability/cytotoxicity. *Nat. Protocols* 3, 1125–1131.
- Ricklin, D., Reis, E.S., Mastellos, D.C., Gros, P., Lambris, J.D., 2016. Complement component C3 – the “Swiss Army Knife” of innate immunity and host defense. *Immunol. Rev.* 274, 33–58.
- Risgård, H.U., Luskow, F., Pleissner, D., Lundgreen, K., López, M., 2013. Effect of salinity on filtration rates of mussels *Mytilus edulis* with special emphasis on dwarfed mussels from the low-saline Central Baltic Sea. *Helgol. Mar. Res.* 67, 591–598.
- Rosa, R.D., Santini, A., Fievet, J., Bulet, P., Destoumieux-Garzon, D., Bachere, E., 2011. Big Defensins, a diverse family of antimicrobial peptides that follows different patterns of expression in hemocytes of the oyster *Crassostrea gigas*. *PLoS One* 6.
- Roy, R., Chauhan, L.K.S., Das, M., Tripathi, A., Dwivedi, P.D., 2014. Phagocytic cells internalize ZnO particles by FcγII/III-receptor pathway. *Immunobiology* 219, 746–755.
- Sathe, P., Laxman, K., Myint, M.T.Z., Dobretsov, S., Richter, J., Dutta, J., 2017. Bioinspired nano-coatings for biofouling prevention by photocatalytic redox reactions. *Sci. Rep.* 7, 3624. <https://doi.org/10.1038/s41598-017-03636-6>.
- Schmitt, P., Rosa, R.D., Duperthuy, M., de Lorigeril, J., Bachere, E., Destoumieux-Garzon, D., 2012. The antimicrobial defense of the Pacific oyster, *Crassostrea gigas*. How diversity may compensate for scarcity in the regulation of resident/pathogenic microflora. *Front. Microbiol.* 3, 160.
- Schmitz, M., Baekelandt, S., Bequet, S., Kestemont, P., 2017. Chronic hyperosmotic stress inhibits renal Toll-like receptors expression in striped catfish (*Pangasianodon hypophthalmus*, Sauvage) exposed or not to bacterial infection. *Dev. Comp. Immunol.* 73, 139–143.
- Seo, J.K., Crawford, J.M., Stone, K.L., Noga, E.J., 2005. Purification of a novel arthropod defensin from the American oyster, *Crassostrea virginica*. *Biochem. Biophys. Res. Commun.* 338, 1998–2004.
- Shaw, B.J., Handy, R.D., 2011. Physiological effects of nanoparticles on fish: a comparison of nanometals versus metal ions. *Environ. Int.* 37, 1083–1097.
- Sheir, S., Handy, R., 2010. Tissue injury and cellular immune responses to cadmium chloride exposure in the common mussel *Mytilus edulis*: modulation by lipopolysaccharide. *Arch. Environ. Contam. Toxicol.* 59, 602–613.
- Shi, W., Han, Y., Guo, C., Zhao, X.G., Liu, S.X., Su, W.H., et al., 2017. Immunotoxicity of nanoparticle nTiO₂ to a commercial marine bivalve species, *Tegillarca granosa*. *Fish & Shellfish Immunology* 66, 300–306.

- Singh, B.P., Vij, S., Hati, S., 2014. Functional significance of bioactive peptides derived from soybean. *Peptides* 54, 171–179.
- Sohrin, Y., Urushihara, S., Nakatsuka, S., Kono, T., Higo, E., Minami, T., Norisuye, K., Umetani, S., 2008. Multielemental determination of GEOTRACES key trace metals in seawater by ICPMS after preconcentration using an ethylenediaminetriacetic acid chelating resin. *Anal. Chem.* 80 (16), 6267–6273.
- Sokolova, I.M., 2009. Apoptosis in molluscan immune defense. *Invertebr. Surviv. J.* 6, 49–58.
- Sokolova, I.M., Wu, F., Falfushynska, H., Piontkivska, H., 2019. Interactive effects of salinity and ZnO nanoparticles on the blue mussel *Mytilus edulis* (data set). PANGAEA <https://doi.org/10.1594/PANGAEA.908851>.
- Stuckas, H., Knöbel, L., Schade, H., Breusing, C., Hinrichsen, H.-H., Bartel, M., et al., 2017. Combining hydrodynamic modelling with genetics: can passive larval drift shape the genetic structure of Baltic *Mytilus* populations? *Mol. Ecol.* 26, 2765–2782.
- Telesh, I.V., Schubert, H., Skarlato, S.O., 2011. Revisiting Remane's concept: evidence for high plankton diversity and a protistan species maximum in the horohaliniacum of the Baltic Sea. *Mar. Ecol. Prog. Ser.* 421, 1–11.
- Thompson, E.L., Taylor, D.A., Nair, S.V., Birch, G., Coleman, R., Raftos, D.A., 2012. Optimal acclimation periods for oysters in laboratory-based experiments. *J. Molluscan Stud.* 78, 304–307.
- Turabekova, M., Rasulev, B., Theodore, M., Jackman, J., Leszczynska, D., Leszczynski, J., 2014. Immunotoxicity of nanoparticles: a computational study suggests that CNTs and C-60 fullerenes might be recognized as pathogens by Toll-like receptors. *Nano-scale* 6, 3488–3495.
- Vautier, S., MacCallum, D.M., Brown, G.D., 2012. C-type lectin receptors and cytokines in fungal immunity. *Cytokine* 58, 89–99.
- Volanakis, J.E., 1990. Participation of C3 and its ligands in complement activation. *Curr. Top. Microbiol. Immunol.* 153, 1–21.
- Wang, Y.J., Hu, M.H., Cheung, S.G., Shin, P.K.S., Lu, W.Q., Li, J.L., 2012. Immune parameter changes of hemocytes in green-lipped mussel *Perna viridis* exposure to hypoxia and hyposalinity. *Aquaculture* 356, 22–29.
- Wang, J., Wang, L., Yang, C., Jiang, Q., Zhang, H., Yue, F., et al., 2013. The response of mRNA expression upon secondary challenge with *Vibrio anguillarum* suggests the involvement of C-lectins in the immune priming of scallop *Chlamys farreri*. *Developmental & Comparative Immunology* 40, 142–147.
- Wang, Y.J., Hu, M.H., Li, Q.Z., Li, J.L., Lin, D.H., Lu, W.Q., 2014. Immune toxicity of TiO₂ under hypoxia in the green-lipped mussel *Perna viridis* based on flow cytometric analysis of hemocyte parameters. *Sci. Total Environ.* 470, 791–799.
- Wang, L.L., Zhang, H., Wang, L.L., Zhang, D.X., Lv, Z., Liu, Z.Q., et al., 2017. The RNA-seq analysis suggests a potential multi-component complement system in oyster *Crassostrea gigas*. *Dev. Comp. Immunol.* 76, 209–219.
- Wang, B., Zhang, J., Chen, C., Xu, G., Qin, X., Hong, Y., et al., 2018a. The size of zinc oxide nanoparticles controls its toxicity through impairing autophagic flux in A549 lung epithelial cells. *Toxicol. Lett.* 285, 51–59.
- Wang, F., Gómez-Sintes, R., Boya, P., 2018b. Lysosomal membrane permeabilization and cell death. *Traffic* 19, 918–931.
- Wang, F., Salvati, A., Boya, P., 2018c. Lysosome-dependent cell death and deregulated autophagy induced by amine-modified polystyrene nanoparticles. *Open Biol.* 8.
- Ward, A.E., Rosenthal, B.M., 2014. Evolutionary responses of innate immunity to adaptive immunity. *Infect. Genet. Evol.* 21, 492–496.
- Wesche, H., Henzel, W.J., Shillinglaw, W., Li, S.Y., Cao, Z.D., 2013. MyD88: an adapter that recruits IRAK to the IL-1 receptor complex (reprinted from *immunity*, vol 7, pg 837–847, 1997). *J. Immunol.* 190, 5–15.
- Williams, R.J., Harrison, S., Keller, V., Kuenen, J., Lofts, S., Praetorius, A., et al., 2019. Models for assessing engineered nanomaterial fate and behaviour in the aquatic environment. *Curr. Opin. Environ. Sustain.* 36, 105–115.
- Winckler, J., 1974. Vitalfärbung von Lysosomen und anderen Zellorganellen der Ratte mit Neutralrot. *Prog. Histochem. Cytochem.* 6, III–89.
- Wu, F., Cui, S., Sun, M., Xie, Z., Huang, W., Huang, X., et al., 2018. Combined effects of ZnO NPs and seawater acidification on the haemocyte parameters of thick shell mussel *Mytilus coruscus*. *Sci. Total Environ.* 624, 820–830.
- Xu, M.S., Wu, J., Ge, D.L., Wu, C.W., Chi, C.F., Lv, Z.M., et al., 2018. A novel toll-like receptor from *Mytilus coruscus* is induced in response to stress. *Fish & Shellfish Immunology* 78, 331–337.
- Yang, H., Fung, S.Y., Xu, S.Y., Sutherland, D.P., Kollmann, T.R., Liu, M.Y., et al., 2015. Amino acid-dependent attenuation of toll-like receptor signaling by peptide-gold nanoparticle hybrids. *ACS Nano* 9, 6774–6784.
- Yung, M.M.N., Mouneyrac, C., Leung, K.M.Y., 2014. Ecotoxicity of zinc oxide nanoparticles in the marine environment. In: Bhushan, B. (Ed.), *Encyclopedia of Nanotechnology*. Springer Netherlands, Dordrecht, pp. 1–17.
- Yung, M.M.N., Wong, S.W.Y., Kwok, K.W.H., Liu, F.Z., Leung, Y.H., Chan, W.T., et al., 2015. Salinity-dependent toxicities of zinc oxide nanoparticles to the marine diatom *Thalassiosira pseudonana*. *Aquat. Toxicol.* 165, 31–40.
- Yung, M.M.N., Kwok, K.W.H., Djuricic, A.B., Giesy, J.P., Leung, K.M.Y., 2017. Influences of temperature and salinity on physicochemical properties and toxicity of zinc oxide nanoparticles to the marine diatom *Thalassiosira pseudonana*. *Sci. Rep.* 7.
- Zhang, L.L., Li, L., Guo, X.M., Litman, G.W., Dishaw, L.J., Zhang, G.F., 2015. Massive expansion and functional divergence of innate immune genes in a protostome. *Sci. Rep.* 5.
- Zhang, Y., Nguyen, K.C., Caldwell, D., Fine, J.H., Lefebvre, D.E., Tayabali, A.F., 2017. Immune responses during single and repeated murine endotracheal exposures of zinc oxide nanoparticles. *NanoImpact* 7, 54–65.
- Zheng, L., Zhang, L., Lin, H., McIntosh, M.T., Malacrida, A.R., 2005. Toll-like receptors in invertebrate innate immunity. *ISJ* 2, 105–113.
- Zhou, H.L., Gong, X.Q., Lin, H.Y., Chen, H.M., Huang, D.T., Li, D., et al., 2018. Gold nanoparticles impair autophagy flux through shape-dependent endocytosis and lysosomal dysfunction. *J. Mater. Chem. B* 6, 8127–8136.

7.3. Season-dependent effects of ZnO nanoparticles and elevated temperature on bioenergetics of the blue mussel *Mytilus edulis*

Wu, FL, Sokolov, E. P, Dellwig, O. and Sokolova, I. M. (2021). Chemosphere 263, 127780.

DOI: <https://doi.org/10.1016/j.chemosphere.2020.127780>





Season-dependent effects of ZnO nanoparticles and elevated temperature on bioenergetics of the blue mussel *Mytilus edulis*

Fangli Wu ^a, Eugene P. Sokolov ^b, Olaf Dellwig ^c, Inna M. Sokolova ^{a, d, *}

^a Department of Marine Biology, Institute for Biological Sciences, University of Rostock, Rostock, Germany

^b Leibniz Institute for Baltic Sea Research, Leibniz ScienceCampus Phosphorus Research, Rostock, Warnemünde, Germany

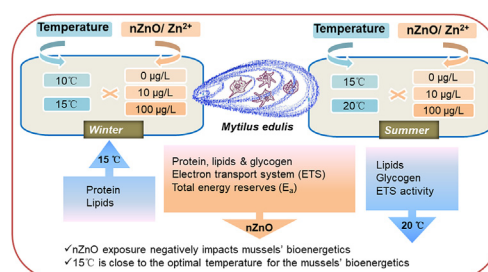
^c Department of Marine Geology, Leibniz Institute for Baltic Sea Research Warnemünde, Rostock, Germany

^d Department of Maritime Systems, Interdisciplinary Faculty, University of Rostock, Rostock, Germany

HIGHLIGHTS

- Combined effects of temperature and nZnO on mussels' bioenergetics were studied.
- In summer and winter, nZnO exposure depleted glycogen stores of the mussels.
- In summer, nZnO exposure suppressed mitochondrial activity and lipid levels.
- Warming (+5 °C) increased mussels' energy reserves in winter but not in summer.

GRAPHICAL ABSTRACT



ARTICLE INFO

Article history:

Received 27 April 2020

Received in revised form

17 July 2020

Accepted 18 July 2020

Available online 12 August 2020

Handling Editor: Jim Lazorchak

Keywords:

Warming

nZnO

Mussel

Energy reserves

Mitochondria

Electron transport activity

Oxidative phosphorylation

Proton leak

Lipid

Carbohydrate

ABSTRACT

Input of ZnO nanoparticles (nZnO) from multiple sources have raised concerns about the potential toxic effects on estuarine and coastal organisms. The toxicity of nZnO and its interaction with common abiotic stressors (such as elevated temperature) are not well understood in these organisms. Here, we examined the bioenergetics responses of the blue mussel *Mytilus edulis* exposed for 21 days to different concentrations of nZnO or dissolved zinc (Zn^{2+}) (0, 10, 100 $\mu g L^{-1}$) and two temperatures (ambient and 5 °C warmer) in winter and summer. Exposure to nZnO had little effect on the protein and lipid levels, but led to a significant depletion of carbohydrates and a decrease in the electron transport system (ETS) activity. Qualitatively similar but weaker effects were found for dissolved Zn. In winter mussels, elevated temperature (15 °C) led to elevated protein and lipid levels increasing the total energy content of the tissues. In contrast, elevated temperature (20 °C) resulted in a decrease in the lipid and carbohydrate levels and suppressed ETS in summer mussels. These data indicate that moderate warming in winter (but not in summer) might partially compensate for the bioenergetics stress caused by nZnO toxicity in *M. edulis* from temperate areas such as the Baltic Sea.

© 2020 Elsevier Ltd. All rights reserved.

1. Introduction

With the global rise in nanotechnology, manufactured

* Corresponding author. Department of Marine Biology, Institute for Biological Sciences, University of Rostock, Rostock, Germany.

E-mail address: inna.sokolova@uni-rostock.de (I.M. Sokolova).

nanoparticles (<100 nm) are increasingly released into coastal marine ecosystems (Garner and Keller, 2014; Williams et al., 2019). The nanoscale zinc oxides (nZnO) are commonly used as anti-fouling agents, UV screens and antimicrobials. Probabilistic models accounting for the production and emission of nZnO predict concentrations of nZnO of >100 $\mu\text{g kg}^{-1}$ in the sediment and >100 $\mu\text{g l}^{-1}$ in the coastal waters (Coll et al., 2016; Yung et al., 2014). This raises concerns about the potential impact of nZnO pollution on coastal marine ecosystems (Bondarenko et al., 2013; Williams et al., 2019). Exposure to nZnO can negatively affect growth (Hanna et al., 2013; Muller et al., 2014), immunity (Wu et al., 2018, 2020), redox balance (Buffet et al., 2012; Trevisan et al., 2014) and reproduction (Fabrega et al., 2012) of marine organisms. However, the toxic mechanisms of environmentally relevant levels of nZnO in marine organisms are not yet fully understood. Furthermore, due to the wide fluctuations of abiotic factors (such as temperature, salinity, or pH) that can affect both the physicochemical properties of nanoparticles (Yung et al., 2017) and the physiological responses of the organisms (Somero et al., 2016), assessment of the potential effects of abiotic variability on nanoparticle toxicity is needed for ecological risk assessment of nanopollutants (Holmstrup et al., 2010; Wu et al., 2018, 2020).

Temperature is a key abiotic factor affecting all aspects of performance of ectotherms due to its direct effects on the rates of biochemical and physiological reactions (Somero et al., 2016). In temperate ecosystems, benthic invertebrates are commonly exposed to elevated temperatures due to the seasonal warming as well as the global climate change (IPCC, 2014). The recent consensus models predict a 3–6 °C increase in the global mean air temperatures by the end of the 21st century. Northern and central Europe are warming even faster with the predicted increase of 5–8 °C until the end of the 21st century (IPCC, 2013). Elevated temperatures can strongly enhance the toxicity of dissolved metals in aquatic organisms (Bagwe et al., 2015; Hallman and Brooks, 2016; Heugens Eh et al., 2003; Nardi et al., 2017; Sokolova, 2004; Sokolova and Lannig, 2008) but little is known about the temperature-dependent effects on the biological responses to the metal-containing nanoparticles in marine ectotherms (Andrade et al., 2019; Falfushynska et al., 2019b; Kumar et al., 2020; Mos et al., 2017). Furthermore, because seasonality is an important factor affecting all aspects of physiology of temperate mussels including stress tolerance (Bagwe et al., 2015; Cherkasov et al., 2010; Ioannou et al., 2009; Katsikatsou et al., 2012; Múgica et al., 2015; Marigómez et al., 2017), it is important to consider season in assessing the temperature-dependent responses to nanopollution. Here, we focused on the potential modulating effects of seasonality and elevated temperature on the metabolic response of the blue mussels *M. edulis* to nZnO toxicity by comparing the effects of a similar degree of warming (+5 °C above the ambient) in winter and summer mussels.

Energy metabolism of aquatic ectotherms is susceptible to temperature and pollutants (Sokolova et al., 2011). The ability to maintain energy homeostasis is a major factor determining stress tolerance of aquatic organisms and sustainability of their populations under multiple stress scenarios (Sokolova, 2013; Sokolova et al., 2012). Nanoparticle exposure can impact energy metabolism of aquatic ectotherms. Thus, exposures to waterborne TiO₂ and Ag nanoparticles suppressed feeding activities, decreased food absorption efficiency, impaired digestion and diminished the aerobic scope for growth of marine mussels and clams (Hu et al., 2017; Kong et al., 2019; Saggese et al., 2016; Saidani et al., 2019; Shang et al., 2020). Studies in freshwater mussels (*Unio tumidus*) showed that the energy status of these organisms was negatively affected by nZnO (as reflected in the depletion of tissue energy reserves and a decrease in ATP levels) and that these impacts were

modulated by environmental temperature (Falfushynska et al., 2019b). However, to the best of our knowledge, no studies of the bioenergetics consequences of temperature-nZnO interactions have been conducted in marine bivalves.

The aim of our present study was to determine the interactive effects of seasonal warming and acclimation at elevated temperatures on bioenergetic responses to nZnO pollution in the blue mussels *Mytilus edulis*. The blue mussels are common sentinel species for environmental stress assessment (Beyer et al., 2017; Bricker et al., 2014) that play important ecological and economical roles in the coastal environment (Kijewski et al., 2011; Mathiesen et al., 2017). As filter feeders, mussels can accumulate nanomaterials and are susceptible to their toxicity (Beyer et al., 2017; Rocha et al., 2015). We hypothesized that the nZnO exposure will cause disturbance of the energy status of the mussels as reflected in the impaired mitochondrial activity and the decrease in the energy reserves (including carbohydrates, lipids, and in the case of extreme stress, proteins). We also hypothesized that the negative effects of nZnO on bioenergetics might be exacerbated by the seasonal warming and/or acclimation at the elevated temperatures. To test these hypotheses, we measured the tissue levels of energy reserves (including proteins, lipids and carbohydrates), electron transport system (ETS) activity, mitochondrial capacity for respiration and ATP synthesis, and cellular energy allocation (CEA) as an integrative index of the energy status (De Coen and Janssen, 2003) in *M. edulis* exposed for 21 days to different nZnO concentrations (0, 10, 100 $\mu\text{g l}^{-1}$) under ambient and elevated (+5 °C) temperature in winter and summer. To assess whether the effects of nZnO on bioenergetics might be due to the increase in intracellular Zn, we measured accumulation of Zn and levels of the metal-binding proteins (metallothioneins) as markers for intracellular Zn in the mussels exposed to different temperatures and pollutants. Our study provides new insights into the bioenergetic mechanisms underlying the combined effects of elevated temperature and nZnO of *M. edulis* and has important implications for understanding the effects of warming on the mussels' populations from polluted estuaries and coastal zones.

2. Materials and methods

2.1. Animal collection and maintenance

The wild blue mussels *M. edulis* (56 ± 6 mm shell length) were collected near Warnemünde, Germany (54°10'49.602"N, 12°05'21.991"E) in late October (winter experiment) and June (summer experiment). The mussels were transported to the University of Rostock within 2 h of collection in a cooler lined with the seawater-soaked paper towels. Mussels with no shell damage were selected, and the shell surface was cleaned from epibionts. Mussels were acclimated to the following laboratory conditions for two weeks: the mussels used in the winter experiment maintained at salinity 15 (practical salinity scale) and temperature 10 °C, those in the summer experiment maintained at salinity 15 and temperature 15 °C. All mussels were kept in recirculated temperature-controlled aquaria with aeration, UV-water treatment, protein skimmer, and a moving bed biofilter. The temperature of 10 °C in the winter experiment and the temperature of 15 °C in the summer experiment were close to the respective temperatures in the mussels' habitat at the time of collection and thus considered ambient (control) temperatures in this study. Elevated temperatures (+5 °C above the respective controls) were chosen to represent the predicted warming in the southern Baltic Sea according to the climate change scenarios (IPCC, 2013).

2.2. Experimental exposures and tissue collection

After the preliminary acclimation, the mussels were randomly assigned to one of the ten experimental groups and exposed for 21 days in 12: 12 light: dark regime at salinity 15 to the different combinations of temperature and Zn exposure. The duration of experimental exposures (21 days) was chosen because in temperate marine bivalves, 2–3 weeks are required to reach a new physiological steady-state after an environmental shift (Khlebovich, 2017; Thompson et al., 2012). Within each season, two factors were tested in a fully crossed design with two temperatures levels (10 and 15 °C as ambient and elevated temperature in the winter, and 15 and 20 °C as ambient and elevated temperature in the summer, respectively) and five Zn treatments: no Zn addition as a control, nZnO or dissolved Zn at 10 $\mu\text{g l}^{-1}$ Zn and 100 $\mu\text{g l}^{-1}$ Zn (the low and high Zn levels, respectively). Exposures to 10 and 100 $\mu\text{g l}^{-1}$ of nZnO were within the range of predicted environmental concentrations of nZnO (Coll et al., 2016; Yung et al., 2014). Exposure to dissolved Zn (as ZnSO_4) was used to test whether the toxic effects of nZnO might be due to the potential release of Zn^{2+} . Each of the ten experimental groups was randomly subdivided and placed into three replicate tanks (6 l) per treatment, each tank containing 20 mussels. Artificial seawater was made with the Instant Ocean® sea salt and supplemented with 20% of the filtered natural Baltic seawater (salinity ~12) to achieve salinity 15.

A static renewal design was used with the water change and nZnO or ZnSO_4 additions every two days. ZnO nanoparticles (nZnO) (average particle size 30 nm, hydrodynamic size $\sim 817 \pm 174$ nm and zeta-potential -9.6 mV at salinity 15) were purchased from Sigma-Aldrich Sweden AB (Stockholm, Sweden). Suspensions of nZnO or ZnSO_4 solutions were added to experimental water during every water change and vigorously aerated to maintain particles in suspension. No mortality of the mussels occurred during the experiment. The mussels were fed at least 2 h before every water change with a commercial blend of live algae containing *Nannochloropsis oculata*, *Phaeodactylum* sp. and *Chlorella* sp. (Premium Reef Blend, CoralSands, Wiesbaden, Germany) per manufacturer's instructions.

After 21 days of experimental exposure, mussels were dissected on ice. Soft tissues were collected, blotted with filter paper, shock-frozen and stored at -80 °C. Whole soft tissue was ground under the liquid nitrogen, the powder was aliquoted and stored at -80 °C until further analyses.

2.3. Determination of Zn concentrations in the seawater and the mussels' body

Before each water change, seawater samples (14.5 ml) were collected from experimental tanks, acidified with trace-metal grade HNO_3 and stored at $+4$ °C for further analysis. Zn concentration in seawater samples was measured by inductively coupled plasma mass spectrometry (ICP-MS) (iCAP Q; Thermo Fisher Scientific) as described elsewhere (Dellwig et al., 2019; Lagerstrom et al., 2013; Sohrin et al., 2008; Wu et al., 2020). Accuracy (2.4%) and precision (7.4%) were verified by the international seawater reference material NASS-7.

Whole soft tissue powder (~ 300 mg) of the mussels was dried in an incubator at 70 °C, and digested with 30% H_2O_2 . The samples were incubated at 70 °C overnight to evaporate H_2O_2 , digested in 65% HNO_3 (trace metal grade) at 70 °C for 24 h, filtered through 0.45 μm filters and kept at $+4$ °C for further analysis. Zn concentration in the digested soft tissue was determined using inductively coupled plasma-optical emission spectrometry (ICP-OES) (iCAP 7400 Duo, Thermo Fisher Scientific) as described elsewhere (Wu et al., 2020). Accuracy (5.0%) and precision (1.1%) were verified by the international reference material SGR-1b.

2.4. Electron transport system (ETS) activity in the whole soft tissue

ETS activity was measured in the whole body extracts of the mussels by a 2-(4-iodophenyl)-3-(4-nitrophenyl)-5-phenyl tetrazolium chloride (INT) reduction assay using a SpectraMax ID3 Multi-Mode Microplate Reader (Molecular Devices, USA) at 20 °C as described elsewhere (Falfushynska et al., 2019c; Haider et al., 2018). For each sample, the non-mitochondrial reduction of INT-tetrazolium was determined by adding 0.7 mM KCN (an inhibitor of the terminal ETS enzyme cytochrome c oxidase) and 10 μM rotenone (an inhibitor of the ETS Complex I) instead of NAD(P)H solution for blank reading. Specific ETS activity of the tissues was calculated based on the rate of formazan formation using an extinction coefficient of 15.9 $\text{mM}^{-1} \text{cm}^{-1}$ at 490 nm and corrected for the light path (0.523 ± 0.023 cm). The ETS activity was calculated as a difference in the activity in the absence and presence of the ETS inhibitors and expressed as $\text{nM O}_2 \text{min}^{-1} \text{g}^{-1}$ wet tissue mass using the stoichiometric equivalent of 1 μmol formazan to 0.5 $\mu\text{mol O}_2$.

2.5. Mitochondrial oxygen consumption and ATP synthesis capacity

Mitochondria were isolated from the digestive gland, which is one of the most metabolically active tissues in mussels, as described elsewhere (Falfushynska et al., 2019a). Briefly, ~ 0.6 – 1 g of the digestive gland tissue (pooled from 2 to 3 mussels) was homogenized in an ice-cold homogenization media containing 100 mM sucrose, 200 mM KCl, 100 mM NaCl, 8 mM ethylene glycol-bis(2-aminoethylether)-N,N,N',N'-tetraacetic acid (EGTA), 50 $\mu\text{g l}^{-1}$ aprotinin, 1 mM phenylmethylsulfonyl fluoride (PMSF), and 30 mM 2-[4-(2-hydroxyethyl)piperazin-1-yl]ethanesulfonic acid (HEPES), pH 7.5. Mitochondria were isolated by differential centrifugation at 4 °C (Falfushynska et al., 2019a), and resuspended in ice-cold assay media containing 185 mM sucrose, 130 mM KCl, 10 mM NaCl, 30 mM HEPES, 10 mM glucose, 1 mM MgCl_2 , 10 mM KH_2PO_4 and 1% bovine serum albumin (BSA), pH 7.2.

Oxygen consumption rate (\dot{M}_{O_2}) of isolated mitochondria was measured with a substrate mixture of pyruvate, malate and succinate at 15 °C using a high resolution respirometer Oxygraph 2 k (Oroboros, Innsbruck, Austria). Baseline mitochondrial \dot{M}_{O_2} (indicative of the proton leak, i.e. the respiration needed to counteract the sum of all futile cation cycles that dissipate the mitochondrial membrane potential), \dot{M}_{O_2} of actively phosphorylating mitochondria (indicative of OXPHOS capacity), and activities of the ETS and cytochrome c oxidase (COX) were measured as described in an earlier report (Falfushynska et al., 2019a). Mitochondrial \dot{M}_{O_2} was expressed as $\mu\text{mol O}_2 \text{min}^{-1} \text{g}^{-1}$ mitochondrial protein. The respiratory control ratio (RCR) was calculated by dividing the OXPHOS respiration by the baseline (proton leak) respiration (Estabrook, 1967). The OXPHOS coupling efficiency was calculated as follows: $\text{CE}_{\text{OXPHOS}} = 1 - [\text{LEAK}/\text{OXPHOS}]$, where LEAK and OXPHOS are the respiration rates of the mitochondria in the baseline (leak) and actively phosphorylating states, respectively (Gnaiger, 2012). The apparent reserve ETS and COX capacity were calculated as the ratio of ETS to OXPHOS respiration, and of COX to ETS respiration, respectively (Gnaiger, 2012).

2.6. Tissue energy reserves

2.6.1. Lipids, proteins and carbohydrates in the whole soft tissue

Lipid concentration was measured in the whole soft tissue using a standard colorimetric method with chloroform-methanol extraction (Van Handel, 1985). Protein concentrations were determined using Biorad Bradford Protein Assay Kit according to the manufacturer's instructions (Bio-Rad, Hercules, CA, USA) with

bovine serum albumin (BSA) as a standard. Carbohydrate concentrations were measured with the phenol-sulphuric acid method (Masuko et al., 2005). Other details of analyses can be found in our previous reports (Falfushynska et al., 2019a, 2019c; Haider et al., 2018). The absorbance of lipids, proteins and carbohydrates was determined at 490 nm, 595 nm and 492 nm, respectively, by a SpectraMax ID3 Multi-Mode Microplate Reader (Molecular devices, USA). Concentrations of lipid and proteins were expressed in mg g⁻¹ wet mass. Concentrations of carbohydrates were expressed as μmol glucose equivalents g⁻¹ wet mass.

2.6.2. Cellular energy allocation (CEA)

Because marine mussels can use different energy compounds (lipids, carbohydrates and proteins) interchangeably depending on the compound availability and physiological status (Gosling, 1992; Haider et al., 2018), determination of the total energy content vs. potential energy expenditure is important to assess the overall bioenergetics condition of an organism. Total energy reserve (Ea) of the mussels was calculated by transforming the measured protein, lipid and carbohydrate content into energy equivalents (Gnaiger, 1983). The potential energy expenditure (Ec) was calculated by converting the ETS activity into energy equivalents using oxy-enthalpic equivalents for combustion of an average lipid, carbohydrate and protein mixture (484 J mmol⁻¹ O₂) (Gnaiger, 1983; Verslycke et al., 2004a). The cellular energy allocation (CEA) (as an integrative index of the energy status) was calculated as a ratio of total energy reserve (Ea) to the potential energy expenditure (Ec) (DeCoen and Janssen, 1997).

2.7. Metallothioneins (MTs) assay

Total concentration of metallothioneins (MTs) in the whole body of the mussels was measured using 5,5-dithio-bis-(2-nitrobenzoic acid) (DTNB) reduction method (Viarengo et al., 1997). The tissue was homogenized (1:3 v/v) in an ice-cold buffer (0.5 M sucrose, 20 mM Tris, 0.5 mM phenyl methyl sulfonyl fluoride (PMSF) and 0.01% β -mercaptoethanol, pH 8.6). The samples were centrifuged at 16,000 g at 4 °C for 60 min. The large-molecular-weight proteins were precipitated with 200 μl of -20 °C absolute ethanol and 15 μl chloroform and removed by centrifugation at 6,000 g at 4 °C for 12 min. The supernatant was mixed with three volumes of -20 °C absolute ethanol, vortexed, cooled at -20 °C for 1 h, and centrifuged at 6,000 g for 12 min. The pellet containing MTs was washed twice with 1 ml of the washing buffer made up with 2.5 ml chloroform and 30 ml Tris-sucrose solution (20 mM Tris and 0.5 mM sucrose) adjusted to 250 ml with absolute ethanol and cooled to -20 °C. The pellet was dissolved in 100 μl Tris-EDTA buffer (5 mM Tris and 1 mM EDTA), mixed with 0.5 ml of 0.43 mM DTNB, and incubated for 15 min at room temperature. Absorbance was measured at 412 nm using a SpectraMax ID3 Multi-Mode Microplate Reader (Molecular Devices, USA). The levels of MTs were calculated assuming the following relationship: 20 μmol GSH = 1 μmol MT = 8000 μg MT, and expressed as μg of MTs g⁻¹ wet tissue mass.

2.8. Statistical analysis

Data analysis was performed by IBM® SPSS® Statistics ver. 22.0.0.0 (IBM Corp., Armonk, NY, USA) and GraphPad Prism ver. 7.02 (GraphPad Software Inc., La Jolla, CA, USA). Pilot analysis showed no effects of replicate tanks on the studied traits ($P > 0.05$); therefore, individual mussels were used as biological replicates in all subsequent analyses. The data were tested for normality with the Shapiro-Wilk's test and homogeneity of variance with Levine test. Not-normally distributed data were Box-Cox transformed. The

effects of temperature, Zn treatment and their interactions on the studied traits were analyzed by two-way ANOVA with temperature and Zn exposure as fixed factors. The factor "Temperature" had two levels (ambient and elevated temperature). The factor "Zn treatment" had five levels (control – no Zn addition, 10 $\mu\text{g l}^{-1}$ nZnO, 100 $\mu\text{g l}^{-1}$ nZnO, 10 $\mu\text{g l}^{-1}$ dissolved Zn or 100 $\mu\text{g l}^{-1}$ dissolved Zn). Tukey's Honest Significant Differences (HSD) test was used to compare the pairs of means among different Zn treatments at each fixed temperature. The significant effects of temperature were tested for each Zn treatment using a Student's t-test. To reduce the dimensionality of the data set, principal component analysis (PCA) was carried out using XLSTAT®2014, and a biplot was graphed including the measured variables and the individual mussels from different exposure groups. The number of biological replicates was 6–7 for isolated mitochondria and 5 for all other traits. The results were expressed as the means \pm the standard error of the mean (SEM), and the differences were considered statistically significant if $P < 0.05$.

3. Results

3.1. Zn content in seawater and the soft body of mussels

The total Zn concentration in the seawater (in $\mu\text{g l}^{-1}$) was 17.56 ± 1.40 in the control, 27.93 ± 3.54 and 27.79 ± 1.77 in 10 $\mu\text{g l}^{-1}$ nZnO and Zn²⁺ exposures, respectively, and 68.76 ± 4.58 and 94.67 ± 5.55 in 100 $\mu\text{g l}^{-1}$ nZnO and Zn²⁺ exposures, respectively ($N = 12$). The total Zn concentration in the soft tissues of the mussels was not affected by the elevated temperature or Zn exposure ($P > 0.05$), whereas exposure to high concentration of nZnO led to a significant Zn accumulation in the mussels' tissues (Fig. 1A and B).

3.2. Metallothioneins (MTs)

MTs levels in the mussels' soft tissues were significantly affected by the temperature and the season ($P < 0.05$), but no significant ($P > 0.05$) interactive effect was detected (Tables 1–3). MTs was not significantly affected by the nZnO/Zn²⁺ treatments within each temperature group in winter or summer mussels. Elevated temperature significantly increased MTs levels in the winter mussels exposed to control and low nZnO treatment (Fig. 1C and D).

3.3. Bioenergetics markers

Protein levels were significantly affected by temperature and Zn exposure in the winter mussels ($P < 0.05$), but the interactions between temperature and Zn exposure were not detected ($P > 0.05$) (Tables 1–3). In winter mussels, protein levels decreased in high nZnO/Zn²⁺ treatments (Fig. 2A), while acclimation at the elevated temperature significantly increased the protein content of the control group and the mussels exposed to 10 $\mu\text{g l}^{-1}$ nZnO or Zn²⁺. In summer mussels, no significant effects of the elevated temperature or nZnO/Zn²⁺ treatments on the protein levels were detected ($P > 0.05$) (Fig. 2A and B).

Lipid levels were significantly affected by Zn exposure in summer (but not in winter) mussels (Tables 1 and 2). Statistically significant effects of temperature and the interaction between Zn exposure and temperature were observed in summer mussels (Tables 1–3). Elevated temperature increased the body lipid content of the control group and the mussels exposed to 100 $\mu\text{g l}^{-1}$ nZnO or Zn²⁺ in the winter (Fig. 2C). In summer, acclimation at the elevated temperature led to a decrease in the body lipid content of the control group and the mussels exposed to 100 $\mu\text{g l}^{-1}$ nZnO or Zn²⁺ (Fig. 2D). High nZnO treatments led to a decrease in lipid

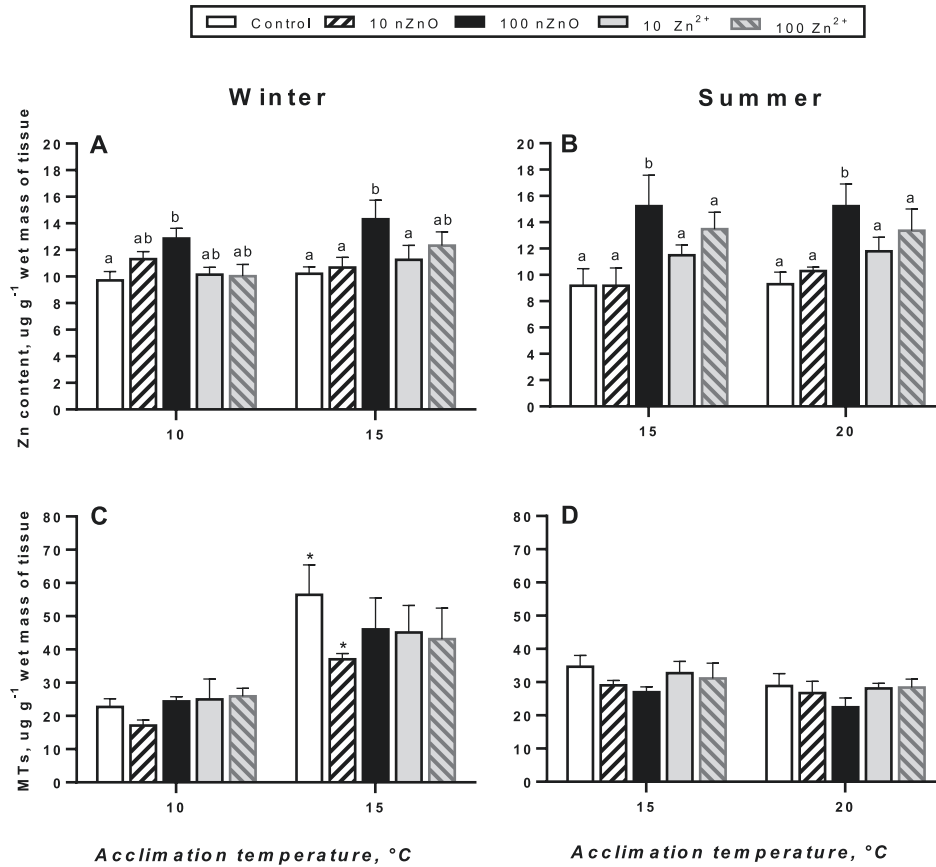


Fig. 1. Zn content (A, B) and metallothionein levels (C, D) in the soft tissues of *M. edulis* exposed to different concentrations of nZnO or Zn²⁺ (0, 10 and 100 µg l⁻¹) and temperatures for 21 days. Winter mussels – A, C; Summer mussels – B, D. Different letters indicate significant differences among nZnO or Zn²⁺ treatments within fixed temperature level (Tukey HSD test, P < 0.05), and asterisks indicate significant differences between two temperatures within the same Zn treatment group (t-test, P < 0.05). N = 5.

Table 1

Two-way ANOVA analyses of the studied biomarkers of *M. edulis* exposed to different combinations of Zn treatment and temperature in winter experiment. Temperature: 10 and 15 °C; Zn treatment: control, 10 µg l⁻¹ nZnO, 100 µg l⁻¹ nZnO, 10 µg l⁻¹ Zn²⁺, and 100 µg l⁻¹ Zn²⁺; ETS: electron transport system activity; Ea: total energy reserve; CEA: cellular energy allocation; MTs: metallothionein. P: P-value. Degrees of freedom (df) for the error were 40 for all studied traits. Significant effects are highlighted in bold.

Source	df	Tissue Zn content		Protein		Lipid		Carbohydrate		ETS		Ea		CEA		MTs	
		F	P	F	P	F	P	F	P	F	P	F	P	F	P	F	P
		Temperature	1	2.945	0.096	23.920	<0.001	127.409	<0.001	5.885	0.020	3.143	0.084	165.590	<0.001	75.295	<0.001
Zn treatment	4	4.898	0.004	6.194	0.001	2.888	0.054	33.059	<0.001	6.626	<0.001	7.642	<0.001	3.856	0.010	1.003	0.417
Temperature * Zn	4	0.794	0.538	1.139	0.352	1.421	0.245	7.556	<0.001	0.979	0.430	2.036	0.108	3.966	0.008	0.623	0.649

Table 2

Two-way ANOVA analyses of the studied biomarkers of *M. edulis* exposed to different combinations of Zn treatment and temperature in summer experiment. Temperature: 15 and 20 °C; Zn treatment: control, 10 µg l⁻¹ nZnO, 100 µg l⁻¹ nZnO, 10 µg l⁻¹ Zn²⁺, and 100 µg l⁻¹ Zn²⁺; ETS: electron transport system activity; Ea: total energy reserve; CEA: cellular energy allocation; MTs: metallothionein. P: P-value. Degrees of freedom (df) for the error were 40 for all studied traits. Significant effects are highlighted in bold.

Source	df	Tissue Zn content		Protein		Lipid		Carbohydrate		ETS		Ea		CEA		MTs	
		F	P	F	P	F	P	F	P	F	P	F	P	F	P	F	P
		Temperature	1	0.107	0.746	4.522	0.056	20.141	<0.001	15.475	<0.001	30.089	<0.001	25.798	<0.001	3.201	0.081
Zn treatment	4	6.648	0.001	1.176	0.336	7.106	<0.001	7.144	<0.001	22.203	<0.001	8.53	<0.001	6.467	<0.001	1.744	0.159
Temperature * Zn	4	0.063	0.992	0.363	0.833	2.685	0.045	0.642	0.636	0.671	0.616	2.275	0.078	1.944	0.122	0.121	0.974

content at the ambient temperature in summer mussels but not in their winter counterparts (compared with the respective controls

not exposed to metals) (Fig. 2C and D).

Temperature and Zn exposure had significant effects on the

Table 3
Two-way ANOVA analyses of the studied biomarkers of *M. edulis* exposed to different combinations of Zn treatment and season at 15 °C. Season: summer and winter; Zn treatment: control, 10 $\mu\text{g l}^{-1}$ nZnO, 100 $\mu\text{g l}^{-1}$ nZnO, 10 $\mu\text{g l}^{-1}$ Zn²⁺, and 100 $\mu\text{g l}^{-1}$ Zn²⁺; ETS: electron transport system activity; Ea: total energy reserve; CEA: cellular energy allocation; MTs: metallothionein. P: P-value. Degrees of freedom (df) for the error were 40 for all studied traits. Significant effects are highlighted in bold.

Source	df	Tissue Zn content		Protein		Lipid		Carbohydrate		ETS		Ea		CEA		MTs	
		F	P	F	P	F	P	F	P	F	P	F	P	F	P	F	P
Season	1	0.004	0.953	32.980	<0.001	6.491	0.015	0.315	0.578	62.254	<0.001	0.324	0.573	45.887	<0.001	16.000	<0.001
Zn treatment	4	5.513	0.002	5.761	<0.001	6.836	<0.001	8.018	<0.001	15.924	<0.001	11.154	<0.001	7.328	<0.001	1.269	0.298
Season * Zn	4	0.418	0.794	1.273	0.297	0.513	0.726	1.392	0.254	2.300	0.076	0.510	0.729	1.669	0.176	0.473	0.755

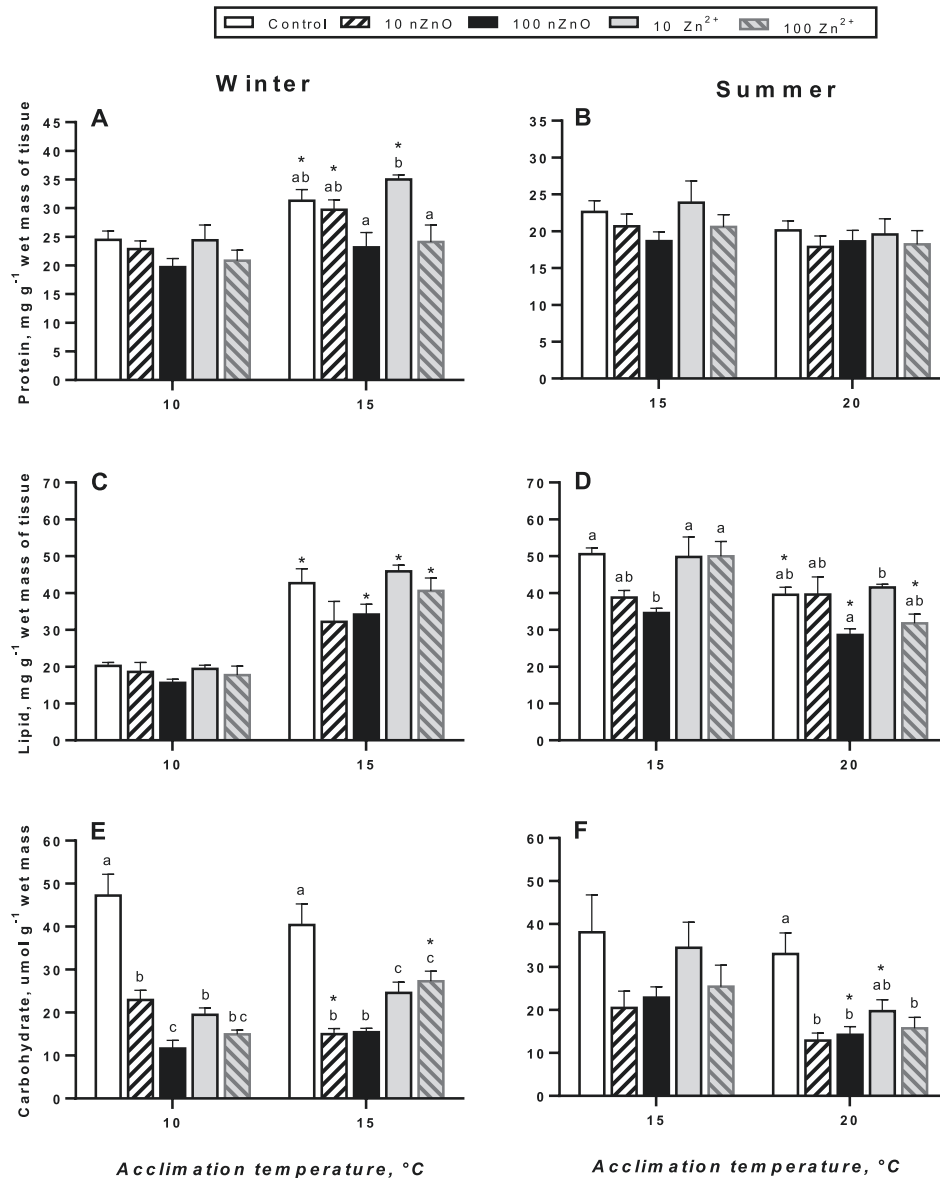


Fig. 2. Protein (A, B), lipid (C, D) and carbohydrate (E, F) content in soft tissues of *M. edulis* exposed to combinations of nZnO or Zn²⁺ (0, 10 and 100 $\mu\text{g l}^{-1}$) and temperature for 21 days. Winter mussels – A, C, E; Summer mussels – B, D, F. Different letters indicate significant differences among nZnO or Zn²⁺ treatments within fixed temperature level (Tukey HSD test, $P < 0.05$), and asterisks indicate significant differences between two temperatures within the same Zn treatment group (t -test, $P < 0.05$). $N = 5$.

carbohydrate levels of the mussels' body, and the interactive effect between temperature and Zn exposure was found in the winter (Tables 1 and 2). Elevated temperature increased carbohydrate

levels in the winter mussels exposed to 100 $\mu\text{g l}^{-1}$ Zn²⁺ (Fig. 2E). In summer, acclimation at the elevated temperatures led to a decrease in the carbohydrate content in the mussels exposed to 10 $\mu\text{g l}^{-1}$

Zn²⁺ and 100 µg l⁻¹ nZnO. The carbohydrate content of the mussels' body decreased with increasing nZnO or dissolved Zn concentrations. This trend was significant in all temperature treatment groups except for the 15 °C-acclimated summer mussels (Fig. 2E and F).

Total energy reserve (Ea) was affected by temperature and Zn exposure, but no significant interactions between Zn treatment and temperature were found (Tables 1–3). Ea decreased in the winter and summer mussels exposed to high nZnO regardless of the temperature (Fig. 3A and B). Acclimation at the elevated temperature increased Ea within the respective Zn treatment group in the winter but not in the summer (Fig. 3A and B).

ETS activity in the whole tissue was affected by temperature, Zn exposure and season, but no significant factor interactions were detected (Tables 1–3). ETS activity generally decreased with

increasing nZnO or dissolved Zn concentrations at each temperature level in both winter and summer mussels (Fig. 3C and D). In summer mussels, combined exposures to elevated temperature and high nZnO/Zn²⁺ further decreased ETS activity (Fig. 3D). In winter, acclimation at the elevated temperature had no significant effect on the ETS activity when compared within each Zn treatment group (Fig. 3C and D).

Functional traits of the isolated mitochondria from the digestive gland including the ATP synthesis capacities, mitochondrial proton leak, and the maximum ETS and COX activities were not strongly affected by the acclimation temperature or Zn exposures in the winter mussels (Table 4). The mitochondrial coupling (assessed as RCR or OXPHOS coupling efficiency) or the apparent ETS and COX capacity did not change in response to temperature acclimation or Zn exposures in the winter mussels (summer mussels were not

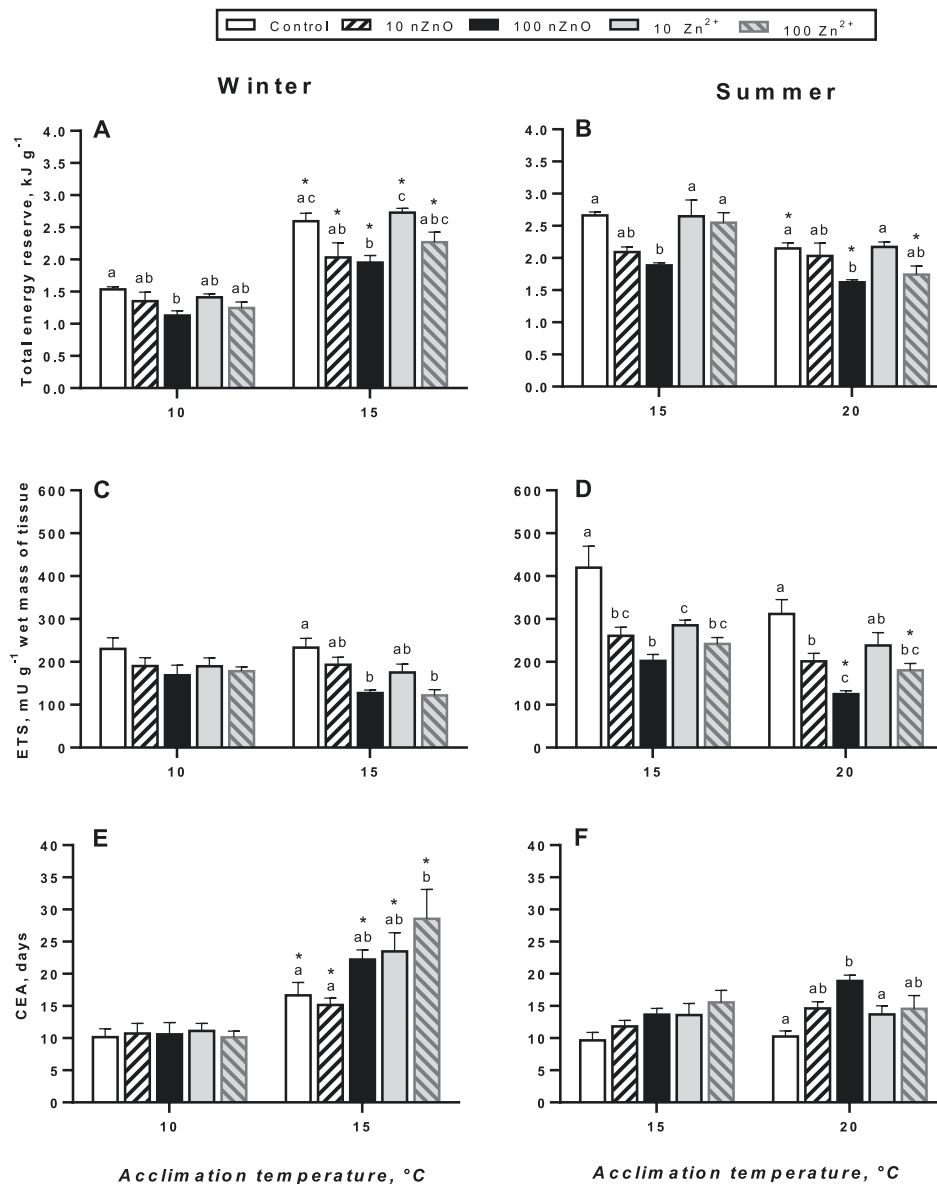


Fig. 3. Total energy reserve (A, B), ETS activity (C, D) and cellular energy allocation (E, F) of *M. edulis* exposed to combinations of nZnO or Zn²⁺ (0, 10 and 100 µg l⁻¹) and temperature during 21 days. Winter mussels – A, C, E; Summer mussels – B, D, F. Different letters indicate significant differences among nZnO or Zn²⁺ treatments within fixed temperature level (Tukey HSD test, P < 0.05), and asterisks indicate significant differences between two temperatures within the same Zn treatment group (t-test, P < 0.05). N = 5.

Table 4
Effects of the acclimation temperature combined with nZnO or dissolved Zn exposure on mitochondrial bioenergetics of *M. edulis*. Mitochondria were isolated from the digestive gland of the winter mussels acclimated at different temperatures and exposed either to control conditions, 100 $\mu\text{g l}^{-1}$ of nZnO or 100 $\mu\text{g l}^{-1}$ of Zn^{2+} . All mitochondrial traits were assayed at 15 °C. Proton leak – baseline oxygen consumption of non-phosphorylating mitochondria (leak state); OXPHOS activity – oxygen consumption of mitochondria during oxidative phosphorylation (OXPHOS) indicative of the ATP synthesis capacity, ETS – electron transport system, RCR – respiratory control ratio. Explanations of the derived indices (RCR, OXPHOS coupling efficiency and the reserve ETS and COX capacity) are provided in the Materials and Methods. Proton leak, OXPHOS activity, ETS activity and COX activity are expressed as $\mu\text{mol O}_2 \text{min}^{-1} \text{g}^{-1}$ mitochondrial protein. The derived indices have no units. For the proton leak, values that do not share the same letter, are significantly different ($P < 0.05$). For all other traits, no significant differences were found between the experimental treatment groups. N = 6–7.

Source	Acclimation conditions					
	10 °C			15 °C		
	Control	nZnO	Zn^{2+}	Control	nZnO	Zn^{2+}
Proton leak	2.24 ± 0.30 ^{ab}	2.17 ± 0.27 ^{ab}	2.18 ± 0.20 ^{ab}	2.54 ± 0.21 ^{ab}	3.12 ± 0.35 ^b	2.04 ± 0.18 ^a
OXPHOS activity	6.41 ± 1.30	6.03 ± 1.72	6.96 ± 0.97	4.65 ± 1.10	6.43 ± 0.99	5.68 ± 0.18
ETS activity	6.92 ± 1.41	6.40 ± 1.74	8.95 ± 0.83	6.48 ± 1.36	8.50 ± 0.60	5.73 ± 1.22
COX activity	19.91 ± 2.64	19.69 ± 2.95	20.62 ± 3.12	15.21 ± 1.78	18.74 ± 2.61	17.34 ± 1.72
RCR	2.87 ± 0.46	2.49 ± 0.51	3.17 ± 0.22	1.72 ± 0.24	2.10 ± 0.24	3.89 ± 0.85
OXPHOS coupling efficiency	0.61 ± 0.08	0.52 ± 0.11	0.75 ± 0.02	0.59 ± 0.07	0.60 ± 0.04	0.63 ± 0.08
Reserve ETS capacity	1.07 ± 0.03	1.10 ± 0.04	1.33 ± 0.11	1.53 ± 0.31	1.55 ± 0.29	1.03 ± 0.05
Reserve COX capacity	3.39 ± 0.59	3.39 ± 0.59	2.29 ± 0.19	2.93 ± 0.56	2.19 ± 0.24	3.89 ± 0.85

studied) (Table 4).

Cellular energy allocation (CEA) was significantly affected by Zn exposure, temperature (in winter mussels) and season (Tables 1–3). The interactions between Zn treatment and temperature on CEA were significant in the winter (Tables 1–3). CEA was not significantly affected by nZnO or dissolved Zn under the control temperature in each season (Fig. 3E and F). CEA increased in the winter mussels exposed to high Zn^{2+} levels and in the summer mussels exposed to high nZnO concentrations. Furthermore, elevated temperature increased CEA in winter mussels across all Zn treatments (Fig. 3E and F).

3.4. Principal component analysis

Principal component analysis (PCA) revealed that 63.88% and 64.83% of the overall variance of the studied traits were explained by the two first principal components (PC) in the winter and summer experiments, respectively (Fig. 4A and B). In winter mussels, PC 1 expressed 38.39% of overall variance and separated the groups exposed to the ambient and elevated temperatures (Fig. 4A). PC 2 explained 25.49% of the overall variance; this axis presented a Zn-specific response since control group was separated from Zn exposures along this axis (Fig. 4A). In summer mussels, PC 1 and PC 2 explained 44.90% and 19.93% of the overall variance, respectively, with a similar pattern of group separation as found in the winter mussels (Fig. 4B). Tissue levels of proteins, lipids, carbohydrates, MTs, and Ea had high positive associations with the PC 1 in both the winter and summer mussels (Fig. 4A and B).

4. Discussion

4.1. Bioaccumulation of nZnO or Zn^{2+} in mussels

Nanomaterials can pose potential risks to marine life due to the harmful effects of the nanoparticles and the release of trace metals in marine environments (Chae and An, 2017; Yung et al., 2014). In our present study, no Zn accumulation in the soft tissues of the mussels was found when exposed to 10 and 100 $\mu\text{g l}^{-1}$ of Zn^{2+} or 10 $\mu\text{g l}^{-1}$ of nZnO. A modest but significant accumulation of Zn in the mussels' body was observed at high concentration (100 $\mu\text{g l}^{-1}$) of nZnO. The integrated PCA-based analysis of the biomarker profiles also showed that the tissue Zn content tightly correlates with the 2nd principal component that separates the groups of mussels exposed to high nZnO levels from other experimental groups. Overall, these findings indicate that tissue Zn concentrations are

tightly regulated by the mussels in the low concentration range of nZnO but accumulate when the ambient nZnO levels exceed a certain threshold (in this study, 100 $\mu\text{g l}^{-1}$). Similarly, no Zn accumulation was found in the soft tissues of mussels *Elliptio complanata* exposed for 21 days to 10 $\mu\text{g l}^{-1}$ of nZnO or Zn^{2+} (Gagne et al., 2016), *Dreissena polymorpha* exposed for 96 h to 25 $\mu\text{g l}^{-1}$ of nZnO or Zn^{2+} (Gagne et al., 2019), and the mussels *Mytilus galloprovincialis* exposed for 21–28 days to 10–100 $\mu\text{g l}^{-1}$ of nZnO or Zn^{2+} (Li et al., 2018). In *M. galloprovincialis*, Zn accumulation only occurred during prolonged exposures to high concentrations ($\geq 0.5 \text{ mg l}^{-1}$) of nZnO (Hanna et al., 2013; Muller et al., 2014) consistent with our present findings.

Metallothioneins play an important role in the binding of free intracellular metals including Zn^{2+} and in protection against oxidative stress as ROS scavengers (Davis and Cousins, 2000; Yin et al., 2014). In our present study, no significant change in the total metallothionein levels was observed in *M. edulis* exposed to nZnO or Zn^{2+} . This is consistent with the lack of bioaccumulation of Zn that could act as metallothionein inducer (Ruttikay-Nedecky et al., 2013). The lack of MT upregulation also indicates that oxidative injury is not a major toxicity mechanism for nZnO or Zn^{2+} in the concentration range used in our present study. This finding is consistent with the earlier published work in bivalves exposed to low environmentally relevant levels of these pollutants (Falfushynska et al., 2015, 2017; Gagne et al., 2019; Marisa et al., 2016). Interestingly, the metallothionein levels increased during acclimation to elevated temperature in winter mussels indicating that upregulation of this antioxidant might be important for the redox homeostasis during temperature stress. Seasonal acclimatization to elevated temperatures in the summer mussels blunted this increase indicating that other antioxidant mechanisms might be involved in the response to long-term seasonal acclimatization as opposed to short-term (three weeks) experimental warming.

4.2. Bioenergetic responses to temperature and nZnO

Levels of energy reserves have important implications for tolerance of organisms towards toxic substances, and depletion of energy reserves is an early sign of toxicity occurring before other biological activities such as growth, respiration, or reproduction are impaired (Smolders et al., 2003). Pollutant exposure in aquatic invertebrates often leads to elevated energy costs for detoxification, damage repair and stress protection (Berenbaum and Zangerl, 1994; Sokolova, 2013; Sokolova et al., 2012). Furthermore, immune stress and inflammatory reactions caused by nanomaterials

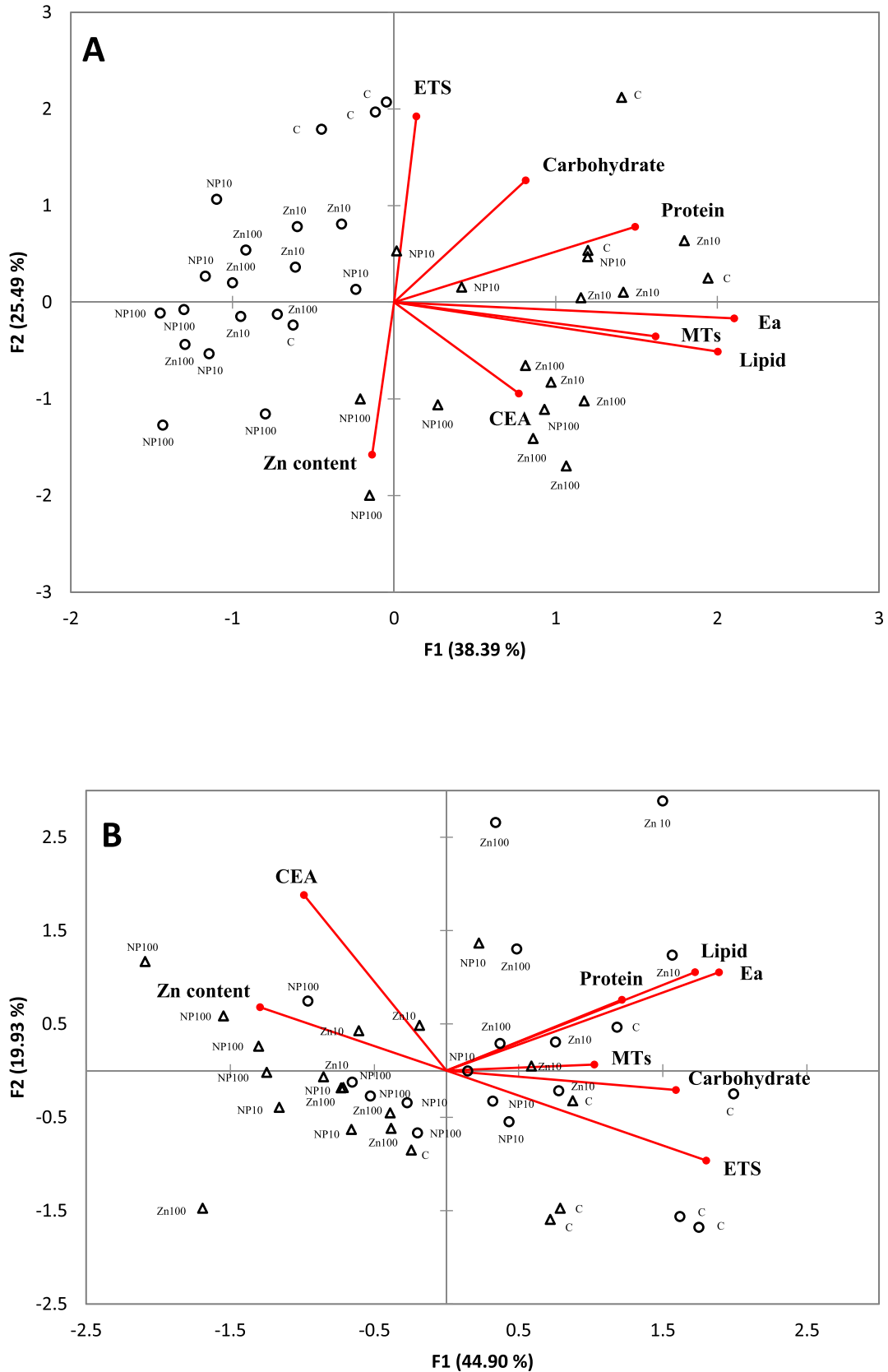


Fig. 4. Principal component analysis (PCA) biplot integrating all measured biomarkers of *M. edulis* exposed to different combinations of nZnO or Zn²⁺ (0, 10 and 100 µg l⁻¹) and temperature. Winter mussels – A; summer mussels – B. Biomarker abbreviations: ETS – electron transport system activity; Ea – total energy reserve; CEA – cellular energy allocation; MTs – metallothioneins. Experimental treatment groups: ○ – ambient temperature; △ – elevated temperature; C – control (no Zn addition); 10NP – 10 µg l⁻¹ nZnO; 100NP – 100 µg l⁻¹ nZnO; 10Zn – 10 µg l⁻¹ ionic Zn; 100Zn – 100 µg l⁻¹ ionic Zn.

(Ansar et al., 2017; Attia et al., 2018; Wu et al., 2020) can increase the energy demand (Wang and Ye, 2015). Elevated energy demand of the mussels exposed to nanopollutants might therefore deplete the organism's energy reserves especially as the feeding activities are impaired by the nanoparticle exposure (Hu et al., 2017; Kong et al., 2019; Saggese et al., 2016; Saidani et al., 2019; Shang et al., 2020). Glycogen and lipids are the major contributors to the energy storage in marine mollusks (Smolders et al., 2003; Sokolova, 2013). In our present study, a significant depletion of carbohydrates (that consist of ~90% of glycogen; Sokolova, unpublished data) was found in *M. edulis* exposed to nZnO or Zn²⁺. A similar decrease in the glycogen content was found in the freshwater mussels *Unio tumidus* exposed to 250 µg l⁻¹ of nZnO (Falfushynska et al., 2019b) and in the clams *Ruditapes philippinarum* exposed to 0.1 and 1.0 mg l⁻¹ of multi-walled carbon nanotubes (De Marchi et al., 2017). Exposure to 100 µg l⁻¹ of nZnO also led to a decrease in the lipid content in the tissues of summer mussels indicating that carbohydrates mobilization cannot fully cover the energy costs in the combined temperature and nZnO stress. Similarly, the lipid reserve was negatively affected in the blue mussels *M. edulis* exposed to 10 µg l⁻¹ nZnO for 14 days (Falfushynska et al., 2019c) and in the gills of freshwater mussels *U. tumidus* exposed to 250 µg l⁻¹ nZnO for 14 days (Falfushynska et al., 2019b). Taken together, these findings indicate that glycogen is mobilized to cover the elevated energy costs caused by the nanoparticle exposure in marine mussels, while the lipid breakdown might contribute under the conditions of extreme energy demand such as during the combined exposures to high temperature and nanopollutants. The total amount of available energy (Ea) decreased in the tissue of the mussels exposed to 100 µg l⁻¹ of nZnO in both seasons and acclimation temperatures reflecting depletion of carbohydrates and lipids.

The protein content of *M. edulis* tissues remained stable during all exposures to Zn²⁺ and nZnO, regardless of the season and acclimation temperature. These findings are consistent with the notion that the proteins are used as a last-resort fuel during extreme energy demand (Albentosa et al., 2007; Haider et al., 2018). In the freshwater mussels, *U. tumidus*, high concentrations of nZnO (250 µg l⁻¹) led to a slight but significant decrease in the protein content of the gills and the digestive gland, but this response varied between different mussel populations (Falfushynska et al., 2019b). Overall, protein catabolism does not appear a major energy source under the environmentally relevant nZnO exposures in bivalves thus indicating that these exposures do not elicit extremely high energy demand.

The mitochondrial ETS activity reflects the amount and functional activity of the mitochondria and can serve as an index of both the tissue energy demand and ATP synthesis capacity (Fanslow et al., 2001; Ivanina et al., 2012, 2016; Kurochkin et al., 2011). In our present study, the whole-body ETS activity of the mussels decreased in a concentration-dependent manner in nZnO and Zn²⁺ exposures at 15 and 20 °C, indicating a decline in the capacity for ATP synthesis. Given that the ETS activities of isolated mitochondria of mussels were relatively insensitive to nZnO and Zn²⁺ exposures (Table 4), these changes in the whole-body ETS capacity likely reflect a decline in the mitochondrial abundance. A decrease in ETS activity was also found in the freshwater mussels *U. tumidus* exposed to 250 µg l⁻¹ nZnO (Falfushynska et al., 2019b) and in oysters *Crassostrea gigas* exposed to 4 mg l⁻¹ nZnO (Trevisan et al., 2014). Trace metals including Zn²⁺ are toxic to animal mitochondria (Lemire et al., 2008), and Zn²⁺ release was proposed as a mechanism of the mitochondrial toxicity of nZnO (Chevallet et al., 2016). However, in our present study no major Zn accumulation or induction of metallothioneins was found during nZnO or Zn²⁺ exposures indicating that an increase in intracellular Zn²⁺ is not

likely to explain the observed suppression of ETS activity in the mussels. Other mechanisms (such as direct interactions of nZnO with mitochondria or secondary ROS-dependent damage to ETS complexes) might contribute to the mitochondrial dysfunction in nZnO and Zn²⁺ exposed mussels and require further investigation.

It is worth noting that an integrative index of the energy status, CEA, appeared less sensitive as an indicator of nZnO-induced stress than the levels of energy reserves and ETS activity considered separately. In earlier studies, both increases and decreases of CEA in response to elevated temperature and pollutant exposures have been reported in aquatic invertebrates (DeCoen and Janssen, 1997; Erk et al., 2008, 2011; Gomes et al., 2015; Smolders et al., 2003; Verheyen and Stoks, 2020; Verslycke et al., 2004b). In our present study, elevated CEA was found in the warm-acclimated winter mussels (reflecting higher levels of energy reserves) and in the warm-acclimated summer mussels exposed to 100 µg l⁻¹ nZnO (reflecting suppressed ETS activity). Depletion of energy reserves found in the mussels exposed to 100 µg l⁻¹ nZnO was not reflected in the CEA because of the concomitant decrease in ETS activity. This indicates that CEA should be used with caution because opposing changes in Ea and ETS activity might mask the stressor effects on the energy status.

Environmental temperature is an important factor affecting energy homeostasis of marine bivalves (Sokolova, 2013; Sokolova et al., 2011). Our present study shows that the temperature is the dominant factor affecting the bioenergetic markers profiles in *M. edulis*, as shown by the PCA analysis where most of the studied bioenergetic traits had high loadings on the 1st principal component separating the groups of mussels acclimated at different temperatures. In bivalves, the availability of energy reserves can be affected by temperature (Andrade et al., 2019; Falfushynska et al., 2019b; Scott-Fordsmann and Weeks, 2000). In our present study, the protein and lipid content as well as the total energy reserves increased in the mussels exposed to warming (15 °C) in winter but decreased in response to warming (20 °C) in summer. This indicates that the effects of warming on *M. edulis* differ between the seasons with the winter warming having beneficial, and summer warming – deleterious effects. Similarly, *M. edulis* exposed to 22 °C showed a decrease in the glycogen content compared to their counterparts maintained at 16 °C (Clements et al., 2018). Previous studies showed that most populations of *M. edulis* occur at the seawater temperatures <20 °C, and none persist at the sea surface temperature >23 °C (Fly and Hilbish, 2013; Fly et al., 2015). Therefore, 20 °C can be considered close to the ecological tolerance limit for the European *M. edulis*. This hypothesis is supported by the observation that oxygen consumption rates of *M. edulis* from the same population as used in our present study were suppressed by the temperatures >22 °C (Falfushynska et al., 2019a).

Our present study shows that despite high general stress tolerance of a eurybiont marine bivalve such as *M. edulis*, environmentally relevant concentrations of nZnO have negative impacts of bioenergetics of these organisms. A predicted increase in the seawater temperature combined with nZnO pollution might negatively affect the Baltic Sea mussels in summer which is a critical period for the temperate mussel populations when reproduction takes place (Gosling, 1992; Kijewski et al., 2011). With the rapidly increasing industrial production of nanoparticles, their toxic effects on marine organisms including mussels will continue to rise and require protective measures to limit the inputs of nanopollutants and mitigate their effects on marine ecosystems.

Declaration of competing interest

The authors declare that they have no known competing financial interests or personal relationships that could have

appeared to influence the work reported in this paper.

Acknowledgements

This work was in part supported by the China Scholarship Council (CSC) to FW, by the Research Training Group 'Baltic TRANSCOAST' funded by the DFG (Deutsche Forschungsgemeinschaft) under grant number GRK 2000 to IMS, and by the funding line Strategic Networks of the Leibniz Association within the scope of the Leibniz ScienceCampus Phosphorus Research Rostock (www.sciencecampus-rostock.de) to ES and IMS. We thank Fei Ye and Joydeep Dutta (KTH Royal Institute of Technology, Sweden) for their assistance with the nanoparticle characterization, and Mirza Nusrat Noor for the help with ETS testing. The project metadata are submitted to PANGAEA® Data Publisher open access database. This is Baltic TRANSCOAST publication no. GRK 2000/000X*.

Appendix A. Supplementary data

Supplementary data to this article can be found online at <https://doi.org/10.1016/j.chemosphere.2020.127780>.

Authors' contributions

FW - conceptualization, Methodology, Investigation, Data curation, Validation, Visualization, Formal analysis, Funding acquisition, Writing - original draft, writing -review & editing; EPS - methodology, Investigation, Data curation, Validation, Funding acquisition, Writing - review & editing; OD - methodology, Investigation, Data curation, Validation, Writing - review & editing; IMS - conceptualization, Methodology, Visualization, Formal analysis, Supervision, Resources, Funding acquisition, Writing - review & editing.

References

- Albentosa, M., Fernandez-Reiriz, M.J., Labarta, U., Perez-Camacho, A., 2007. Response of two species of clams, *Ruditapes decussatus* and *Venerupis pullastra*, to starvation: physiological and biochemical parameters. *Comp. Biochem. Physiol. B Biochem. Mol. Biol.* 146, 241–249.
- Andrade, M., De Marchi, L., Pretti, C., Chiellini, F., Morelli, A., Figueira, E., Rocha, R.J.M., Soares, A., Freitas, R., 2019. The impacts of warming on the toxicity of carbon nanotubes in mussels. *Mar. Environ. Res.* 145, 11–21.
- Ansar, S., Abudawood, M., Hamed, S.S., Aleem, M.M., 2017. Exposure to zinc oxide nanoparticles induces neurotoxicity and proinflammatory response: amelioration by hesperidin. *Biol. Trace Elem. Res.* 175, 360–366.
- Attia, H., Nounou, H., Shalaby, M., 2018. Zinc oxide nanoparticles induced oxidative DNA damage, inflammation and apoptosis in rat's brain after oral exposure. *Toxics* 6.
- Bagwe, R., Beniash, E., Sokolova, I.M., 2015. Effects of cadmium exposure on critical temperatures of aerobic metabolism in eastern oysters *Crassostrea virginica* (Gmelin, 1791). *Aquat. Toxicol.* 167, 77–89.
- Berenbaum, M.R., Zangerl, A.R., 1994. Costs of inducible defense: protein limitation, growth, and detoxification in *parsnip webworms*. *Ecology* 75, 2311–2317.
- Beyer, J., Green, N.W., Brooks, S., Allan, I.J., Ruus, A., Gomes, T., Brate, L.L.N., Schoyen, M., 2017. Blue mussels (*Mytilus edulis* spp.) as sentinel organisms in coastal pollution monitoring: a review. *Mar. Environ. Res.* 130, 338–365.
- Bondarenko, O., Juganson, K., Ivask, A., Kasemets, K., Mortimer, M., Kahru, A., 2013. Toxicity of Ag, CuO and ZnO nanoparticles to selected environmentally relevant test organisms and mammalian cells in vitro: a critical review. *Arch. Toxicol.* 87, 1181–1200.
- Bricker, S., Lauenstein, G., Maruya, K., 2014. NOAA's Mussel Watch Program: incorporating contaminants of emerging concern (CECs) into a long-term monitoring program. *Mar. Pollut. Bull.* 81, 289–290.
- Buffet, P.E., Amiard-Triquet, C., Dybowska, A., Riso-de Faverney, C., Guibolini, M., Valsami-Jones, E., Mouneyrac, C., 2012. Fate of isotopically labeled zinc oxide nanoparticles in sediment and effects on two endobenthic species, the clam *Scrobicularia plana* and the ragworm *Hediste diversicolor*. *Ecotoxicol. Environ. Saf.* 84, 191–198.
- Chae, Y., An, Y.-J., 2017. Effects of micro- and nanoplastics on aquatic ecosystems: current research trends and perspectives. *Mar. Pollut. Bull.* 124, 624–632. <https://doi.org/10.1016/j.marpolbul.2017.01.070>.
- Cherkasov, A.S., Taylor, C., Sokolova, I.M., 2010. Seasonal variation in mitochondrial responses to cadmium and temperature in eastern oysters *Crassostrea virginica* (Gmelin) from different latitudes. *Aquat. Toxicol.* 97, 68–78.
- Chevallet, M., Gallet, B., Fuchs, A., Jouneau, P.H., Um, K., Mintz, E., Michaud-Soret, I., 2016. Metal homeostasis disruption and mitochondrial dysfunction in hepatocytes exposed to sub-toxic doses of zinc oxide nanoparticles. *Nanoscale* 8, 18495–18506.
- Clements, J.C., Hicks, C., Tremblay, R., Comeau, L.A., 2018. Elevated seawater temperature, not pCO₂, negatively affects post-spawning adult mussels (*Mytilus edulis*) under food limitation. *Conservation physiology* 6, cox078–cox078.
- Coll, C., Notter, D., Gottschalk, F., Sun, T.Y., Som, C., Nowack, B., 2016. Probabilistic environmental risk assessment of five nanomaterials (nano-TiO₂, nano-Ag, nano-ZnO, CNT, and fullerenes). *Nanotoxicology* 10, 436–444.
- Davis, S.R., Cousins, R.J., 2000. Metallothionein expression in animals: a physiological perspective on function. *J. Nutr.* 130, 1085–1088.
- De Coen, W.M., Janssen, C.R., 2003. The missing biomarker link: relationships between effects on the cellular energy allocation biomarker of toxicant-stressed *Daphnia magna* and corresponding population characteristics. *Environ. Toxicol. Chem.* 22, 1632–1641.
- De Marchi, L., Neto, V., Pretti, C., Figueira, E., Chiellini, F., Morelli, A., Soares, A., Freitas, R., 2017. The impacts of seawater acidification on *Ruditapes philippinarum* sensitivity to carbon nanoparticles. *Environmental Science-Nano* 4, 1692–1704.
- DeCoen, W.M., Janssen, C.R., 1997. The use of biomarkers in *Daphnia magna* toxicity testing. 2. Digestive enzyme activity in *Daphnia magna* exposed to sublethal concentrations of cadmium, chromium and mercury. *Chemosphere* 35, 1053–1067.
- Dellwig, O., Wegwerth, A., Schnetger, B., Schulz, H., Arz, H.W., 2019. Dissimilar behaviors of the geochemical twins W and Mo in hypoxic-euxinic marine basins. *Earth Sci. Rev.* 193, 1–23.
- Erk, M., Ivankovic, D., Strizak, Z., 2011. Cellular energy allocation in mussels (*Mytilus galloprovincialis*) from the stratified estuary as a physiological biomarker. *Mar. Pollut. Bull.* 62, 1124–1129.
- Erk, M., Muysen, B.T.A., Ghekiere, A., Janssen, C.R., 2008. Metallothionein and cellular energy allocation in the estuarine mysid shrimp *Neomysis integer* exposed to cadmium at different salinities. *J. Exp. Mar. Biol. Ecol.* 357, 172–180.
- Estabrook, R.W., 1967. Mitochondrial respiratory control and the polarographic measurements in mitochondria. *Methods Enzymol.* 10, 41–47.
- Fabrega, J., Tantra, R., Amer, A., Stolpe, B., Tomkins, J., Fry, T., Lead, J.R., Tyler, C.R., Galloway, T.S., 2012. Sequestration of zinc from zinc oxide nanoparticles and life cycle effects in the sediment dweller amphipod *Corophium volutator*. *Environ. Sci. Technol.* 46, 1128–1135.
- Falfushynska, H., Gnatyshyna, L., Horyn, O., Sokolova, I., Stoliar, O., 2017. Endocrine and cellular stress effects of zinc oxide nanoparticles and nifedipine in marsh frogs *Pelophylax ridibundus*. *Aquat. Toxicol.* 185, 171–182.
- Falfushynska, H., Gnatyshyna, L., Yurchak, I., Sokolova, I., Stoliar, O., 2015. The effects of zinc nanooxide on cellular stress responses of the freshwater mussels *Unio tumidus* are modulated by elevated temperature and organic pollutants. *Aquat. Toxicol.* 162, 82–93.
- Falfushynska, H., Sokolova, E.P., Haider, F., Oppermann, C., Kragl, U., Ruth, W., Stock, M., Glufke, S., Winkel, E.J., Sokolova, I.M., 2019a. Effects of a common pharmaceutical, atorvastatin, on energy metabolism and detoxification mechanisms of a marine bivalve *Mytilus edulis*. *Aquat. Toxicol.* 208, 47–61.
- Falfushynska, H.I., Gnatyshyna, L.L., Ivanina, A.V., Khoma, V.V., Stoliar, O.B., Sokolova, I.M., 2019b. Bioenergetic responses of freshwater mussels *Unio tumidus* to the combined effects of nano-ZnO and temperature regime. *Sci. Total Environ.* 650, 1440–1450.
- Falfushynska, H.I., Wu, F.L., Ye, F., Kasianchuk, N., Dutta, J., Dobretsov, S., Sokolova, I.M., 2019c. The effects of ZnO nanostructures of different morphology on bioenergetics and stress response biomarkers of the blue mussels *Mytilus edulis*. *Sci. Total Environ.* 694.
- Fanslow, D.L., Nalepa, T.F., Johengen, T.H., 2001. Seasonal changes in the respiratory electron transport system (ETS) and respiration of the zebra mussel, *Dreissena polymorpha* in Saginaw Bay, Lake Huron. *Hydrobiologia* 448, 61–70.
- Fly, E.K., Hilbish, T.J., 2013. Physiological energetics and biogeographic range limits of three congeneric mussel species. *Oecologia* 172, 35–46.
- Fly, E.K., Hilbish, T.J., Wetthey, D.S., Rognstad, R.L., 2015. Physiology and biogeography: the response of European mussels (*Mytilus* spp.) to climate change. *Am. Malacol. Bull.* 33, 136–149.
- Gagne, F., Auclair, J., Trepanier, S., Turcotte, P., Pilote, M., Gagnon, C., 2016. The impact of zinc oxide nanoparticles in freshwater mussels exposed to municipal effluents. *Isj-Invertebrate Survival Journal* 13, 281–290.
- Gagne, F., Auclair, J., Turcotte, P., Gagnon, C., Peyrot, C., Wilkinson, K., 2019. The influence of surface waters on the bioavailability and toxicity of zinc oxide nanoparticles in freshwater mussels. *Comparative Biochemistry and Physiology C-Toxicology & Pharmacology* 219, 1–11.
- Garner, K.L., Keller, A.A., 2014. Emerging patterns for engineered nanomaterials in the environment: a review of fate and toxicity studies. *J. Nanoparticle Res.* 16, 28.
- Gnaiger, E., 1983. Calculation of energetic and biochemical equivalents of respiratory oxygen consumption. In: Gnaiger, E., Forstner, H. (Eds.), *Polarographic Oxygen Sensors*. Springer Berlin Heidelberg, Berlin, Heidelberg, pp. 337–345.
- Gnaiger, E., 2012. Mitochondrial Pathways and Respiratory Control: an Introduction to OXPHOS Analysis. *Mitochondrial Physiological Network (MiPNet)* 17.18, *OROBOROS MiPNet Publications 2012*. Innsbruck, pp. 1–64. Open access: <http://>

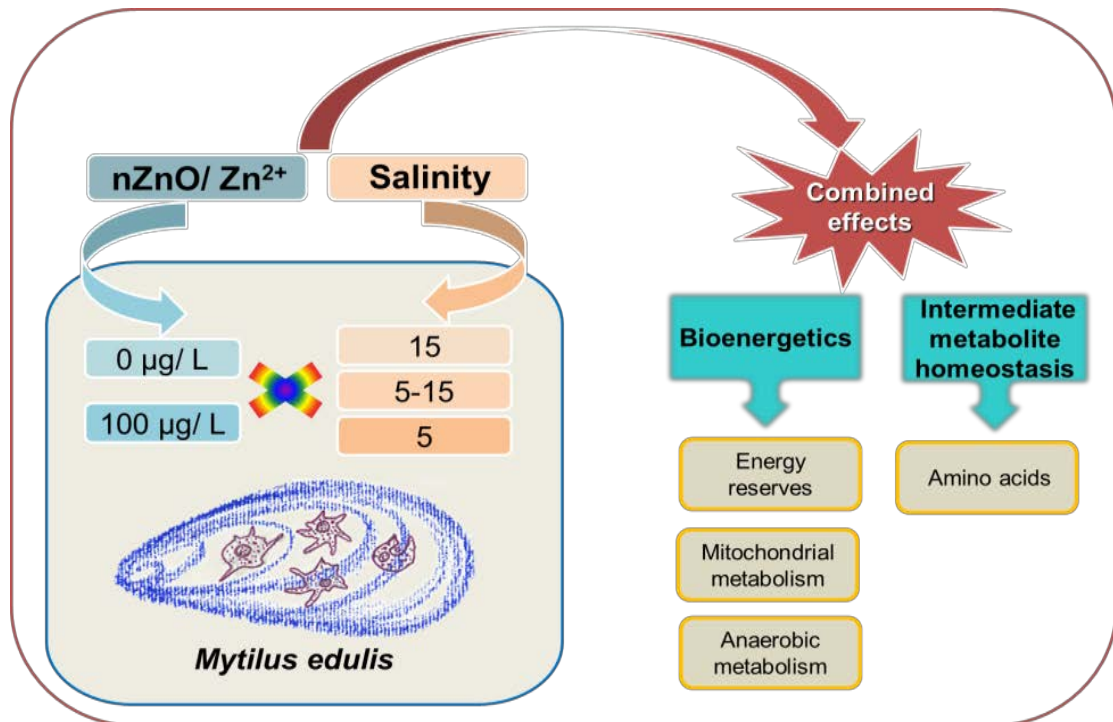
- www.bioblast.at/index.php/Gnaiger_2012_MitoPathways.
- Gomes, S.I.L., Scott-Fordsmand, J.J., Amorim, M.J.B., 2015. Cellular energy allocation to assess the impact of nanomaterials on soil invertebrates (enchytraeids): the effect of Cu and Ag. *Int. J. Environ. Res. Publ. Health* 12, 6858–6878.
- Gosling, E.M., 1992. *The Mussel Mytilus: Ecology, Physiology, Genetics, and Culture*. Elsevier, Amsterdam, New York.
- Haider, F., Sokolov, E.P., Sokolova, I.M., 2018. Effects of mechanical disturbance and salinity stress on bioenergetics and burrowing behavior of the soft-shell clam *Mya arenaria*. *J. Exp. Biol.* 221.
- Hallman, T.A., Brooks, M.L., 2016. Metal-mediated climate susceptibility in a warming world: larval and latent effects on a model amphibian. *Environ. Toxicol. Chem.* 35, 1872–1882.
- Hanna, S.K., Miller, R.J., Muller, E.B., Nisbet, R.M., Lenihan, H.S., 2013. Impact of engineered zinc oxide nanoparticles on the individual performance of *Mytilus galloprovincialis*. *PLoS One* 8, 7.
- Heugens Eh, T., J. R., C. H., K. M., J. H.A., M. V.S.N., W. A., 2003. Temperature-dependent effects of cadmium on *Daphnia magna*: accumulation versus sensitivity. *Environ. Sci. Technol.* 37, 2145–2151.
- Holmstrup, M., Bindsbol, A.M., Oostingh, G.J., Duschl, A., Scheil, V., Kohler, H.R., Loureiro, S., Soares, A., Ferreira, A.L.G., Kienle, C., et al., 2010. Interactions between effects of environmental chemicals and natural stressors: a review. *Sci. Total Environ.* 408, 3746–3762.
- Hu, M., Lin, D., Shang, Y., Hu, Y., Lu, W., Huang, X., Ning, K., Chen, Y., Wang, Y., 2017. CO₂-induced pH reduction increases physiological toxicity of nano-TiO₂ in the mussel *Mytilus coruscus*. *Sci. Rep.* 7, 40015–40015.
- Ioannou, S., Anestis, A., P'rtner, H.O., Michaelidis, B., 2009. Seasonal patterns of metabolism and the heat shock response (HSR) in farmed mussels *Mytilus galloprovincialis*. *J. Exp. Mar. Biol. Ecol.* 381, 136–144.
- IPCC, 2013. *Climate Change 2013: the Physical Science Basis*.
- IPCC, 2014. *Climate change 2014: synthesis report*. In: Contribution of Working Groups I, II and III to the Fifth Assessment Report of the Intergovernmental Panel on Climate Change.
- Ivanina, A.V., Kurochkin, I.O., Leamy, L., Sokolova, I.M., 2012. Effects of temperature and cadmium exposure on the mitochondria of oysters (*Crassostrea virginica*) exposed to hypoxia and subsequent reoxygenation. *J. Exp. Biol.* 215, 3142–3154.
- Ivanina, A.V., Nesmelova, I., Leamy, L., Sokolov, E.P., Sokolova, I.M., 2016. Intermittent hypoxia leads to functional reorganization of mitochondria and affects cellular bioenergetics in marine molluscs. *J. Exp. Biol.* 219, 1659–1674.
- Katsikatsou, M., Anestis, A., Poertner, H.-O., Vratisstas, A., Aligizaki, K., Michaelidis, B., 2012. Field studies and projections of climate change effects on the bearded horse mussel *Modiolus barbatus* in the Gulf of Thermaikos, Greece. *Mar. Ecol. Prog. Ser.* 449, 183–196.
- Khlebovich, V.V., 2017. Acclimation of animal organisms: basic theory and applied aspects. *Biology Bulletin Reviews* 7, 279–286.
- Kijewski, T., Smietanka, B., Zbawicka, M., Gosling, E., Hummel, H., Wenne, R., 2011. Distribution of *Mytilus* taxa in European coastal areas as inferred from molecular markers. *J. Sea Res.* 65, 224–234.
- Kong, H., Wu, F., Jiang, X., Wang, T., Hu, M., Chen, J., Huang, W., Bao, Y., Wang, Y., 2019. Nano-TiO₂ impairs digestive enzyme activities of marine mussels under ocean acidification. *Chemosphere* 237, 124561.
- Kumar, N., Chandan, N.K., Wakchaure, G.C., Singh, N.P., 2020. Synergistic effect of zinc nanoparticles and temperature on acute toxicity with response to biochemical markers and histopathological attributes in fish. *Comp. Biochem. Physiol. C Toxicol. Pharmacol.* 229, 108678.
- Kurochkin, I.O., Etkorn, M., Buchwalter, D., Leamy, L., Sokolova, I.M., 2011. Top-down control analysis of the cadmium effects on molluscan mitochondria and the mechanisms of cadmium-induced mitochondrial dysfunction. *Am. J. Physiol. Regul. Integr. Comp. Physiol.* 300, R21–R31.
- Lagerstrom, M.E., Field, M.P., Seguret, M., Fischer, L., Hann, S., Sherrell, R.M., 2013. Automated on-line flow-injection ICP-MS determination of trace metals (Mn, Fe, Co, Ni, Cu and Zn) in open ocean seawater: application to the GEOTRACES program. *Mar. Chem.* 155, 71–80.
- Lemire, J., Mailloux, R., Appanna, V.D., 2008. Zinc toxicity alters mitochondrial metabolism and leads to decreased ATP production in hepatocytes. *J. Appl. Toxicol.* 28, 175–182.
- Li, J.J., Schiavo, S., Dong, X.L., Rametta, G., Miglietta, M.L., Oliviero, M., Wu, C.W., Manzo, S., 2018. Early ecotoxic effects of ZnO nanoparticle chronic exposure in *Mytilus galloprovincialis* revealed by transcription of apoptosis and antioxidant-related genes. *Ecotoxicology* 27, 369–384.
- Múgica, M., Sokolova, I.M., Izagirre, U., Marigómez, I., 2015. Season-dependent effects of elevated temperature on stress biomarkers, energy metabolism and gamete development in mussels. *Mar. Environ. Res.* 103, 1–10.
- Marigómez, I., Múgica, M., Izagirre, U., Sokolova, I.M., 2017. Chronic environmental stress enhances tolerance to seasonal gradual warming in marine mussels. *PLoS One* 12, e0174359.
- Marisa, I., Matozzo, V., Munari, M., Binelli, A., Parolini, M., Martucci, A., Franceschini, E., Brianese, N., Marin, M.G., 2016. In vivo exposure of the marine clam *Ruditapes philippinarum* to zinc oxide nanoparticles: responses in gills, digestive gland and haemolymph. *Environ. Sci. Pollut. Res. Int.* 23, 15275–15293.
- Masuko, T., Minami, A., Iwasaki, N., Majima, T., Nishimura, S.I., Lee, Y.C., 2005. Carbohydrate analysis by a phenol-sulfuric acid method in microplate format. *Anal. Biochem.* 339, 69–72.
- Mathiesen, S.S., Thyrring, J., Hemmer-Hansen, J., Berge, J., Sukhotin, A., Leopold, P., Bekaert, M., Sejr, M.K., Nielsen, E.E., 2017. Genetic diversity and connectivity within *Mytilus* spp. in the subarctic and Arctic. *Evolutionary Applications* 10, 39–55.
- Mos, B., Kaposi, K.L., Rose, A.L., Kelaher, B., Dworjanyn, S.A., 2017. Moderate ocean warming mitigates, but more extreme warming exacerbates the impacts of zinc from engineered nanoparticles on a marine larva. *Environ. Pollut.* 228, 190–200.
- Muller, E.B., Hanna, S.K., Lenihan, H.S., Miller, R., Nisbet, R.M., 2014. Impact of engineered zinc oxide nanoparticles on the energy budgets of *Mytilus galloprovincialis*. *J. Sea Res.* 94, 29–36.
- Nardi, A., Mincarelli, L.F., Benedetti, M., Fattorini, D., d'Errico, G., Regoli, F., 2017. Indirect effects of climate changes on cadmium bioavailability and biological effects in the Mediterranean mussel *Mytilus galloprovincialis*. *Chemosphere* 169, 493–502.
- Rocha, T.L., Gomes, T., Sousa, V.S., Mestre, N.C., Bebianno, M.J., 2015. Ecotoxicological impact of engineered nanomaterials in bivalve molluscs: an overview. *Mar. Environ. Res.* 111, 74–88.
- Ruttikay-Nedecky, B., Nejdil, L., Gumulec, J., Zitka, O., Masarik, M., Eckschlager, T., Stiborova, M., Adam, V., Kizek, R., 2013. The role of metallothionein in oxidative stress. *Int. J. Mol. Sci.* 14, 6044–6066.
- Saggese, I., Sarà, G., Dondero, F., 2016. Silver nanoparticles affect functional bioenergetic traits in the invasive red sea mussel *brachidontes pharaonis*. *BioMed Res. Int.* 1872351. <https://doi.org/10.1155/2016/1872351>.
- Saidani, W., Sellami, B., Khazri, A., Mezni, A., Dellali, M., Joubert, O., Sheehan, D., Beyrem, H., 2019. Metal accumulation, biochemical and behavioral responses on the Mediterranean clams *Ruditapes decussatus* exposed to two photocatalyst nanocomposites (TiO₂ NPs and AuTiO₂NPs). *Aquat. Toxicol.* 208, 71–79.
- Scott-Fordsmand, J.J., Weeks, J.M., 2000. Biomarkers in earthworms. In: Ware, G.W. (Ed.), *Reviews of Environmental Contamination and Toxicology*, vol. 165, pp. 117–159 vol. 165.
- Shang, Y., Wu, F., Wei, S., Guo, W., Chen, J., Huang, W., Hu, M., Wang, Y., 2020. Specific dynamic action of mussels exposed to TiO₂ nanoparticles and seawater acidification. *Chemosphere* 241, 125104.
- Smolders, R., De Boeck, G., Blust, R., 2003. Changes in cellular energy budget as a measure of whole effluent toxicity in zebrafish (*Danio rerio*). *Environ. Toxicol. Chem.* 22, 890–899.
- Sohrin, Y., Urushihara, S., Nakatsuka, S., Kono, T., Higo, E., Minami, T., Norisuye, K., Umetani, S., 2008. Multielemental determination of GEOTRACES key trace metals in seawater by ICP-MS after preconcentration using an ethylenediaminetetraacetic acid chelating resin. *Anal. Chem.* 80, 6267–6273.
- Sokolova, I.M., 2004. Cadmium effects on mitochondrial function are enhanced by elevated temperatures in a marine poikilotherm, *Crassostrea virginica* Gmelin (*Bivalvia: ostreidae*). *J. Exp. Biol.* 207, 2639–2648.
- Sokolova, I.M., 2013. Energy-limited tolerance to stress as a conceptual framework to integrate the effects of multiple stressors. *Integr. Comp. Biol.* 53, 597–608.
- Sokolova, I.M., Frederick, M., Bagwe, R., Lannig, G., Sukhotin, A.A., 2012. Energy homeostasis as an integrative tool for assessing limits of environmental stress tolerance in aquatic invertebrates. *Mar. Environ. Res.* 79, 1–15.
- Sokolova, I.M., Lannig, G., 2008. Interactive effects of metal pollution and temperature on metabolism in aquatic ectotherms: implications of global climate change. *Clim. Res.* 37, 181–201.
- Sokolova, I.M., Sukhotin, A.A., Lannig, G., 2011. Stress effects on metabolism and energy budgets in mollusks. In: Abele, D., Zenteno-Savin, T., Vazquez-Medina, J. (Eds.), *Oxidative Stress in Aquatic Ecosystems*. Blackwell Wiley, Boston etc., pp. 263–280.
- Somero, G.N., Lockwood, B.L., Tomanek, L., 2016. *Biochemical Adaptation: Response to Environmental Challenges, from Life's Origins to the Anthropocene*.
- Thompson, E.L., Taylor, D.A., Nair, S.V., Birch, G., Coleman, R., Raftos, D.A., 2012. Optimal acclimation periods for oysters in laboratory-based experiments. *J. Molluscan Stud.* 78, 304–307.
- Trevisan, R., Delapiedra, G., Mello, D.F., Arl, M., Schmidt, E.C., Meder, F., Monopoli, M., Cargnin-Ferreira, E., Bouzon, Z.L., Fisher, A.S., et al., 2014. Gills are an initial target of zinc oxide nanoparticles in oysters *Crassostrea gigas*, leading to mitochondrial disruption and oxidative stress. *Aquat. Toxicol.* 153, 27–38.
- Van Handel, E., 1985. Rapid determination of total lipids in mosquitoes. *J. Am. Mosq. Contr. Assoc.* 1, 302–304.
- Verheyen, J., Stoks, R., 2020. Negative bioenergetic responses to pesticides in damselfly larvae are more likely when it is hotter and when temperatures fluctuate. *Chemosphere* 243, 125369.
- Verslycke, T., Roast, S.D., Widdows, J., Jones, M.B., Janssen, C.R., 2004a. Cellular energy allocation and scope for growth in the estuarine mysid *Neomysis integer* (Crustacea: mysidacea) following chlorpyrifos exposure: a method comparison. *J. Exp. Mar. Biol. Ecol.* 306, 1–16.
- Verslycke, T., Roast, S.D., Widdows, J., Jones, M.B., Janssen, C.R., 2004b. Cellular energy allocation and scope for growth in the estuarine mysid *Neomysis integer* (Crustacea: mysidacea) following chlorpyrifos exposure: a method comparison. *J. Exp. Mar. Biol. Ecol.* 306, 1–16.
- Viarengo, A., Ponzano, E., Dondero, F., Fabbri, R., 1997. A simple spectrophotometric method for metallothionein evaluation in marine organisms: an application to Mediterranean and Antarctic molluscs. *Mar. Environ. Res.* 44, 69–84.
- Wang, H., Ye, J.P., 2015. Regulation of energy balance by inflammation: common theme in physiology and pathology. *Rev. Endocr. Metab. Disord.* 16, 47–54.
- Williams, R.J., Harrison, S., Keller, V., Kuenen, J., Loftis, S., Praetorius, A., Svendsen, C., Vermeulen, L.C., van Wijnen, J., 2019. Models for assessing engineered nanomaterial fate and behaviour in the aquatic environment. *Current Opinion in Environmental Sustainability* 36, 105–115.

- Wu, F., Falfushynska, H., Dellwig, O., Piontkivska, H., Sokolova, I.M., 2020. Interactive effects of salinity variation and exposure to ZnO nanoparticles on the innate immune system of a sentinel marine bivalve, *Mytilus edulis*. *Sci. Total Environ.* 712, 136473.
- Wu, F.L., Cui, S.K., Sun, M., Xie, Z., Huang, W., Huang, X.Z., Liu, L.P., Hu, M.H., Lu, W.Q., Wang, Y.J., 2018. Combined effects of ZnO NPs and seawater acidification on the haemocyte parameters of thick shell mussel & *Mytilus coruscus*. *Sci. Total Environ.* 624, 820–830.
- Yin, X., Zhou, S.S., Zheng, Y., Tan, Y., Kong, M.Y., Wang, B., Feng, W.K., Epstein, P.N., Cai, J., Cai, L., 2014. Metallothionein as a compensatory component prevents intermittent hypoxia-induced cardiomyopathy in mice. *Toxicol. Appl. Pharmacol.* 277, 58–66.
- Yung, M.M.N., Kwok, K.W.H., Djurišić, A.B., Giesy, J.P., Leung, K.M.Y., 2017. Influences of temperature and salinity on physicochemical properties and toxicity of zinc oxide nanoparticles to the marine diatom *Thalassiosira pseudonana*. *Sci. Rep.* 7, 3662.
- Yung, M.M.N., Mouneyrac, C., Leung, K.M.Y., 2014. Ecotoxicity of zinc oxide nanoparticles in the marine environment. In: Bhushan, B. (Ed.), *Encyclopedia of Nanotechnology*. Springer Netherlands, Dordrecht, pp. 1–17.

7.4. Salinity-dependent effects of ZnO nanoparticles on bioenergetics and intermediate metabolite homeostasis in a euryhaline marine bivalve, *Mytilus edulis*

Noor, M. N, Wu, F, Sokolov, E. P, Falfushynska, H, Timm, S, Haider, F. and Sokolova, I. M. (2021). Science of The Total Environment 774, 145195

DOI: <https://doi.org/10.1016/j.scitotenv.2021.145195>





Salinity-dependent effects of ZnO nanoparticles on bioenergetics and intermediate metabolite homeostasis in a euryhaline marine bivalve, *Mytilus edulis*

Mirza Nusrat Noor^{a,1}, Fangli Wu^{a,1}, Eugene P. Sokolov^b, Halina Falfushynska^{a,c}, Stefan Timm^d, Fouzia Haider^a, Inna M. Sokolova^{a,e,*}

^a Department of Marine Biology, Institute for Biological Sciences, University of Rostock, Rostock, Germany

^b Leibniz Institute for Baltic Sea Research, Leibniz Science Campus Phosphorus Research, Warnemünde, Rostock, Germany

^c Department of Human Health, Physical Rehabilitation and Vital Activity, Ternopil V. Hnatiuk National Pedagogical University, Ternopil, Ukraine

^d Department of Plant Physiology, University of Rostock, Rostock, Germany

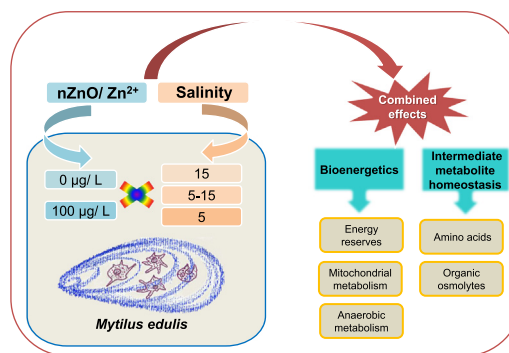
^e Department of Maritime Systems, Interdisciplinary Faculty, University of Rostock, Rostock, Germany



HIGHLIGHTS

- Combined effects of nZnO and salinity stress have been investigated in mussels.
- Exposure to nZnO had weak effects on energy or intermediate metabolite homeostasis.
- Zn²⁺ was metabolically more damaging to the Baltic Sea mussels than nZnO.
- Fluctuating salinity (5–15) was bioenergetically less stressful than low salinity (5).
- The biological effects of nZnO and Zn²⁺ became less detectable under salinity stress.

GRAPHICAL ABSTRACT



ARTICLE INFO

Article history:

Received 29 November 2020

Received in revised form 2 January 2021

Accepted 10 January 2021

Available online 11 February 2021

Editor: Julian Blasco

Keywords:

Nanopollutants
Osmotic stress
Stressor interactions
Cell volume regulation
Bioenergetics
Mitochondrial function

ABSTRACT

Engineered nanoparticles including ZnO nanoparticles (nZnO) are important emerging pollutants in aquatic ecosystems creating potential risks to coastal ecosystems and associated biota. The toxicity of nanoparticles and its interaction with the important environmental stressors (such as salinity variation) are not well understood in coastal organisms and require further investigation. Here, we examined the interactive effects of 100 µg l⁻¹ nZnO or dissolved Zn (as a positive control for Zn²⁺ release) and salinity (normal 15, low 5, and fluctuating 5–15) on bioenergetics and intermediate metabolite homeostasis of a keystone marine bivalve, the blue mussel *Mytilus edulis* from the Baltic Sea. nZnO exposures did not lead to strong disturbances in energy or intermediate metabolite homeostasis regardless of the salinity regime. Dissolved Zn exposures suppressed the mitochondrial ATP synthesis capacity and coupling as well as anaerobic metabolism and modified the free amino acid profiles in the mussels indicating that dissolved Zn is metabolically more damaging than nZnO. The environmental salinity regime strongly affected metabolic homeostasis and altered physiological and biochemical responses to nZnO or dissolved Zn in the mussels. Exposure to low (5) or fluctuating (5–15) salinity affected the physiological condition, energy metabolism and homeostasis, as well as amino acid metabolism in *M. edulis*. Generally, fluctuating salinity (5–15) appeared bioenergetically less stressful than constantly hypoosmotic stress (salinity 5) in

* Corresponding author at: Department of Marine Biology, Institute for Biological Sciences, University of Rostock, Rostock, Germany.

E-mail address: inna.sokolova@uni-rostock.de (I.M. Sokolova).

¹ These authors contributed equally to the work.

M. edulis indicating that even short (24 h) periods of recovery might be sufficient to restore the metabolic homeostasis in this euryhaline species. Notably, the biological effects of nZnO and dissolved Zn became progressively less detectable as the salinity stress increased. These findings demonstrate that habitat salinity must be considered in the biomarker-based assessment of the toxic effects of nanopollutants on coastal organisms.

© 2021 Elsevier B.V. All rights reserved.

1. Introduction

Coastal ecosystems are among the most threatened ecosystems worldwide due to urbanization, pollution, global climate change and habitat degradation (Borgwardt et al., 2019; Cloern et al., 2016). A recent analysis of the integrated risks from human activities ranked chemical pollution as the highest risk for the coastal waters and biota (Borgwardt et al., 2019). Engineered nanoparticles (i.e. particles with at least one dimension <100 nm) are important emerging pollutants creating potential risks to coastal ecosystems and associated biota (Coll et al., 2016; Gottschalk et al., 2009; Piccinno et al., 2011). Nano-zinc oxide (nZnO) is a common nanomaterial with an estimated global production of 10 Mt (Stoller and Ochando-Pulido, 2020) extensively used in industry, agriculture, medicine, textiles, packaging, and cosmetics (Beegam et al., 2016; Martínez-Carmona et al., 2018; Narayanan et al., 2012). About 10% of all produced nZnO is released from the technosphere into the environment, with >95% of this amount entering the aquatic ecosystems and accumulating in the water and sediments (Gottschalk et al., 2015). Models predict that the present-day concentrations of nZnO may reach ~900 $\mu\text{g l}^{-1}$ in the European surface waters (Coll et al., 2016) and exceed 100–300 $\mu\text{g kg}^{-1}$ in the sediments (Gottschalk et al., 2015). ZnO has been classified as ecotoxic by the EU hazard classification and as a priority pollutant by the US Environmental Protection Agency (US EPA, 2002). The toxicity assessment of nZnO is based on the assumption that the toxic effects are caused by the ion shedding by nZnO (US EPA, 2002). However, recent studies indicate that nanomaterials including nZnO may display significantly different toxic mechanisms from those of dissolved metals (Falfushynska et al., 2015; Falfushynska et al., 2019b; Falfushynska et al., 2019d; Wu et al., 2020b). Furthermore, potential interactions of nanoparticle toxicity with other abiotic stressors (such as salinity, temperature, or pH) have not been extensively studied (Auffan et al., 2014; Falfushynska et al., 2015; Falfushynska et al., 2019b; Mos et al., 2017; Wu et al., 2020b; Yung et al., 2017; Yung et al., 2015). This limits our ability to understand the impacts of coastal nanopollution in the environmentally realistic contexts and adds to the uncertainty of risk assessment (Cabral et al., 2019).

Salinity variation is an important environmental stressor in estuaries, coastal areas and closed basins such as the Baltic Sea (Stigebrandt, 2001). The Baltic Sea salinity varies spatially from >20 to <1 PSU (practical salinity units) from southwest to northeast and fluctuates over time due to the variation in the saltwater influx, evaporation and precipitation (HELCOM, 2016). The Baltic Sea coast is a highly populated area receiving pollution (including nanoparticles) from multiple point-and non-point sources (Moreno and Amelung, 2009; Tovar-Sánchez et al., 2013). Benthic bivalves such as the blue mussels (*Mytilus* spp.) are important sentinel organisms to assess nanoparticle toxicity because of their global distribution, important ecological roles as ecosystem engineers and high vulnerability to nanoparticle exposure due to their suspension-feeding habits (Beyer et al., 2017). Exposures to environmentally relevant concentrations of nZnO were shown to negatively impact the physiological performance and health status of marine organisms including the blue mussels leading to bioenergetics disturbances and suppression of growth (Hanna et al., 2013; Muller et al., 2014; Wu et al., 2021), immune impairments (Wu et al., 2018; Wu et al., 2020b) and onset of the cellular damage, inflammation and apoptosis (Falfushynska et al., 2019c). Furthermore, the toxic effects of

nZnO in marine organisms can be modulated by the ambient salinity due to the direct effects of salinity on the nanoparticle properties (such as aggregation, solubility and sedimentation) (Yung et al., 2017), as well as through the interactive effects of nanoparticles and salinity on physiology of marine organisms (Auffan et al., 2014; Park et al., 2014; Wang and Wang, 2014; Wu et al., 2020b; Yung et al., 2015). However, the interactive effects of salinity and nanopollutants on the health and performance of marine organisms in the environmentally realistic contexts are not yet well understood and require further investigation.

Metabolic homeostasis plays an important role in organismal tolerance to stressors including pollutants and salinity stress (Sokolova et al., 2012; Sokolova and Lannig, 2008; Sokolova et al., 2011). Exposure to pollutants may negatively affect an organism's bioenergetics by increasing the energy demand for basal maintenance including detoxification, stress protection and damage repair, and/or by reducing the energy gain through the negative effects on feeding and metabolic conversion of food energy into ATP (Sokolova, 2013; Sokolova et al., 2011). Salinity stress can also have negative impact on energy metabolism of the mussels due to the elevated costs of intracellular osmoregulation, suppression of feeding activity and impairment of the cellular metabolism (Berger and Kharazova, 1997; Gosling, 1992; Riisgård et al., 2013). The disturbances of the energy homeostasis can have direct impacts on the physiological performance and fitness-related functions of an organism such as growth, activity or reproduction (Sokolova, 2013; Sokolova et al., 2012). Therefore, investigations of the metabolic consequences of stress exposures provide an excellent tool to link the cellular and molecular stress mechanisms to the organismal performance and thus the population-level outcomes of multiple stressors including nanopollutants and salinity stress.

The aim of the present study was to assess the interactive effects of nZnO (100 $\mu\text{g l}^{-1}$ Zn) and salinity stress on bioenergetics and intermediate metabolite homeostasis of a keystone marine bivalve, the blue mussel *Mytilus edulis*. The mussels are economically important and ecologically dominant species in the benthic ecosystem of the Baltic Sea (Gosling, 1992; Jansson and Kautsky, 1977). They are commonly exposed to pollutants (including nZnO) and salinity variations in their habitats and thus serve as an excellent model species to investigate the interactive effects of nanopollutants and salinity stress (Canesi et al., 2012; Wu et al., 2020b). Here, we hypothesized that combined exposures to nZnO and salinity stress might negatively impact the energy homeostasis of the mussels by increasing the energy demand and/or suppressing the aerobic capacity for ATP production in the mussels. We also hypothesized that nZnO exposure may affect the intermediate nitrogen metabolism of the mussels causing shifts in the organic osmolytes (such as the free amino acids) and thus interfering with intracellular osmoregulation. To test these hypotheses, we measured the tissue levels of energy reserves (lipids, carbohydrates and proteins), body condition index, and the mitochondrial aerobic capacity in the whole tissue and isolated mitochondria of the mussels. To assess whether exposure to the combined salinity and nZnO stress might result in aerobic energy deficiency and lead to the onset of anaerobic metabolism, accumulation of anaerobic end products (succinate and lactate) was determined in the mussel tissues. Tissue water content and the levels of free amino acids were measured to determine whether the osmoregulatory response to salinity shifts is negatively affected by nZnO exposures in *M. edulis*.

2. Materials and methods

2.1. Animal collection and maintenance

The adult blue mussels (shell length 5.23 ± 0.37 cm, $N = 170$) were collected in February 2019 in Warnemünde harbor area ($54^{\circ}10'49.602''$ N, $12^{\circ}05'21.991''$ E) near Rostock, Germany, and transported to University of Rostock within 2 h of collection. The Baltic Sea is a zone of introgression between two closely related groups of mussels, *M. edulis* and *M. grossulus*, and the studied population of natural hybrids has been designated *M. edulis* due to the predominance of *M. edulis* genes in its genetic makeup (Falfushynska et al., 2019a; Stuckas et al., 2017). Based on the seasonal progression of mussel gametogenesis in the studied region of the Baltic Sea (Benito et al., 2019), the mussels used in this study were expected to be at the early to advanced stages of gametogenesis. The visual inspection of the gonads during dissection (see "Tissue collection" below) confirmed the presence of gametes in the gonads of the experimental mussels, albeit the development stage of the gametes could not be determined. The mussel shells were cleaned from epibionts and acclimated for at least a week at 10°C and salinity 15. These salinity and temperature conditions were similar to the habitat conditions at the time of collection. The seawater used for the maintenance and all experimental exposures was prepared by mixing 90% of artificial seawater (Tropic Marin®) with 10% of the filtered Baltic seawater. The mussels were kept in a thermally controlled recirculated aquaria ($10.1 \pm 0.9^{\circ}\text{C}$, $N = 102$, salinity 15.6 ± 0.7 , $N = 26$) equipped with a multi-step filtration system including a moving bed biofilter, UV water treatment and protein skimmer. During the preliminary acclimation and experimental treatments, the mussels were fed ad libitum on alternate days with live phytoplankton blend containing *Nannochloropsis oculata*, *Phaeodactylum* sp. and *Chlorella* sp. (Premium Reef Blend, CoralSands, Wiesbaden, Germany).

2.2. Experimental exposures

Experimental exposure conditions were identical to those described in our earlier study (Wu et al., 2020b). Briefly, after the preliminary acclimation, mussels were randomly divided into nine groups and exposed for three weeks in 12:12 light:dark regime to different salinity and Zn conditions. A fully crossed experimental design was used with three salinity regimes (normal salinity 15; low salinity 5; and fluctuating salinity with the daily change between salinities 15 and 5), and three levels of Zn exposure including control (no Zn^{2+} or nZnO addition), nZnO or dissolved Zn corresponding to $100 \mu\text{g Zn l}^{-1}$. For fluctuating salinity, a square wave change was used as follows: 22 h at salinity 15, followed by 2 h at salinity 10, and 22 h at salinity 5. This cycle was repeated for three weeks of exposure. For each experimental treatment, five replicate tanks were used. Average salinity was 15.6 ± 0.66 ($N = 26$) for the normal salinity treatment and the high-salinity phase of the fluctuating salinity regime, and 5.22 ± 0.66 ($N = 42$) for the low salinity treatment and the low-salinity phase of the fluctuating salinity regime. Commercial ZnO nanoparticles (nZnO) (average particle size 30 nm) were purchased from Sigma-Aldrich Sweden AB (Stockholm, Sweden). The suspensions of nanoparticles ($10 \mu\text{g ml}^{-1}$) had the following characteristics: at salinity 5, the hydrodynamic size with a major peak at 854 ± 172 nm and zeta-potential of 2.9 mV; at salinity 15, the hydrodynamic size with a major peak at 817 ± 174 nm and zeta-potential -9.6 mV (Wu et al., 2020b). A static-renewal exposure regime was used with water change and Zn supplementation every other day (except in the fluctuating salinity regime where the water was changed and Zn added daily during salinity change). Suspensions of nZnO were added to experimental water to achieve the nominal concentration of $100 \mu\text{g l}^{-1}$ Zn during every water change and maintained in suspension by vigorous aeration. For dissolved Zn exposures, $100 \mu\text{g l}^{-1}$ Zn^{2+} (as ZnSO_4) was added during every water change. All exposures were conducted at $10 \pm 1^{\circ}\text{C}$. During preliminary acclimation

and experimental exposures, mussels were fed before every water change with a commercial blend of live algae containing *Nannochloropsis oculata*, *Phaeodactylum* sp. and *Chlorella* sp. (Premium Reef Blend, CoralSands, Wiesbaden, Germany) per manufacturer's instructions. During experimental exposures, mortality was $<5\%$ in the normal and fluctuating salinity groups and $\sim 16\%$ in the low salinity group. Mortality was not affected by the Zn treatment ($P > 0.05$; data not shown). The total Zn concentrations in the seawater were reported in our earlier study using the same exposures and were 3.7 ± 0.5 , 88.1 ± 3.6 , and $80.2 \pm 2.2 \mu\text{g l}^{-1}$ in the control, Zn^{2+} , and nZnO exposures, respectively (Wu et al., 2020b). Dissolved Zn concentrations were the same in the control and nZnO exposed water indicating minimal dissolution of nZnO (Wu et al., 2020b). The mussels exposed to dissolved Zn (but not to nZnO) accumulated Zn in their soft tissues to approximately the same extent regardless of the exposure salinity (Wu et al., 2020b).

2.3. Tissue collection

After three weeks of exposure, mussels were collected, dissected on ice and their soft tissues (mean mass: 2.53 ± 0.72 g, $N = 90$) immediately shock-frozen in liquid nitrogen. Mussels from the fluctuating salinity regime were collected during the high salinity (15) phase. Soft tissues were ground under liquid nitrogen and stored at -80°C until further analyses. Whole-body samples were used to determine the content of carbohydrates, proteins and lipids, the mitochondrial electron transport system (ETS) activity and concentrations of metabolites. A separate batch of mussels (12–15 per treatment group) was used to isolate the mitochondria from the digestive gland tissue to assess the mitochondrial respiratory and ATP synthesis capacity. A subsample (5 mussels per treatment group) was used to determine the body water content. For all experimental mussels, the wet mass of the soft tissues was determined, and the shell width, length and height were measured to the nearest mm using calipers. The sample sizes (N) were 8–10 per treatment group for the whole-body bioenergetics traits and metabolite concentrations, $N = 6$ for the activity of isolated mitochondria, and $N = 5$ for the body water content.

2.4. Determination of energy reserves and ETS activity

Lipid, carbohydrate and protein concentrations were measured in the whole-body homogenates of the mussels using colorimetric methods in a SpectraMax M2 microplate reader (Molecular Devices GmbH, Biberach-an-der-Riß, Germany) as described elsewhere (Haider et al., 2018). Total energy reserve (E_a) was calculated by transforming the measured protein, lipid and carbohydrate into energy equivalents using their respective energy of combustion: 24 kJ g^{-1} for proteins, 39.5 kJ g^{-1} for lipids and 17.5 kJ g^{-1} for carbohydrates (Gnaiger, 1983).

ETS activity was measured in the whole body of mussels with a 2-(4-iodophenyl)-3-(4-nitrophenyl)-5-phenyl tetrazolium chloride (INT) reduction assay using a SpectraMax M2 microplate reader (Molecular Devices GmbH, Biberach-an-der-Riß, Germany) as described elsewhere (DeCoen and Janssen, 1997; Haider et al., 2018). Specific ETS activity of the tissues ($\mu\text{mol O}_2 \text{ min}^{-1} \text{ mg wet tissue mass}$) was calculated using an extinction coefficient of formazan of $15.9 \text{ mM}^{-1} \text{ cm}^{-1}$ and corrected for the light path (0.523 ± 0.023 cm) and the activity of non-mitochondrial reductases. The ETS activity was expressed as $\text{nM O}_2 \text{ min}^{-1} \text{ g}^{-1}$ wet tissue mass. The potential energy expenditure (E_c) was calculated based on the ETS flux assuming the stoichiometric equivalent of $1 \mu\text{mol formazan}$ to $0.5 \mu\text{mol O}_2$ and using oxyenthalpic equivalents for combustion of an average lipid, glycogen and protein mixture ($484 \text{ J mmole}^{-1} \text{ O}_2$) (Gnaiger, 1983; Verslycke et al., 2004). The cellular energy allocation (CEA) was calculated as a ratio of E_a to E_c (Verslycke et al., 2004).

2.5. Mitochondrial assays

Mitochondria were isolated from the digestive gland, which is one of the most metabolically active tissues in mussels as described elsewhere (Falfushynska et al., 2019d). Briefly, ~0.6–1 g of the digestive gland tissue (pooled from 3 to 4 mussels) was homogenized in an ice-cold homogenization media containing 100 mM sucrose, 200 mM KCl, 100 mM NaCl, 8 mM ethylene glycol-bis(2-aminoethylether)-N,N,N',N'-tetraacetic acid (EGTA), 50 $\mu\text{g l}^{-1}$ aprotinin, 1 mM phenylmethylsulfonyl fluoride (PMSF), 2 mM sodium orthovanadate, 30 mM taurine and 30 mM 2-[4-(2-hydroxyethyl)piperazin-1-yl]ethanesulfonic acid (HEPES), pH 7.5 using several passes of a Potter–Elvehjem homogenizer at 200 rotations min^{-1} . Mitochondria were isolated by differential centrifugation at 4 °C and resuspended in ice-cold assay media (AM: 185 mM sucrose, 130 mM KCl, 10 mM NaCl, 30 mM HEPES, 10 mM glucose, 1 mM MgCl_2 , 10 mM KH_2PO_4 and 1% bovine serum albumin (BSA), pH 7.2). Oxygen consumption of isolated mitochondria was measured using an Oxygraph 2k high resolution respirometer (Oroboros, Innsbruck, Austria) at 10 °C in the AM with 5 mM pyruvate, 2 mM malate and 10 mM succinate to stimulate ETS flux through the mitochondrial Complexes I and II. The following traits were assessed: ADP-stimulated respiration (in the presence of 2.5 mM ADP) as a measure of the maximum oxidative phosphorylation (OXPHOS) rate; resting respiration (indicative of the mitochondrial proton leak) in the presence of 2.5 μM oligomycin to inhibit mitochondrial F_0 , F_1 -ATPase; maximum activity of the mitochondrial ETS (measured with 7.5 μM of an uncoupler carbonyl cyanide *m*-chlorophenyl hydrazone); maximum activity of cytochrome c oxidase (CCO) measured with 0.5 mM *N,N,N',N'*-tetramethyl-*p*-phenylenediamine (TMPD) and 2 mM ascorbate as substrates in the presence of 2.5 μM antimycin A to inhibit electron flux through the upstream mitochondrial complexes. Protein concentrations in mitochondrial suspensions were measured using Biorad Bradford Protein Assay Kit according to the manufacturer's instructions (Bio-Rad, Hercules, CA, USA) using BSA as a standard. Mitochondrial respiration was expressed as $\mu\text{mol O}_2 \text{ min}^{-1} \text{ g}^{-1}$ mitochondrial protein. The apparent reserve ETS capacity (ratio of ETS to OXPHOS respiration), reserve CCO capacity (ratio of CCO to OXPHOS activity) and electron transport (ET) and OXPHOS coupling efficiencies were calculated as described elsewhere (Doerrier et al., 2018). Briefly, the ET coupling efficiency was calculated as 1-PL/ETS, where PL and ETS are the oxygen consumption of the resting and uncoupled mitochondria, respectively. The OXPHOS coupling efficiency was calculated as 1-PL/OXPHOS, where PL and OXPHOS are the oxygen consumption of the resting and actively phosphorylating mitochondria, respectively.

2.6. Metabolite analyses

To measure the concentration of metabolites including the free amino acids and anaerobic end products (succinate and lactate), 100 mg of whole soft tissue was extracted with 1.0 ml of 80% ethanol containing 1 $\mu\text{g ml}^{-1}$ of 2-(*N*-morpholino)ethanesulfonic acid (MES) as an internal standard. After vigorous shaking, samples were centrifuged at 13,000 $\times\text{g}$ and 4 °C for 10 min. The supernatant was freeze-dried (Unicryo MC2L –60 °C, Martinsreid, Germany) and stored at –80 °C until further analyses. The extracts were dissolved in MS-grade distilled water (ROTISOLV® LC-MS-grade, Roth, Germany), filtered through 0.2 μm filters (Omnifix®-F, Braun, Germany) and analyzed using the high performance liquid chromatograph-mass spectrometer LCMS-8050 system (Shimadzu, Japan) with electrospray ionization (ESI) as described elsewhere (Haider et al., 2020). Separation was carried out on a pentafluorophenylpropyl (PFPP) column (Supelco Discovery HS FS, 3 μm , 150 \times 2.1 mm) using a consecutive gradient of 1 min 0.1% formic acid, 95% water, 5% acetonitrile, within 15 min linear

gradient to 0.1% formic acid, 5% water, 95% acetonitrile, 10 min 0.1% formic acid, 5% water, 95% acetonitrile to elute the samples. For the identification and quantification of metabolites, LC-MS/MS method package for primary metabolites Ver. 2. (Shimadzu, P/N 225-24862-92) and the LabSolutions software package (Shimadzu, Japan) were used (Haider et al., 2020). The signal intensity (peak area) of the target compounds was normalized to the peak of the internal standard (MES) and quantified using calibration with authentic standard substances (Merck, Germany) for each compound. The concentrations were expressed in $\mu\text{g g}^{-1}$ wet tissue mass. Because the specific amino acid biosynthesis pathways are not well studied in *Mytilus*, we classified the amino acids as essential or non-essential based on the reported capacity for amino acid synthesis in mollusks (Fitzgerald and Szmant, 1997). We considered Arg, His, Lys, Phe, Thr, Trp and Val (for which no biosynthetic capacity was found in mollusks), as well as Met, Ser, Ile, Leu and Pro (that can be synthesized in some but not all mollusks) essential amino acids (Fitzgerald and Szmant, 1997). All other studied FAAs were considered non-essential. To assess the diversity of FAA pool in the mussels' tissues, the Shannon-Wiener diversity index (H) was calculated (Ortiz-Burgos, 2016).

2.7. Condition index

Condition index (CI) was calculated using ratio to the dry soft body mass to shell volume as described elsewhere (Lobel et al., 1991). Ten mussels were randomly selected per each treatment group, and their total mass, whole body soft tissue mass, shell length, shell width and shell height were recorded. Dry tissue mass was calculated based on the percentage of the water in the soft body mass in each group. The CI was calculated as follows:

$$\text{CI} = \text{DW}/\text{SV},$$

where DW is the dry mass of the whole soft tissue (mg) and SV is the shell volume (cm^3) calculated as shell length \times shell width \times shell height (in cm). The tissue water content was determined in five randomly selected mussels from each experimental treatment group as the difference in the wet and dry soft body mass (the latter determined after drying at 60 °C for 72 h until the constant mass).

2.8. Statistical analyses

Shapiro-Wilk test and Levine's test were used to test for normality of the data distribution and the homogeneity of variances, respectively. Statistical outliers were detected by the box-and-whiskers plots and discarded from the further analyses. There was no pattern of outlier distribution among different treatment groups and 0–3 outliers per group were detected. For the data deviating from the normal distribution, Box-Cox transformation was used. The effects of salinity regime, Zn exposures and their interactions on bioenergetics traits, condition index, tissue water content and metabolite concentrations were tested by two-way ANOVA. Salinity regime and Zn exposure were treated as fixed factors with three levels each. The post-hoc Tukey's Honest Significant Differences (HSD) test was used to test for significant differences between the pairs of means of interest. Normalized, Box-Cox transformed data were subjected to the principal component analysis (PCA) to reduce the dimensionality of the data set and identify the potential biomarker signatures of different experimental exposures. Discriminant analysis with stepwise module was performed to assess the ability of the studied biomarkers to distinguish between the different treatment groups. Statistical analyses were performed using IBM® SPSS® Statistics ver. 22.0.0.0 (IBM Corp., Armonk, NY, USA). Data are expressed as means \pm the standard error of the mean unless indicated otherwise. Differences were considered significant if $P < 0.05$.

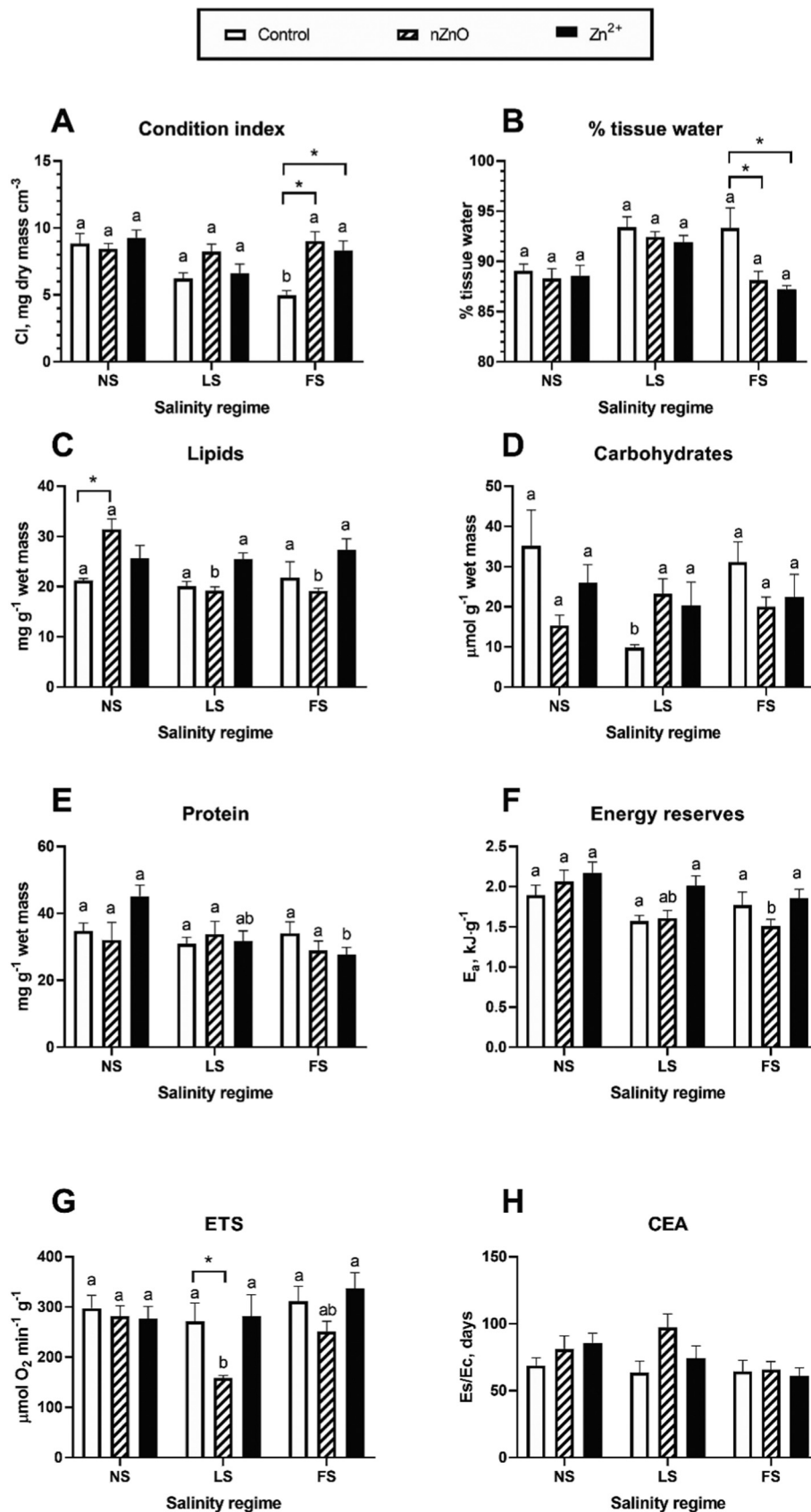


Fig. 1. Effects of salinity acclimation and exposure to different forms of Zn ($100 \mu\text{g l}^{-1}$) on physiological and bioenergetics parameters in the whole soft tissues of the blue mussels *M. edulis*. Salinity regimes: NS – salinity 15, LS – salinity 5, FS – fluctuating salinity between 15 and 5. Different letters indicate values that are significantly different between different salinity regimes within the same Zn exposure group ($P < 0.05$). Please note that the comparison of the means among different salinity treatments is confined to a single Zn treatment group (i.e. within the control, nZnO-exposed or Zn²⁺-exposed groups); therefore, the letters marking different Zn treatment groups cannot be compared to each other. Asterisks indicate values that are significantly different between different Zn treatments within the same acclimation salinity ($P < 0.05$). A – body condition index, B – soft tissue water content, C–E – tissue concentrations of lipids, carbohydrates and proteins, and F – total energy content of the soft tissues. N = 4–5 for the tissue water content, N = 10 for all other traits.

3. Results

3.1. Condition index

Exposure to low and fluctuating salinity led to a decrease in the condition index of *M. edulis* from 8.8 mg cm⁻³ under the normal salinity regime to 6.2 and 5.0 mg cm⁻³ in the low and fluctuating salinity, respectively (Fig. 1A). This decline was significant at the fluctuating but not low salinity (Table 1; Fig. 1A). Exposure to nZnO or dissolved Zn had no effect on the CI under the normal and low salinity conditions, but mitigated the negative effects of osmotic stress under the fluctuating salinity regime, so that the condition index in the nZnO- and Zn²⁺-exposed mussels acclimated to the fluctuating salinity (9.0 and 8.3 mg cm⁻³, respectively) were similar to the CI of the control mussels (8.8 mg cm⁻³).

3.2. Water content

The body water content of the mussels was 88–89% at the normal salinity (Fig. 1B). Exposure to the low or fluctuating salinity led to an increase in the body water content to 92–93%. Under the low salinity regime, this increase was found in all Zn treatment groups. Under the fluctuating salinity regime, an increase in the body water content was only found in the control mussels, but not in those exposed to nZnO or dissolved Zn (Fig. 1B).

3.3. Whole-organism energy status

Acclimation salinity and Zn exposure had no effect on the tissue lipid content of *M. edulis* except for a modest but statistically significant increase in nZnO-exposed group at normal salinity (Table 1, Fig. 1C). The tissue levels of carbohydrates significantly decreased in the control mussels (but not in their counterparts exposed to nZnO or dissolved Zn) exposed to low salinity (Fig. 1D). Fluctuating salinity had no effect on the tissue carbohydrate content of the mussels, regardless of the Zn exposure regime (Fig. 1D). Protein concentrations remained stable in the tissues of the mussels regardless of the acclimation salinity or Zn exposure (Fig. 1E). Overall, the total energy content of the mussels' body was lower in nZnO-exposed mussels at low and fluctuating salinity compared with their counterparts exposed to the normal salinity, albeit this decrease was only statistically significant in the fluctuating salinity group ($P < 0.05$) (Fig. 1F). Similarly, the whole-body activity of the mitochondrial electron transport system (ETS) was suppressed by nZnO exposure in the mussels acclimated at low or fluctuating salinity albeit

Table 1

ANOVA: effects of acclimation salinity and Zn exposure on the whole-body bioenergetics traits and water content of *M. edulis*. F values with the degrees of freedom for the effect and the error (in subscript) and P-values are given. Significant effects are highlighted in bold.

Parameters	Salinity	Zn treatments	Salinity * Zn
Protein content	F_{2,79} = 3.49 P = 0.035	F _{2,79} = 0.71 P = 0.496	F _{4,79} = 2.33 P = 0.063
Carbohydrate content	F _{2,77} = 0.641 P = 0.530	F _{2,77} = 1.393 P = 0.254	F_{4,77} = 3.26 P = 0.016
Lipid content	F_{2,77} = 4.22 P = 0.018	F_{2,77} = 6.39 P = 0.003	F_{4,77} = 5.42 P = 0.001
Total energy reserves	F_{2,81} = 7.21 P = 0.001	F_{2,81} = 5.33 P = 0.007	F _{4,81} = 1.20 P = 0.317
Cellular energy allocation	F_{2,79} = 3.35 P = 0.040	F _{2,79} = 2.90 P = 0.061	F _{4,79} = 1.47 P = 0.221
Condition index	F_{2,81} = 7.79 P = 0.001	F_{2,81} = 8.40 P = 0.000	F_{4,81} = 4.50 P = 0.002
% water content	F_{2,33} = 13.43 P = 0.000	F_{2,33} = 6.50 P = 0.004	F _{4,33} = 2.50 P = 0.061
ETS	F_{2,79} = 3.74 P = 0.028	F_{2,79} = 5.02 P = 0.009	F _{4,79} = 1.39 P = 0.244

this trend was only statistically significant at the low salinity (Fig. 1G). Salinity and Zn exposure had no effect on the CEA index in *M. edulis* (Fig. 1H).

3.4. Mitochondrial activity

The baseline respiration of the isolated mitochondria (indicative of the proton leak) was not affected by the acclimation salinity or Zn exposure (Tables 2, 3). OXPHOS activity was suppressed in the mitochondria of the mussels exposed to dissolved Zn but not in those exposed to nZnO (Table 4). This was reflected in a lower coupling efficiency of OXPHOS in the mitochondria from the mussels exposed to dissolved Zn (Table 3). ETS activity followed a trend similar to OXPHOS (Table 3). CCO activity (and as a consequence, the reserve CCO capacity) was higher in the mitochondria from *M. edulis* acclimated at low salinity (5) compared to their counterparts kept at the normal (15) or fluctuating (5–15) salinity (Table 3). Reserve ETS capacity was the highest in the mussels maintained at the fluctuating salinity compared to other salinity acclimation groups (Table 3).

3.5. Anaerobic end products

Exposure to low salinity (5) led to a strong accumulation of succinate in the tissues of *M. edulis* indicating onset of anaerobic metabolism (Table 4, Fig. 2). This trend was found in the control and nZnO-exposed mussels (but not in those exposed to dissolved Zn) under the low salinity regime (Fig. 2). Notably, succinate accumulation was also observed during transition from salinity 15 to salinity 5 in the fluctuating salinity regime, with an ~27-fold increase (from 0.06 ± 0.01 μmol g⁻¹ to 1.73 ± 0.20 μmol g⁻¹ at salinity 15 and 5, respectively; $P < 0.05$) in succinate content within 22 h of salinity change. Succinate content of the tissues of mussels collected at salinity 15 under the fluctuating salinity regime did not differ from that of the mussels constantly maintained at salinity 15 (Fig. 2).

3.6. Total FAA content

Exposure to low and fluctuating salinity led to a significant decrease of the total FAA content of the mussels' soft tissues from ~26 μmol g⁻¹

Table 2

ANOVA: effects of the acclimation salinity, Zn exposure and their interactions on the bioenergetics traits of isolated mitochondria from the digestive gland of *M. edulis*. Values of F with degrees of freedom for the effect and the error (in subscript) and P values are given. Significant effects ($P < 0.05$) are highlighted in bold. Oxygen consumption (MO₂) of the mitochondria in different states (resting representative of the proton leak, phosphorylating, uncoupled ETS and CCO) were measured in μmol O₂ min⁻¹ g⁻¹ mitochondrial protein. Reserve ETS capacity and reserve CCO capacity were calculated as the ratio of the ETS/OXPHOS flux and CCO/OXPHOS flux, respectively. OXPHOS and electron transport coupling efficiency were calculated as described elsewhere (Doerrier et al., 2018). PL – proton leak, CE – coupling efficiency.

Mitochondrial traits	Salinity	Zn exposure	Salinity * Zn exposure
Resting (PL) MO ₂	F _{2,49} = 1.17 P = 0.319	F _{2,49} = 2.38 P = 0.103	F _{4,49} = 0.30 P = 0.875
OXPHOS MO ₂	F _{2,49} = 0.853 P = 0.432	F_{2,49} = 4.56 P = 0.015	F _{4,49} = 0.61 P = 0.657
ETS MO ₂	F _{2,49} = 0.04 P = 0.958	F _{2,49} = 2.51 P = 0.092	F _{4,49} = 1.13 P = 0.353
CCO MO ₂	F_{2,49} = 7.25 P = 0.002	F _{2,49} = 1.76 P = 0.183	F _{4,49} = 0.45 P = 0.769
Reserve CCO capacity	F_{2,49} = 5.16 P = 0.009	F_{2,49} = 4.77 P = 0.013	F _{4,49} = 2.40 P = 0.062
Reserve ETS capacity	F_{2,49} = 3.88 P = 0.027	F _{2,49} = 1.32 P = 0.276	F _{4,49} = 1.21 P = 0.320
OXPHOS CE	F _{2,43} = 2.93 P = 0.064	F_{2,43} = 4.79 P = 0.013	F _{4,43} = 1.58 P = 0.198
ET CE	F _{2,42} = 2.38 P = 0.105	F _{2,42} = 2.73 P = 0.077	F _{4,42} = 2.10 P = 0.097

Table 3Effects of acclimation salinity and Zn exposure on mitochondrial bioenergetics of *M. edulis*.Mitochondria were isolated from the digestive gland tissue of *M. edulis* exposed to different salinity and Zn regimes. Oxygen consumption (MO_2) of the mitochondria in different states (resting representative of the proton leak, phosphorylating, uncoupled ETS and CCO) were measured in $\mu\text{mol O}_2 \text{ min}^{-1} \text{ g}^{-1}$ mitochondrial protein. Reserve ETS capacity and reserve CCO capacity were calculated as the ratio of the ETS/OXPPOS flux and CCO/OXPPOS flux, respectively. OXPPOS and electron transport coupling efficiency were calculated as described elsewhere (Doerrier et al., 2018). PL – proton leak, CE – coupling efficiency. N = 6.

	Normal salinity			Low salinity			Fluctuating salinity		
	C	nZnO	μ	C	nZnO	Zn ²⁺	C	nZnO	Zn ²⁺
Resting (PL) MO_2	4.47 ± 1.00	3.81 ± 0.81	3.79 ± 0.85	3.86 ± 0.25	3.86 ± 0.43	2.62 ± 0.35	3.69 ± 0.58	3.65 ± 0.27	2.75 ± 0.26
OXPPOS MO_2	7.62 ± 2.28	7.18 ± 1.98	6.13 ± 1.57	8.50 ± 0.98	8.11 ± 1.31	4.57 ± 0.70	5.75 ± 0.85	7.85 ± 0.97	3.96 ± 0.26
ETS MO_2	11.23 ± 3.40	7.94 ± 1.97	8.30 ± 2.14	10.32 ± 0.86	11.55 ± 1.58	6.70 ± 10.2	8.68 ± 0.91	11.87 ± 1.50	8.00 ± 0.83
CCO MO_2	25.79 ± 6.29	28.56 ± 4.46	26.27 ± 3.87	31.46 ± 2.24	42.12 ± 2.69	33.48 ± 4.88	24.86 ± 1.93	26.69 ± 3.46	23.57 ± 1.62
Reserve ETS capacity	1.48 ± 0.14	1.20 ± 0.15	1.37 ± 0.10	1.24 ± 0.05	1.46 ± 0.09	1.52 ± 0.22	1.57 ± 0.19	1.52 ± 0.09	2.04 ± 0.21
Reserve CCO capacity	2.54 ± 0.25	4.06 ± 0.45	3.64 ± 0.43	3.10 ± 0.21	3.89 ± 0.41	5.40 ± 1.00	3.09 ± 0.58	2.27 ± 0.14	3.26 ± 0.35
OXPPOS CE	0.26 ± 0.05	0.30 ± 0.12	0.21 ± 0.09	0.55 ± 0.05	0.44 ± 0.08	0.23 ± 0.08	0.25 ± 0.28	0.46 ± 0.07	0.17 ± 0.03
ET CE	0.53 ± 0.05	0.54 ± 0.07	0.39 ± 0.07	0.64 ± 0.02	0.62 ± 0.05	0.47 ± 0.06	0.49 ± 0.08	0.64 ± 0.05	0.61 ± 0.02

wet mass at salinity 15 to ~11 $\mu\text{mol g}^{-1}$ wet mass at salinity 5, and ~19 $\mu\text{mol g}^{-1}$ wet mass at the fluctuating salinity (5–15) (Table 4, Figs. 3 and 4A). At the normal salinity (15), exposure to dissolved Zn

(but not nZnO) led to a decrease in the total FAA content (Fig. 4A). At low or fluctuating salinity, Zn exposure had no effect on the total FAA concentrations in the mussels' tissues (Fig. 4A).

Table 4ANOVA: Effects of the acclimation salinity, Zn exposure and their interactions on the tissue levels of FAA and succinate in *M. edulis*.Values of F with degrees of freedom for the effect and the error (in subscript) and P values are given. Significant effects ($P < 0.05$) are highlighted in bold.

Metabolites	Salinity	Zn exposure	Salinity * Zn exposure
Total FAAs	F_{2,75} = 125.12 P < 0.001	F_{2,75} = 19.59 P < 0.001	F_{4,75} = 3.96 P = 0.006
Asparagine	F_{2,78} = 56.23 P < 0.001	F_{2,78} = 3.49 P = 0.036	F _{4,78} = 1.46 P = 0.224
Aspartate	F_{2,77} = 131.40 P < 0.001	F_{2,77} = 49.79 P < 0.001	F_{4,77} = 6.44 P < 0.001
Serine	F_{2,76} = 52.44 P < 0.001	F_{2,76} = 5.74 P = 0.005	F_{4,76} = 3.14 P = 0.019
Alanine	F_{2,80} = 12.34 P < 0.001	F_{2,80} = 13.89 P < 0.001	F _{4,80} = 0.56 P = 0.695
Glycine	F_{2,77} = 168.39 P < 0.001	F_{2,77} = 24.40 P < 0.001	F_{4,77} = 3.73 P = 0.008
Glutamine	F_{2,79} = 10.36 P < 0.001	F _{2,79} = 2.48 P = 0.090	F_{4,79} = 3.30 P = 0.015
Threonine	F_{2,76} = 5.04 P = 0.009	F _{2,76} = 0.73 P = 0.485	F_{4,76} = 6.12 P < 0.001
Methionine sulfoxide	F_{2,75} = 12.10 P < 0.001	F_{2,75} = 10.84 P < 0.001	F_{4,75} = 7.55 P < 0.001
Glutamate	F_{2,79} = 19.47 P < 0.001	F _{2,79} = 0.45 P = 0.640	F_{4,79} = 4.59 P = 0.002
Proline	F_{2,78} = 3.36 P = 0.040	F _{2,78} = 0.47 P = 0.624	F_{4,78} = 8.98 P < 0.001
Lysine	F_{2,79} = 9.61 P < 0.001	F _{2,79} = 1.99 P = 0.144	F_{4,79} = 3.72 P = 0.008
Histidine	F_{2,76} = 9.95 P < 0.001	F_{2,76} = 6.55 P = 0.002	F_{4,76} = 3.53 P = 0.011
Arginine	F_{2,80} = 12.34 P < 0.001	F_{2,80} = 13.89 P < 0.001	F _{4,80} = 0.56 P = 0.695
Valine	F_{2,78} = 3.73 P = 0.028	F_{2,78} = 6.19 P = 0.003	F_{4,78} = 3.65 P = 0.009
Methionine	F_{2,77} = 24.70 P < 0.001	F _{2,77} = 1.34 P = 0.269	F _{4,77} = 1.60 P = 0.184
Tyrosine	F_{2,78} = 4.88 P = 0.010	F _{2,78} = 1.23 P = 0.297	F_{4,78} = 4.43 P = 0.003
Isoleucine	F_{2,78} = 8.83 P < 0.001	F _{2,78} = 1.28 P = 0.283	F_{4,78} = 4.91 P = 0.001
Leucine	F_{2,74} = 5.57 P = 0.006	F _{2,74} = 2.22 P = 0.115	F_{4,74} = 3.46 P = 0.012
Phenylalanine	F_{2,77} = 20.10 P < 0.001	F_{2,77} = 7.45 P = 0.001	F_{4,77} = 4.80 P = 0.002
Tryptophan	F_{2,73} = 30.24 P < 0.001	F_{2,73} = 27.62 P < 0.001	F_{4,73} = 6.54 P < 0.001
Taurine	F _{2,78} = 0.35 P = 0.707	F_{2,78} = 10.82 P < 0.001	F_{4,78} = 7.69 P < 0.001
Succinate	F_{2,74} = 46.57 P < 0.001	F_{2,74} = 23.09 P < 0.001	F_{4,74} = 16.14 P < 0.001

Acclimation to low salinity led to a considerable rearrangement of the FAA composition in the mussels' tissues and an increase in the FAA diversity (indicated by the higher value of the Shannon-Wiener index H) (Fig. 3). In control and nZnO-exposed mussels maintained at the fluctuating salinity, the composition and diversity of the FAA pool was similar to those kept under the normal salinity (15) (Fig. 3). In all salinity regimes, exposure to dissolved Zn changed the composition of the FAA pool (most notably, decreasing the fraction of Gly and increasing the proportion of Ile) compared to the control or nZnO-exposed mussels at the same salinity (Fig. 3).

3.7. Free amino acids content

Acclimation salinity, Zn exposure and their interactions had significant effects on the tissue levels of most studied FAAs (Table 4). For all FAAs (except Asn, Ala, Arg and Met), the effect of the Salinity × Zn exposure interactions was significant indicating that Zn exposure has different effects on FAA content depending on the acclimation salinity (Table 4).

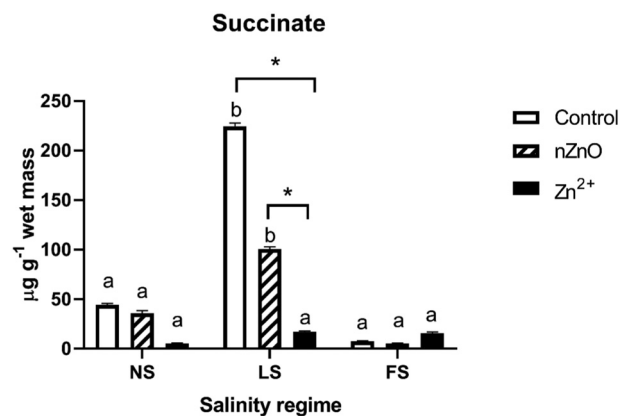


Fig. 2. Effects of salinity acclimation and exposure to different forms of Zn ($100 \mu\text{g l}^{-1}$) on succinate content in the whole soft tissues of the blue mussels *M. edulis*. Salinity regimes: NS – salinity 15, LS – salinity 5, FS – fluctuating salinity between 15 and 5. Different letters indicate values that are significantly different between different salinity regimes within the same Zn exposure group ($P < 0.05$). Please note that the comparison of the means among different salinity treatments is confined to a single Zn treatment group (i.e. within the control, nZnO-exposed or Zn²⁺-exposed groups); therefore, the letters marking different Zn treatment groups cannot be compared to each other. Asterisks indicate values that are significantly different between different Zn treatments within the same acclimation salinity ($P < 0.05$). N = 8–10.

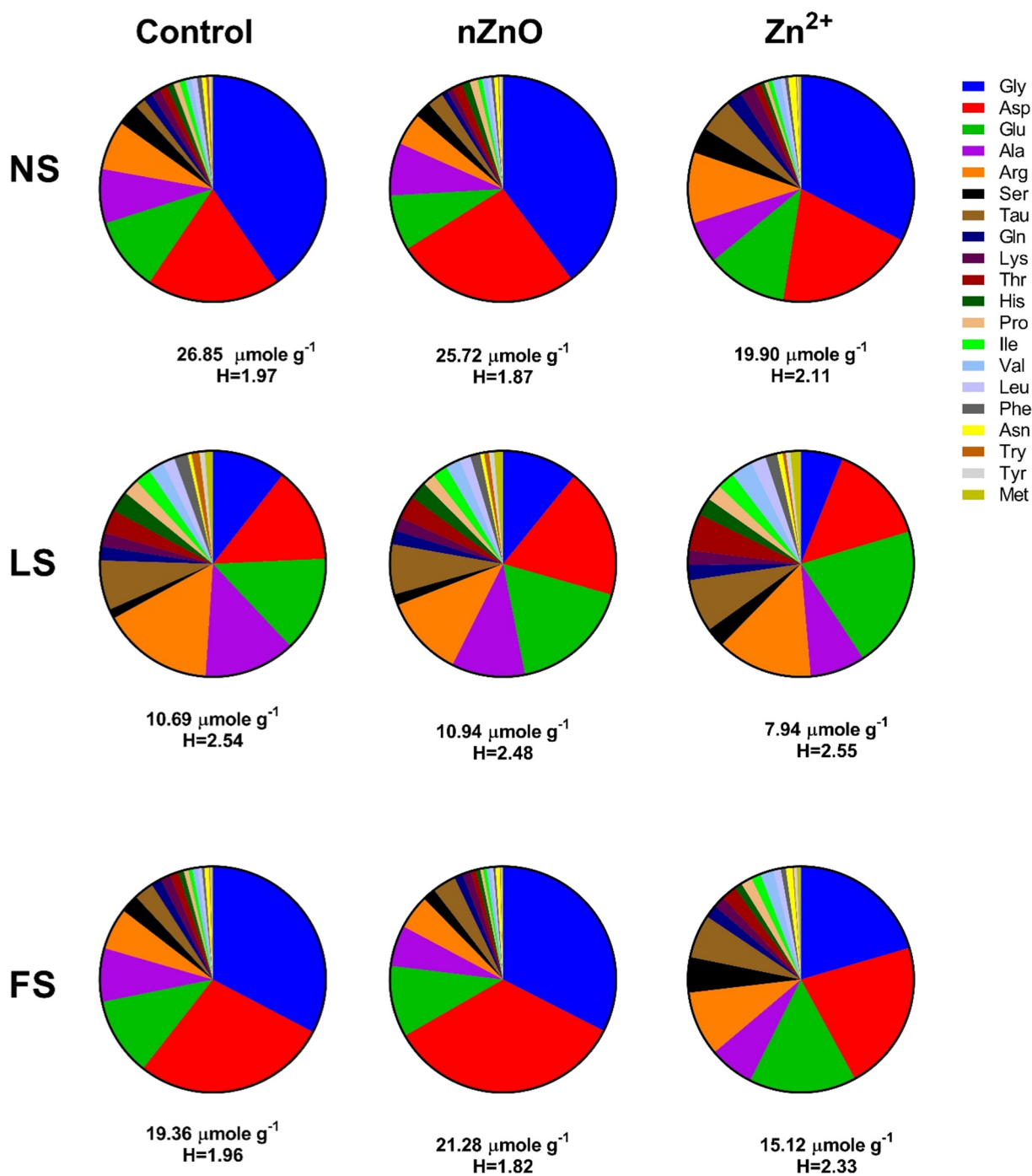


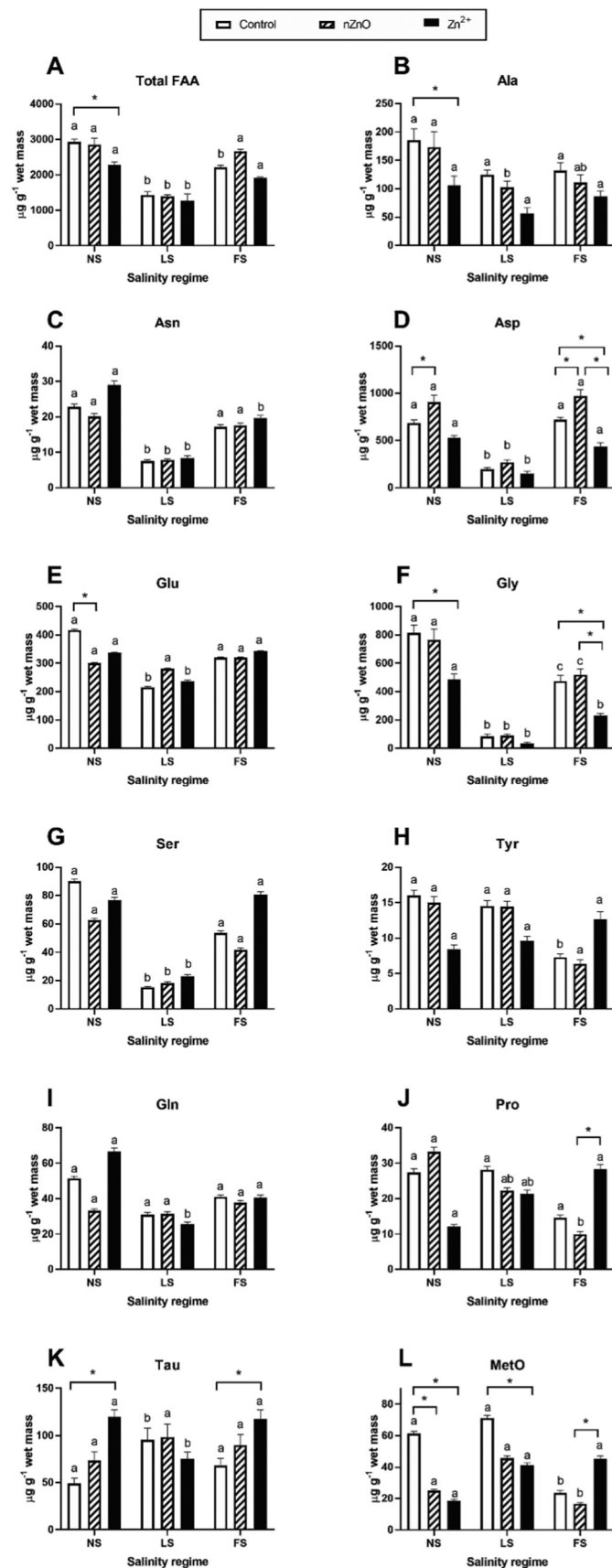
Fig. 3. Effects of salinity acclimation and exposure to different forms of Zn ($100 \mu\text{g l}^{-1}$) on amino acid composition in the whole soft tissues of the blue mussels *M. edulis*. Salinity regimes: NS – salinity 15, LS – salinity 5, FS – fluctuating salinity between 15 and 5. A total concentration of free amino acid and amino acid diversity index (H) are given under each pie chart. The charts are based on the mean values for each experimental treatment group (N = 8–10 per group).

Out of nine studied non-essential amino acids, the concentrations of five (Asn, Asp, Glu, Gly, and Ser) decreased in the mussels exposed to low salinity (Fig. 4C, D, E, F, G), whereas the tissue content of Ala, Tyr, Gln and Pro did not change (Fig. 4B, H, I, J). Unlike non-essential FAAs, acclimation to the low salinity (5) had no effect on the tissue levels of the ten studied essential amino acids (Fig. 5). Acclimation at the fluctuating salinity regime led to a modest decline in the total FAA levels in the mussel tissues reflecting a decrease in the concentrations of non-essential (Gly, Tyr) and essential (Ile, Leu, Phe and Trp) amino acids (Fig. 4F,H, and 5C, D, G, I). Tissue levels of taurine increased in the mussels exposed to low and fluctuating salinity stress but this trend was only statistically significant ($P < 0.05$) at low salinity (Fig. 4K).

Methionine sulfoxide (MetO), a product of oxidation of Met, decreased in the mussels acclimated under the fluctuating (but not under the constantly low) salinity regime compared with those kept at the normal salinity (Fig. 4L).

Exposure to nZnO did not affect the tissue levels of FAAs in a consistent manner except for an increase in the Asp levels in nZnO-exposed mussels (Fig. 4D). This trend was statistically significant ($P < 0.05$) under the normal and fluctuating salinity but not under the constantly low salinity regime. With regard to other FAAs, the effects of the nZnO exposure were modest and strongly salinity-dependent. Thus, under the normal salinity (15) conditions, Glu, Phe, and Trp content decreased in response to nZnO exposures (Figs. 4, 5). These trends were not

observed in the mussels kept under the low or fluctuating salinity. Levels of all other studied FAAs did not change in response to nZnO. Tissue levels of MetO tended to decrease in nZnO-exposed mussels



compared to their control counterparts but this tendency was only significant under the normal salinity regime (Fig. 4L).

Unlike nZnO, exposure to dissolved Zn affected tissue levels of multiple FAAs (Fig. 4A, F). The most consistent patterns were shown by Gly (decreasing in Zn²⁺-exposed mussels at all studied salinity regimes), Phe and Trp (decreasing in Zn²⁺-exposed mussels at the normal and fluctuating salinity) and Tau (increasing in Zn²⁺-exposed mussels at the normal and fluctuating salinity) (Figs. 4F, K and 5G, I). Furthermore, under the normal salinity conditions exposure to dissolved Zn led to a decrease in Ala and His (Figs. 4B, 5B), whereas under the fluctuating salinity conditions exposure to dissolved Zn led to the elevated levels of Pro, Thr and Val (Figs. 4J, 5H, J). Under the low salinity regime, dissolved Zn exposure had no effect on the FAA levels in the mussels' tissues (Figs. 4, 5). Tissue levels of MetO declined in Zn²⁺-exposed mussels at the normal and low salinity and increased under the fluctuating salinity regime (Fig. 4L).

3.8. Data integration

The principal component (PCA) and discriminant analysis based on the integrated biomarker profile showed a strong differentiation of the groups acclimated to the low salinity (LS) from those maintained under the normal (NS) and fluctuating (FS) salinity, as well as clear separation of the NS and FS groups (Fig. 6). The PCA analysis identified two first principal components (PCs) jointly explaining 49% of the variation in the biomarker levels. The 1st PC (29% variation) separated the NS and FS groups (Fig. 6A) and had high loadings of the concentrations of essential FAAs His, Arg, Val, Met, Ile, Leu, Phe, and Trp as well as Asp, Tyr, and MetO (Fig. 6B; Supplementary Table 2). The 2nd PC (20% variation) separated the LS-exposed mussels from the other two experimental groups (Fig. 6A) and had high loadings of anaerobic metabolism markers (Asp, succinate and total carbohydrate levels) as well as Ser, Gly, Lys, and Tau (Fig. 6B; Supplementary Table 2). The discriminant analysis showed high Mahalanobis distances between the LS and NS ($D^2 = 302$) and the LS and FS ($D^2 = 332$) groups, and a smaller distance ($D^2 = 41$) between the LS and NS groups, consistent with the PCA analysis. The traits that significantly contributed to the discriminant model ($P < 0.05$) separating the groups included concentrations of Gly, Asp, Ser, Phe, MetO, as well as succinate and AMP (Supplementary Table 3).

Effects of the Zn treatment on the integrated metabolite biomarker profile of the mussels (as revealed by the PCA and discriminant analysis) strongly depended on the acclimation salinity regime (Figs. 7, 8, and 9). Generally, the biomarker profiles clearly separated the three experimental groups (control, nZnO and dissolved Zn exposures) under the normal salinity regime (Fig. 7A) but not under the low (Fig. 8A) or fluctuating (Fig. 9A) salinity.

Under the normal (15) salinity regime, the metabolite profiles of the control group separated from the nZnO- and Zn²⁺-exposed groups along the 1st principal component axis explaining 27% of the total variation and mostly associated with the whole-body levels of Ala, Gly, Thr, Pro, His, Val, Tyr, Ile, Leu, Phe, Try and MetO (Fig. 7B). The group exposed to dissolved Zn was associated with the higher levels of these biomarkers compared to the nZnO-exposed and control groups (Fig. 7A). The nZnO exposed group was separated from other experimental

Fig. 4. Effects of salinity acclimation and exposure to different forms of Zn ($100 \mu\text{g l}^{-1}$) on the tissue levels of the putative non-essential amino acids and amino acid derivatives in the blue mussels *M. edulis*. Salinity regimes: NS – salinity 15, LS – salinity 5, FS – fluctuating salinity between 15 and 5. Different letters indicate values that are significantly different between different salinity regimes within the same Zn exposure group ($P < 0.05$). Please note that the comparison of the means among different salinity treatments is confined to a single Zn treatment group (i.e. within the control, nZnO-exposed or Zn²⁺-exposed groups); therefore, the letters marking different salinity groups cannot be compared to each other. Asterisks indicate values that are significantly different between different Zn treatments within the same acclimation salinity ($P < 0.05$). A – total FAA content; B–J – concentrations of different proteinogenic amino acids, K – taurine, L – methionine sulfoxide. N = 8–10.

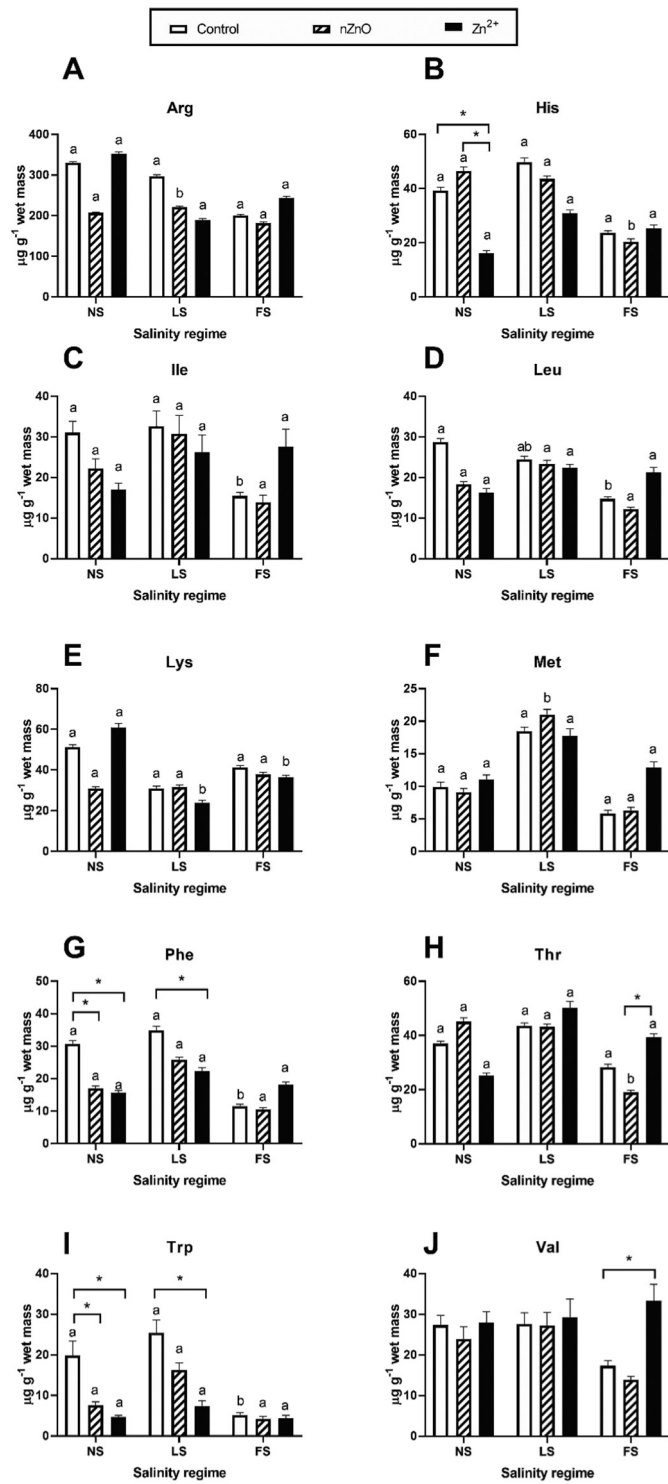


Fig. 5. Effects of salinity acclimation and exposure to different forms of Zn ($100 \mu\text{g l}^{-1}$) on the tissue levels of the putative essential amino acids in the blue mussels *M. edulis*. Salinity regimes: NS – salinity 15, LS – salinity 5, FS – fluctuating salinity between 15 and 5. Different letters indicate values that are significantly different between different salinity regimes within the same Zn exposure group ($P < 0.05$). Please note that the comparison of the means among different salinity treatments is confined to a single Zn treatment group (i.e. within the control, nZnO-exposed or Zn^{2+} -exposed groups); therefore, the letters marking different Zn treatment groups cannot be compared to each other. Asterisks indicate values that are significantly different between different Zn treatments within the same acclimation salinity ($P < 0.05$). A–J – concentrations of different proteinogenic amino acids. N = 8–10.

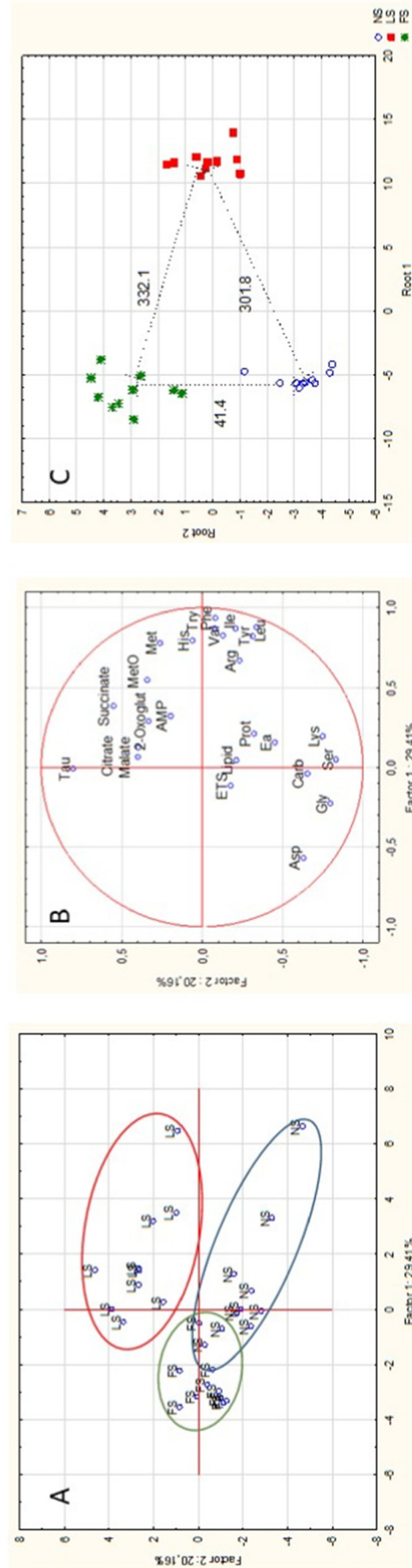


Fig. 6. Principal component analysis (PCA) and discriminant analysis biplots integrating all measured biomarkers of *M. edulis* acclimated at different salinity conditions. Only the mussels maintained under the control conditions (without addition of nZnO or dissolved Zn) were used in the analyses. Experimental treatment groups: NS – salinity 15, LS – salinity 5, FS – fluctuating salinity between 15 and 5. A – the position of samples from different salinity regimes in the plane of the two first principal components. B – the variable-based plot showing the associations of the respective biomarkers with the two first principal components. C – the discriminant analysis biplot of the different salinity regimes based on the multibiomarker profiles. Numbers next to the lines indicate the Mahalanobis distance between the respective groups.

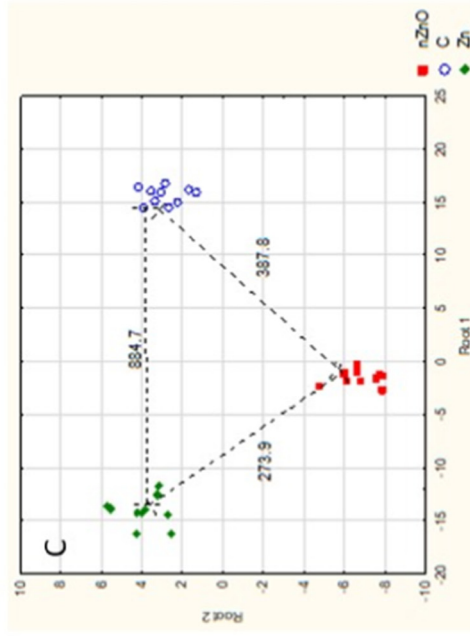
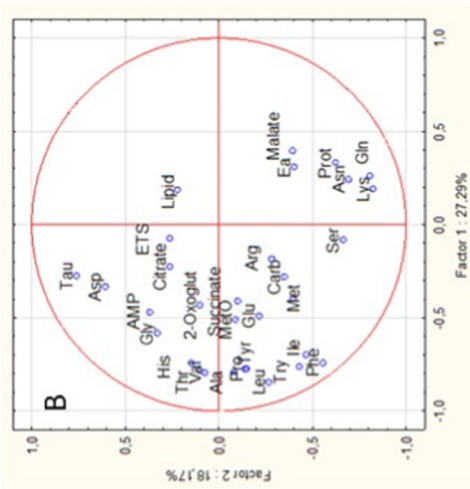
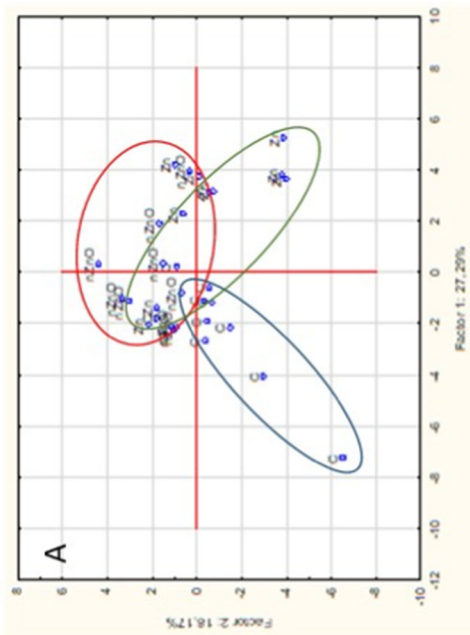


Fig. 7. Principal component analysis (PCA) and discriminant analysis biplots integrating all measured biomarkers of *M. edulis* from different Zn treatment groups acclimated at the normal salinity (15). Experimental treatment groups: C – controls, nZnO – mussels exposed to $100 \mu\text{g l}^{-1}$ of nZnO, Zn – mussels exposed to $100 \mu\text{g l}^{-1}$ of dissolved Zn. A – the position of samples from different Zn exposure groups in the plane of the two first principal components. B – the variable-based plot showing the associations of the respective biomarkers with the two first principal components. C – the discriminant analysis biplot of the different Zn exposure based on the multibiomarker profiles. Numbers next to the lines indicate the Mahalanobis distance between the respective groups.

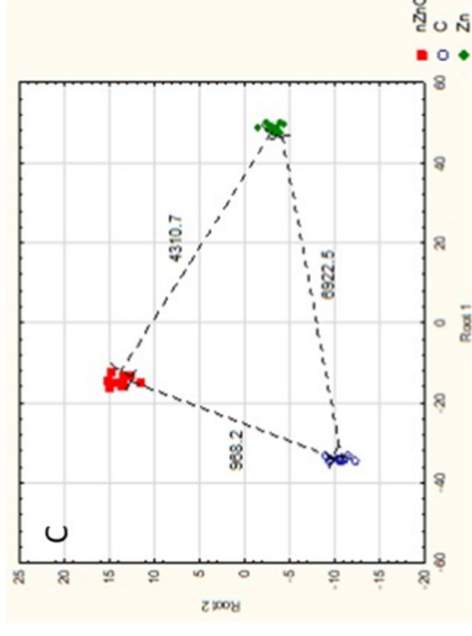
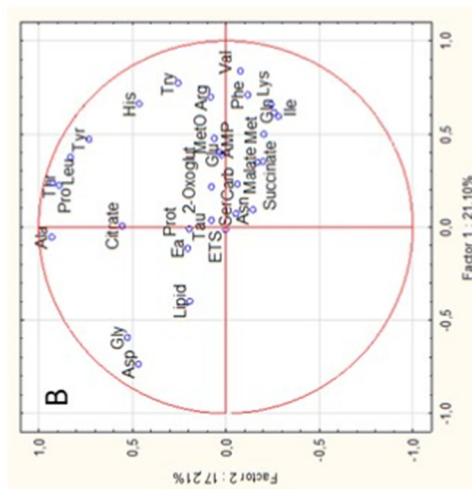
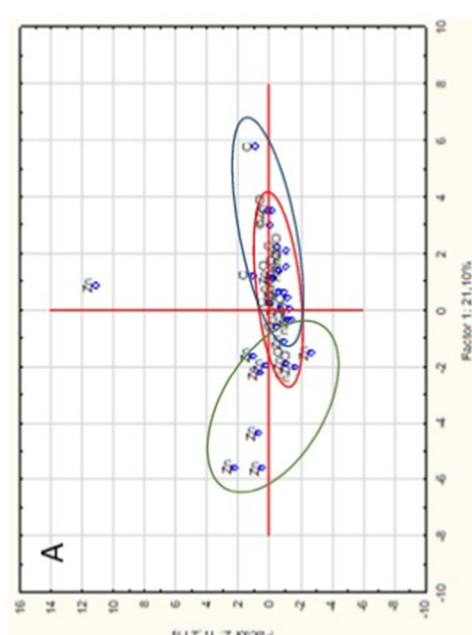


Fig. 8. Principal component analysis (PCA) and discriminant analysis biplots integrating all measured biomarkers of *M. edulis* from different Zn treatment groups acclimated at the low salinity (5). Experimental treatment groups: C – controls, nZnO – mussels exposed to $100 \mu\text{g l}^{-1}$ of nZnO, Zn – mussels exposed to $100 \mu\text{g l}^{-1}$ of dissolved Zn. A – the position of samples from different Zn exposure groups in the plane of the two first principal components. B – the variable-based plot showing the associations of the respective biomarkers with the two first principal components. C – the discriminant analysis biplot of the different Zn exposure based on the multibiomarker profiles. Numbers next to the lines indicate the Mahalanobis distance between the respective groups.

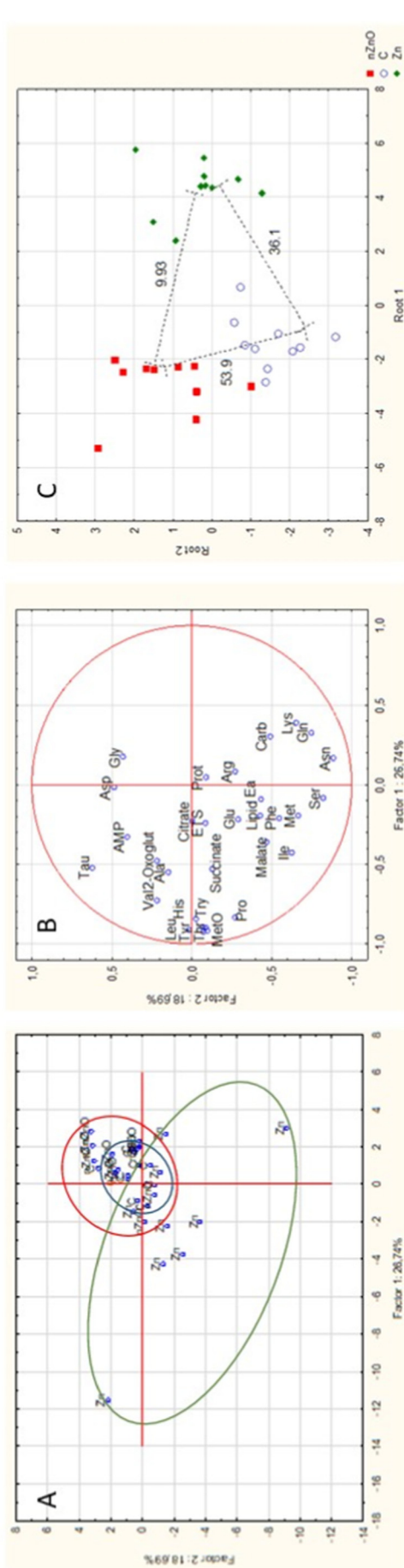


Fig. 9. Principal component analysis (PCA) and discriminant analysis biplots integrating all measured biomarkers of *M. edulis* from different Zn treatment group acclimated at the fluctuating salinity (5–15). Experimental treatment groups: C – controls, nZnO – mussels exposed to $100 \mu\text{g l}^{-1}$ of dissolved Zn, A – the position of samples from different Zn exposure groups in the plane of the two first principal components. B – the variable-based plot showing the associations of the respective biomarkers with the two first principal components. C – the discriminant analysis biplot of the different Zn exposure based on the multibiomarker profiles. Numbers next to the lines indicate the Mahalanobis distance between the respective groups.

groups along the 2nd PC axis (explaining 18% of the data variation) that had high positive loadings of the body levels of Asp and Tau and high negative loadings of the Asn, Ser, Gln, Lys and total protein levels (Fig. 7B; Supplementary Table 4). The discriminant analysis indicated the highest Mahalanobis distance ($D^2 = 885$) between the control and Zn^{2+} -exposed groups, whereas the distances between the nZnO-exposed groups and two other treatments were 274–388 (Fig. 7C). The biomarkers significantly contributing to the discriminant function between the control, nZnO and Zn^{2+} -exposed groups under the normal (15) salinity regime included the whole-body concentrations of Val, Leu, Phe, Try, Tau, MetO, citrate, malate, lipid and protein content, as well as the ETS activity (Supplementary Table 5).

The PCA analysis of the metabolite profiles in the mussels acclimated to low (5) salinity identified two PCs jointly explaining 38% of the data variation (Supplementary Table 6). Under the low (5) salinity regime, the metabolite profiles of the control group separated from the Zn^{2+} -exposed group along the 1st principal component axis explaining 21% of the total variation and associated with the body levels of Asp, Gly, Gln, Lys, His, Arg, Val, Ile, Phe and Try (Fig. 8B). Most of these markers (except Asp and Gly) were higher in the Zn^{2+} -exposed group (Fig. 8B; Supplementary Table 6). The position of the control and nZnO-exposed groups showed considerable overlap in the plane of the two first principal components (Fig. 8A). The discriminant analysis indicated the highest Mahalanobis distance ($D^2 = 6922$) between the control and Zn^{2+} -exposed groups, followed by the distance between the nZnO- and Zn^{2+} -exposed groups ($D^2 = 4311$) (Fig. 8C). The control and nZnO-exposed groups were less differentiated ($D^2 = 968$). The biomarkers significantly contributing to the discriminant model under the low (5) salinity regime included the whole-body concentrations of Asp, Ser, Val, Ile, Leu, Try, Glu, Tyr, Phe, Asn, Lys, Met, MetO, citrate, 2-oxoglutarate, AMP, the total lipid content, and the ETS activity (Supplementary Table 7).

The PCA analysis of the metabolite profiles in the mussels acclimated to the fluctuating (5–15) salinity identified two PCs jointly explaining 45% of the data variation (Fig. 9A, Supplementary Table 8). Under the fluctuating (5–15) salinity regime, the metabolite profiles of the control and nZnO-exposed groups overlapped (Fig. 9A). The position of the Zn^{2+} -exposed group (except a single sample) was shifted towards the negative values of the 2nd PC (Fig. 9A). The 1st PC had high loadings of the body concentrations of Ala, Thr, Pro, His, Val, Tyr, Leu, Try, Tau and MetO, and PC2 had high loadings of Asn, Ser, Gln, Lys, Met, Ile, Phe and Tau (Fig. 9B; Supplementary Table 8). The discriminant analysis showed a broad spread within each experimental group with modest Mahalanobis distances ($D^2 = 10$ –54) between all groups (Fig. 9C). Under the fluctuating salinity regime, the biomarkers significantly contributing to the discriminant model included the whole-body concentrations of Asp, Ile, Val and Met (Supplementary Table 9).

4. Discussion

Our study showed that exposure to low (5) or fluctuating (5–15) salinity affected the physiological condition, energy metabolism and homeostasis, as well as amino acid metabolism in a euryhaline marine bivalve *M. edulis*. Impacts of nZnO and dissolved Zn on the energy and amino acid metabolism were relatively mild and most pronounced under the normal salinity regime. Except for a few studied metabolic traits (including the body lipid content, ETS activity, and concentrations of Asp and Glu), the effects of dissolved Zn were similar or stronger than the effects of nZnO. Generally, the metabolic biomarker profiles could distinguish the nZnO and Zn^{2+} exposed groups from the controls under the normal salinity conditions (15) but this diagnostic ability was lost in the mussels exposed to the low or fluctuating salinity reflecting the dominant effects of the osmotic stress on the mussels' physiology compared with the effects of the environmentally relevant, low concentrations of dissolved and nanoparticulate Zn.

4.1. Effects of salinity regime on the physiological condition and energy status of the mussels

Physiological condition of a euryhaline marine bivalve *M. edulis* was robust against the osmotic stress. The body condition index (CI) remained unchanged in the mussels exposed for three weeks to chronically low salinity (5), while a modest decrease in CI under the fluctuating salinity conditions reflected an increase in the body water content rather than a major loss of the body mass. Aerobic metabolism of *M. edulis* was also unaffected by osmotic stress under the conditions of our present study. Thus, the ETS activity (a composite index of the mitochondrial abundance and respiratory capacity) of the mussels' body did not change under the conditions of low or fluctuating salinity. The lack of the whole-body ETS response to osmotic stress was supported by the studies of the isolated mitochondria. Thus, the mitochondrial proton leak (indicative of the mitochondrial activity needed to counteract all futile proton and cation cycles and to maintain the membrane potential in resting mitochondria) as well as OXPHOS capacity were similar in the mussels' mitochondria regardless of the acclimation salinity regime. The OXPHOS and ETS coupling efficiency also remained unchanged under different salinity conditions. Interestingly, activity of cytochrome c oxidase (CCO), the terminal oxidase of the ETS, increased in the mussels acclimated to chronically low salinity. The physiological implications of this increase are not clear because CCO has a relatively high excess capacity (~2–4-fold higher than the activity of the ETS) and thus is unlikely to be a rate-controlling enzyme under the conditions of this study. Studies indicate that the apparent CCO capacity of animal cells is tuned to support the periodical bouts of high ATP demand (Gnaiger et al., 1998a; Gnaiger et al., 1998b; Lemieux et al., 2017) so that elevated CCO activity in low salinity-acclimated mussels might indicate periods of high energy demand, possibly due to the needs of osmoregulation during hypoosmotic stress.

Hypoosmotic stress led to onset of anaerobic metabolism in the mussels as indicated by strong accumulation of an anaerobic end product, succinate, and depletion of the glycolytic substrates (glycogen and aspartate) in the mussels exposed to low salinity (5). Accumulation of succinate and depletion of aspartate were also found in *M. edulis* during the low salinity (5) phase of the fluctuating salinity regime (Supplementary Table 1) indicating a rapid onset of anaerobiosis during salinity downshift. This trend was reversed during increase of salinity back to 15 (Supplementary Table 1). Stimulation of anaerobic pathways during hypoosmotic stress has also been reported for other bivalves including mytilids. Thus, in *Mytilus galloprovincialis*, hypoosmotic stress (salinity 19) suppressed the activity of pyruvate kinase (PK), an enzyme that channels the glycolytic substrate towards aerobic oxidation, compared to the mussels acclimated at salinity 38 (De Vooys and Holwerda, 1986). In facultative anaerobes such as bivalve mollusks, pyruvate kinase (PK) and phosphoenolpyruvate carboxykinase (PEPCK) compete for a common substrate, phosphoenolpyruvate (PEP), at the so called PEP branch point, with PK channeling PEP to aerobic oxidation via formation of pyruvate and PEPCK converting PEP to oxaloacetate that eventually leads to anaerobic succinate production by the mitochondrial fumarate reductase (Bayne, 2017; Saz, 1971; Zammit and Newsholme, 1978). The suppression of PK under hypoosmotic stress thus would favor anaerobic metabolism of carbohydrates resulting in the succinate production (Bayne, 2017; Saz, 1971; Zammit and Newsholme, 1978). Overall, onset of partial anaerobiosis under the hypoosmotic stress (salinity 5) in our present study indicates transition into a bioenergetically unsustainable (pessimum) environmental range of the mussels (Sokolova, 2013; Sokolova et al., 2012) and is consistent with the observations that salinity 5 is close to the tolerance limit of *M. edulis* (Gosling, 1992).

4.2. Effects of nZnO and dissolved Zn on the physiological condition and energy status of the mussels

Effects of Zn-containing exposures on the body condition index and energy (carbohydrates and lipids) reserves of the mussels varied

depending on the acclimation salinity as shown by the significant interactions between salinity and Zn exposure ($P < 0.05$). Exposure to nZnO and dissolved Zn had a positive effect on the body condition under the fluctuating salinity regime, preventing an increase in the body water content (and the associated decrease in the body condition index) caused by the fluctuating salinity. Under the normal and constant low salinity, nZnO and dissolved Zn had no effect on the body condition index. Effects of dissolved Zn on the cellular water transport has been reported in animal model systems (such as *Xenopus* oocytes) (Németh-Cahalan et al., 2007) and plants (Rygal et al., 1992; Sridhar et al., 2007); however, to the best of our knowledge, no studies exist for the mechanisms of Zn effects on water transport of marine invertebrates. Further studies are needed to determine the mechanisms of Zn effects on intracellular osmoregulation and water transport in the mussels and explain why these effects are only apparent under the fluctuating salinity regime.

Exposure to nZnO or dissolved Zn exposure had no effect on the body levels of energy reserves of the mussels except a modest but statistically significant increase of the body lipid content of nZnO-exposed mussels at the normal salinity. These findings are in contrast to an earlier study that found a decrease in the body energy reserves (glycogen in winter and lipids in summer) during exposure to $100 \mu\text{g l}^{-1}$ of nZnO in the Baltic Sea mussels (Wu et al., 2021). A decrease in the tissue lipid and glycogen content was also reported in freshwater mussels *Unio tumidus* exposed to $250 \mu\text{g l}^{-1}$ of nZnO (Falfushynska et al., 2019b). These findings indicate variable effects of nZnO on the energy reserves of the mussels, even within the same species. Albeit the limited amount of available data precludes broad generalizations, the observed nZnO effects on the energy reserves of the mussels were modest indicating that exposure to environmentally relevant nZnO concentrations does not result in a major energy deficit in the mussels (this study; Falfushynska et al., 2019b; Wu et al., 2021).

Mitochondrial metabolism of the mussels was differently responsive to nZnO and dissolved Zn exposures. Exposure to nZnO led to a decrease in the whole-body ETS capacity in the mussels. A similar decrease has been reported for *M. edulis* in other studies (Falfushynska et al., 2019c; Wu et al., 2021). Interestingly, activity of isolated mitochondria was not altered in the nZnO-exposed mussels (Wu et al., 2021; this study) indicating that the observed drop in the whole-body ETS capacity reflects a decrease in the mitochondrial abundance rather than the quality of the mitochondria. A study in the isolated mitochondria of rats showed that treatment with nZnO inhibits mitochondrial respiration, and leads to the elevated ROS production and collapse of the mitochondrial membrane potential (Li et al., 2012). However, in the latter study high nZnO concentrations ($5\text{--}50 \text{ mg l}^{-1}$) were added directly to the mitochondrial suspension (Li et al., 2012), and the physiological relevance of this exposure route remains unclear. Unlike nZnO, exposure to dissolved Zn negatively affected the OXPHOS activity (indicative of the ATP synthesis capacity) and OXPHOS coupling efficiency in the mitochondria of *M. edulis*. Zn is a known mitochondrial toxin negatively affecting mitochondrial respiration and ATP synthesis in a variety of animals including bivalves (Akberali and Earnshaw, 1982; Dineley et al., 2003; Lemire et al., 2008; Pivovarov et al., 2014). Given a strong mitochondrial toxicity of Zn^{2+} and the lack of effects of nZnO, our study indicates that intracellular release on Zn^{2+} during nZnO exposures does not achieve the threshold required to damage the mitochondrial functions in *M. edulis*.

Unlike mitochondrial activity, anaerobic metabolism of the mussels (assessed by succinate accumulation) was unaltered during exposures to $100 \mu\text{g l}^{-1}$ of nZnO. Under the normal and fluctuating salinity regimes, dissolved Zn likewise has no effect on succinate accumulation, whereas at the low salinity exposure to dissolved Zn suppressed succinate accumulation. In mammals, Zn^{2+} activate succinate dehydrogenase activity (Yamaguchi et al., 1981; Yamaguchi et al., 1982). If a similar mechanism exists in bivalves, it might explain the reversal of succinate accumulation caused by the hypoosmotic stress by exposure

to dissolved Zn in *M. edulis*. To the best of our knowledge, no studies have addressed the effects of Zn²⁺ exposure on anaerobic glycolysis of bivalves. In the Manila clam *Ruditapes philippinarum*, acute (48 h) exposure to 20 µg l⁻¹ Hg²⁺ led to accumulation of succinate and lactate indicating onset of partial anaerobiosis to compensate for insufficient aerobic ATP production (Liu et al., 2011). Likewise, activation of glycolysis (indicated by accumulation of succinate and lactate and depletion of glycogen) was reported in the green mussels *Perna perna* exposed to Cd (20 µg l⁻¹), Cu (50 µg l⁻¹), or a mixture of these metals (Wu and Wang, 2010). The lack of succinate accumulation in the blue mussels exposed to 100 µg l⁻¹ of nZnO or dissolved Zn (this study) indicates that these concentrations are within the tolerance range of the mussels requiring no compensatory increase in anaerobic glycolysis (Sokolova, 2013). This notion is in line with the generally recognized lower toxicity of Zn compared to Cd, Cu or Hg (Amiard et al., 1986; Jomova and Valko, 2011; Zalups and Koropatnick, 2010).

4.3. Effects of salinity regime on the FAA pool of the mussels

The free amino acids (FAAs) play important and multifarious roles in physiology of marine invertebrates including mollusks as compatible osmolytes, intermediaries in nitrogen excretion, energy sources, biosynthetic precursors (e.g. in gluconeogenesis) and building blocks for proteins. Therefore, shifts in the FAA profiles due to the abiotic stressors such as salinity or pollutants can have major impacts on the energy metabolism, nitrogen homeostasis and biosynthetic capacities of an organism. Our study indicates that acclimation to low salinity has a major impact on the size and the composition of the FAA pool of the blue mussels. This is also reflected in the strong differentiation of the metabolite profiles of the low salinity-acclimated mussels from both the normal and fluctuating salinity groups shown by the multivariate (PCA and discriminant) analyses. The total concentration of FAAs in the mussels' body decreased during acclimation to the low salinity reflecting the need for isosmotic cell volume regulation (Berger and Kharazova, 1997; Yancey, 2005). This decrease was largely due to the loss of glycine, a dominant amino acid in the FAA pool in *M. edulis*. As a result, the molecular diversity of the amino acid pool increased in the mussels acclimated to low salinity (to H ~ 2.5–2.6 compared with H ~ 1.9–2.1 at salinity 15) reflecting greater evenness of the relative FAA concentrations. Glycine is commonly used as a compatible osmolyte for isosmotic cell volume regulation in marine osmoconformers including mussels (Haider et al., 2019; Livingstone et al., 1979; Shumway et al., 1977; Zurburg and De Zwaan, 1981). Thus, in *M. edulis* from the Atlantic coast, an acute salinity downshift (32 → 10 or 30 → 15) led to a major decrease in the tissues Gly content (Livingstone et al., 1979; Shumway et al., 1977). Similarly, low-salinity acclimation of the sediment-dwelling soft shell clam *Mya arenaria* led to an ~98% decrease in the body Gly content, from ~1240 µg g⁻¹ body mass at salinity 15 to <30 µg g⁻¹ body mass at salinity 5 (Haider et al., 2019). A decrease in the concentrations of other, less abundant FAAs also contributes to the overall decrease in the tissue osmolyte content during salinity downshift in bivalves including *M. edulis*, but these contributions are quantitatively less important (Haider et al., 2019; Livingstone et al., 1979; Shumway et al., 1977; this study).

The body content of most FAA (14 out of 20 studied, including all essential amino acids) was preserved in the tissue of *M. edulis* acclimated to the low salinity despite an ~2.5-fold decrease in the total FAA pool. Likewise, in *M. edulis* from the Atlantic coast acclimated at the near-ocean salinity (30–32), most essential FAAs were conserved during acute hypoosmotic stress (salinity 15–10) except Thr and Arg that showed a modest decline (Livingstone et al., 1979; Shumway et al., 1977). The preferential conservation of essential FAAs during the salinity downshift could minimize the potential negative effect of isosmotic cell volume regulation under the lower salinity condition on biosynthetic capacities (including the protein synthesis) of the mussels. Interestingly, unlike the blue mussels, the Baltic soft-shell clams did not

conserve essential amino acids (except Arg) during 15 → 5 salinity downshift (Haider et al., 2019). This indicates that different species and/or populations of bivalves employ different strategies to balance the needs of osmoregulation and protein biosynthesis during hypoosmotic stress.

Acclimation to the fluctuating salinity (5–15) resulted in a decrease in the total concentration of the FAAs in the body of the Baltic *M. edulis* to the levels intermediate between those of the normal and low salinity groups. This decrease was mostly associated with the depletion of glycine in the mussel tissues. However, unlike low salinity acclimation, exposure to the fluctuating salinity led to a substantial (by ~50–60%) decrease in the body content of several essential amino acids including Leu, Ile and Phe in the body of *M. edulis*. It is worth noting that in our present study the samples for the FAA analysis were taken near the end of the high-salinity cycle of the fluctuating salinity regime (i.e. ~22 h after the 5 → 15 salinity upshift). Additional samples collected at the end of the low salinity cycle (i.e. ~22 h after the 15 → 5 salinity downshift) showed further significant decreases in the content of Asp, Glu and Tyr, as well as multiple essential amino acids (Lys, Val, Ile, Leu, Phe, and Try) in the mussels body (Supplementary Table 1). These findings indicate that unlike the constantly low salinity, exposure to fluctuating salinity might have a negative impact on protein biosynthesis of the mussels due to the potential limitation of essential amino acids.

4.4. Salinity-dependent effects of Zn on multibiomarker and FAA profiles of the mussels

Effects of nZnO and/or dissolved Zn exposures on the multibiomarker profile of the mussels were strongly dependent on the salinity context as shown by the significant ($P < 0.05$) salinity × Zn exposure interaction in ANOVA and the results of the multivariate analyses. Generally, the effects of dissolved Zn exposures on the biomarker profile of *M. edulis* were stronger than those on nZnO regardless of the salinity regime. The differentiation of the biomarker profiles of the Zn-exposed mussels from the control groups was pronounced at the normal salinity (15) and collapsed under the osmotic stress. Thus, the PCA analysis showed minimal overlap of the control mussels with the nZnO or Zn²⁺ exposed groups under the normal salinity conditions, whereas at the low salinity only Zn²⁺-exposed group was differentiated from the other two, and under the fluctuating salinity conditions the profiles of all three experimental groups overlapped (cf. Figs. 7A, 8A, and 9A). Furthermore, different biomarkers contributed to the separation of the control, nZnO and Zn²⁺-exposed groups depending on the salinity regime. Under the normal and constantly low salinity, multiple biomarkers (12 and 19 at salinities 15 and 5, respectively, including concentrations of several amino acids, TCA cycle intermediates and bioenergetic markers) significantly differentiated between the experimental treatment groups. Under the fluctuating salinity regime, only Asp, Ile, Val and Met concentrations contributed to the discriminant function separating the treatment groups. These findings indicate that none of the studied biomarkers is universally applicable for assessing the impacts of nZnO or Zn²⁺ exposures in the field populations of the mussels as the nature of the responsive biomarkers as well as the degree of response strongly depend on the ambient salinity.

Analysis of the changes in concentrations of individual FAAs supports the notion of the greater effects of dissolved Zn compared to nZnO on the amino acid metabolism of the mussels, as well as a strong dependence of these effects of ambient salinity. Generally, exposure to nZnO had no consistent effects on FAA levels in *M. edulis*. Thus, there was a modest but significant increase in Asp (at the normal and the fluctuating salinity), as well as decreases in Glu, Phe and Trp content (at the normal salinity only) in nZnO-exposed mussels, but no changes in the levels of other FAAs. Unlike nZnO, exposure to 100 µg l⁻¹ of dissolved Zn under the normal salinity (15) regime led to a depletion of several essential and non-essential amino acids including the most abundant

amino acid, Gly, as well as Ala, His, Phe, and Trp. Similar to salinity 15, fluctuating salinity combined with dissolved Zn exposure led to a decrease in the tissue content of Gly in the mussels. Depletion of Gly was also found in the Manila clam (*R. philippinarum*) exposed for 48 h to $20 \mu\text{g l}^{-1}$ of Hg^{2+} (Liu et al., 2011) and in the green mussels *Perna perna* exposed for 1–2 weeks to $20 \mu\text{g l}^{-1}$ of Cd^{2+} (Wu and Wang, 2010). Glycine and its derivatives are recognized as antioxidant and cytoprotective compounds in animals (Pérez-Torres et al., 2017; Razak et al., 2017) that protect against toxicity of trace metals including Cd, Co, Cu, Fe, As, Hg, Cr, and Pb (Heidari et al., 2018; Shafiekhani et al., 2019). The mechanisms of the cytoprotective action of glycine are not yet fully understood but are likely linked to its role as a precursor for the synthesis of glutathione, an essential antioxidant and metal-chelating agent in animals (Lu, 2013). Depletion of glycine in the bivalves exposed to dissolved Zn (this study), Hg^{2+} (Liu et al., 2011) or Cd^{2+} (Wu and Wang, 2010) might thus indicate increased synthesis of glutathione for metal detoxification. Furthermore, exposure to dissolved metals (including Hg, Cu, Ag and Cd) can suppress the transepithelial transport (and therefore inhibit uptake) of glycine as was shown in annelids *Enchytraeus albidus* and *Hediste (Nereis) diversicolor* (Siebers and Ehlers, 1979). Therefore, depletion of glycine in the tissues of Zn^{2+} exposed mussels in our present study might reflect a combination of suppressed uptake and increased utilization of this amino acid for detoxification purposes.

Tissue content of taurine was not affected by nZnO in *M. edulis* but significantly increased during exposure to dissolved Zn at the normal (15) and fluctuating (5–15) salinity. Taurine is an important osmolyte in bivalves (Yancey, 2005), and this increase could osmotically compensate for the loss of other FAAs in Zn^{2+} -exposed mussels. However, the compensation was incomplete, as shown by the lower total FAA content in Zn^{2+} exposed mussels compared to their control counterparts. Alternatively, upregulation of taurine might be a protective mechanism against mitochondrial damage and oxidative stress during Zn^{2+} exposures. In vertebrates including fish and mammals, taurine mitigates metal toxicity and suppresses metal accumulation as was shown in the goldfish exposed to cadmium (Choi et al., 2013) and in rats exposed to zinc, cadmium, aluminum, mercury or lead (Agha et al., 2014; Flora et al., 2004; Hwang and Wang, 2001; Yeh et al., 2009; Yeh et al., 2011). Furthermore, taurine improves mitochondrial function, enhances ATP synthesis capacity and mitigates ROS production in a variety of animals including bivalves (Hansen et al., 2010; Jong et al., 2012; Sokolov and Sokolova, 2019). Upregulation of taurine (or its precursor hypotaurine) has been found in marine mussels collected from a metal polluted area (Kwon et al., 2012) or experimentally exposed to metals (including cadmium, copper or mercury) in the lab (Liu et al., 2011; Wu and Wang, 2010; Zhang et al., 2011). Interestingly, the tissue levels of methionine sulfoxide (MetO) decreased in Zn^{2+} -exposed mussels (except under the conditions of the fluctuating salinity where MetO levels in the Zn^{2+} -exposed mussels were similar to the baseline). Methionine sulfoxide is formed by the oxidation of the thiol group in methionine and serves as a biomarker of the oxidative damage in the cell (Cabreiro et al., 2006). A decrease in MetO levels during exposure to dissolved Zn might thus indicate less oxidative damage to the proteins, possibly as a result of elevated levels of antioxidants such as taurine and glutathione.

Acclimation to low (5) salinity disrupted the responses of the FAA pool to nZnO and dissolved Zn in the mussels. Thus, unlike under the normal or fluctuating salinity, at low salinity there was no decline in Gly or increase in Tau in Zn^{2+} -exposed mussels compared to their control counterparts. Generally, the FAA levels in low-salinity acclimated mussels were preserved regardless of Zn exposures. These data indicate that the effects of extreme hypoosmotic stress (salinity 5, close to the lower tolerance limit of *M. edulis*) may overshadow the relatively minor impacts of sublethal exposures to metal-containing pollutants, precluding reliable detection of the pollutant-induced physiological stress.

4.5. Conclusions and outlook

Environmental salinity regime strongly affects metabolic homeostasis in a sentinel marine bivalve, the blue mussel *M. edulis*, and has strong implications for the physiological and biochemical responses to nanopollutants (nZnO) and dissolved Zn. Generally, fluctuating salinity (5–15) appeared bioenergetically less stressful than constantly hypoosmotic stress (salinity 5) in *M. edulis* indicating that even short (24 h) periods of recovery might be sufficient to restore the metabolic homeostasis in this euryhaline species. In our present study, the biological effects of nZnO and dissolved Zn (assessed by multiple metabolic biomarkers) became progressively less detectable as the salinity stress increased. In mussels, environmentally relevant concentrations ($100 \mu\text{g l}^{-1}$) of nZnO did not lead to strong disturbances in energy or intermediate metabolite homeostasis regardless of the salinity regime. Exposure to similar concentrations of dissolved Zn suppressed the mitochondrial OXPHOS capacity and coupling as well as anaerobic metabolism and modified the FAA profiles in mussels. These findings indicate that nZnO is metabolically less damaging to the Baltic Sea mussels than dissolved Zn. Similar to our present study, earlier research showed that the biomarker responses to a variety of pollutants (including nanoparticles) can be modified by temperature (Falfushynska et al., 2015; Falfushynska et al., 2019b; Falfushynska et al., 2018; Múgica et al., 2015; Wu et al., 2021), feeding (Blanco-Rayón et al., 2019a; Blanco-Rayón et al., 2019b), reproductive status (Blanco-Rayón et al., 2020; González-Fernández et al., 2017; Roznere et al., 2014), and salinity (Wu et al., 2020a). These findings have important implications for the multibiomarker-based assessment of the pollutant effects in marine sentinel organisms including systems-based approaches such as metabolomics (Campillo et al., 2015; Cappello et al., 2015; Deng et al., 2017; Digilio et al., 2016; Fasulo et al., 2012; Ji et al., 2016; Kwon et al., 2012; Liu et al., 2011; Lu et al., 2016; Vosloo et al., 2002), and emphasize the importance of establishing an environment-specific baseline for each sentinel population in which the biomarker-based stress assessment is to be conducted.

CRedit authorship contribution statement

Mirza Nusrat Noor: Methodology, Investigation, Data curation, Validation, Formal analysis, Writing – original draft, Writing – review & editing. **Fangli Wu:** Methodology, Investigation, Data curation, Validation, Funding acquisition, Writing – review & editing. **Eugene P. Sokolov:** Methodology, Investigation, Data curation, Validation, Formal analysis, Writing – review & editing. **Halina Falfushynska:** Investigation, Methodology, Data curation, Formal analysis, Funding Acquisition, Writing - review & editing. **Stefan Timm:** Methodology, Investigation, Data curation, Validation, Writing – review & editing. **Fouzia Haider:** Methodology, Investigation, Data curation, Validation, Writing – review & editing. **Inna M. Sokolova:** Conceptualization, Methodology, Visualization, Formal analysis, Supervision, Resources, Funding acquisition, Writing – original draft, Writing – review & editing.

Declaration of competing interest

The authors declare that they have no known competing financial interests or personal relationships that could have appeared to influence the work reported in this paper.

Acknowledgements

This work was in part supported by the Research Training Group 'Baltic TRANSCOAST' funded by the DFG (Deutsche Forschungsgemeinschaft) under grant number GRK 2000 to IMS, Alexander von Humboldt Fellowship to HF, Erasmus Mundus Program "European MSc in Marine Environment and Resources" to MNN, the China Scholarship Council (CSC) to FW, and the Leibniz Science Campus

“Phosphorus Research Rostock” to ES. We thank Fei Ye and Joydeep Dutta (KTH Royal Institute of Technology, Sweden) for their assistance with the nanoparticle characterization. The LC-MS equipment at the University of Rostock was funded through the Hochschulbauförderungsgesetz program (GZ: INST 264/125-1 FUGG). This is Baltic TRANSCOAST publication no. GRK2000/00042.

Appendix A. Supplementary data

Supplementary data to this article can be found online at <https://doi.org/10.1016/j.scitotenv.2021.145195>.

References

- Agha, F.E., Youness, E.R., Selim, M.M., Ahmed, H.H., 2014. Nephroprotective potential of selenium and taurine against mercuric chloride induced nephropathy in rats. *Ren. Fail.* 36, 704–716.
- Akberali, H.B., Earnshaw, M.J., 1982. Studies of the effects of zinc on the respiration of mitochondria from different tissues in the bivalve mollusc *Mytilus edulis* (L.). *Compar. Biochem. Physiol. C Compar. Pharmacol.* 72, 149–152.
- Amiard, J.C., Amiard-Triquet, C., Berthet, B., Métayer, C., 1986. Contribution to the ecotoxicological study of cadmium, lead, copper and zinc in the mussel *Mytilus edulis*. *Mar. Biol.* 90, 425–431.
- Auffan, M., Matson, C.W., Rose, J., Arnold, M., Proux, O., Fayard, B., Liu, W., Chaurand, P., Wiesner, M.R., Bottero, J.Y., et al., 2014. Salinity-dependent silver nanoparticle uptake and transformation by Atlantic killifish (*Fundulus heteroclitus*) embryos. *Nanotoxicology* 8, 167–176.
- Bayne, B.L., 2017. *Metabolic Expenditure*. vol. 41. Academic Press, London, pp. 331–415.
- Beegam, A., Prasad, P., Jose, J., Oliveira, M., Costa, F.G., Soares, A.M.V.M., Gonçalves, P.P., Trindade, T., Kalarikkal, N., Thomas, S., et al., 2016. Environmental fate of zinc oxide nanoparticles: risks and benefits. In: Soloneski, S., Larramendy, M. (Eds.), *Toxicology – New Aspects to This Scientific Conundrum*. InTech.
- Benito, D., Ahvo, A., Nuutinen, J., Bilbao, D., Saenz, J., Etxebarria, N., Lekube, X., Izagirre, U., Lehtonen, K.K., Marigómez, I., et al., 2019. Influence of season-dependent ecological variables on biomarker baseline levels in mussels (*Mytilus trossulus*) from two Baltic Sea subregions. *Sci. Total Environ.* 689, 1087–1103.
- Berger, V.J., Kharazova, A.D., 1997. Mechanisms of salinity adaptations in marine molluscs. In: Naumov, A.D., Hummel, H., Sukhotin, A.A., Ryland, J.S. (Eds.), *Interactions and Adaptation Strategies of Marine Organisms*. Springer Netherlands, Dordrecht, pp. 115–126.
- Beyer, J., Green, N., Brooks, S., Allan, I., Ruus, A., Gomes, T., Bråte, I.L., Schøyen, M., 2017. Blue mussels (*Mytilus edulis* spp.) as sentinel organisms in coastal pollution monitoring: a review. *Mar. Environ. Res.* 130.
- Blanco-Rayón, E., Guilhermino, L., Irazola, M., Ivanina, A.V., Sokolova, I.M., Izagirre, U., Marigómez, I., 2019a. The influence of short-term experimental fasting on biomarker responsiveness in oil WAF exposed mussels. *Aquat. Toxicol.* 206, 164–175.
- Blanco-Rayón, E., Ivanina, A.V., Sokolova, I.M., Marigómez, I., Izagirre, U., 2019b. Food-type may jeopardize biomarker interpretation in mussels used in aquatic toxicological experimentation. *PLoS One* 14, e0220661.
- Blanco-Rayón, E., Ivanina, A.V., Sokolova, I.M., Marigómez, I., Izagirre, U., 2020. Sex and sex-related differences in gamete development progression impinge on biomarker responsiveness in sentinel mussels. *Sci. Total Environ.* 740, 140178.
- Borgwardt, F., Robinson, L., Trauner, D., Teixeira, H., Nogueira, A.J.A., Lillebø, A.I., Piet, G., Kuemmerlen, M., O'Higgins, T., McDonald, H., et al., 2019. Exploring variability in environmental impact risk from human activities across aquatic ecosystems. *Sci. Total Environ.* 652, 1396–1408.
- Cabral, H., Fonseca, V., Sousa, T., Costa Leal, M., 2019. Synergistic effects of climate change and marine pollution: an overlooked interaction in coastal and estuarine areas. *Int. J. Environ. Res. Public Health* 16, 2737.
- Cabreiro, F., Picot, C.R., Friguet, B., Petropoulos, I., 2006. Methionine sulfoxide reductases: relevance to aging and protection against oxidative stress. *Ann. N. Y. Acad. Sci.* 1067, 37–44.
- Campillo, J.A., Sevilla, A., Albentosa, M., Bernal, C., Lozano, A.B., Cánovas, M., León, V.M., 2015. Metabolomic responses in caged clams, *Ruditapes decussatus*, exposed to agricultural and urban inputs in a Mediterranean coastal lagoon (Mar Menor, SE Spain). *Sci. Total Environ.* 524–525, 136–147.
- Canesi, L., Ciacci, C., Fabbri, R., Marcomini, A., Pojana, G., Gallo, G., 2012. Bivalve molluscs as a unique target group for nanoparticle toxicity. *Mar. Environ. Res.* 76, 16–21.
- Cappello, T., Maisano, M., Giannetto, A., Parrino, V., Mauceri, A., Fasulo, S., 2015. Neurotoxicological effects on marine mussel *Mytilus galloprovincialis* caged at petrochemical contaminated areas (eastern Sicily, Italy): 1H NMR and immunohistochemical assays. *Compar. Biochem. Physiol. C Toxicol. Pharmacol.* 169, 7–15.
- Choi, K.-S., Yoo, I.-S., Shin, K.-O., Chung, K.-H., 2013. Effects of taurine on cadmium exposure in muscle, gill, and bone tissues of Carassius auratus. *Nutr. Res. Pract.* 7, 22–25.
- Cloern, J.E., Abreu, P.C., Carstensen, J., Chauvaud, L., Elmgren, R., Grall, J., Greening, H., Johansson, J.O.R., Kahru, M., Sherwood, E.T., et al., 2016. Human activities and climate variability drive fast-paced change across the world's estuarine-coastal ecosystems. *Glob. Chang. Biol.* 22, 513–529.
- Coll, C., Notter, D., Gottschalk, F., Sun, T., Som, C., Nowack, B., 2016. Probabilistic environmental risk assessment of five nanomaterials (nano-TiO₂, nano-Ag, nano-ZnO, CNT, and fullerenes). *Nanotoxicology* 10, 436–444.
- De Vooy, C.G.N., Holwerda, D.A., 1986. Anaerobic metabolism in sublittoral living *Mytilus galloprovincialis* lam. In the Mediterranean—III. The effect of anoxia and osmotic stress on some kinetic parameters of adductor muscle pyruvate kinase. *Compar. Biochem. Physiol. B Compar. Biochem.* 85, 217–221.
- DeCoen, W.M., Janssen, C.R., 1997. The use of biomarkers in *Daphnia magna* toxicity testing. 2. Digestive enzyme activity in *Daphnia magna* exposed to sublethal concentrations of cadmium, chromium and mercury. *Chemosphere* 35, 1053–1067.
- Deng, Y., Zhang, Y., Lemos, B., Ren, H., 2017. Tissue accumulation of microplastics in mice and biomarker responses suggest widespread health risks of exposure. *Sci. Rep.* 7, 46687.
- Digilio, G., Sforzini, S., Cassino, C., Robotti, E., Oliveri, C., Marengo, E., Musso, D., Osella, D., Viarengo, A., 2016. Haemolymph from *Mytilus galloprovincialis*: response to copper and temperature challenges studied by ¹H-NMR metabolomics. *Compar. Biochem. Physiol. C Toxicol. Pharmacol.* 183–184, 61–71.
- Dineley, K.E., Votyakova, T.V., Reynolds, I.J., 2003. Zinc inhibition of cellular energy production: implications for mitochondria and neurodegeneration. *J. Neurochem.* 85, 563–570.
- Doerrier, C., Garcia-Souza, L.F., Krumschnabel, G., Wohlfarter, Y., Mészáros, A.T., Gnaiger, E., 2018. High-resolution Fluorescence Respirometry and OXPHOS protocols for human cells, permeabilized fibers from small biopsies of muscle, and isolated mitochondria. In: Palmeira, C.M., Moreno, A.J. (Eds.), *Mitochondrial Bioenergetics: Methods and Protocols*. Springer New York, New York, NY, pp. 31–70.
- Falfushynska, H., Gnatyshyna, L., Yurchak, I., Sokolova, I., Stoliar, O., 2015. The effects of zinc nanoxide on cellular stress responses of the freshwater mussels *Unio tumidus* are modulated by elevated temperature and organic pollutants. *Aquat. Toxicol.* 162, 82–93.
- Falfushynska, H., Sokolov, E.P., Haider, F., Oppermann, C., Kragl, U., Ruth, W., Stock, M., Glufke, S., Winkel, E.J., Sokolova, I.M., 2019a. Effects of a common pharmaceutical, atorvastatin, on energy metabolism and detoxification mechanisms of a marine bivalve *Mytilus edulis*. *Aquat. Toxicol.* 208, 47–61.
- Falfushynska, H.L., Gnatyshyna, L.L., Ivanina, A.V., Sokolova, I.M., Stoliar, O.B., 2018. Detoxification and cellular stress responses of unionid mussels *Unio tumidus* from two cooling ponds to combined nano-ZnO and temperature stress. *Chemosphere* 193, 1127–1142.
- Falfushynska, H.L., Gnatyshyna, L.L., Ivanina, A.V., Khoma, V.V., Stoliar, O.B., Sokolova, I.M., 2019b. Bioenergetic responses of freshwater mussels *Unio tumidus* to the combined effects of nano-ZnO and temperature regime. *Sci. Total Environ.* 650, 1440–1450.
- Falfushynska, H.L., Wu, F., Ye, F., Kasianchuk, N., Dutta, J., Dobretsov, S., Sokolova, I.M., 2019c. The effects of ZnO nanostructures of different morphology on bioenergetics and stress response biomarkers of the blue mussels *Mytilus edulis*. *Sci. Total Environ.* 694, 133717.
- Falfushynska, H.L., Wu, F., Ye, F., Kasianchuk, N., Dutta, J., Dobretsov, S., Sokolova, I.M., 2019d. The effects of ZnO nanostructures of different morphology on bioenergetics and stress response biomarkers of the blue mussels *Mytilus edulis*. *Sci. Total Environ.* 694, 133717.
- Fasulo, S., Iacono, F., Cappello, T., Corsaro, C., Maisano, M., D'Agata, A., Giannetto, A., De Domenico, E., Parrino, V., Lo Paro, G., et al., 2012. Metabolomic investigation of *Mytilus galloprovincialis* (Lamarck 1819) caged in aquatic environments. *Ecotoxicol. Environ. Saf.* 84, 139–146.
- Fitzgerald, L.M., Szmant, A.M., 1997. Biosynthesis of 'essential' amino acids by scleractinian corals. *Biochem. J.* 322 (Pt 1), 213–221.
- Flora, S.J., Pande, M., Bhaduria, S., Kannan, G.M., 2004. Combined administration of taurine and meso 2,3-dimercaptosuccinic acid in the treatment of chronic lead intoxication in rats. *Hum. Exp. Toxicol.* 23, 157–166.
- Gnaiger, E., 1983. Calculation of energetic and biochemical equivalents of respiratory oxygen consumption. In: Gnaiger, E., Forstner, H. (Eds.), *Polarographic Oxygen Sensors: Aquatic and Physiological Applications*. Springer Berlin Heidelberg, Berlin, Heidelberg, pp. 337–345.
- Gnaiger, E., Lassnig, B., Kuznetsov, A., Rieger, G., Margreiter, R., 1998a. Mitochondrial oxygen affinity, respiratory flux control and excess capacity of cytochrome c oxidase. *J. Exp. Biol.* 201, 1129–1139.
- Gnaiger, E., Lassnig, B., Kuznetsov, A.V., Margreiter, R., 1998b. Mitochondrial respiration in the low oxygen environment of the cell effect of ADP on oxygen kinetics. *Biochim. Biophys. Acta (BBA) Bioenerg.* 1365, 249–254.
- González-Fernández, C., Albentosa, M., Sokolova, I., 2017. Interactive effects of nutrition, reproductive state and pollution on molecular stress responses of mussels, *Mytilus galloprovincialis* Lamarck, 1819. *Mar. Environ. Res.* 131, 103–115.
- Gosling, E.M., 1992. *The Mussel Mytilus: Ecology, Physiology, Genetics, and Culture*. Elsevier, Amsterdam, New York.
- Gottschalk, F., Sonderer, T., Scholz, R.W., Nowack, B., 2009. Modeled environmental concentrations of engineered nanomaterials (TiO₂, ZnO, Ag, CNT, fullerenes) for different regions. *Environ. Sci. Technol.* 43, 9216–9222.
- Gottschalk, F., Lassen, C., Kjoelholm, J., Christensen, F., Nowack, B., 2015. Modeling flows and concentrations of nine engineered nanomaterials in the Danish environment. *Int. J. Environ. Res. Public Health* 12, 5581–5602.
- Haider, F., Sokolov, E.P., Sokolova, I.M., 2018. Effects of mechanical disturbance and salinity stress on bioenergetics and burrowing behavior of the soft-shell clam *Mya arenaria*. *J. Exp. Biol.* 221.
- Haider, F., Sokolov, E.P., Timm, S., Hagemann, M., Blanco Rayón, E., Marigómez, I., Izagirre, U., Sokolova, I.M., 2019. Interactive effects of osmotic stress and burrowing activity on protein metabolism and muscle capacity in the soft shell clam *Mya arenaria*. *Comp. Biochem. Physiol. A Mol. Integr. Physiol.* 228, 81–93.
- Haider, F., Falfushynska, H.L., Timm, S., Sokolova, I.M., 2020. Effects of hypoxia and reoxygenation on intermediary metabolite homeostasis of marine bivalves *Mytilus edulis* and *Crasostrea gigas*. *Comp. Biochem. Physiol. A Mol. Integr. Physiol.* 242, 110657.

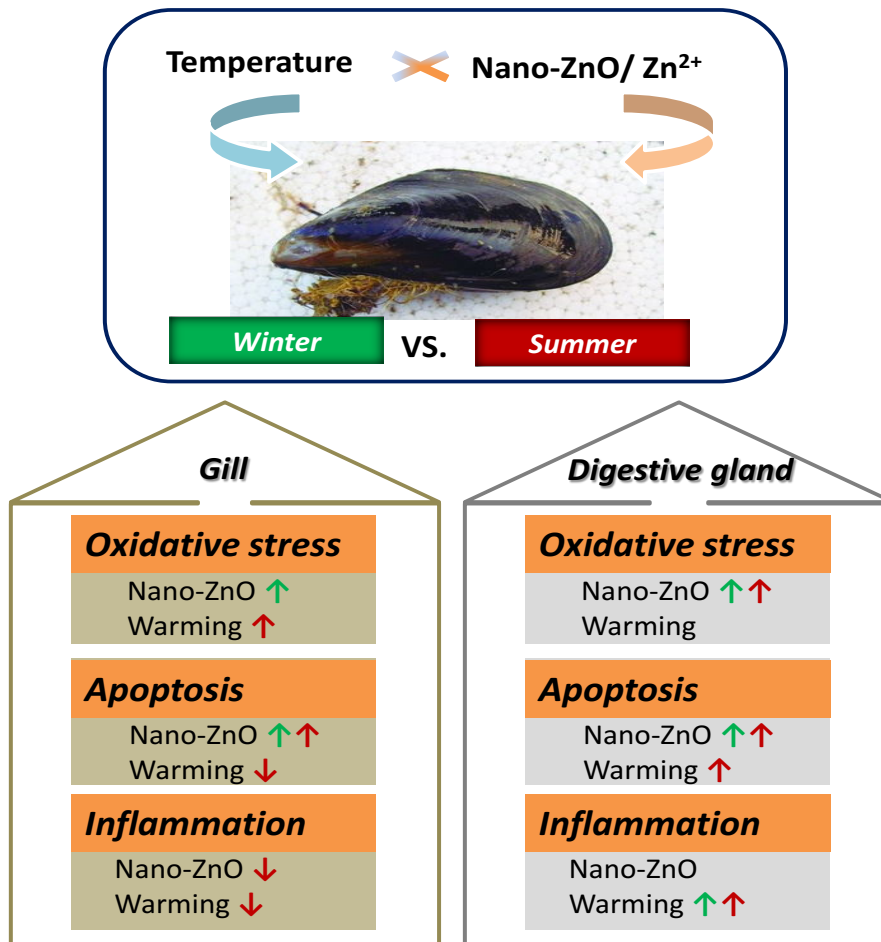
- Hanna, S.K., Miller, R.J., Muller, E.B., Nisbet, R.M., Lenihan, H.S., 2013. Impact of engineered zinc oxide nanoparticles on the individual performance of *Mytilus galloprovincialis*. *PLoS One* 8, e61800.
- Hansen, S.H., Andersen, M.L., Cornett, C., Gradinaru, R., Grunnet, N., 2010. A role for taurine in mitochondrial function. *J. Biomed. Sci.* 17, S23.
- Heidari, R., Mohammadi, H., Ahmadi, A., Ghanbarinejad, V., Kasra, F., Khosravi, A., 2018. Protective effect of glycine and tri-methyl glycine (betaine) against heavy metals-induced oxidative stress in liver-derived post-nuclear supernatant (PNS). *Trends Pharm. Sci.* 4.
- HELCOM, 2016. Hydrography and Oxygen in the Deep Sea Basins.
- Hwang, D.-F., Wang, L., 2001. Effect of taurine on toxicity of cadmium in rats. *Toxicology* 167, 173–180.
- Jansson, A.-M., Kautsky, N., 1977. Quantitative survey of hard bottom communities in a Baltic archipelago. In: Ceidigh, B.F., Keegan P.O., Boaden, P.J.S. (Eds.), *Biology of Benthic Organisms*. Pergamon, pp. 359–366.
- Ji, C., Wang, Q., Wu, H., Tan, Q., Wang, W.-X., 2016. A metabolomic study on the biological effects of metal pollutants in oysters *Crassostrea sikamea*. *Mar. Pollut. Bull.* 102, 216–222.
- Jomova, K., Valko, M., 2011. Advances in metal-induced oxidative stress and human disease. *Toxicology* 283, 65–87.
- Jong, C.J., Azuma, J., Schaffer, S., 2012. Mechanism underlying the antioxidant activity of taurine: prevention of mitochondrial oxidant production. *Amino Acids* 42, 2223–2232.
- Kwon, Y.K., Jung, Y.S., Park, J.C., Seo, J., Choi, M.S., Hwang, G.S., 2012. Characterizing the effect of heavy metal contamination on marine mussels using metabolomics. *Mar. Pollut. Bull.* 64, 1874–1879.
- Lemieux, H., Blier, P.U., Gnaiger, E., 2017. Remodeling pathway control of mitochondrial respiratory capacity by temperature in mouse heart: electron flow through the Q-junction in permeabilized fibers. *Sci. Rep.* 7, 2840.
- Lemire, J., Mailloux, R., Appanna, V.D., 2008. Zinc toxicity alters mitochondrial metabolism and leads to decreased ATP production in hepatocytes. *J. Appl. Toxicol.* 28, 175–182.
- Li, J.-h., Liu, X.-r., Zhang, Y., Tian, F.-f., Zhao, G.-y., Yu, Q.-l.-y., Jiang, F.-l., Liu, Y., 2012. Toxicity of nano zinc oxide to mitochondria. *Toxicol. Res.* 1, 137–144.
- Liu, X., Zhang, L., You, L., Cong, M., Zhao, J., Wu, H., Li, C., Liu, D., Yu, J., 2011. Toxicological responses to acute mercury exposure for three species of Manila clam *Ruditapes philippinarum* by NMR-based metabolomics. *Environ. Toxicol. Pharmacol.* 31, 323–332.
- Livingstone, D.R., Widdows, J., Fieth, P., 1979. Aspects of nitrogen metabolism of the common mussel *Mytilus edulis*: adaptation to abrupt and fluctuating changes in salinity. *Mar. Biol.* 53, 41–55.
- Lobel, P.B., Bajdik, C.D., Belkhole, S.P., Jackson, S.E., Longrich, H.P., 1991. Improved protocol for collecting mussel watch specimens taking into account sex, size, condition, shell shape, and chronological age. *Arch. Environ. Contam. Toxicol.* 21, 409–414.
- Lu, S.C., 2013. Glutathione synthesis. *Biochim. Biophys. Acta Gen. Subj.* 1830, 3143–3153.
- Lu, Y., Zhang, Y., Deng, Y., Jiang, W., Zhao, Y., Geng, J., Ding, L., Ren, H., 2016. Uptake and accumulation of polystyrene microplastics in zebrafish (*Danio rerio*) and toxic effects in liver. *Environ. Sci. Technol.* 50, 4054–4060.
- Martínez-Carmona, M., Gun'ko, Y., Vallet-Regí, M., 2018. ZnO nanostructures for drug delivery and theranostic applications. *Nanomaterials (Basel, Switzerland)* 8, 268.
- Moreno, A., Amelung, B., 2009. Climate change and tourist comfort on Europe's beaches in summer: a reassessment. *Coast. Manag.* 37, 550–568.
- Mos, B., Kaposi, K.L., Rose, A.L., Kelaher, B., Dworjanyan, S.A., 2017. Moderate ocean warming mitigates, but more extreme warming exacerbates the impacts of zinc from engineered nanoparticles on a marine larva. *Environ. Pollut.* 228, 190–200.
- Múgica, M., Sokolova, I.M., Izagirre, U., Marigómez, I., 2015. Season-dependent effects of elevated temperature on stress biomarkers, energy metabolism and gamete development in mussels. *Mar. Environ. Res.* 103, 1–10.
- Muller, E.B., Hanna, S.K., Lenihan, H.S., Miller, R.J., Nisbet, R.M., 2014. Impact of engineered zinc oxide nanoparticles on the energy budgets of *Mytilus galloprovincialis*. *J. Sea Res.* 94, 29–36.
- Narayanan, P.M., Wilson, W.S., Abraham, A.T., Sevanan, M., 2012. Synthesis, characterization, and antimicrobial activity of zinc oxide nanoparticles against human pathogens. *BioNanoScience* 2, 329–335.
- Németh-Cahalan, K.L., Kalman, K., Froger, A., Hall, J.E., 2007. Zinc modulation of water permeability reveals that aquaporin 0 functions as a cooperative tetramer. *J. Gen. Physiol.* 130, 457–464.
- Ortiz-Burgos, S., 2016. Shannon-weaver diversity index. In: Kennish, M.J. (Ed.), *Encyclopedia of Estuaries*. Springer Netherlands, Dordrecht, pp. 572–573.
- Park, J., Kim, S., Yoo, J., Lee, J.-S., Park, J.-W., Jung, J., 2014. Effect of salinity on acute copper and zinc toxicity to *Tigriopus japonicus*: the difference between metal ions and nanoparticles. *Mar. Pollut. Bull.* 85, 526–531.
- Pérez-Torres, I., Zúñiga-Muñoz, A.M., Guarnier-Lans, V., 2017. Beneficial effects of the amino acid glycine. *Mini-Rev. Med. Chem.* 17, 15–32.
- Piccinno, F., Gottschalk, F., Seeger, S., Nowack, B., 2011. Industrial Production Quantities and Uses of Ten Engineered Nanomaterials in Europe and the World.
- Pivovarova, N.B., Stanika, R.I., Kazanina, G., Villanueva, I., Andrews, S.B., 2014. The interactive roles of zinc and calcium in mitochondrial dysfunction and neurodegeneration. *J. Neurochem.* 128, 592–602.
- Razak, M.A., Begum, P.S., Viswanath, B., Rajagopal, S., 2017. Multifarious beneficial effect of nonessential amino acid, glycine: a review. *Oxidative Med. Cell. Longev.* 2017, 1716701.
- Riisgård, H.U., Lüsrow, F., Pleissner, D., Lundgreen, K., López, M.Á.P., 2013. Effect of salinity on filtration rates of mussels *Mytilus edulis* with special emphasis on dwarfed mussels from the low-saline Central Baltic Sea. *Helgol. Mar. Res.* 67, 591–598.
- Roznere, I., Watters, G.T., Wolfe, B.A., Daly, M., 2014. Nontargeted metabolomics reveals biochemical pathways altered in response to captivity and food limitation in the freshwater mussel *Amblema plicata*. *Compar. Biochem. Physiol. D Genom. Proteom.* 12, 53–60.
- Rykol, J., Arnold, W.M., Zimmermann, U., 1992. Zinc and salinity effects on membrane transport in *Chara connivens*. *Plant Cell Environ.* 15, 11–23.
- Saz, H.J., 1971. Facultative anaerobiosis in the invertebrates: pathways and control systems. *Am. Zool.* 11, 125–135.
- Shafiekhani, M., Ommati, M.M., Azarpira, N., Heidari, R., Salarian, A.A., 2019. Glycine supplementation mitigates lead-induced renal injury in mice. *J. Exp. Pharmacol.* 11, 15–22.
- Shumway, S.E., Gabbott, P.A., Youngson, A., 1977. The effect of fluctuating salinity on the concentrations of free amino acids and ninhydrin-positive substances in the adductor muscles of eight species of bivalve molluscs. *J. Exp. Mar. Biol. Ecol.* 29, 131–150.
- Siebers, D., Ehlers, U., 1979. Heavy metal action on transintegumentary absorption of glycine in two annelid species. *Mar. Biol.* 50, 175–179.
- Sokolov, E.P., Sokolova, I.M., 2019. Compatible osmolytes modulate mitochondrial function in a marine osmoconformer *Crassostrea gigas* (Thunberg, 1793). *Mitochondrion* 45, 29–37.
- Sokolova, I.M., 2013. Energy-limited tolerance to stress as a conceptual framework to integrate the effects of multiple stressors. *Integr. Comp. Biol.* 53, 597–608.
- Sokolova, I.M., Lannig, G., 2008. Interactive effects of metal pollution and temperature on metabolism in aquatic ectotherms: implications of global climate change. *Clim. Res.* 37, 181–201.
- Sokolova, I.M., Sukhotin, A.A., Lannig, G., 2011. Stress effects on metabolism and energy budgets in mollusks. In: Abele, D., Zenteno-Savín, T., Vazquez-Medina, J. (Eds.), *Oxidative Stress in Aquatic Ecosystems*. Blackwell Wiley, Boston etc., pp. 263–280.
- Sokolova, I.M., Frederich, M., Bagwe, R., Lannig, G., Sukhotin, A.A., 2012. Energy homeostasis as an integrative tool for assessing limits of environmental stress tolerance in aquatic invertebrates. *Mar. Environ. Res.* 79, 1–15.
- Sridhar, B.B.M., Han, F.X., Diehl, S.V., Monts, D.L., Su, Y., 2007. Effects of Zn and Cd accumulation on structural and physiological characteristics of barley plants. *Braz. J. Plant Physiol.* 19, 15–22.
- Stigebrandt, A., 2001. Physical oceanography of the Baltic Sea. In: Wulff, F.V., Rahm, L.A., Larsson, P. (Eds.), *A Systems Analysis of the Baltic Sea, Vol. 148: Ecological Studies (Analysis and Synthesis)*. Springer, Berlin, Heidelberg.
- Stoller, M., Ochando-Pulido, J., 2020. ZnO Nano-particles production intensification by means of a spinning disk reactor. *Nanomaterials* 10, 1321.
- Stuckas, H., Knöbel, L., Schade, H., Breusing, C., Hinrichsen, H.-H., Bartel, M., Langguth, K., Melzner, F., 2017. Combining hydrodynamic modelling with genetics: can passive larval drift shape the genetic structure of Baltic *Mytilus* populations? *Mol. Ecol.* 26, 2765–2782.
- Tovar-Sánchez, A., Sánchez-Quiles, D., Basterretxea, G., Benedé, J.L., Chisvert, A., Salvador, A., Moreno-Garrido, I., Blasco, J., 2013. Sunscreen products as emerging pollutants to coastal waters. *PLoS One* 8, e65451.
- US EPA, 2002. National Recommended Water Quality Criteria EPA-822-R-02-047. Office of Science and Technology.
- Verslycke, T., Roast, S.D., Widdows, J., Jones, M.B., Janssen, C.R., 2004. Cellular energy allocation and scope for growth in the estuarine mysid *Neomysis integer* (Crustacea: Mysidacea) following chlorpyrifos exposure: a method comparison. *J. Exp. Mar. Biol. Ecol.* 306, 1–16.
- Vosloo, A., van Aardt, W.J., Mienie, L.J., 2002. Sublethal effects of copper on the freshwater crab *Potamonautes warreni*. *Compar. Biochem. Physiol. Pt A Mol. Integr. Physiol.* 133, 695–702.
- Wang, J., Wang, W.-x., 2014. Salinity influences on the uptake of silver nanoparticles and silver nitrate by marine medaka (*Oryzias latipes*): salinity influences on silver nanoparticle uptake by marine medaka. *Environ. Toxicol. Chem.* 33, 632–640.
- Wu, F., Cui, S., Sun, M., Xie, Z., Huang, W., Huang, X., Liu, L., Hu, M., Lu, W., Wang, Y., 2018. Combined effects of ZnO NPs and seawater acidification on the haemocyte parameters of thick shell mussel *Mytilus coruscus*. *Sci. Total Environ.* 624, 820–830.
- Wu, F., Falfushynska, H., Dellwig, O., Piontkivska, H., Sokolova, I.M., 2020a. Interactive effects of salinity variation and exposure to ZnO nanoparticles on the innate immune system of a sentinel marine bivalve, *Mytilus edulis*. *Sci. Total Environ.* 712, 136473.
- Wu, F., Falfushynska, H., Dellwig, O., Piontkivska, H., Sokolova, I.M., 2020b. Interactive effects of salinity variation and exposure to ZnO nanoparticles on the innate immune system of a sentinel marine bivalve, *Mytilus edulis*. *Sci. Total Environ.* 712, 136473.
- Wu, F., Sokolov, E.P., Dellwig, O., Sokolova, I.M., 2021. Season-dependent effects of ZnO nanoparticles and elevated temperature on bioenergetics of the blue mussel *Mytilus edulis*. *Chemosphere* 263, 127780.
- Wu, H., Wang, W.-X., 2010. NMR-based metabolomic studies on the toxicological effects of cadmium and copper on green mussels *Perna viridis*. *Aquat. Toxicol.* 100, 339–345.
- Yamaguchi, M., Kura, M., Okada, S., 1981. Zinc accumulation and succinate dehydrogenase activation in hepatic mitochondria of rats orally administered zinc sulfate. *Chem. Pharm. Bull. (Tokyo)* 29, 2370–2374.
- Yamaguchi, M., Kura, M., Okada, S., 1982. Role of zinc as an activator of mitochondrial function in rat liver. *Biochem. Pharmacol.* 31, 1289–1293.
- Yancey, P.H., 2005. Organic osmolytes as compatible, metabolic and counteracting cytoprotectants in high osmolarity and other stresses. *J. Exp. Biol.* 208, 2819–2830.
- Yeh, Y.H., Lee, Y.T., Hsieh, Y.L., Hwang, D.F., 2011. Dietary taurine reduces zinc-induced toxicity in male Wistar rats. *J. Food Sci.* 76, T90–T98.
- Yeh, Y.-H., Lee, Y.-T., Hsieh, H.-S., Hwang, D.-F., 2009. Effect of taurine on toxicity of aluminum in rats. *Eur. e-J. Clin. Nutr. Metab.* 4, e187–e192.
- Yung, M.M.N., Wong, S.W.Y., Kwok, K.W.H., Liu, F.Z., Leung, Y.H., Chan, W.T., Li, X.Y., Djuricic, A.B., Leung, K.M.Y., 2015. Salinity-dependent toxicities of zinc oxide nanoparticles to the marine diatom *Thalassiosira pseudonana*. *Aquat. Toxicol.* 165, 31–40.
- Yung, M.M.N., Kwok, K.W.H., Djuricic, A.B., Giesy, J.P., Leung, K.M.Y., 2017. Influences of temperature and salinity on physicochemical properties and toxicity of zinc oxide nanoparticles to the marine diatom *Thalassiosira pseudonana*. *Sci. Rep.* 7.

- Zalups, R.K., Koropatnick, J., 2010. Cellular and Molecular Biology of Metals. CRC Press, Taylor & Francis Corp., Boca Raton, London, New York.
- Zammit, V.A., Newsholme, E.A., 1978. Properties of pyruvate kinase and phosphoenolpyruvate carboxykinase in relation to the direction and regulation of phosphoenolpyruvate metabolism in muscles of the frog and marine invertebrates. *Biochem. J.* 174, 979–987.
- Zhang, L., Liu, X., You, L., Zhou, D., Wu, H., Li, L., Zhao, J., Feng, J., Yu, J., 2011. Metabolic responses in gills of Manila clam *Ruditapes philippinarum* exposed to copper using NMR-based metabolomics. *Mar. Environ. Res.* 72, 33–39.
- Zurburg, W., De Zwaan, A., 1981. The role of amino acids in anaerobiosis and osmoregulation in bivalves. *J. Exp. Zool.* 215, 315–325.

7.5. Interactive effects of ZnO nanoparticles and temperature on molecular and cellular stress responses of the blue mussel *Mytilus edulis*

Wu, FL, Sokolov, E. P., Khomich, A., Fettkenhauer, C., Schnell, G., Seitz, H. and Sokolova, I. M. (2021). *Science of The Total Environment* 818, 151785.

DOI: <https://doi.org/10.1016/j.scitotenv.2021.151785>





Interactive effects of ZnO nanoparticles and temperature on molecular and cellular stress responses of the blue mussel *Mytilus edulis*



Fangli Wu^a, Eugene P. Sokolov^b, Andrei Khomich^{a,c}, Christian Fettkenhauer^d, Georg Schnell^e, Hermann Seitz^{e,f}, Inna M. Sokolova^{a,g,*}

^a Department of Marine Biology, Institute for Biological Sciences, University of Rostock, Rostock, Germany

^b Leibniz Institute for Baltic Sea Research, Leibniz Science Campus Phosphorus Rostock, Warnemünde, Germany

^c International Sakharov Environmental Institute of Belarusian State University, Minsk, Belarus

^d Anton Paar Germany GmbH, Ostfildern, Germany

^e Microfluidics, Faculty of Mechanical Engineering and Marine Technology, University of Rostock, Rostock, Germany

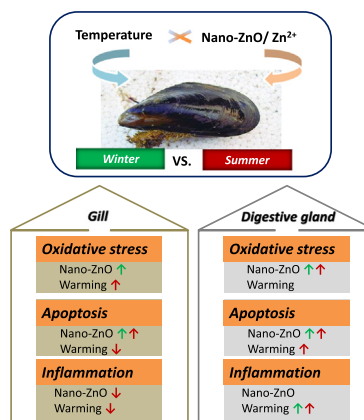
^f Department Life, Light & Matter, University of Rostock, Rostock, Germany

^g Department of Maritime Systems, Interdisciplinary Faculty, University of Rostock, Rostock, Germany

HIGHLIGHTS

- Interactive effects of temperature and nano-ZnO on mussels were investigated.
- Nano-ZnO caused oxidative injury and induced apoptosis.
- No significant inflammatory response to nano-ZnO was observed.
- Dissolved Zn appeared less toxic than nano-ZnO.
- The cellular stress response to nano-ZnO was modified by warming and season.

GRAPHICAL ABSTRACT



ARTICLE INFO

Article history:

Received 31 August 2021

Received in revised form 4 November 2021

Accepted 14 November 2021

Available online 19 November 2021

Editor: Julian Blasco

Keywords:

Temperature

Nano-ZnO

Mussel

ABSTRACT

Temperature is an important abiotic factor that modulates all aspects of ectotherm physiology, including sensitivity to pollutants. Nanoparticles are emerging pollutants in coastal environments, and their potential to cause toxicity in marine organisms is a cause for concern. Here we studied the interactive effects of temperature (including seasonal and experimental warming) on sublethal toxicity of ZnO nanoparticles (nano-ZnO) in a model marine bivalve, the blue mussel *Mytilus edulis*. Molecular markers were used to assess the pollutant-induced cellular stress responses in the gills and the digestive gland of mussels exposed for 21 days to $10 \mu\text{g l}^{-1}$ and $100 \mu\text{g l}^{-1}$ of nano-ZnO or dissolved Zn under different temperature regimes including ambient temperature (10°C and 15°C in winter and summer, respectively) or experimental warming ($+5^\circ\text{C}$). Exposure to high concentration ($100 \mu\text{g l}^{-1}$) of nano-ZnO caused oxidative injury to proteins and lipids and induced a marked apoptotic response indicated by increased transcript levels of apoptosis-related genes p53, caspase 3 and the MAPK pathway (JNK and p38) and decreased mRNA expression of anti-apoptotic Bcl-2. No significant induction of inflammatory cytokine-related response (TGF- β and NF- κ B) of tissues was observed in nano-ZnO

Abbreviations: ZnO nanoparticles, nano-ZnO; LPO, lipid peroxidation; PC, protein carbonyls; p53, tumor protein p53; p38, p38 mitogen-activated protein kinases; JNK, c-Jun N-terminal kinase; COX, cyclooxygenase; Bcl-2, B-cell lymphoma2; NF- κ B, nuclear factor κ B (p100/p105); TGF- β , transforming growth factor-beta.

* Corresponding author at: Department of Maritime Systems, Interdisciplinary Faculty, University of Rostock, Rostock, Germany.

E-mail address: inna.sokolova@uni-rostock.de (I.M. Sokolova).

Gill
 Digestive gland
 Seasonality
 Oxidative stress
 Apoptosis
 Inflammation

exposed-mussels. Furthermore, the oxidative injury and apoptotic response could differentiate the effects of nano-ZnO from those of dissolved Zn in the mussels. This study revealed that oxidative stress and stress-related transcriptional responses to nano-ZnO were strongly modified by warming and season in the mussels. No single biomarker could be shown to consistently respond to nano-ZnO in all experimental groups, which implies that multiple biomarkers are needed to assess nano-ZnO toxicity to marine organisms under the variable environmental conditions of coastal habitats.

© 2021 Elsevier B.V. All rights reserved.

1. Introduction

With the widespread application and release of manufactured nanomaterials, nanoparticles accumulate in the coastal and marine environments posing a potential threat to marine organisms and human health (Garner and Keller, 2014; Williams et al., 2019). Coastal marine ecosystems are particularly vulnerable to emerging pollutants including nanoparticles as they serve as a sink of (nano)pollutants from terrestrial and riverine sources (Linders et al., 2018; Williams et al., 2019). Zinc oxide nanoparticles (nano-ZnO) are used in various products (Williams et al., 2019), and raise concerns due to their high predicted environmental concentrations and potential toxicity (Coll et al., 2016; Hong et al., 2021). There is increasing evidence of ecotoxicity of nano-ZnO in marine ecosystems (Czyżowska and Barbasz, 2020; Katsumiti et al., 2016; Li et al., 2018; Ma et al., 2013; Wu et al., 2020; Yung et al., 2017), but the impacts and mechanisms of nano-ZnO toxicity are not yet well understood.

The toxic mechanisms of nanoparticles have been extensively investigated in the context of nanomaterials safety and the potential risks to human health (Gerloff et al., 2017; Halappanavar et al., 2020). These studies made clear that traditional toxicology approaches to hazard and risk assessment of individual nanomaterials are unfeasible due to enormous diversity of nanoparticles and their derivatives (Costa and Fadeel, 2016; Halappanavar et al., 2020). The challenge is even greater in ecotoxicology where the diversity of affected organisms and their environments needs to be taken into account. These challenges make the mechanistic understanding of the nanoparticle toxicity especially important as it allows predicting adverse organismal outcomes based on the perturbation of cellular stress response pathways that can be measured more easily, reliably and often non-invasively (Gerloff et al., 2017; Halappanavar et al., 2020). Studies in humans and mammalian models showed that the key molecular events in nanoparticle toxicity involve oxidative stress, stimulation of pro-inflammatory responses, and dysregulation of cell survival pathways that might lead to the damage of target organs, morbidity or mortality (Gerloff et al., 2017; Halappanavar et al., 2020; Luo et al., 2020). Earlier studies in aquatic organisms indicated that similar pathways (including apoptosis, inflammation and redox misbalance) might also be involved in nanoparticle toxicity during environmental exposures in water and sediment (Castro-Bugallo et al., 2014; Falfushynska et al., 2019a; Marisa et al., 2016; Schiavo et al., 2016; Wu et al., 2020). However, the flexibility and robustness of the cellular stress response mechanisms under the conditions of natural environmental variability such as fluctuations of temperature, that can affect the organisms' physiology as well as the behavior of nanomaterials are not well understood (Ma et al., 2013; Yung et al., 2014). This gap in knowledge limits our ability to assess the nanoparticle toxicity to marine organisms and predict their adverse outcomes in polluted coastal ecosystems.

Temperature is a key abiotic factor that affects ectotherms' physiology (Schiedek et al., 2007) and modulate the toxic responses of organisms (Sokolova and Lannig, 2008). Surface seawater temperature naturally varies in coastal environments due to the diurnal and seasonal cycles, and the mean surface water temperature is increasing at a rate of -0.11 – 0.13 °C per decade (IPCC, 2019) with some areas (including the Baltic Sea) warming considerably faster than the global average (Knibbusch et al., 2019). Recent studies in marine ectotherms reported

the interacting effects of nano-ZnO and temperature on marine organisms (Lai et al., 2020; Yung et al., 2017). Thus, toxicity of nano-ZnO (LC_{50} , 0.84 mg l⁻¹) to a copepod *Tigriopus japonicus* was upregulated with increasing temperature with the lowest toxicity observed at 15 °C (Lai et al., 2020). In a marine diatom *Thalassiosira pseudonana* toxicity of nano-ZnO (0.5 – 50 mg l⁻¹) was significantly greater at 30 °C (near the species' upper thermal limit) than other studied temperatures (Yung et al., 2017). Elevated temperature also modulated metabolic responses to nano-ZnO in marine mussels *Mytilus edulis* so that a 5 °C warming lessened the nano-ZnO-induced metabolic disturbance during winter but increased it in summer (Wu et al., 2021). Generally, temperature does not strongly effect nano-ZnO properties (such as the solubility and aggregation behavior) in the environmentally relevant range of temperatures and nanoparticle concentrations (Yung et al., 2017), so that the temperature-induced modulation of the nanoparticle toxicity in marine organisms is most likely mediated by the changes in the organisms' physiology (Holmstrup et al., 2010; Wu et al., 2021). These physiological alterations might be reflected in the changes of the respective molecular and cellular pathways of nano-ZnO toxicity such as induction of inflammation, oxidative stress or alteration of cell survival pathways (Gerloff et al., 2017; Halappanavar et al., 2020; Luo et al., 2020).

The aim of this study was to assess the responses of cellular stress mechanisms (including oxidative stress, inflammation, and cell survival pathways) to nano-ZnO (10 µg l⁻¹ and 100 µg l⁻¹) under different temperature regimes in a common marine mussel, *M. edulis*. The blue mussels (*Mytilus* spp.) represent excellent sentinel species for ecotoxicological assessment in marine habitats (Beyer et al., 2017; Bricker et al., 2014). Nano-ZnO particles and their aggregates can be retained by the mussel gills, ingested, and internalized by endocytosis (Al-Sid-Cheikh et al., 2013; Joubert et al., 2013; Rocha et al., 2015). We used biomarker-based approach focusing on oxidative stress indicators (PC and LPO) and transcription pattern of marker genes in the cell survival (caspase 3, Bcl-2, p53, p38 and JNK) and inflammation (COX, NF-κB, and TGF-β) pathways of *M. edulis*. The oxidative stress and molecular biomarkers were measured in the soft tissues (gill and digestive gland) of the mussels exposed for 21 days to different combinations of nano-ZnO and temperature in winter and summer. The gills (as a key site of nanoparticle uptake) and the digestive gland (as the main organ for nanoparticles accumulation) (Al-Sid-Cheikh et al., 2013; Hull et al., 2011) were used as target tissues in our present study. We hypothesized that the nano-ZnO exposure will cause oxidative stress and activate apoptosis and inflammation pathways in the mussels, and that the toxic effects of nano-ZnO will be mitigated by mild warming in winter but exacerbated by more extreme thermal stress in summer.

2. Materials and methods

2.1. Nanoparticles preparations and physicochemical characterization

Commercial ZnO nanoparticles (nano-ZnO) (particle size <100 nm (TEM), average particle size ≤ 40 nm (APS), pH 7.5 ± 1.5 and without coating agent; catalog number 721077) were purchased from Sigma-Aldrich Sweden AB (Stockholm, Sweden). Since nano-ZnO tend to form aggregates in seawater, the aggregate size distribution of nano-ZnO in the seawater (100 mg l⁻¹, salinity 15) at different temperatures

(10, 15 and 20 °C) were analyzed by relative frequency (intensity weighted) of particle diameters using dynamic light scattering (DLS) (Litesizer 500, Anton Paar GmbH, Graz, Austria). Aggregation tendency and stability of aggregates in the seawater (100 mg l⁻¹, salinity 15) at 20 °C was characterized by Zeta potential measurement. The Zeta potential of nano-ZnO was determined at a pH value of 7.0 using electrophoretic light scattering (ELS) (Litesizer 500, Anton Paar GmbH, Graz, Austria). Further details of preparation and characterization of nano-ZnO are provided in SI Appendix.

2.2. Animal collection and maintenance

The exposure conditions of the mussels *M. edulis* used in the present study were similar to those described elsewhere (Wu et al., 2021). Briefly, the mussels *M. edulis* (shell length is 56 ± 6 mm) were collected from the same mussel bed in Warnemünde, Germany (54°10'49.602"N, 12°05'21.991"E) in late October 2018 (winter experiment: salinity 10–16 (practical salinity scale); the average seawater temperature ~ 10 °C) and June 2019 (summer experiment: salinity 10–16; the average seawater temperature ~ 15 °C). Before the experiment, mussels were kept in recirculated temperature-controlled aquariums for two weeks at salinity 15 and temperature 10 °C (winter) or 15 °C (summer). Water was changed every two days, and the mussels were fed ad libitum 2 h before every water change with a commercial blend of live marine phytoplankton containing *Nannochloropsis oculata*, *Phaeodactylum tricornutum* and *Chlorella* sp. (cell size: 2–20 µm, density: 2.5 × 10⁸ cells ml⁻¹) (Premium Reef Blend, CoralSands, Germany) per manufacturer's instructions during the preliminary acclimation and experimental exposures.

2.3. Experimental exposures and tissue collection

After two-week acclimation, the mussels were randomly divided into ten treatments and exposed for three-weeks in triplicates for each treatment with 20 mussels per replicate (6 l seawater). The randomly chosen groups of mussels were either kept at the same temperature as during the preliminary acclimation, or immediately transferred to a warmer (+5 °C) temperature. Within each season, a full factorial design was implemented including two temperatures (10 and 15 °C in winter, 15 and 20 °C in the summer) and five Zn treatments: control (without Zn addition), nano-ZnO at 10 µg l⁻¹ Zn or 100 µg l⁻¹ Zn, and dissolved Zn (as ZnSO₄) at 10 µg l⁻¹ or 100 µg l⁻¹ Zn. These concentrations (10 µg l⁻¹ and 100 µg l⁻¹) are later referred to as low and high nano-ZnO or Zn levels, respectively. The predicted no-effect concentration (PNEC) of nano-ZnO is 0.2–5 µg l⁻¹ (Chen et al., 2018; Coll et al., 2016; Hong et al., 2021); therefore, the experimental nano-ZnO concentrations used in our present study represent sub-lethal toxic concentrations and are close to the range of the concentrations predicted for polluted coastal areas (Boxall et al., 2007; Coll et al., 2016; Hong et al., 2021). Exposure to dissolved Zn was used to as a positive control for Zn²⁺ effects such as might be caused by nano-ZnO dissolution. Warming (+5 °C above the respective control temperature) was selected to represent the predicted warming in the southern Baltic Sea based on climate change scenarios (IPCC, 2019).

A static-renewal design was used with the water change every two days. New aliquots of sonicated suspensions of nano-ZnO or ZnSO₄ solutions were added during every water change to maintain the nominal target concentrations. No release of dissolved Zn was detected in the seawater in nano-ZnO exposures (data not shown). No mussels died during the experiment. After exposures, the animals were dissected on ice. The gill and digestive gland were collected, shock-frozen and stored at -80 °C until further analysis.

2.4. Oxidative stress traits

Lipid peroxidation (LPO) was tested using a thiobarbituric acid assay in the gill and digestive gland, separately (N = 5–6) (Ohkawa et al.,

1979). The tissue was homogenized and sonicated in 50 mM phosphate buffer (1:10 w/v), incubated for 10 min with 50% trichloroacetic acid (1:2 v/v), and the supernatant was used for LPO measurements. Samples or blanks (50 mM phosphate buffer) were mixed 1:1 (v:v) with 0.7 mM thiobarbituric acid and boiled for 20 min. The absorbance of thiobarbituric acid-reactive substances (TBARS) as end products of LPO was measured at 532 nm using a SpectraMax ID3 Multi-Mode Microplate Reader (Molecular Devices, USA). A molar extinction coefficient of 1.56 × 10⁵ M⁻¹ cm⁻¹ was used to calculate the LPO level expressed as nmol TBARS g⁻¹ wet tissue mass.

Protein carbonyl (PC) content was determined in the soft tissue (gill or digestive gland) using the 2,4-dinitrophenylhydrazine (DNPH) assay (N = 5–6) (Reznick and Packer, 1994). Proteins were precipitated from the homogenates with 20% trichloroacetic acid (1:2 v/v) and collected by centrifugation (15 min at 5000 ×g and 4 °C). The protein carbonyls were stained with 0.03 M 2,4-DNPH in 2 M HCl (using HCl-treated protein from the same sample as a blank), incubated for 1 h at 37 °C and collected by centrifugation (10 min at 4000 ×g at 4 °C). The pellet was washed with 5% trichloroacetic acid with centrifugations and dissolved in 6 M guanidine hydrochloride. The absorbance was determined at 370 nm in the microplate reader. The concentration of PC was calculated by a molar extinction coefficient of 2.2 × 10⁴ M⁻¹ cm⁻¹ and expressed as nmol g⁻¹ wet mass of soft tissue.

2.5. mRNA expressions of key apoptosis- and inflammation-related genes

The mRNA expression of key apoptosis- and inflammation-related genes including caspase 3, p53, p38, JNK, COX, Bcl-2, NF-κB, and TGF-β were measured in the gill and digestive gland using standard qRT-PCR protocols (N = 6) (Pfaffl, 2001; Steffen et al., 2020). The details of the transcript levels analysis including the total RNA isolation, cDNA synthesis and quantitative real-time PCR including the primer sequences are supplied in SI Appendix and the Supplementary Table 1. The transcript levels of each target gene were normalized by the transcript levels of eEF1 (Pfaffl, 2001) and expressed as fold change in the transcript level in the treatment group relative to the corresponding control group.

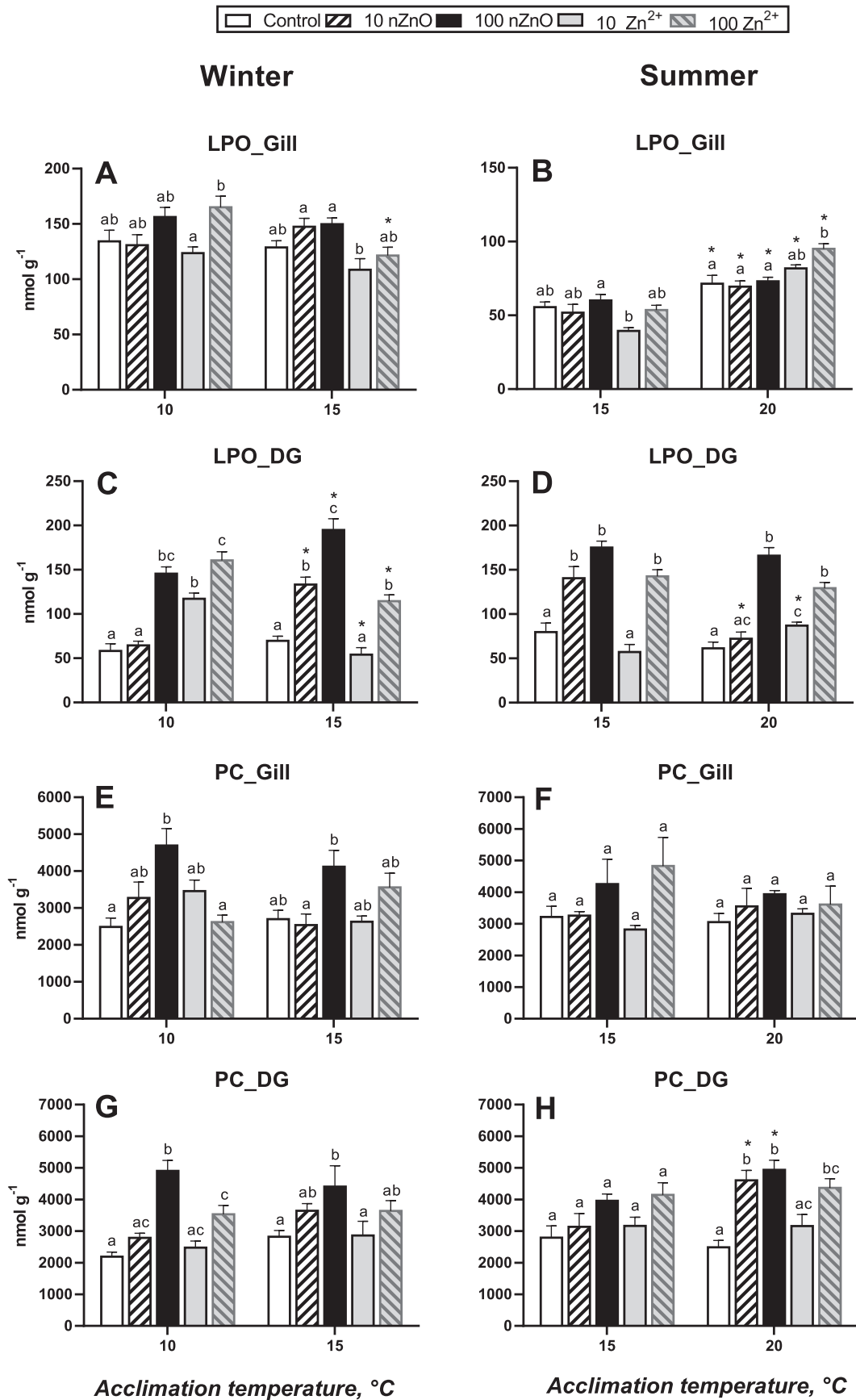
2.6. Statistics analysis

Data analysis was performed using IBM® SPSS® 18.0 and GraphPad Prism 6.0. Prior to analysis, data were checked for the normality using the Shapiro–Wilks test and homogeneity of variances by Levene's test, and Box-Cox transformed if needed. The interactive effects of Zn treatments × temperature (separately for each season), and Zn treatments × season (summer vs. winter at 15 °C) were analyzed by two-way ANOVA. The significant effects of Zn treatments were analyzed using Tukey's HSD multiple range tests at each temperature condition. The significant effect of temperature was tested by Student's *t*-test at each Zn treatment. The PCA and DA analysis were performed on the Box-Cox transformed data. The number of biological replicates was 5–6 for all measured traits and the results are presented as means ± SEM. The differences were considered significant at *P* < 0.05. Further details of the statistical analysis are provided in SI Appendix.

3. Results

3.1. Nano-ZnO characterization

The average aggregate size of nano-ZnO determined from the major peaks of the particle distribution curves of three subsequent measurements in the seawater (100 mg l⁻¹, salinity 15) was 5.21 ± 0.21, 3.72 ± 0.32 and 3.16 ± 0.34 µm at 10, 15 and 20 °C, respectively (Supplementary Fig. 1). The average aggregate size of nano-ZnO was not significantly affected by the temperature in the studied range. The zeta potential of nano-ZnO in the seawater (100 mg l⁻¹, salinity 15) was -8.2 mV at 20 °C.



3.2. Oxidative stress markers

3.2.1. Winter mussels

In gills, the LPO and PC levels generally remained near the baseline in all treatment groups except for a significant increase ($P < 0.05$) in PC levels in the mussels exposed to $100 \mu\text{g l}^{-1}$ of nano-ZnO at 10°C (Fig. 1A, E). In the digestive gland, high concentration ($100 \mu\text{g l}^{-1}$) of nano-ZnO or Zn^{2+} led to a significant increase ($P < 0.05$) in the LPO and PC levels at 10°C and 15°C (Fig. 1C, G). Furthermore, elevated LPO levels were also found in the digestive gland of the mussels exposed to $10 \mu\text{g l}^{-1}$ nano-ZnO at 15°C and $10 \mu\text{g l}^{-1}$ dissolved Zn at 10°C ($P < 0.05$) (Fig. 1C, G).

In the absence of chemical stress, winter warming ($10 \rightarrow 15^\circ\text{C}$) had no effect on the LPO and PC levels in the mussels' tissues (Fig. 1A, C, E, G). In nano-ZnO exposed groups, warming ($10 \rightarrow 15^\circ\text{C}$) had no effect on the LPO and PC level in the mussels' tissues except for significantly enhanced ($P < 0.05$) the LPO content in the digestive gland (Fig. 1A, C, E, G). In the mussels exposed to dissolved Zn, the experimental warming generally decreased ($P < 0.05$) the LPO levels (Fig. 1A, C), but had no effect on PC levels (Fig. 1E, G).

3.2.2. Summer mussels

In the gills of the summer mussels, LPO and PC content was not affected by nano-ZnO and dissolved Zn, except for an increase ($P < 0.05$) in LPO at 20°C combined with dissolved Zn ($100 \mu\text{g l}^{-1}$) (Fig. 1B, F). In the digestive gland of the summer mussels, high concentration of nano-ZnO or dissolved Zn significantly increased ($P < 0.05$) LPO content at each acclimation temperature and PC content at 20°C (Fig. 1D, H). Furthermore, in digestive gland, exposure to $10 \mu\text{g l}^{-1}$ nano-ZnO resulted in a significant increase ($P < 0.05$) in the LPO levels at 15°C and in PC levels at 20°C (Fig. 1D, H). Elevated LPO levels were also found in the digestive gland of the mussels exposed to $10 \mu\text{g l}^{-1}$ dissolved Zn at 20°C ($P < 0.05$) (Fig. 1D, H).

In summer control mussels, the elevated temperature (20°C) generally had no effect on the LPO and PC levels in the control mussels' tissues (Fig. 1B, D, F, H). In the mussels exposed to nano-ZnO, warming ($15 \rightarrow 20^\circ\text{C}$) generally increased ($P < 0.05$) the LPO levels in gill and the PC levels in digestive gland (Fig. 1B, D, F, H). In dissolved Zn exposed groups, warming had no effect on the LPO and PC level in the mussels' tissues except for significantly enhanced ($P < 0.05$) LPO content in the gill (Fig. 1B, D, F, H).

3.3. Molecular markers of apoptosis and inflammation

3.3.1. Winter mussels

At 10°C , exposure to $100 \mu\text{g l}^{-1}$ of nano-ZnO significantly increased ($P < 0.05$) the transcript levels of p53 and JNK in the mussels' gill and the transcript levels of p38 and caspase 3 in the digestive gland (Figs. 2A, E, 4C and 5A). mRNA expression of other studied genes was not significantly influenced by $100 \mu\text{g l}^{-1}$ nano-ZnO in both studied tissues. At 10°C , dissolved Zn exposures (10 or $100 \mu\text{g l}^{-1}$) or low concentration of nano-ZnO ($10 \mu\text{g l}^{-1}$) exposures had no significant effect on the studied transcript levels in the mussels' tissues (Figs. 2-5A, C, E, G).

In winter control mussels, warming (15°C) had no significant effect on the mRNA expression of the studied genes in the gill (Figs. 2-3A, C, E, and G), but significantly increased ($P < 0.05$) the mRNA expression of most studied genes (except for p53, COX and caspase 3) in the digestive gland (Figs. 4-5A, C, E, and G). Acclimation to the elevated temperature (15°C) in winter mitigated the induction of the stress genes by high concentration of nano-ZnO. Thus, at 15°C exposure to nano-ZnO had no significant effect on the transcript level of any of the studied genes

in the gill or digestive gland of *M. edulis* (Figs. 2-5A, C, E, G). Suppression of p53 transcripts in the gill and an increase in NF- κ B mRNA in the digestive gland was observed in the winter mussels exposed to $100 \mu\text{g l}^{-1}$ of dissolved Zn at 15°C ($P < 0.05$) (Figs. 2-5).

3.3.2. Summer mussels

In the gills of the summer mussels, an inhibitory effect of nano-ZnO or dissolved Zn was found for most studied genes (except p53 and JNK) at 15°C (Figs. 2-3B, D, F, H). Exposure to high dissolved Zn ($100 \mu\text{g l}^{-1}$) decreased ($P < 0.05$) the mRNA expression of p38, caspase 3, Bcl-2, NF- κ B and TGF- β in the mussels' gill at 15°C (Figs. 2D, 3B, D, F, H). At 15°C , exposure to $10 \mu\text{g l}^{-1}$ dissolved Zn also decreased ($P < 0.05$) the mRNA expression of p38 in the mussels' gill (Fig. 2D), whereas exposure to $10 \mu\text{g l}^{-1}$ nano-ZnO elevated ($P < 0.05$) the mRNA levels of p53 (Fig. 2B). No significant transcriptional change was found in the mussels' digestive gland in response to nano-ZnO or dissolved Zn exposures at 15°C (Figs. 4-5B, D, F, H).

Elevated summer temperature (20°C) suppressed ($P < 0.05$) transcript levels of p38, JNK, caspase 3 and NF- κ B and increased ($P < 0.05$) the transcript level of Bcl-2 in the gills of the control mussels (Figs. 2D, F, 3B, D and F). Elevated temperature also upregulated ($P < 0.05$) mRNA expression of JNK, COX, NF- κ B and TGF- β in the digestive gland of the control mussels (Figs. 4F, H, 5F, H). Elevated temperature (20°C) exacerbated ($P < 0.05$) the response of several stress genes to the high concentration of nano-ZnO in the digestive gland (Figs. 4D, H, 5B, H) but not in the gill (Figs. 2-3).

3.4. Interaction analysis

In winter mussels, the two-way ANOVA analysis demonstrated significant interactive effects of the Zn exposure \times temperature ($P < 0.05$) for LPO and the mRNA levels of JNK in both gill and digestive gland (Supplementary Tables 2A and 3A). In summer mussels, significant interactive effects of the Zn exposure \times temperature ($P < 0.05$) were reported for LPO and the mRNA levels of p53, COX, caspase 3, Bcl-2 and TGF- β in the gill and for LPO and the mRNA levels of NF- κ B in the digestive gland (Supplementary Tables 2B and 3B). At a common acclimation temperature (15°C), significant effects of the Zn exposure \times season interactions ($P < 0.05$) were reported for all studied biomarkers except PC and the expression of NF- κ B mRNA in the gill, whereas none of the interactions were significant ($P > 0.05$) in the digestive gland (Supplementary Table 4A and B).

3.5. PCA and DA analysis

The PCA analysis revealed that the two first principal components explained 41.59%, 49.79%, 65.76% and 55.97% of overall variance in the winter mussels' gill, the summer mussels' gill, the winter mussels' digestive gland and the summer mussels' digestive gland, respectively (Figs. 6A, D and 7A, D). The PCA and DA results indicated a strong differentiation of $100 \mu\text{g l}^{-1}$ nano-ZnO treatment from other Zn treatments, and clear separation of the warming and normal temperature treatments in both seasons (Figs. 6 and 7).

3.5.1. Winter mussels

In winter mussels, PC 1 (23.07% and 52.05% variation in the gill and digestive gland, respectively) was the main axis connected with Zn treatment (Figs. 6A and 7A). PC 1 had high loadings of p38 and Bcl-2 mRNA levels in the gill, and of the protein carbonyl levels, as well as p53, p38, JNK, caspase 3, NF- κ B and TGF- β mRNA expression in the digestive gland (Figs. 6B and 7B; Supplementary Tables 5 and 6). The

Fig. 1. Oxidative stress biomarkers in the soft tissues of *M. edulis* exposed to different combinations of nano-ZnO or Zn^{2+} and temperature for 21 days. Winter mussels – A, C, E, G; Summer mussels – B, D, F, H; LPO_Gill – lipid peroxidation markers in gill (A, B); LPO_DG – lipid peroxidation markers in digestive gland (C, D); PC_Gill – protein carbonyls in gill (E, F); PC_DG – protein carbonyls in digestive gland (G, H). Different letters indicate significant differences among nano-ZnO or Zn^{2+} treatments within fixed temperature level ($P < 0.05$), and asterisks indicate significant differences between two temperatures within the same Zn treatment group ($P < 0.05$). $N = 5-6$.

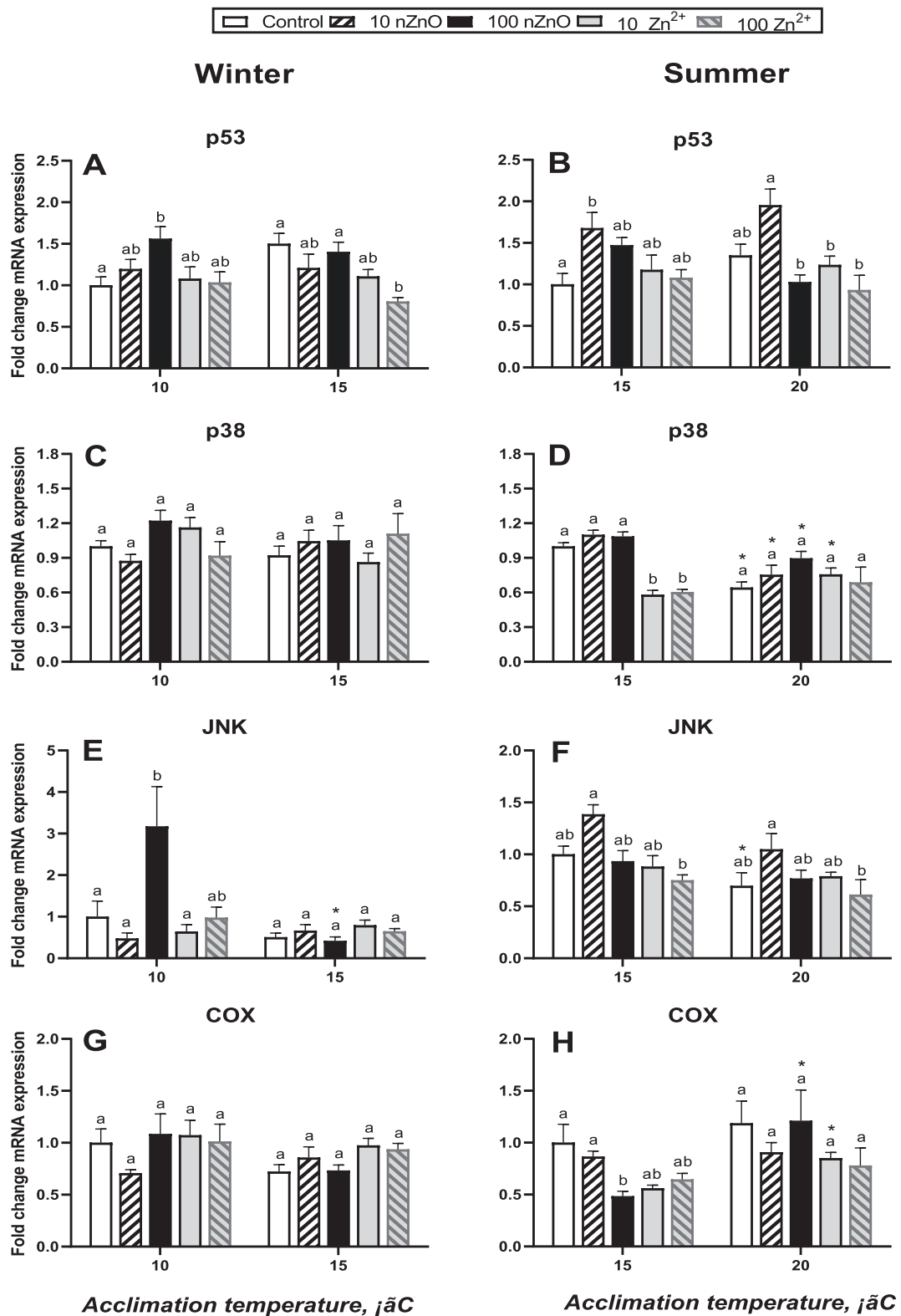


Fig. 2. Cellular stress related-gene expression in gill of *M. edulis* exposed to different combinations of nano-ZnO or Zn²⁺ and temperature for 21 days. Winter mussels – A, C, E, G; Summer mussels – B, D, F, H; p53 (A, B); p38 (C, D); JNK (E, F); COX (G, H). The letters/asterisks have the same meaning as in Fig. 1. N = 6.

PC2 (18.52% and 13.71% variation in gill and digestive gland, respectively) separated warming (15 °C)-exposed mussels from the normal temperature (10 °C) treatment (Figs. 6-7; Supplementary Tables 5 and 6).

DA results indicated a high Mahalanobis distance (D^2) between the controls and 100 $\mu\text{g l}^{-1}$ nano-ZnO treatments ($D^2 = 21.26$ and 8.18 in

the gill at 10 °C and 15 °C, respectively; $D^2 = 42.00$ and 108.49 in the digestive gland at 10 °C and 15 °C, respectively) and the controls and 100 $\mu\text{g l}^{-1}$ Zn²⁺ treatments ($D^2 = 13.81$ and 16.58 in the gill at 10 °C and 15 °C, respectively; $D^2 = 45.45$ and 22.11 in the digestive gland at 10 °C and 15 °C, respectively), and a smaller distance between the controls and 10 $\mu\text{g l}^{-1}$ nano-ZnO or Zn²⁺ treatments, consistent with the

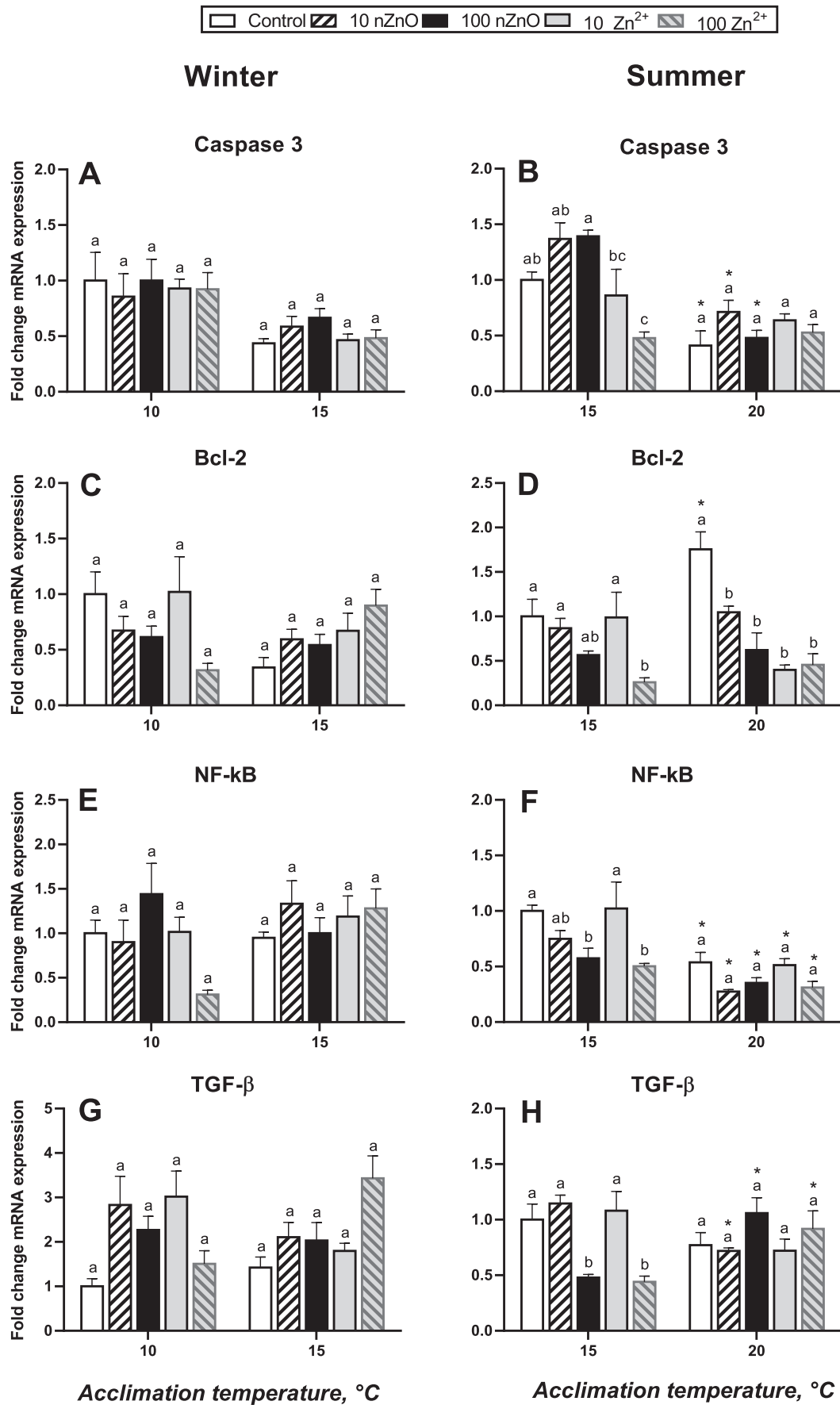


Fig. 3. Cellular stress related-gene expression in gill of *M. edulis* exposed to different combinations of nano-ZnO or Zn²⁺ and temperature for 21 days. Winter mussels – A, C, E, G; Summer mussels – B, D, F, H; Caspase 3 (A, B); Bcl-2 (C, D); NF-κB (E, F); TGF-β (G, H). The letters/asterisks have the same meaning as in Fig. 1. N = 6.

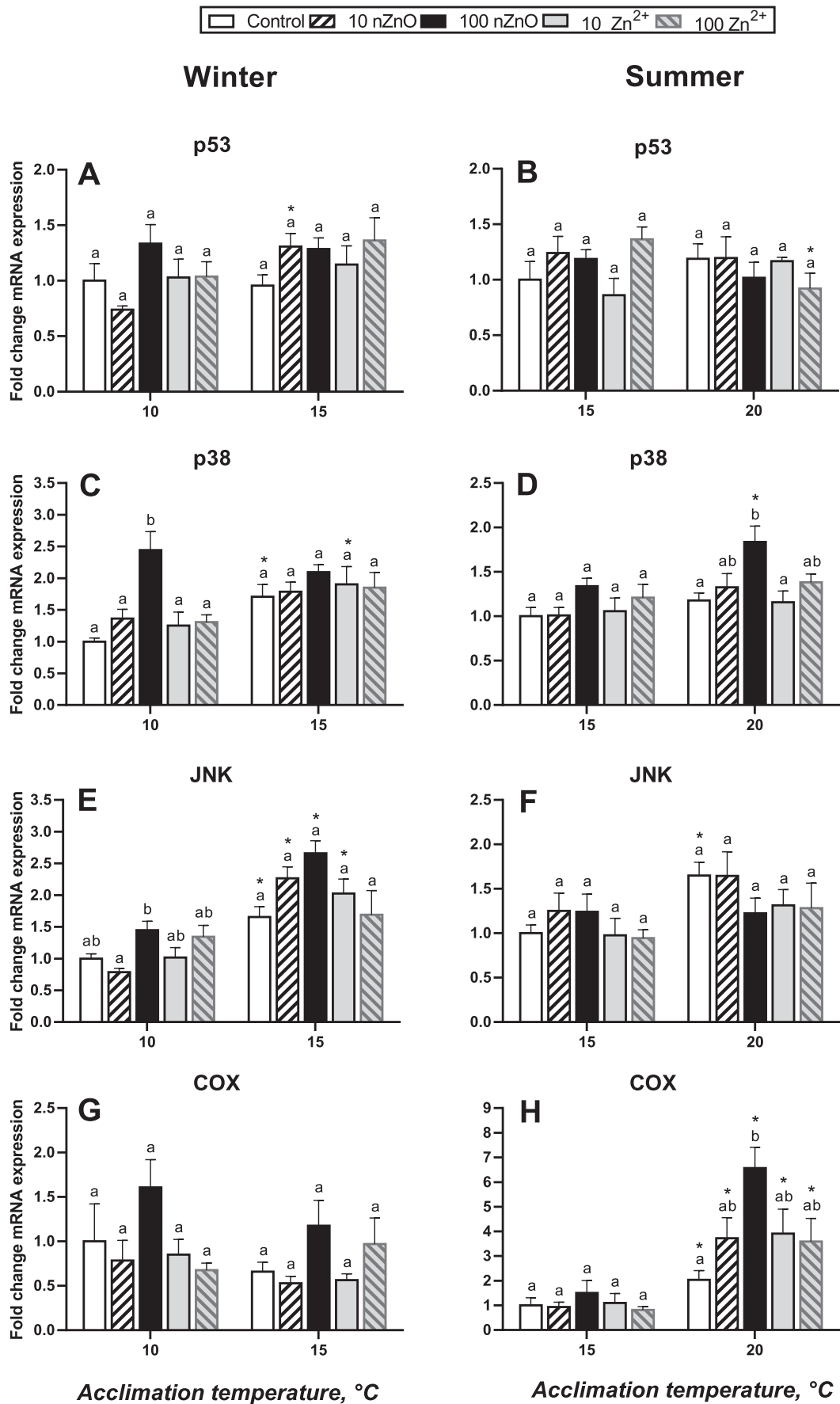


Fig. 4. Cellular stress related-gene expression in digestive gland of *M. edulis* exposed to different combinations of nano-ZnO or Zn²⁺ and temperature for 21 days. Winter mussels – A, C, E, G; Summer mussels – B, D, F, H; p53 (A, B); p38 (C, D); JNK (E, F); COX (G, H). The letters/asterisks have the same meaning as in Fig. 1. N = 6.

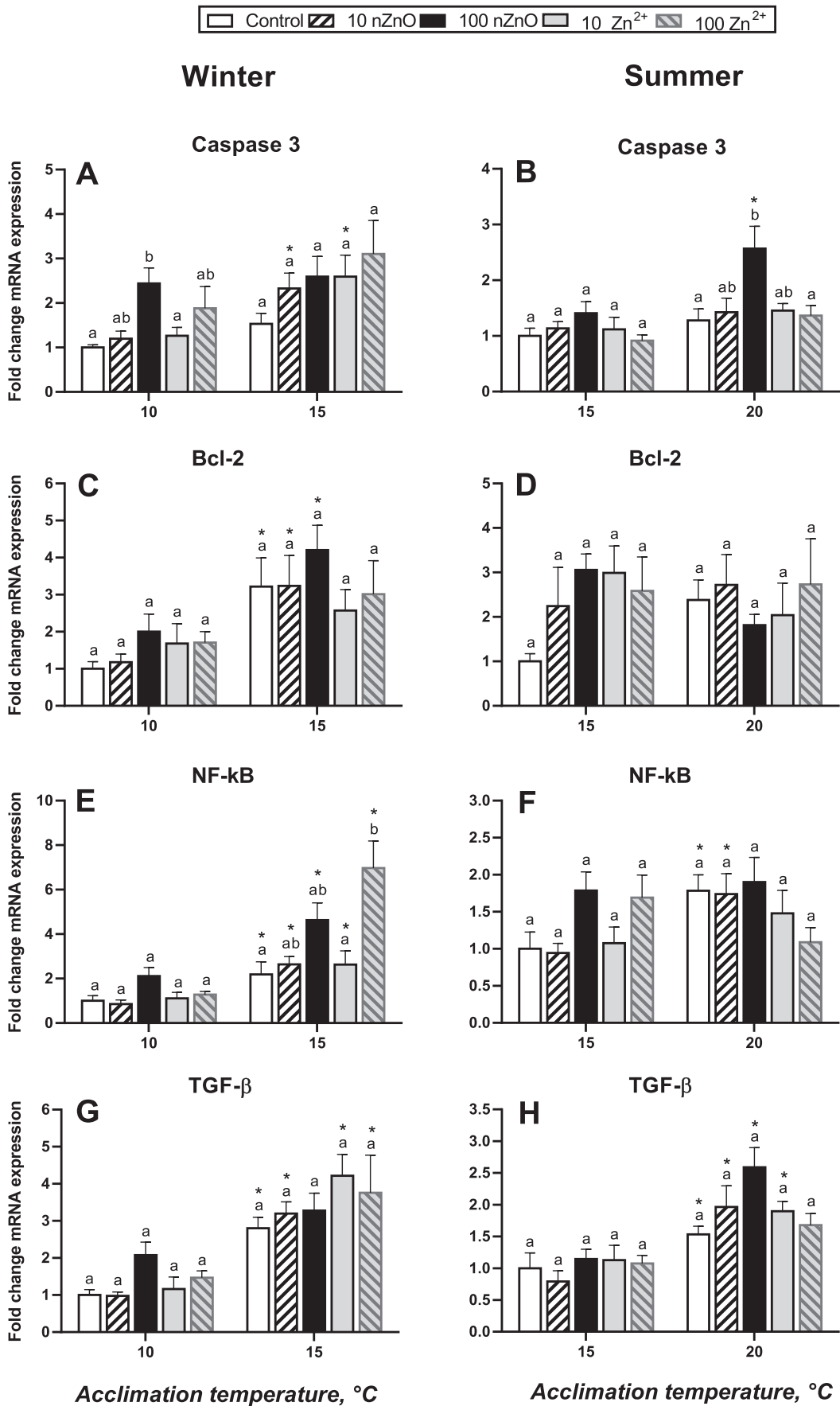


Fig. 5. Cellular stress related-gene expression in digestive gland of *M. edulis* exposed to different combinations of nano-ZnO or Zn²⁺ and temperature for 21 days. Winter mussels – A, C, E, G; Summer mussels – B, D, F, H; Caspase 3 (A, B); Bcl-2 (C, D); NF-κB (E, F); TGF-β (G, H). The letters/asterisks have the same meaning as in Fig. 1. N = 6.

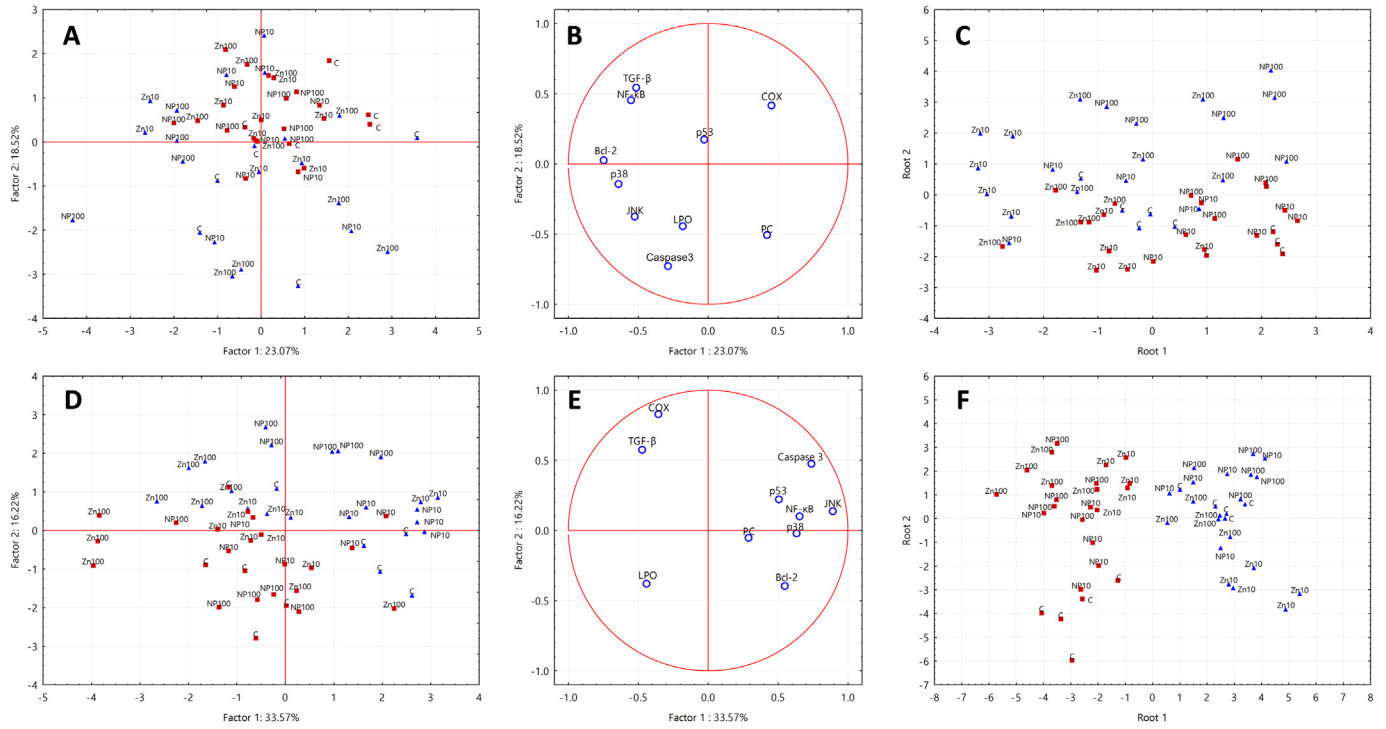


Fig. 6. Biplots originating from PCA and DA analysis integrating all studied biomarkers of gill of *M. edulis* exposed to different experimental conditions. (A, B and C) – winter mussels; (D, E and F) – summer mussels. A, D – the position of samples from different Zn exposure and temperature groups in the plane of the two first principal components; B, E – the variable-based plot showing the associations of the respective biomarkers with the two first principal components; C, F – the discriminant analysis biplot of the different Zn exposure based on the multibiomarker profiles. Experimental treatment groups: The blue triangle (Δ) – normal temperature; the red square (\square) – elevated temperature; C – control (no Zn addition); NP 10–10 $\mu\text{g l}^{-1}$ nano-ZnO; NP 100–100 $\mu\text{g l}^{-1}$ nano-ZnO; Zn 10–10 $\mu\text{g l}^{-1}$ Zn^{2+} ; Zn 100–100 $\mu\text{g l}^{-1}$ Zn^{2+} .

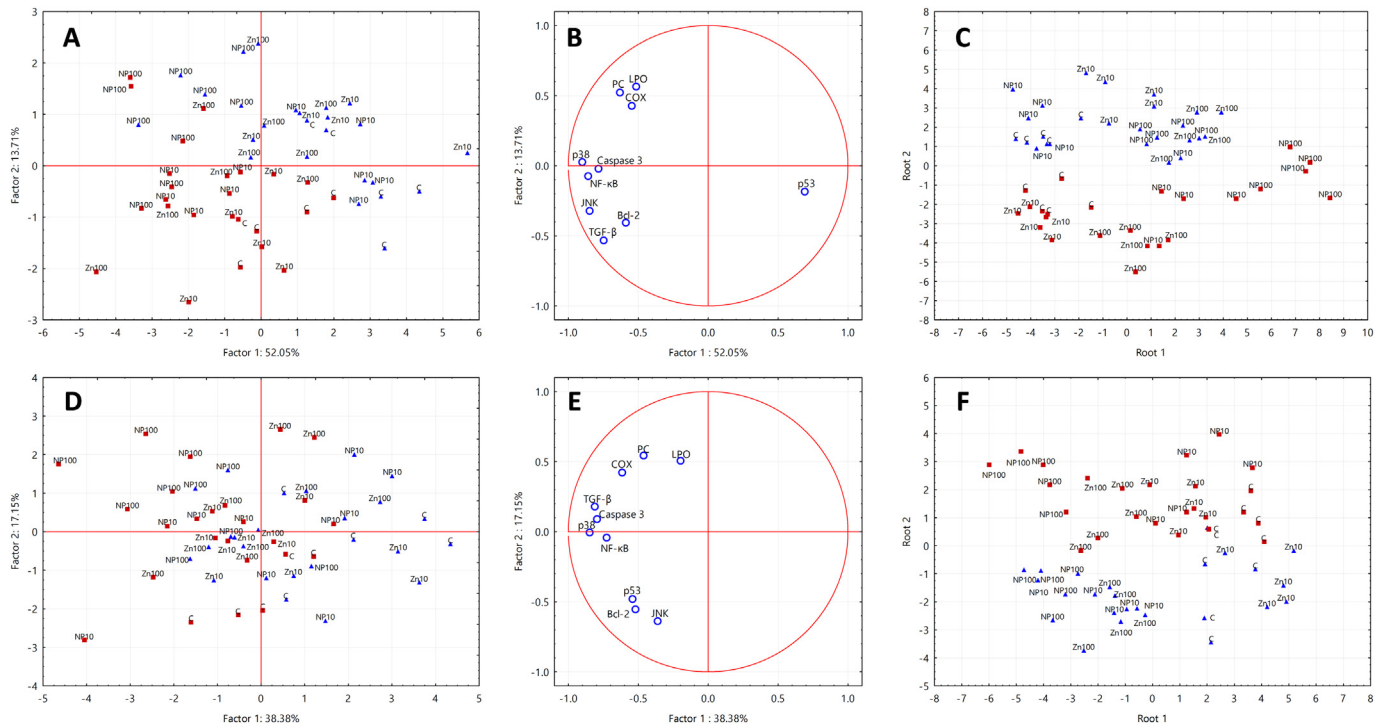


Fig. 7. Biplot originating from PCA and DA analysis integrating all studied biomarkers of digestive gland of *M. edulis* exposed to different studied exposures. (A, B and C) – winter mussels; (D, E and F) – summer mussels. The meaning of the panels A, B, C, D, E and F is the same as that shown in panels A, B, C, D, E and F, respectively. The meaning of experimental treatment groups in this figure is the same as shown in Fig. 6.

PCA analysis (Figs. 6C and 7C; Supplementary Table 11). The studied biomarkers that significantly ($P < 0.05$) contributed to the DA model included LPO, PC and mRNA expression of the JNK and caspase 3 in the gill, and LPO, PC and mRNA expression of the p38, JNK, NF- κ B and TGF- β in the digestive gland (Supplementary Tables 7 and 9).

3.5.2. Summer mussels

In summer mussels' gill, PC1 (33.57% of the total variance) showed a Zn-specific response separating $100 \mu\text{g l}^{-1}$ nano-ZnO or dissolved Zn treatments from other treatments (Fig. 6D). PC1 was associated with the high loadings of p38, JNK, caspase 3 and NF- κ B mRNA (Fig. 6E; Supplementary Table 5). In the gill, PC2 explained 16.22% of the total variance of biomarkers and showed a temperature specific response (Fig. 6D) associated with high loadings of COX mRNA (Fig. 6E; Supplementary Table 5). In the digestive gland, PC1 accounted for 38.38% of the total variance of biomarkers and showed a temperature specific response separating the warming (20°C) from the control (15°C) groups (Fig. 7D) associated with high loadings of p38, COX, caspase 3, NF- κ B and TGF- β transcripts (Fig. 7E; Supplementary Table 6). PC2 explained 17.15% of the total variance of biomarkers in the digestive gland and was associated with Zn exposure (Fig. 7D) and high loadings of JNK mRNA (Fig. 7E; Supplementary Table 6).

DA results demonstrated a high D^2 between the controls and $100 \mu\text{g l}^{-1}$ nano-ZnO treatments ($D^2 = 21.07$ and 34.74 in the gill at 15°C and 20°C , respectively; $D^2 = 40.64$ and 65.53 in the digestive gland at 15°C and 20°C , respectively) and the controls and $100 \mu\text{g l}^{-1}$ Zn $^{2+}$ treatments ($D^2 = 26.20$ and 43.31 in the gill at 15°C and 20°C , respectively; $D^2 = 24.33$ and 32.11 in the digestive gland at 15°C and 20°C , respectively), and a weaker separation between the controls and $10 \mu\text{g l}^{-1}$ nano-ZnO or Zn $^{2+}$ treatments, consistent with the PCA analysis (Figs. 6F and 7F; Supplementary Table 11). Most studied traits (except the mRNA expression of COX and caspase 3) were identified as significant contributors to the DA model ($P < 0.05$) in the gills. In the digestive gland, the significant contributors to the discriminant model included LPO, PC and transcript levels of the JNK and COX (Supplementary Tables 8 and 10).

4. Discussion

4.1. Characterization of nano-ZnO

The measured aggregate size distribution demonstrated the formation of aggregates in the low micrometer range independent of the temperature. This behavior can be explained by the effect of van der Waals forces and the theory of double layer force (DLVO), according to which small charges of neighboring particles (zeta potential $|\zeta| \leq 15$ mV) lead to mutual attraction (Modena et al., 2019; Yung et al., 2014). Furthermore, the aggregation tendency is enhanced by the surrounding salt water, which compresses the electrical double layer and reduces repulsive forces between the nanoparticles due to the high ionic strength (Li et al., 2017; Yung et al., 2014). The measured zeta potential of -8.2 mV confirms the aggregation tendency of nano-ZnO used in the study. Aggregation of nano-ZnO with similar primary particle size into the micrometer-sized aggregates was also observed in previous studies (Li et al., 2017; Wong et al., 2010; Yung et al., 2015). Since mussels can efficiently filter out particles in the size range of $4\text{--}35 \mu\text{m}$ and partially retain even smaller ($<4 \mu\text{m}$) particles (Møhlenberg and Riisgård, 1978; Strohmeier et al., 2012), our results support the notion that nano-ZnO particles and their aggregates are bioavailable to the mussels (Al-Sid-Cheikh et al., 2013; Joubert et al., 2013; Rocha et al., 2015).

4.2. Oxidative stress response to nano-ZnO

Introduction of engineered nanomaterials including ZnO nanoparticles in marine ecosystems carries potential risks to the resident biota

due to the direct toxic effects of the nanomaterials and possible release of trace metals. Oxidative stress has been considered a key mechanism of nano-ZnO toxicity and a hallmark of nano-ZnO-induced injury (Vandebriel and De Jong, 2012; Wang et al., 2014; Xia et al., 2008). The determination of the content of protein carbonyls and end products of lipid peroxidation can thus provide evidence for the oxidative injury induced by nano-ZnO. We predicted that nano-ZnO exposure would lead to oxidative injury manifested as elevated LPO and PC content in mussels (Marisa et al., 2016). Similar to our expectations, increased oxidative lesions (i.e. elevated content of LPO and PC) were observed in the digestive gland of *M. edulis* exposed to high concentrations ($100 \mu\text{g l}^{-1}$) of nano-ZnO. Generally, the oxidative injury caused by nano-ZnO exposures was stronger than the injury caused by dissolved Zn in our study. Furthermore, the oxidative injury induced by nano-ZnO or Zn $^{2+}$ in the gill was weaker than in the digestive gland. The results of our present work are in agreement with earlier studies that showed protein damage in the gills of the oysters *Crassostrea virginica* exposed to 4mg l^{-1} of nano-ZnO for 48 h (Trevisan et al., 2014), and in the whole soft tissue of the mussels *M. edulis* exposed to $100 \mu\text{g l}^{-1}$ nano-ZnO for 14 days (Falfushynska et al., 2019b). Increased LPO concentrations were also reported in the total soft tissues of the brine shrimp *Artemia salina* exposed to $10\text{--}100 \text{mg l}^{-1}$ of nano-ZnO after $24\text{--}96$ h (Ates et al., 2013). However, other studies in marine bivalves failed to detect oxidative damage due to nano-ZnO exposures (Falfushynska et al., 2019b; Marisa et al., 2016). Thus, no accumulation of PC or LPO content was found in the gill and digestive gland of the clam *R. philippinarum* exposed to $1\text{--}10 \mu\text{g l}^{-1}$ of nano-ZnO for 7 days (Marisa et al., 2016). Furthermore, no accumulation of LPO content was also observed in the whole soft tissue of the mussels *M. edulis* exposed to $100 \mu\text{g l}^{-1}$ nano-ZnO for 14 days (Falfushynska et al., 2019b). Notably, these studies that did not report oxidative injury used either lower concentration of nano-ZnO (Marisa et al., 2016) or shorter exposure times (Falfushynska et al., 2019b; Marisa et al., 2016) than the exposure regime in our present study (21 days at $100 \mu\text{g l}^{-1}$ nano-ZnO). Overall, these findings indicate that in marine mussels, high concentrations of nano-ZnO ($100 \mu\text{g l}^{-1}$) and long-term exposure (21 days) induce oxidative injury.

4.3. Apoptotic and inflammatory response to nano-ZnO

In our present study, a marked apoptotic response to the high concentration of nano-ZnO was observed in the mussels, in notable contrast to the effects of dissolved Zn. Apoptosis (a form of programmed cell death) is a highly regulated biological process triggered by extrinsic (e.g. death receptor ligands) or intrinsic (e.g. oxidative stress and other cellular damage) signals in bivalves (Sokolova, 2009). Apoptosis is commonly stimulated by high concentrations of nano-ZnO in different organisms including marine bivalves. In our present study, the induction of apoptosis by $100 \mu\text{g l}^{-1}$ nano-ZnO was indicated by elevated transcript levels of apoptosis-related genes p53 and JNK in the gill, and p38 and caspase 3 in the digestive gland of *M. edulis*. Upregulation of the mRNA expression of the apoptotic proteins caspase 3 (the main executor caspase in the apoptotic cascade (Kiss, 2010; Sokolova, 2009)) was also observed in the zebrafish *Danio rerio* exposed to $25\text{--}50 \text{mg l}^{-1}$ of nano-ZnO (Du et al., 2017) and in the mussels *M. edulis* exposed to $100 \mu\text{g l}^{-1}$ nano-ZnO (Falfushynska et al., 2019b). Similarly, an increase in mRNA expression of the pro-apoptotic protein p53, the Guardian-of-Genome protein that induces apoptosis in response to excessive DNA damage (Singh et al., 2009) was found in the human ovarian cells exposed to $5\text{--}30 \text{mg l}^{-1}$ nano-ZnO (Bai et al., 2017), in the rats exposed to $50\text{--}300 \text{mg kg}^{-1}$ nano-ZnO (El-Shorbagy et al., 2019), in the zebrafish *D. rerio* exposed to $25\text{--}50 \text{mg l}^{-1}$ of nano-ZnO (Du et al., 2017) and in the mussels *M. galloprovincialis* exposed to $100 \mu\text{g l}^{-1}$ nano-ZnO for 72 h (Li et al., 2018).

The MAPK (mitogen-activated protein kinase) pathway (Kyriakis and Avruch, 2012) is another key regulator of the cellular stress

response including apoptosis (Chang and Karin, 2001; Munshi and Ramesh, 2013). Among MAPK-related proteins, p38 (p38 mitogen-activated protein kinase) and JNK (c-Jun N-terminal kinase) play a key role in transducing signals in response to environmental or cellular stress (Chuang et al., 2000; Kyriakis and Avruch, 2012; Owens and Keyse, 2007). Earlier studies have found that nanoparticles including nano-ZnO can activate JNK and p38 MAPK pathway, thereby stimulating apoptosis (Kang et al., 2009; Qu et al., 2020; Wang et al., 2014; Zhao et al., 2019). In our present study, 100 $\mu\text{g l}^{-1}$ nano-ZnO exposures up-regulated the transcript levels of JNK genes in the gill and p38 in the digestive gland of the mussels. Furthermore, we found transcriptional suppression of an anti-apoptotic regulator protein Bcl-2 in response to nano-ZnO or dissolved Zn in the summer mussels' gill. These findings are consistent with earlier reports of transcriptional downregulation of Bcl-2 in human ovarian cells exposed to 5–30 mg l^{-1} nano-ZnO (Bai et al., 2017) and in the rats exposed to 50–300 $\text{mg nano-ZnO kg}^{-1}$ body mass (El-Shorbagy et al., 2019). Suppression of anti-apoptotic genes such as Bcl-2 might reinforce the apoptotic response caused by upregulation of caspases, p53 and the MAPK pathway. These findings support the notion of pro-apoptotic effects of high concentrations of nano-ZnO and highlight the importance of apoptosis as a toxic mechanism of nano-ZnO in the mussels.

Inflammation is a common response to nanomaterials in various organisms including marine bivalves (Chang et al., 2013; Falfushynska et al., 2019b; Martínez-Gutiérrez et al., 2012; Roma et al., 2020). The inflammatory cytokine pathway involving transforming growth factor-beta (TGF- β) and the nuclear factor κB (NF- κB) plays a crucial role in regulation of inflammation (Hoesel and Schmid, 2013; Letterio and Roberts, 1998). Previous studies on *M. edulis* exposed to 100 $\mu\text{g l}^{-1}$ nano-ZnO showed an increase of the transcript levels of inflammatory cytokines TGF- β and NF- κB in the digestive gland (Falfushynska et al., 2019b). However, in our present study the transcript levels of TGF- β and NF- κB were not upregulated by nano-ZnO in mussels. Exposure to nano-ZnO also did not affect mRNA expression of an inflammation-regulating enzyme COX in our present study. In *R. philippinarum*, the key inflammatory response genes AIF1 (allograft inflammatory factor-1) did not change in response to exposures to 0.75 $\mu\text{g l}^{-1}$ of nano-Au for 1–14 days (Volland et al., 2015). Overall, unlike apoptosis, inflammatory response does not appear to be a consistent toxic effect of nano-ZnO in marine bivalves in the studied range of nano-ZnO concentrations.

Overall, our present study shows that the oxidative stress and apoptotic responses of *M. edulis* were induced by high concentrations (100 $\mu\text{g l}^{-1}$) of nZnO exposures in both studied seasons. However, low concentrations (10 $\mu\text{g l}^{-1}$) of nano-ZnO generally had no effect on oxidative stress and transcriptional responses of the blue mussels except for an increase in the oxidative stress markers in the digestive gland (but not in gill). As confirmed by the results of multivariate analyses (Figs. 6 and 7), the cellular stress responses were considerably less sensitive to low concentrations of nZnO than to high concentrations of nZnO, indicating the toxicity of nanomaterials to organisms is concentration-dependent.

Dissolved Zn exposures had no significant effect on the transcript level of apoptotic-related genes in *M. edulis* except for a decrease in the mRNA levels of pro-apoptotic proteins p53 and caspase 3 in some temperature-tissue combinations caused by 100 $\mu\text{g l}^{-1}$ dissolved Zn. An earlier study in *M. edulis* also showed that dissolved Zn exposures did not induce inflammatory and apoptotic response and could (at some Zn^{2+} concentrations) be anti-apoptotic (Falfushynska et al., 2019b). These results support the notion of dissolved Zn as an apoptosis inhibitor (Alexandre et al., 2002; Perry et al., 1997) and suggest that dissolved Zn release from nano-ZnO cannot fully explain the toxic effects of nano-ZnO. The differences between the cellular stress response profile of nano-ZnO vs. dissolved Zn exposures are further corroborated by the results of the multivariate analyses that integrated multiple cellular stress biomarkers (Figs. 6 and 7).

4.4. Modulation of the cellular stress response by season and warming

The oxidative stress, apoptotic and inflammatory responses of *M. edulis* were modulated by warming in both studied seasons, as shown by analysis of individual markers and confirmed by the results of multivariate analyses. In the absence of the chemical stress from nano-ZnO or dissolved Zn, elevated temperature (15 °C) stimulated the expression of apoptosis- (p38, JNK and Bcl-2) and inflammation-related genes (NF- κB and TGF- β) in the digestive gland of the winter mussels. Similarly, in the summer control mussels, warming (20 °C) led to upregulation of the transcript levels of apoptosis- (JNK) and inflammation-related (NF- κB , TGF- β and COX) genes in the digestive gland. These results indicate that in the digestive gland of *M. edulis*, elevated temperature (+5 °C) might induce apoptotic and inflammatory response regardless of the season. The cellular stress response to warming was more complex in the gill, and this tissue appeared to be less sensitive to the negative effects of warming than the digestive gland. Thus, warming had no effect on the studied apoptotic or inflammatory pathways (in winter) or suppressed the transcript levels of apoptosis- and inflammation-related genes p38, JNK, caspase 3 and NF- κB (in summer) in the gills. The suppression of apoptosis and inflammation-related transcript in the gills might reflect a general decrease in cellular stress protection mechanisms in the mussels during summer warming as shown by suppressed mRNA expression of immune genes in hemocytes of *M. edulis* exposed to 20 °C (Wu and Sokolova, 2021). Furthermore, summer warming (20 °C) negatively affected the organismal energy status of *M. edulis* (Wu et al., 2021) indicating a general deterioration of physiological condition. These results support the notion that 20 °C is close to the upper limit of long-term thermal tolerance of the northern European (including the Baltic Sea) *Mytilus* populations (Fly and Hilbish, 2013; Fly et al., 2015). Further studies are needed to determine whether dysregulation of the cellular stress response by warming has implications for the long-term survival of the Baltic Sea mussels *M. edulis* challenged by the climate change-related warming.

Seasonal variations can affect the oxidative stress and DNA integrity in marine bivalves (Pisanelli et al., 2009; Schmidt et al., 2013), consistent with our present findings in the blue mussels. This was reflected in the results of ANOVA analysis for the effect of season and Zn treatment at a common acclimation temperature (15 °C) that showed significant season effects on most of the studied cellular and molecular biomarkers in the mussels. Several studies have shown that season-related changes in seawater salinity and temperature contribute to the seasonal changes in biomarkers in mussels (Bolognesi and Hayashi, 2011; Domouhtsidou and Dimitriadis, 2001). However, in our present study, the seasonal differences in stress biomarker values were observed despite acclimation of the mussels at the same temperature (15 °C) and salinity (15) regime. Another possible reason for seasonal variation in the biomarkers might be a change in reproductive stage of the mussels (reproductive rest in winter vs. spawning in summer in the Baltic Sea *Mytilus* spp. (Benito et al., 2019; Kautsky, 1982)), which is known to affect biomarker levels in bivalves (Benito et al., 2019; Sheehan and Power, 1999).

4.5. Conclusions and outlook

Based on the multi-biomarker analysis, several key elements of the cellular stress response to nano-ZnO could be identified in the blue mussels including an increase in the protein carbonylation and lipid peroxidation and transcriptional modulation of apoptotic genes caspase 3, p53, p38 and JNK. These markers can thus be considered as core elements of nano-ZnO stressors in *M. edulis*. Unlike the adverse outcome pathway for nanoparticle exposures in mammals (Gerloff et al., 2017; Halappanavar et al., 2020; Luo et al., 2020), the inflammatory response does not appear a key event in nano-ZnO toxicity in mussels at environmentally relevant nano-ZnO concentrations. The biomarker profiles

suggest that nano-ZnO is more toxic than dissolved Zn to mussels and indicate differences of the toxic mechanisms of these pollutants. The effects of nano-ZnO on oxidative stress and transcriptional responses of the blue mussels' digestive gland were stronger than that the effects on the gill, which supports a notion that digestive gland is the main organ for nanoparticles accumulation and toxicity in bivalves (Al-Sid-Cheikh et al., 2013; Hull et al., 2011). As a susceptible organ to nanomaterials toxicity, the digestive gland is therefore a tissue of choice for biomarker-based monitoring of the biological effects of nanoparticles in bivalves. The oxidative stress and stress-related transcriptional responses to nano-ZnO were strongly modified by warming and the season in the mussels, so that no single biomarker could be shown to consistently respond to nano-ZnO in all experimental groups. These findings imply that assessment of the biological effects of nano-ZnO using sentinel marine organisms such as mussels must include multiple biomarkers covering key elements of the putative adverse outcome pathways (especially oxidative stress and apoptosis) to capture the stress response signature to nano-ZnO toxicity under the variable environmental conditions of coastal habitats.

CRedit authorship contribution statement

Fangli Wu: Conceptualization, Data curation, Formal analysis, Funding acquisition, Investigation, Methodology, Visualization, Writing – original draft, Writing – review & editing. **Eugene P. Sokolov:** Conceptualization, Formal analysis, Investigation, Methodology, Writing – review & editing. **Andrei Khomich:** Data curation, Formal analysis, Methodology, Visualization, Writing – review & editing. **Christian Fetteshauer:** Data curation, Methodology, Visualization, Writing – review & editing. **Georg Schnell:** Data curation, Methodology, Visualization, Writing – review & editing. **Hermann Seitz:** Data curation, Methodology, Visualization, Writing – review & editing. **Inna M. Sokolova:** Conceptualization, Funding acquisition, Methodology, Supervision, Project administration, Writing – review & editing.

Declaration of competing interest

The authors declare that they have no known competing financial interests or personal relationships that could have appeared to influence the work reported in this paper.

Acknowledgements

This work was in part supported by the Research Training Group 'Baltic TRANSCOAST' funded by the DFG (Deutsche Forschungsgemeinschaft) under grant number GRK 2000 (www.baltic-transcoast.uni-rostock.de) to IMS and the China Scholarship Council (CSC) to FLW. The project metadata are submitted to Zenodo Data Publisher open access database (<https://doi.org/10.5281/zenodo.5070349>). This is Baltic TRANSCOAST publication no. GRK2000/0052.

Appendix A. Supplementary data

Supplementary data to this article can be found online at <https://doi.org/10.1016/j.scitotenv.2021.151785>.

References

Alexandre, S., Rast, C., Nguyen-Ba, G., Vasseur, P., 2002. ZnCl₂ prevents c-myc repression and apoptosis in serum-deprived Syrian hamster embryo cells. *Environ. Toxicol. Pharmacol.* 11, 191–196.

Al-Sid-Cheikh, M., Rouleau, C., Pelletier, E., 2013. Tissue distribution and kinetics of dissolved and nanoparticulate silver in Iceland scallop (*Chlamys islandica*). *Mar. Environ. Res.* 86, 21–28.

Ates, M., Daniels, J., Arslan, Z., Farah, I.O., Rivera, H.F., 2013. Comparative evaluation of impact of Zn and ZnO nanoparticles on brine shrimp (*Artemia salina*) larvae: effects of particle size and solubility on toxicity. *Environ. Sci. Process. Impacts* 15, 225–233.

Bai, D.P., Zhang, X.F., Zhang, G.L., Huang, Y.F., Gurunathan, S., 2017. Zinc oxide nanoparticles induce apoptosis and autophagy in human ovarian cancer cells. *Int. J. Nanomedicine* 12, 6521–6535.

Benito, D., Ahvo, A., Nuutinen, J., Bilbao, D., Saenz, J., Etxebarria, N., Lekube, X., Izagirre, U., Lehtonen, K.K., Marigómez, I., et al., 2019. Influence of season-dependent ecological variables on biomarker baseline levels in mussels (*Mytilus trossulus*) from two Baltic Sea subregions. *Sci. Total Environ.* 689, 1087–1103.

Beyer, J., Green, N.W., Brooks, S., Allan, I.J., Ruus, A., Gomes, T., Brate, I.L.N., Schoyen, M., 2017. Blue mussels (*Mytilus edulis* spp.) as sentinel organisms in coastal pollution monitoring: a review. *Mar. Environ. Res.* 130, 338–365.

Bolognesi, C., Hayashi, M., 2011. Micronucleus assay in aquatic animals. *Mutagenesis* 26, 205–213.

Boxall, A., Chaudhry, Q., Sinclair, C., Jones, A., Aitken, R., Jefferson, B., Watts, C., 2007. Current and Future Predicted Environmental Exposure to Engineered Nanoparticles. Central Science Laboratory, York, UK.

Bricker, S., Lauenstein, G., Maruya, K., 2014. NOAA's mussel watch program: incorporating contaminants of emerging concern (CECs) into a long-term monitoring program. *Mar. Pollut. Bull.* 81, 289–290.

Castro-Bugallo, A., González-Fernández, Á., Guisande, C., Barreiro, A., 2014. Comparative responses to metal oxide nanoparticles in marine phytoplankton. *Arch. Environ. Contam. Toxicol.* 67, 483–493.

Chang, L., Karin, M., 2001. Mammalian MAP kinase signalling cascades. *Nature* 410, 37–40.

Chang, H., Ho, C.C., Yang, C.S., Chang, W.H., Tsai, M.H., Tsai, H.T., Lin, P.P., 2013. Involvement of MyD88 in zinc oxide nanoparticle-induced lung inflammation. *Exp. Toxicol. Pathol.* 65, 887–896.

Chen, G., Peijnenburg, W.J.G.M., Xiao, Y., Vijver, M.G., 2018. Developing species sensitivity distributions for metallic nanomaterials considering the characteristics of nanomaterials, experimental conditions, and different types of endpoints. *Food Chem. Toxicol.* 112, 563–570.

Chuang, S.M., Wang, I.C., Yang, J.L., 2000. Roles of JNK, p38 and ERK mitogen-activated protein kinases in the growth inhibition and apoptosis induced by cadmium. *Carcinogenesis* 21, 1423–1432.

Coll, C., Notter, D., Gottschalk, F., Sun, T.Y., Som, C., Nowack, B., 2016. Probabilistic environmental risk assessment of five nanomaterials (nano-TiO₂, nano-Ag, nano-ZnO, CNT, and fullerene). *Nanotoxicology* 10, 436–444.

Costa, P.M., Fadeel, B., 2016. Emerging systems biology approaches in nanotoxicology: towards a mechanism-based understanding of nanomaterial hazard and risk. *Toxicol. Appl. Pharmacol.* 299, 101–111.

Czyżowska, A., Barbasz, A., 2020. A review: zinc oxide nanoparticles – friends or enemies? *Int. J. Environ. Health Res.* 1–17.

Domouhtsidou, G.P., Dimitriadis, V.K., 2001. Lysosomal and lipid alterations in the digestive gland of mussels, *Mytilus galloprovincialis* (L.) as biomarkers of environmental stress. *Environ. Pollut.* 115, 123–137.

Du, J., Cai, J., Wang, S., You, H., 2017. Oxidative stress and apoptosis to zebrafish (*Danio rerio*) embryos exposed to perfluorooctane sulfonate (PFOS) and ZnO nanoparticles. *Int. J. Occup. Med. Environ. Health* 30, 213–229.

El-Shorbagy, H.M., Eissa, S.M., Sabet, S., El-Ghor, A.A., 2019. Apoptosis and oxidative stress as relevant mechanisms of antitumor activity and genotoxicity of ZnO-NPs alone and in combination with N-acetyl cysteine in tumor-bearing mice. *Int. J. Nanomedicine* 14, 3911–3928.

Falfushynska, H., Sokolov, E.P., Haider, F., Oppermann, C., Kragl, U., Ruth, W., Stock, M., Glufke, S., Winkel, E.J., Sokolova, I.M., 2019a. Effects of a common pharmaceutical, atorvastatin, on energy metabolism and detoxification mechanisms of a marine bivalve *Mytilus edulis*. *Aquat. Toxicol.* 208, 47–61.

Falfushynska, H.I., Wu, F., Ye, F., Kasianchuk, N., Dutta, J., Dobretsov, S., Sokolova, I.M., 2019b. The effects of ZnO nanostructures of different morphology on bioenergetics and stress response biomarkers of the blue mussels *Mytilus edulis*. *Sci. Total Environ.* 694, 133717.

Fly, E.K., Hilbish, T.J., 2013. Physiological energetics and biogeographic range limits of three congeneric mussel species. *Oecologia* 172, 35–46.

Fly, E.K., Hilbish, T.J., Wetthey, D.S., Rognstad, R.L., 2015. Physiology and biogeography: the response of European mussels (*Mytilus* spp.) to climate change. *Am. Malacol. Bull.* 33, 136–149.

Garner, K.L., Keller, A.A., 2014. Emerging patterns for engineered nanomaterials in the environment: a review of fate and toxicity studies. *J. Nanopart. Res.* 16, 28.

Gerloff, K., Landesmann, B., Worth, A., Munn, S., Palosaari, T., Whelan, M., 2017. The adverse outcome pathway approach in nanotoxicology. *Comput. Toxicol.* 1, 3–11.

Halappanavar, S., van den Brule, S., Nymark, P., Gaté, L., Seidel, C., Valentino, S., Zheronkov, V., Høgh Danielsen, P., De Vizcaya, A., Wolff, H., et al., 2020. Adverse outcome pathways as a tool for the design of testing strategies to support the safety assessment of emerging advanced materials at the nanoscale. *Part. Fibre Toxicol.* 17, 16.

Hoesel, B., Schmid, J.A., 2013. The complexity of NF-κB signaling in inflammation and cancer. *Mol. Cancer* 12, 86.

Holmstrup, M., Bindsbol, A.M., Oostingh, G.J., Duschl, A., Scheil, V., Kohler, H.R., Loureiro, S., Soares, A., Ferreira, A.L.G., Kienle, C., et al., 2010. Interactions between effects of environmental chemicals and natural stressors: a review. *Sci. Total Environ.* 408, 3746–3762.

Hong, H., Adam, V., Nowack, B., 2021. Form-specific and probabilistic environmental risk assessment of three engineered nanomaterials (nano-Ag, nano-TiO₂ and nano-ZnO) in European Freshwaters. *Environ. Toxicol. Chem.* 40, 2629–2639.

Hull, M.S., Chaurand, P., Rose, J., Auffan, M., Bottero, J.-Y., Jones, J.C., Schultz, I.R., Vikesland, P.J., 2011. Filter-feeding bivalves store and biodeposit colloidal stably gold nanoparticles. *Environ. Sci. Technol.* 45, 6592–6599.

IPCC, 2019. In: Pörtner, H.-O., Roberts, D.C., Masson-Delmotte, V., Zhai, P., Tignor, M., Poloczanska, E., Mintenbeck, K., Nicolai, M., Okem, A., Petzold, J., Rama, B., Weyer,

- N. (Eds.), Special Report on the Ocean and Cryosphere in a Changing Climate. Cambridge University Press, Cambridge, United Kingdom and New York, NY, USA In press.
- Joubert, Y., Pan, J.F., Buffet, P.E., Pilet, P., Gilliland, D., Valsami-Jones, E., Mouneyrac, C., Amiard-Triquet, C., 2013. Subcellular localization of gold nanoparticles in the estuarine bivalve *Scrobicularia plana* after exposure through the water. *Gold Bull.* 46, 47–56.
- Kang, S.J., Kim, B.M., Lee, Y.J., Hong, S.H., Chung, H.W., 2009. Titanium dioxide nanoparticles induce apoptosis through the JNK/p38-caspase-8-bid pathway in phytohemagglutinin-stimulated human lymphocytes. *Biochem. Biophys. Res. Commun.* 386, 682–687.
- Katsumiti, A., Arostegui, I., Oron, M., Gilliland, D., Valsami-Jones, E., Cajaraville, M.P., 2016. Cytotoxicity of Au, ZnO and SiO₂ NPs using in vitro assays with mussel hemocytes and gill cells: relevance of size, shape and additives. *Nanotoxicology* 10, 185–193.
- Kautsky, N., 1982. Quantitative studies on gonad cycle, fecundity, reproductive output and recruitment in a Baltic *Mytilus edulis* population. *Mar. Biol.* 68, 143–160.
- Kiss, T., 2010. Apoptosis and its functional significance in molluscs. *Apoptosis* 15, 313–321.
- Kniebusch, M., Meier, H.E.M., Neumann, T., Börgel, F., 2019. Temperature variability of the Baltic Sea since 1850 and attribution to atmospheric forcing variables. *J. Geophys. Res. Oceans* 124, 4168–4187.
- Kyriakis, J.M., Avruch, J., 2012. Mammalian MAPK signal transduction pathways activated by stress and inflammation: a 10-year update. *Physiol. Rev.* 92, 689–737.
- Lai, R.W.S., Yung, M.M.N., Zhou, G.-J., He, Y.L., Ng, A.M.C., Djurišić, A.B., Shih, K., Leung, K.M.Y., 2020. Temperature and salinity jointly drive the toxicity of zinc oxide nanoparticles: a challenge to environmental risk assessment under global climate change. *Environ. Sci. Nano* 7, 2995–3006.
- Letterio, J.J., Roberts, A.B., 1998. Regulation of immune responses by TGF- β . *Annu. Rev. Immunol.* 16, 137–161.
- Li, J., Schiavo, S., Rametta, G., Miglietta, M.L., La Ferrara, V., Wu, C., Manzo, S., 2017. Comparative toxicity of nano ZnO and bulk ZnO towards marine algae *Tetraselmis suecica* and *Phaeodactylum tricornutum*. *Environ. Sci. Pollut. Res.* 24, 6543–6553.
- Li, J., Schiavo, S., Xiangli, D., Rametta, G., Miglietta, M.L., Oliviero, M., Changwen, W., Manzo, S., 2018. Early ecotoxic effects of ZnO nanoparticle chronic exposure in *Mytilus galloprovincialis* revealed by transcription of apoptosis and antioxidant-related genes. *Ecotoxicology* 27, 369–384.
- Linders, T., Infantes, E., Joyce, A., Karlsson, T., Ploug, H., Hassellöv, M., Sköld, M., Zetsche, E.-M., 2018. Particle sources and transport in stratified Nordic coastal seas in the Anthropocene. *Elem. Sci. Anth.* 6, 29.
- Luo, Z., Li, Z., Xie, Z., Sokolova, I.M., Song, L., Peijnenburg, W.J.G.M., Hu, M., Wang, Y., 2020. Rethinking Nano-TiO₂ safety: overview of toxic effects in humans and aquatic animals. *Small* 16, 2002019.
- Ma, H., Williams, P.L., Diamond, S.A., 2013. Ecotoxicity of manufactured ZnO nanoparticles – a review. *Environ. Pollut.* 172, 76–85.
- Marisa, I., Matozzo, V., Munari, M., Binelli, A., Parolini, M., Martucci, A., Franceschini, E., Brianese, N., Marin, M.G., 2016. In vivo exposure of the marine clam *Ruditapes philippinarum* to zinc oxide nanoparticles: responses in gills, digestive gland and haemolymph. *Environ. Sci. Pollut. Res.* 23, 15275–15293.
- Martínez-Gutiérrez, F., Thi, E.P., Silverman, J.M., de Oliveira, C.C., Svensson, S.L., Vanden Hoek, A., Sánchez, E.M., Reiner, N.E., Gaynor, E.C., Prydzial, E.L., et al., 2012. Antibacterial activity, inflammatory response, coagulation and cytotoxicity effects of silver nanoparticles. *Nanomedicine* 8, 328–336.
- Modena, M.M., Rühle, B., Burg, T.P., Wuttke, S., 2019. Nanoparticle characterization: what to Measure? *Adv. Mater.* 31, 1901556.
- Møhlenberg, F., Riisgård, H.U., 1978. Efficiency of particle retention in 13 species of suspension feeding bivalves. *Ophelia* 17, 239–246.
- Munshi, A., Ramesh, R., 2013. Mitogen-activated protein kinases and their role in radiation response. *Genes Cancer* 4, 401–408.
- Ohkawa, H., Ohishi, N., Yagi, K., 1979. Assay for lipid peroxides in animal tissues by thiobarbituric acid reaction. *Anal. Biochem.* 95, 351–358.
- Owens, D.M., Keyse, S.M., 2007. Differential regulation of MAP kinase signalling by dual-specificity protein phosphatases. *Oncogene* 26, 3203–3213.
- Perry, D.K., Smyth, M.J., Stennicke, H.R., Salvesen, G.S., Duriez, P., Poirier, G.G., Hannun, Y.A., 1997. Zinc is a potent inhibitor of the apoptotic protease, caspase-3. A novel target for zinc in the inhibition of apoptosis. *J. Biol. Chem.* 272, 18530–18533.
- Pfaffl, M.W., 2001. A new mathematical model for relative quantification in real-time RT-PCR. *Nucleic Acids Res.* 29, 2002–2007.
- Pisanelli, B., Benedetti, M., Fattorini, D., Regoli, F., 2009. Seasonal and inter-annual variability of DNA integrity in mussels *Mytilus galloprovincialis*: a possible role for natural fluctuations of trace metal concentrations and oxidative biomarkers. *Chemosphere* 77, 1551–1557.
- Qu, M., Li, D., Zhao, Y., Yuan, Y., Wang, D., 2020. Exposure to low-dose nanopolystyrene induces the response of neuronal JNK MAPK signaling pathway in nematode *Caenorhabditis elegans*. *Environ. Sci. Eur.* 32, 58.
- Reznick, A.Z., Packer, L., 1994. Oxidative damage to proteins: Spectrophotometric method for carbonyl assay. *Methods in Enzymology*. 233. Academic Press, pp. 357–363.
- Rocha, T.L., Gomes, T., Sousa, V.S., Mestre, N.C., Bebianno, M.J., 2015. Ecotoxicological impact of engineered nanomaterials in bivalve molluscs: an overview. *Mar. Environ. Res.* 111, 74–88.
- Roma, J., Matos, A.R., Vinagre, C., Duarte, B., 2020. Engineered metal nanoparticles in the marine environment: a review of the effects on marine fauna. *Mar. Environ. Res.* 161, 105110.
- Schiavo, S., Oliviero, M., Miglietta, M., Rametta, G., Manzo, S., 2016. Genotoxic and cytotoxic effects of ZnO nanoparticles for *Dunaliella tertiolecta* and comparison with SiO₂ and TiO₂ effects at population growth inhibition levels. *Sci. Total Environ.* 550, 619–627.
- Schiedek, D., Sundelin, B., Readman, J.W., Macdonald, R.W., 2007. Interactions between climate change and contaminants. *Mar. Pollut. Bull.* 54, 1845–1856.
- Schmidt, W., Power, E., Quinn, B., 2013. Seasonal variations of biomarker responses in the marine blue mussel (*Mytilus* spp.). *Mar. Pollut. Bull.* 74, 50–55.
- Sheehan, D., Power, A., 1999. Effects of seasonality on xenobiotic and antioxidant defence mechanisms of bivalve molluscs. *Comp. Biochem. Physiol. C: Pharmacol. Toxicol. Endocrinol.* 123, 193–199.
- Singh, N., Manshian, B., Jenkins, G.J.S., Griffiths, S.M., Williams, P.M., Maffei, T.G.G., Wright, C.J., Doak, S.H., 2009. NanoGenotoxicology: the DNA damaging potential of engineered nanomaterials. *Biomaterials* 30, 3891–3914.
- Sokolova, I.M., 2009. Apoptosis in molluscan immune defense. *Invertebr. Surviv. J.* 6, 49–58.
- Sokolova, I.M., Lannig, G., 2008. Interactive effects of metal pollution and temperature on metabolism in aquatic ectotherms: implications of global climate change. *Clim. Res.* 37, 181–201.
- Steffen, J.B.M., Falfushynska, H.I., Piontkivska, H., Sokolova, I.M., 2020. Molecular biomarkers of the mitochondrial quality control are differently affected by hypoxia-reoxygenation stress in marine bivalves *Crassostrea gigas* and *Mytilus edulis*. *Front. Mar. Sci.* 7.
- Strohmeier, T., Strand, Ø., Alunno-Bruscia, M., Duinker, A., Cranford, P.J., 2012. Variability in particle retention efficiency by the mussel *Mytilus edulis*. *J. Exp. Mar. Biol. Ecol.* 412, 96–102.
- Trevisan, R., Delapiedra, G., Mello, D.F., Arl, M., Schmidt, E.C., Meder, F., Monopoli, M., Cargin-Ferreira, E., Bouzon, Z.L., Fisher, A.S., et al., 2014. Gills are an initial target of zinc oxide nanoparticles in oysters *Crassostrea gigas*, leading to mitochondrial disruption and oxidative stress. *Aquat. Toxicol.* 153, 27–38.
- Vandebriel, R.J., De Jong, W.H., 2012. A review of mammalian toxicity of ZnO nanoparticles. *Nanotechnol. Sci. Appl.* 5, 61–71.
- Volland, M., Hampel, M., Martos-Sitcha, J.A., Trombini, C., Martínez-Rodríguez, G., Blasco, J., 2015. Citrate gold nanoparticle exposure in the marine bivalve *Ruditapes philippinarum*: uptake, elimination and oxidative stress response. *Environ. Sci. Pollut. Res.* 22, 17414–17424.
- Wang, J., Deng, X., Zhang, F., Chen, D., Ding, W., 2014. ZnO nanoparticle-induced oxidative stress triggers apoptosis by activating JNK signaling pathway in cultured primary astrocytes. *Nanoscale Res. Lett.* 9, 117–117.
- Williams, R.J., Harrison, S., Keller, V., Kuenen, J., Lofts, S., Praetorius, A., Svendsen, C., Vermeulen, L.C., van Wijnen, J., 2019. Models for assessing engineered nanomaterial fate and behaviour in the aquatic environment. *Curr. Opin. Environ. Sustain.* 36, 105–115.
- Wong, S.W.Y., Leung, P.T.Y., Djurišić, A.B., Leung, K.M.Y., 2010. Toxicities of nano zinc oxide to five marine organisms: influences of aggregate size and ion solubility. *Anal. Bioanal. Chem.* 396, 609–618.
- Wu, F., Sokolova, I.M., 2021. Immune responses to ZnO nanoparticles are modulated by season and environmental temperature in the blue mussels *Mytilus edulis*. *Sci. Total Environ.* 801, 149786.
- Wu, F.L., Falfushynska, H., Dellwig, O., Piontkivska, H., Sokolova, I.M., 2020. Interactive effects of salinity variation and exposure to ZnO nanoparticles on the innate immune system of a sentinel marine bivalve, *Mytilus edulis*. *Sci. Total Environ.* 712.
- Wu, F., Sokolov, E.P., Dellwig, O., Sokolova, I.M., 2021. Season-dependent effects of ZnO nanoparticles and elevated temperature on bioenergetics of the blue mussel *Mytilus edulis*. *Chemosphere* 263, 127780.
- Xia, T., Kovochich, M., Liong, M., Mädler, L., Gilbert, B., Shi, H., Yeh, J.I., Zink, J.I., Nel, A.E., 2008. Comparison of the mechanism of toxicity of zinc oxide and cerium oxide nanoparticles based on dissolution and oxidative stress properties. *ACS Nano* 2, 2121–2134.
- Yung, M.M.N., Mouneyrac, C., Leung, K.M.Y., 2014. Ecotoxicity of zinc oxide nanoparticles in the marine environment. In: Bhushan, B. (Ed.), *Encyclopedia of Nanotechnology*. Springer Netherlands, Dordrecht, pp. 1–17.
- Yung, M.M.N., Wong, S.W.Y., Kwok, K.W.H., Liu, F.Z., Leung, Y.H., Chan, W.T., Li, X.Y., Djurišić, A.B., Leung, K.M.Y., 2015. Salinity-dependent toxicities of zinc oxide nanoparticles to the marine diatom *Thalassiosira pseudonana*. *Aquat. Toxicol.* 165, 31–40.
- Yung, M.M.N., Kwok, K.W.H., Djurišić, A.B., Giesy, J.P., Leung, K.M.Y., 2017. Influences of temperature and salinity on physicochemical properties and toxicity of zinc oxide nanoparticles to the marine diatom *Thalassiosira pseudonana*. *Sci. Rep.* 7.
- Zhao, X., Rao, Y., Liang, J., Lin, S., Wang, X., Li, Z., Huang, J., 2019. Silver nanoparticle-induced phosphorylation of histone H3 at serine 10 involves MAPK pathways. *Biomolecules* 9, 78.

Supporting Information for “Interactive effects of ZnO nanoparticles and temperature on molecular and cellular stress responses of the blue mussel *Mytilus edulis*”

Fangli Wu¹, Eugene P. Sokolov², Andrei Khomich^{1,3}, Christian Fettkenhauer⁴, Georg Schnell⁵, Hermann Seitz^{5,6}, Inna M. Sokolova^{1,7*}

¹Department of Marine Biology, Institute for Biological Sciences, University of Rostock, Rostock, Germany

²Leibniz Institute for Baltic Sea Research, Leibniz Science Campus Phosphorus Research Rostock, Warnemünde, Germany

³International Sakharov Environmental Institute of Belarusian State University, Minsk, Belarus

⁴Anton Paar Germany GmbH, Ostfildern, Germany

⁵Microfluidics, Faculty of Mechanical Engineering and Marine Technology, University of Rostock, Rostock, Germany

⁶Department Life, Light & Matter, University of Rostock, Rostock, Germany

⁷Department of Maritime Systems, Interdisciplinary Faculty, University of Rostock, Rostock, Germany

*Corresponding author: Inna Sokolova, inna.sokolova@uni-rostock.de

This PDF file includes:

Supplementary text: Description of experimental procedures

Supplementary Figure 1

Supplementary Table 1 to 12

Supplementary References

Characterization of ZnO nanoparticles

Dispersion of ZnO nanoparticles (nano-ZnO) (particle size <100 nm (TEM), average particle size ≤ 40 nm (APS) and pH 7.5 ± 1.5) were purchased from Sigma-Aldrich Sweden AB (Stockholm, Sweden). The morphology and crystal structure of nano-ZnO was visualized by transmission electron micrographs (TEM) and scanning electron micrograph (SEM) in a previous study that used the same batch of nano-ZnO as in the present study (Falfushynska et al., 2019). The surface area of dry nano-ZnO was $35 \text{ m}^2 \text{ g}^{-1}$ and determined by Brunauer–Emmett–Teller (BET) method. A Litesizer 500 (Anton Paar GmbH, Graz, Austria) was used to obtain all dynamic light scattering (DLS) and electrophoretic light scattering (ELS) data. The samples have been irradiated with light of a wavelength of 658 nm. The intensity of all scattered light was measured at 175° . Size and zeta potential analysis measurements have been performed in omega cuvettes. The temperature of the sample was controlled by a Peltier temperature control. The aggregate size distribution of nano-ZnO in the seawater (100 mg l^{-1} , salinity 15) was analyzed at different temperatures (10, 15 and 20°C).

Analysis of molecular markers of apoptosis and inflammation

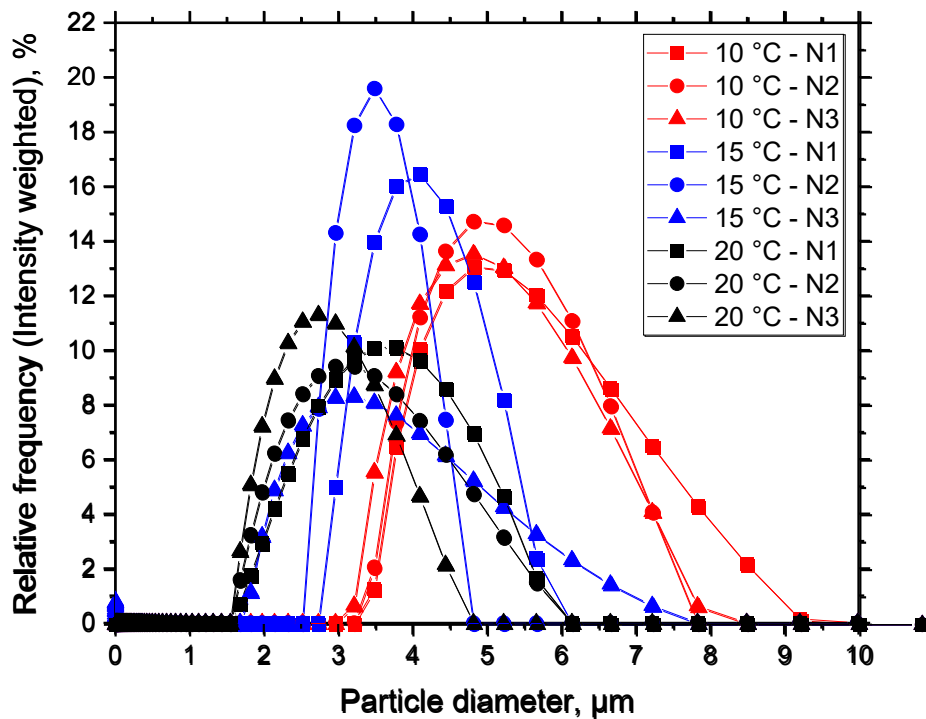
Total RNA was extracted from the soft tissues (gill and digestive gland) using TRIzol reagent (Thermo Fisher Scientific, Berlin, Germany) and cleaned up from the possible DNA contamination with TURBO DNA-free Kit (Thermo Fisher Scientific, Berlin, Germany) following the manufacturer's protocol. cDNA was obtained from $2.0 \mu\text{g}$ of purified RNA by High Capacity cDNA Reverse Transcription Kit (Thermo Fisher Scientific, Berlin, Germany) according to the manufacturer's instructions. qRT-PCR was performed using StepOnePlus™ Real-Time PCR System Thermal Cycling Block (Applied Biosystems, Thermo Fisher Scientific, Berlin, Germany) and Biozym Blue S'Green qPCR Mix Separate ROX kit (Biozym Scientific GmbH, Hessisch Oldendorf, Germany). The reaction mixture containing $2 \mu\text{l}$ of cDNA, $1.6 \mu\text{l}$ of each forward and

reverse primer (to the final concentration of 0.4 μM), 10 μl of 2 \times qPCR S'Green BlueMix and ROX additive mixture and 4.8 μl PCR grade water were added to the wells of 96 well PCR plates, sealed (RT-PCR Seal foil, Roth, Karlsruhe, Germany) and briefly centrifuged to eliminate air bubbles and collect the contents. The cycling parameters were as follows: 95 $^{\circ}\text{C}$ for 20 s to activate the polymerase followed by 40 cycles of 3 s at 95 $^{\circ}\text{C}$ and 15 s at 60 $^{\circ}\text{C}$. Signal readout was conducted at the primer-specific reading temperature at the end of each cycle (Supplementary Table 1). Following amplification, a melt curve analysis was performed to ensure that a single PCR product was amplified. In each run, serial dilutions of a cDNA standard were amplified to determine amplification efficiency (Pfaffl, 2001). In a pilot analysis, we tested three housekeeping genes (the eukaryotic elongation factor 1 (eEF1), tubulin and β -actin) and chose eEF1 that showed the least variation among and within the experimental groups for normalization of the target gene expression. The apparent amplification efficiency was calculated for each primer pair, and the expression of the target genes was normalized against the expression of the eukaryotic elongation factor eEF1 as described elsewhere (Pfaffl, 2001). The results was expressed as fold change in mRNA expression in the treated group relative to the mRNA expression in the respective control group (no Zn additions and ambient temperature corresponding to 10 $^{\circ}\text{C}$ in winter and 15 $^{\circ}\text{C}$ in summer).

Statistical analysis

Data analysis was performed by statistical software IBM® SPSS® Statistics ver. 18.0 (IBM Corp., Armonk, NY, USA) and GraphPad Prism ver. 6.0 (GraphPad Software Inc., La Jolla, CA, USA). Prior to significance analysis, data were checked for the normality using the Shapiro–Wilk's test and homogeneity of variances by Levene's test. Data that was not-normally distributed was Box-Cox transformed. The effects of Zn treatment, temperature regime and their interactions on the studied traits were tested by two-way analysis of variance (ANOVA). Similarly, the interactive effects of Zn treatment and Season at fixed temperature (15 $^{\circ}\text{C}$) were tested for each studied traits

by two-way ANOVA. The factor “Zn treatment” had five levels (control – no Zn addition, 10 $\mu\text{g l}^{-1}$ nano-ZnO, 100 $\mu\text{g l}^{-1}$ nano-ZnO, 10 $\mu\text{g l}^{-1}$ dissolved Zn or 100 $\mu\text{g l}^{-1}$ dissolved Zn). The factor “Temperature” had two levels (ambient temperature and elevated temperature). The factor “Season” had two levels (winter and summer). The significant effects of Zn treatments were analyzed using Tukey’s HSD post hoc multiple range tests at each fixed temperature regime, and the significant effects of temperature were analyzed by a Student’s *t* test at each fixed Zn treatment. To reduce the dimensionality of the data set normalized, normalized, Box-Cox transformed data were subjected to the principal component analysis (PCA). Discriminant analysis with stepwise module was performed to assess the ability of the studied biomarkers to distinguish between the different treatment groups. The number of biological replicates was 5-6 for all measured traits. The results are expressed as the means \pm the standard error (SE) and the significant effects were considered as $P < 0.05$.



Supplementary Figure 1. Distribution of intensity-weighted aggregate size of nano-ZnO suspended in the seawater (100 mg l^{-1} , salinity 15) at different temperatures (10, 15 and $20 \text{ }^{\circ}\text{C}$). Measurements were repeated three times ($N=3$).

Supplementary Table 1. Primer sequences for the target and housekeeping genes used for qPCR.

NCBI accession numbers of the sequences used for primer design are given. Because *M. edulis* does not yet have a completely sequenced genome assembly, in those cases where no sequence information was available for *M. edulis*, we used homologous sequences from closely related *Mytilus* species (*M. galloprovincialis*, or *M. coruscus*) to generate primers. For TGF- β we used earlier published primers from *M. coruscus* (Qi et al., 2019).

Gene	Forward primer (3'-5')	Reverse primer (3'-5')	NCBI accession #	T _{read}	Primer efficiency	Product length
p53	AAGCTGGCTCAGAAATGGGTC	TTCGACTGCCCGTCTACCCTA	AY579472	78 °C	96%	140
p38	GATGACAGGTTAATGTGGCTACCAG	ACTAGGAGTTCCCAACAAGGACAG	KP713439.1	75 °C	86%	196
JNK	CCTTTTATGGCAGCAGCGGTG	AAAATCCAGTGCCCGATGGT	MH603332.1	76 °C	99%	182
COX	CATTAGTCAAGAACGAAAGTCAAGAG	GCCTGCCGAGTCAATTGAAG	F1490762.1	78 °C	98%	-
Caspase 3	ACGACAGCTAGTTCACCAGG	CCACCAGAAGAGGAGTTCCG	HQ424453.1	76 °C	89%	108
Bcl-2	CGGTGGTTGGCAAAGGATTTG	CGCCATTGGCGCTAATTACAC	KC545829.1	75 °C	107%	118
NF- κ B	TGGATGATGAGGCCAAACC	TGAAAGTCACCATGTGACGG	KF051275.1	76 °C	118%	103
TGF- β	TGCGGGTAAAAACCAAGACCA	TCCCTGGCGGCTTCAATTAC	-	76 °C	93%	-

Supplementary Table 2. Two-way ANOVA analysis of the molecular and cellular stress biomarkers in gill of *M. edulis* exposed to different combinations of Zn treatment and temperature. Temperature: 10 and 15 °C in winter; 15 and 20 °C in summer. Zn treatment: control, 10 µg l⁻¹ nano-ZnO, 100 µg l⁻¹ nano-ZnO, 10 µg l⁻¹ Zn²⁺, and 100 µg l⁻¹ Zn²⁺.

MS: mean square; P: p-value. Degrees of freedom (d.f.) for the error were 48 for all studied traits. Significant effects are highlighted in bold.

A. Winter.

Source	LPO		PC		p53		p38		JNK							
	MS	F	P	MS	F	P	MS	F	P	MS	F	P				
Temperature	1	1459.083	4.279	0.045	2.49E-06	0.553	0.461	0.056	0.258	0.614	0.043	0.526	0.472	0.115	2.151	0.149
Zn treatment	4	1916.266	5.620	0.001	3.00E-05	6.654	< 0.001	1.052	4.852	0.002	0.054	0.655	0.626	0.093	1.738	0.157
T * Zn	4	1188.808	3.487	0.016	1.15E-05	2.558	0.053	0.474	2.186	0.085	0.118	1.436	0.237	0.230	4.303	0.005
	df	COX		Caspase 3		Bcl-2		NF-κB		TGF-β						
Temperature	1	0.149	0.149	1.134	0.292	4.829	24.384	0.000	0.034	0.070	0.793	1.702	5.861	0.019	0.178	0.770
Zn treatment	4	0.157	0.163	1.238	0.307	0.099	0.500	0.736	0.296	0.600	0.664	0.683	2.352	0.067	0.911	3.946
T * Zn	4	0.005	0.139	1.059	0.387	0.081	0.409	0.801	1.344	2.729	0.040	1.304	4.491	0.004	0.781	3.386

B. Summer.

Source	MS	F	P	MS	F	P	MS	F	P	MS	F	P			
	LPO			PC			p53			p38					
Temperature	8490.886	115.379	<0.001	2.28E-10	0.048	0.829	0.005	0.079	0.780	0.030	9.032	0.004	1.052	10.912	0.002
Zn treatment	324.082	4.404	0.005	1.14E-08	2.383	0.067	0.443	7.304	<0.001	0.032	9.556	<0.001	0.565	5.859	0.001
T * Zn	532.194	7.232	<0.001	4.91E-09	1.025	0.406	0.116	1.909	0.124	0.021	6.357	<0.001	0.050	0.521	0.720
	COX			Caspase 3			Bcl-2			NF-κB			TGF-β		
Temperature	0.180	10.105	0.003	0.516	33.687	<0.001	0.027	0.706	0.405	6.935	37.175	<0.001	0.068	1.945	0.169
Zn treatment	0.044	2.452	0.058	0.086	5.602	0.001	0.443	11.388	<0.001	1.005	5.389	0.001	0.126	3.608	0.012
T * Zn	0.053	2.983	0.028	0.078	5.065	0.002	0.131	3.371	0.016	0.093	0.499	0.737	0.363	10.347	<0.001

Supplementary Table 3. Two-way ANOVA analysis of the molecular and cellular stress biomarkers in digestive gland of *M. edulis* exposed to different combinations of Zn treatment and temperature. Temperature: 10 and 15 °C in winter; 15 and 20 °C in summer. Zn treatment: control, 10 µg l⁻¹ nano-ZnO, 100 µg l⁻¹ nano-ZnO, 10 µg l⁻¹ Zn²⁺, and 100 µg l⁻¹ Zn²⁺.

MS: mean square; P: p-value. Degrees of freedom (d.f.) for the error were 48 for all studied traits. Significant effects are highlighted in bold.

A. Winter.

Source	df	LPO			PC			p53			p38			JNK		
		MS	F	P	MS	F	P	MS	F	P	MS	F	P	MS	F	P
Temperature	1	211.604	0.648	0.425	0.132	2.895	0.097	0.438	5.890	0.019	0.049	11.043	0.002	0.127	51.043	<0.001
Zn treatment	4	1.80E+04	55.272	<0.001	0.620	13.641	<0.001	0.145	1.953	0.116	0.024	5.514	0.001	0.008	3.308	0.018
T * Zn	4	8307.239	25.452	<0.001	0.071	1.569	0.201	0.116	1.554	0.201	0.009	1.998	0.109	0.007	2.626	0.045
	df	COX			Caspase 3			Bcl-2			NF-κB			TGF-β		
Temperature	1	0.093	0.198	0.658	3.620	14.132	<0.001	0.083	19.618	<0.001	16.379	51.638	<0.001	14.449	67.815	<0.001
Zn treatment	4	1.289	2.747	0.083	0.840	3.279	0.018	0.004	0.912	0.464	1.989	6.271	<0.001	0.323	1.515	0.212
T * Zn	4	0.191	0.407	0.803	0.368	1.435	0.236	0.002	0.407	0.803	0.377	1.190	0.327	0.387	1.816	0.140

B. Summer.

Source	MS	F	P	MS	F	P	MS	F	P	MS	F	P				
		LPO				PC				p53						
Temperature	6.147	6.797	0.013	2.81E+06	5.389	0.025	0.004	0.115	0.736	0.618	8.483	0.005	0.013	6.490	0.014	
Zn treatment	42.330	46.806	<0.001	5.78E+06	11.085	<0.001	0.019	0.496	0.739	0.294	4.037	0.006	0.002	0.835	0.509	
T * Zn	8.593	9.501	<0.001	1.35E+06	2.580	0.052	0.075	1.957	0.115	0.017	0.236	0.917	0.001	0.635	0.640	
		COX				Caspase 3				Bcl-2				NF-κB		
Temperature	26.360	51.550	<0.001	1.718	10.117	0.003	0.076	0.120	0.731	0.303	3.280	0.076	2.224	42.677	<0.001	
Zn treatment	1.031	2.016	0.016	0.522	3.070	0.024	0.517	0.811	0.524	0.136	1.473	0.224	0.096	1.849	0.134	
T * Zn	0.289	0.566	0.689	0.076	0.449	0.773	1.320	2.071	0.099	0.242	2.619	0.046	0.054	1.031	0.400	
														TGF-β		

Supplementary Table 4. Two-way ANOVA analysis of the molecular and cellular stress biomarkers in gill/ digestive gland of *M. edulis* exposed to different combinations of Zn treatment and season at 15 °C. Season: winter and summer. Zn treatment: control, 10 µg l⁻¹ nano-ZnO, 100 µg l⁻¹ nano-ZnO, 10 µg l⁻¹ Zn²⁺, and 100 µg l⁻¹ Zn²⁺.

MS: mean square; P: p-value. Degrees of freedom (d.f.) for the error were 48 for all studied traits. Significant effects are highlighted in bold.

A. Gill.

Source	LPO			PC			p53			p38			JNK			
	MS	F	P	MS	F	P	MS	F	P	MS	F	P	MS	F	P	
Season	6.314	245.400	<0.001	3.05E-08	5.622	0.023	2.338	95.646	<0.001	8.351	416.192	<0.001	0.016	0.775	0.383	
Zn treatment	0.325	12.637	<0.001	3.03E-08	5.599	0.001	0.110	4.517	0.004	0.303	15.090	<0.001	0.058	2.739	0.039	
Season * Zn	0.738	28.693	<0.001	4.81E-09	0.888	0.480	0.083	3.402	0.016	0.214	10.650	<0.001	0.060	2.850	0.034	
	df	COX			Caspase 3			Bcl-2			NF-κB			TGF-β		
Season	1	6.890	102.381	<0.001	74.359	541.288	<0.001	41.462	151.646	<0.001	22.300	97.599	<0.001	75.038	509.362	<0.001
Zn treatment	4	0.243	3.607	0.012	1.076	7.832	<0.001	0.460	1.681	0.170	0.313	1.371	0.258	0.370	2.515	0.054
Season * Zn	4	0.323	4.795	0.002	0.369	2.688	0.042	2.209	8.081	<0.001	0.308	1.349	0.266	1.457	9.888	<0.001

B. Digestive gland.

Source	MS	F	P	MS	F	P	MS	F	P	MS	F	P	MS	F	P	
		LPO				PC				p53				p38		
		COX				Caspase 3				Bcl-2				NF-κB		
		TGF-β				JNK										
df																
Season	1	0.034	0.000	0.993	1.52E+04	0.021	0.885	2.295	21.525	<0.001	0.011	2.487	0.121	0.014	8.811	0.005
Zn treatment	4	2.77E+04	64.717	<0.001	3.35E+06	4.691	0.003	0.343	3.220	0.020	0.007	1.522	0.210	0.004	2.740	0.039
Season * Zn	4	990.343	2.316	0.074	5.01E+05	0.701	0.596	0.064	0.605	0.661	0.001	0.250	0.908	0.001	0.476	0.753
		COX				Caspase 3				Bcl-2				NF-κB		
		TGF-β				JNK										
Season	1	91.631	190.327	<0.001	28.266	134.164	<0.001	18.567	31.493	<0.001	18.901	66.570	<0.001	10.168	44.580	<0.001
Zn treatment	4	0.502	1.043	0.394	0.290	1.375	0.256	1.156	1.961	0.115	1.993	7.019	<0.001	0.183	0.802	0.530
Season * Zn	4	0.146	0.303	0.875	0.189	0.898	0.472	0.826	1.401	0.247	0.163	0.573	0.684	0.106	0.466	0.760

Supplementary Table 5. Factor loadings for the first two principal components of the molecular and cellular stress related biomarkers of gill of *M. edulis* exposed to different combinations of Zn treatment and temperature in both winter and summer experiment.

Traits with high loadings (>0.6 absolute value) are highlighted in bold.

Variable	Winter		Summer	
	Factor 1	Factor 2	Factor 1	Factor 2
p53	-0.028117	0.169716	0.506058	0.221027
p38	-0.640950	-0.142717	0.633959	-0.020793
JNK	-0.522558	-0.378860	0.892112	0.135744
COX	0.453987	0.412546	-0.353464	0.827922
Caspase3	-0.283819	-0.732238	0.740488	0.471667
Bcl-2	-0.747375	0.026524	0.552076	-0.396939
NF-κB	-0.551608	0.448797	0.654019	0.095924
TGF-β	-0.512681	0.542076	-0.470755	0.575276
LPO	-0.181739	-0.443389	-0.436297	-0.382231
PC	0.421104	-0.510745	0.291912	-0.054605

Supplementary Table 6. Factor loadings for the first two principal components of the molecular and cellular stress related biomarkers of digestive gland of *M. edulis* exposed to different combinations of Zn treatment and temperature in both winter and summer experiment.

Traits with high loadings (>0.6 absolute value) are highlighted in bold.

Variable	Winter		Summer	
	Factor 1	Factor 2	Factor 1	Factor 2
p53	0.692993	-0.189453	-0.537169	-0.481876
p38	-0.898818	0.023427	-0.847821	-0.010195
JNK	-0.843851	-0.326301	-0.361640	-0.639223
COX	-0.544757	0.425021	-0.614351	0.418689
Caspase3	-0.783131	-0.025169	-0.791624	0.089169
Bcl-2	-0.584535	-0.411021	-0.520195	-0.555214
NF-κB	-0.856702	-0.074601	-0.722072	-0.043636
TGF-β	-0.748100	-0.534870	-0.807703	0.176618
LPO	-0.510953	0.562425	-0.193355	0.504784
PC	-0.631086	0.519916	-0.462323	0.542740

Supplementary Table 7. Discriminant Function Stepwise Analysis of the molecular and cellular stress related biomarkers of gill of *M. edulis* exposed to different combinations of Zn treatment and temperature in winter experiment.

Values that significantly discriminate studied groups ($P < 0.05$) are shown in red. Wilks' Lambda: 0.01081, $F_{90.220} = 2.3260$, $P < 0.001$.

	Wilks' Lambda	Partial Lambda	F-remove (2,16)	P-value	1-Toler. (R-Sqr.)
p53	0.015750	0.686450	1.573317	0.167029	0.212699
p38	0.011926	0.906563	0.355008	0.947691	0.386623
JNK	0.017841	0.605999	2.239467	0.046260	0.304492
COX	0.015525	0.696395	1.501665	0.191089	0.300994
Caspase3	0.020583	0.525248	3.113307	0.008773	0.360803
Bcl-2	0.012814	0.843739	0.637911	0.756047	0.409469
NF- κ B	0.017426	0.620426	2.107301	0.059776	0.228561
TGF- β	0.016417	0.658553	1.785877	0.111347	0.345276
LPO	0.020718	0.521842	3.156101	0.008105	0.217896
PC	0.021196	0.510056	3.308622	0.006124	0.370663

Supplementary Table 8. Discriminant Function Stepwise Analysis of the molecular and cellular stress related biomarkers of gill of *M. edulis* exposed to different combinations of Zn treatment and temperature in summer experiment.

Values that significantly discriminate studied groups ($P < 0.05$) are shown in red. Wilks' Lambda: 0.00025, $F_{90.220} = 5.8680$, $P < 0.001$.

	Wilks' Lambda	Partial Lambda	F-remove (2,16)	P-value	1-Toler. (R-Sqr.)
p53	0.000549	0.457574	4.083180	0.001554	0.460367
p38	0.000510	0.492207	3.553512	0.003932	0.495941
JNK	0.000476	0.526850	3.093360	0.009103	0.761319
COX	0.000397	0.632155	2.004292	0.072998	0.663959
Caspase3	0.000361	0.696019	1.504333	0.190138	0.498736
Bcl-2	0.000686	0.366081	5.964537	0.000080	0.584037
NF- κ B	0.000714	0.351585	6.352463	0.000046	0.513935
TGF- β	0.000651	0.385512	5.490275	0.000161	0.297744
LPO	0.000892	0.281381	8.796773	0.000002	0.170231
PC	0.000412	0.609901	2.203099	0.049638	0.284071

Supplementary Table 9. Discriminant Function Stepwise Analysis of the molecular and cellular stress related biomarkers of digestive gland of *M. edulis* exposed to different combinations of Zn treatment and temperature in winter experiment.

Values that significantly discriminate studied groups ($P < 0.05$) are shown in red. Wilks' Lambda: 0.00103, $F_{90.220} = 4.3058$, $P < 0.001$.

	Wilks' Lambda	Partial Lambda	F-remove (2,16)	P-value	1-Toler. (R-Sqr.)
p53	0.001205	0.853967	0.58902	0.795868	0.355812
p38	0.002084	0.493728	3.53195	0.004087	0.787267
JNK	0.002088	0.492761	3.54564	0.003988	0.684126
COX	0.001563	0.658411	1.78701	0.111105	0.722162
Caspase3	0.001358	0.757812	1.10081	0.390784	0.460864
Bcl-2	0.001167	0.881967	0.46097	0.889344	0.258831
NF- κ B	0.002652	0.388027	5.43237	0.000176	0.758376
TGF- β	0.002330	0.441634	4.35488	0.000981	0.706845
LPO	0.006762	0.152164	19.19198	0.000000	0.377983
PC	0.001761	0.584363	2.44992	0.030801	0.447305

Supplementary Table 10. Discriminant Function Stepwise Analysis of the molecular and cellular stress related biomarkers of digestive gland of *M. edulis* exposed to different combinations of Zn treatment and temperature in summer experiment.

Values that significantly discriminate studied groups ($P < 0.05$) are shown in red. Wilks' Lambda: 0.00213, $F_{90.220} = 3.6178$, $P < 0.001$.

	Wilks' Lambda	Partial Lambda	F-remove (2,16)	P-value	1-Toler. (R-Sqr.)
p53	0.003017	0.706646	1.42991	0.218330	0.594326
p38	0.002663	0.800537	0.85822	0.570779	0.518752
JNK	0.004126	0.516661	3.22230	0.007174	0.590702
COX	0.004884	0.436484	4.44690	0.000842	0.493766
Caspase3	0.003318	0.642551	1.91613	0.086594	0.557215
Bcl-2	0.002967	0.718553	1.34914	0.253112	0.431442
NF- κ B	0.003063	0.696101	1.50375	0.190346	0.463684
TGF- β	0.003160	0.674576	1.66165	0.141262	0.468977
LPO	0.014703	0.144998	20.31065	0.000000	0.350957
PC	0.004138	0.515274	3.24024	0.006941	0.174342

Supplementary Table 11. Squared Mahalanobis distances of discriminant Function

Stepwise Analysis of *M. edulis* exposed to different combinations of Zn treatment and temperature.

Experimental treatment groups: NP 10 – 10 $\mu\text{g l}^{-1}$ nano-ZnO; NP 100 –100 $\mu\text{g l}^{-1}$ nano-ZnO; Zn 10 – 10 $\mu\text{g l}^{-1}$ Zn^{2+} ; Zn 100 –100 $\mu\text{g l}^{-1}$ Zn^{2+} .

Season	Temperature	Tissues	Groups	NP 10	NP 100	Zn 10	Zn 100
winter	10	gill	control	4.2303	21.2557	11.9201	13.8051
winter	15	digestive gland	control	3.2166	8.1847	7.7188	16.5778
summer	15	gill	control	10.2058	21.0735	23.4558	26.1979
summer	20	digestive gland	control	25.1009	34.7387	44.0608	43.3106
winter	10	gill	control	5.7368	42.0068	17.4675	45.4548
winter	15	digestive gland	control	32.0314	108.4905	4.7265	22.1057
summer	15	gill	control	19.9945	40.6373	9.5200	24.3284
summer	20	digestive gland	control	12.5518	65.5275	8.3628	32.1099

Supplementary References

Falfushynska, H. I., Wu, F., Ye, F., Kasianchuk, N., Dutta, J., Dobretsov, S. and Sokolova, I. M. (2019). The effects of ZnO nanostructures of different morphology on bioenergetics and stress response biomarkers of the blue mussels *Mytilus edulis*. *Science of The Total Environment* **694**, 133717.

Pfaffl, M. W. (2001). A new mathematical model for relative quantification in real-time RT-PCR. *Nucleic Acids Research* **29**, 2002-2007.

Qi, P., Huang, H., Guo, B., Liao, Z., Liu, H., Tang, Z. and He, Y. (2019). A novel interleukin-1 receptor-associated kinase-4 from thick shell mussel *Mytilus coruscus* is involved in inflammatory response. *Fish & Shellfish Immunology* **84**, 213-222.

Curriculum Vitae

Name: Fangli Wu
Date of birth: 20.01.1993
Place of birth: Gansu Province, P. R. China

Education and research experience

Since 05/2022 **Maternity leave**

Since 10/2021 **Study in Institute of Biological Sciences, University of Rostock**

Topic: "The combined effect of ZnO nanoparticles and hypoxia on the immunity and cellular stress response in the blue mussels *Mytilus edulis*"

Supervisor: Prof. Dr. Inna M. Sokolova

10/2018–09/2021 **PhD study in Institute of Biological Sciences, University of Rostock**

Topic: "Bioenergetics, immunity and cellular and molecular stress responses to ZnO nanoparticles are modulated by environmental temperature and salinity in the blue mussels *Mytilus edulis*"

Supervisor: Prof. Dr. Inna M. Sokolova

09/2015–06/2018 **Master study in College of Fisheries and Life Science, Shanghai Ocean University**

Master thesis: "Combined effects of seawater acidification and nanoparticles on the immunity, digestion and special dynamic action of thick shell mussel"

Supervisors: Prof. Dr. Weiqun Lv, Prof. Dr. Youji Wang

09/2011–06/2015 **Bachelor study in College of Fisheries and Life Science, Shanghai Ocean University**

Bachelor thesis: "Classification and characterization of hemocytes from two Asian horseshoe crab species *Tachypleus tridentatus* and *Carcinoscorpius rotundicauda*"

Supervisor: Prof. Dr. Youji Wang

08/2008–06/2011 **High school study at Qinan First high school**

List of Publications (*related to the PhD thesis)

14) *Wu FL, Sokolov, E. P., Khomich, A., Fettkenhauer, C., Schnell, G., Seitz, H. and Sokolova, I. M. (2022). Interactive effects of ZnO nanoparticles and temperature on molecular and cellular stress responses of the blue mussel *Mytilus edulis*. Science of The Total Environment 818, 151785.

13) *Wu FL and Sokolova, I. M. (2021). Immune responses to ZnO nanoparticles are modulated by season and environmental temperature in the blue mussels *Mytilus edulis*. Science of The Total Environment 801, 149786.

12) *Noor, N M.#, Wu FL#, Sokolov, E. P., Sokolova, I. M. (2021). Salinity-dependent effects of ZnO nanoparticles on bioenergetics and intermediate metabolite homeostasis in a euryhaline marine bivalve, *Mytilus edulis*. Science of the Total Environment 774, 145195.

equal contribution authors

11) *Wu FL, Sokolov, E. P., Dellwig, O. and Sokolova, I. M. (2020). Season-dependent effects of ZnO nanoparticles and elevated temperature on bioenergetics of the blue mussel *Mytilus edulis*. Chemosphere 263, 127780.

10) *Wu FL, Falfushynska, H., Dellwig, O., Piontkivska, H. and Sokolova, I. M. (2020). Interactive effects of salinity variation and exposure to ZnO nanoparticles on the innate immune system of a sentinel marine bivalve, *Mytilus edulis*. Science of the Total Environment 712, 136473.

9) Shang, Y.#, Wu FL#, Wei, S., Guo, W., Chen, J., Huang, W., Hu, M. and Wang, Y. (2020). Specific dynamic action of mussels exposed to TiO₂ nanoparticles and seawater acidification. Chemosphere 241, 125104.

equal contribution authors

8) Wu FL, Xie, Z., Yan, M., Li, Q., Song, J., Hu, M. and Wang, Y. (2019). Classification and characterization of hemocytes from two Asian horseshoe crab species *Tachypleus tridentatus* and *Carcinoscorpius rotundicauda*. Scientific Reports 9, 1-10.

7) Kong, H.#, Wu FL#, Jiang, X., Wang, T., Hu, M., Chen, J., Huang, W., Bao, Y. and Wang, Y. (2019). Nano-TiO₂ impairs digestive enzyme activities of marine mussels under ocean acidification. Chemosphere 237, 124561.

equal contribution authors

6) Wu FL, Xie, Z., Lan, Y., Dupont, S., Sun, M., Cui, S., Huang, X., Huang, W., Liu, L. and Hu, M. (2018). Short-term exposure of *Mytilus coruscus* to decreased pH and salinity change impacts immune parameters of their haemocytes. Frontiers in Physiology 9, 166.

5) Wu FL, Cui, S., Sun, M., Xie, Z., Huang, W., Huang, X., Liu, L., Hu, M., Lu, W. and Wang, Y. (2018). Combined effects of ZnO NPs and seawater acidification on the haemocyte

parameters of thick shell mussel *Mytilus coruscus*. Science of the Total Environment 624, 820-830.

4) Wu FL, Wang T, Cui SK, Xie Z, Dupont S, Zeng JN, Gu HX, Kong H, Hu MH, Lu WQ, Wang YJ. (2017). Effects of seawater pH and temperature on foraging behavior of the Japanese stone crab *Charybdis japonica*. Marine Pollution Bulletin 120: 99-108.

3) Wu FL, Kong H, Shang YY, Zhou ZQ, Gul Y, Liu QG, Hu MH. (2017). Histopathological alterations in triangle sail mussel (*Hyriopsis cumingii*) exposed to toxic cyanobacteria (*Microcystis aeruginosa*) under hypoxia. Aquaculture 467: 182-189.

2) Hu M, Wu FL, Yuan M, Liu Q, Wang Y. (2016). Combined effects of toxic cyanobacteria *Microcystis aeruginosa* and hypoxia on the physiological responses of triangle sail mussel *Hyriopsis cumingii*. Journal of Hazardous Materials 306: 24-33.

1) Hu M, Wu FL, Yuan M, Li Q, Gu Y, Wang Y, Liu Q. (2015). Antioxidant responses of triangle sail mussel *Hyriopsis cumingii* exposed to harmful algae *Microcystis aeruginosa* and hypoxia. Chemosphere 139: 541-549.

Contribution to Conferences

6) Wu FL, Sokolova, I. M. Poster: Combined effects of nZnO and temperature on hemocyte responses of the blue mussel *Mytilus edulis*. 20th International symposium on Pollutant Responses In Marine Organisms. Charleston, SC, United States, 2019.

5) Wu FL, Wang YJ. Oral presentation: Haemocyte responses to salinity change and seawater acidification in the thick shell mussel *Mytilus coruscus*. The Eighteenth National Symposium on Shellfish. Xian, China, October 10-12, 2017.

4) Wu FL, Wang YJ. Poster: Hemocyte responses of the thick shell mussel *Mytilus coruscus* exposed to nano-ZnO and seawater acidification. The Fourth Symposium on Ecological Toxicology. Hangzhou, China, April 25-28, 2017.

3) Wu FL, Hu M, Wang Y. Poster: Ocean acidification impairs feeding behaviour and physiology of the brown crab *Cancer pagurus*. The Tenth Symposium on shrimp and crab farming. Shanghai, China, November 12-13, 2016.

2) Wu FL, Sui YM, Hu MH, Wang YJ. Poster: Effect of pH and DO on immune responses of the thick shell mussel *Mytilus coruscus*. The Symposium on life science and human health. Anhui, China, December 4- 6, 2015.

1) Wu FL, Hu MH, Wang YJ. Poster: Combined effects of seawater acidification and high temperature on haemocyte parameters in the thick shell mussel *Mytilus coruscus*. The Seventeenth National Symposium on Shellfish. Changsha, China, October 14-16, 2015.